CYCLONE ACTIVITY, PRECIPITATION AND MARINE STORMINESS IN THE EASTERN MEDITERRANEAN REGION: ANALYSIS OF REGIONAL CLIMATE SCENARIO SIMULATIONS

Lionello Piero[(1)], Boldrin Ugo[(2)], Cogo Stefano[(2)], De Zolt Simona[(2)], Giorgi Filippo[(3)], Galati Maria Barbara[(1)], Sanna Antonella[(1) (4)], Vicentini Giulia[(2)]

[(1)]University of Lecce, Italy, [(2)]University of Padua, Italy, [(3)]ICTP, International Center for Theoretical Physics, Italy, [(4)]ARPA-Piemonte, Italy

ABSTRACT

This study is based on a set of simulations carried out at ICTP in Trieste with a regional climate model (called RegCM). The A2 and B2 scenario for the period 2070-2100 are described and compared with a CTR simulation based on the 1960-1990 green house gas concentration. The monthly precipitation and synoptic variability fields are considered. Wave fields are computed with a wave model (called WAM) forced using the RegCM wind fields. Results show a statistically significant reduction of cyclone activity, precipitation, and wave height over most of the annual cycle in the A2 scenario. In the B2 scenario changes are smaller than in A2 and often they are not significant. In general, results suggest milder and drier weather conditions in scenario simulations in the Eastern Mediterranean.

INTRODUCTION

Cyclones are a frequent component of Mediterranean weather (see Lionello et al, 2006b for a review). The Northern Hemisphere storm track presents a separate branch crossing the Mediterranean region, with areas of cyclogenesis in the western Mediterranean and of prevalent cyclolysis in the Central and Eastern Mediterranean. The cyclones in the Mediterranean region can be quite intense and are responsible for hazardous events, but are also beneficial as they are the main source of precipitation in the region for most of the year. Cyclogenesis in the Mediterranean region is primarily caused by orographic effects, but the latent heat release, which is an usual mechanism of intensification of cyclogenesis, is important too, especially in fall and winter, when the basin becomes a considerable heat reservoir.

In this study we analyze the climate change signal of cyclones, of precipitation and ocean waves, which are associated with them. Heavy rain events are associated with cyclones as humid Mediterranean air is advected against the slopes of the mountain ridges surrounding the basin. The interaction of the atmospheric circulation produced by cyclones with orography and land-sea distribution contributes to the Mediterranean regional winds and, therefore, to the generation of ocean waves. It is particularly important to identify the climate change of the precipitation regime, because of the irregular and limited (especially in summer) water availability in the region and the environmental and societal problems that water scarcity could produce in future (Lionello et al. 2006a). Wave regimes are important in general for the coast, which with its 46000km length is an important component of the Mediterranean environment.

Two different approaches are used to analyze the cyclone activity (e.g. Lionello et al 2006b): a "lagrangian" approach based on a cyclone trajectory identification algorithm and an "eulerian" approach based on computation of SLP standard deviation. The maps shown here (fig.1) result from the Eulerian approach. A band-pass filter is applied to the SLP fields, which retains the variability in the 1-7 day period, and the SLP standard deviation is computed. For brevity, the standard deviation of the band pass filtered SLP fields is called "synoptic signal".

DATA

This study is based on three 30-year long regional climate simulations, one for present day conditions (1961-1990, CTR experiment) and two for future conditions (2071-2100) under the A2 and B2 IPCC scenarios, which are characterized by a high and low emission level, respectively. The climate simulations are carried out using the regional climate model RegCM (Giorgi et al. 1993a,b) driven at the lateral boundaries by meteorological fields from the Hadley Centre global atmospheric model HadAM3H at 1.25×1.875 lat-lon horizontal resolution (Jones et al. 2001). Sea surface temperatures (SSTs) are obtained from corresponding simulations with the Hadley Centre global coupled model HadCM3 (Jones et al. 2001). The model grid spacing is 50 km and the model domain covers the European region and adjacent oceans. For more information on the model and for a general discussion of the simulations, the reader is referred to Giorgi et al. (2004a,b). In this study we analyse the six-hourly SLP (Sea Level Pressure) fields for the assessment of the cyclone climate and the corresponding precipitation fields. The surface wind fields produced by RegCM are used as forcing of the WAM (WAMDI group, 1987) model for the computation of the ocean wave field. The WAM model is implemented in the whole Mediterranean Sea with a 0.25deg resolution and the resulting three-hourly SWH (Significant Wave Height) and mean wave direction fields are analysed.

THE CLIMATE CHANGE SIGNAL

Fig.1 shows the difference of synoptic signal between the A2 and CTR simulations (values in hPa). The negative values (green areas) denote lower signal in the A2 scenario. Only areas where the change is statistically significant at the 95% confidence level according to the Mann-Whitney test are filled with colours. Reduction is significant for most of the year, but for a moderate increase over some continental area from June to August. During the first part of the year (from January to May) reduction mostly located over the Asian and African countries, while European countries are more affected during the second part of the year from September to November. The overall reduction of cyclone activity is consistent with previous studies (Lionello et al., 2002 and Pinto et al, 2006) based on global climate simulations.

Figure 2 shows the difference of monthly accumulated precipitation (values in mm). The precipitation increase in the northern part of the area from January to March is consistent with the increase of the synoptic signal in the northern corner of the map. Precipitation diminishes during the remaining part of the year over most areas and the reduction is particularly large in autumn. It is interesting that the increase of synoptic signal in June and July does not produce a corresponding increase of precipitation. A possible explanation is its association with advection of dry air from the north which would produce hardly any precipitation.

Figure 3 shows the results of the wave field simulations (SWH values in metres). Analysis consider four seasons according to Lionello and Sanna (2006): winter (Dec-Mar), spring (Apr-May), Summer (Jun-Sep), Autumn (Oct-Nov). The left column shows the seasonal average fields, the right column the areas where the climate change signal (difference between A2 and CTR) is significant. Arrows are used to show change of mean wave direction. Attenuation of wave activity takes places for the whole year in the A2 scenario, being particularly large in winter. Only in summer, in the central Levantine basin, the waves generated by the Etesian winds are higher in the A2 scenario than in the CTR simulation. These changes are consistent with those of the synoptic signal. The B2 scenario (not shown) presents a similar behaviour, but with smaller magnitude, suggesting a climate change signal increasing with the emission level.

DISCUSSION

The link between the considered variables is not simple and linear. Besides changes of synoptic signal, other quantities, such as air humidity and stability, are important for precipitation, and besides transient winds associated with the passage of cyclones, mean wind regimes are important for waves. Moreover the link is not local, because precipitation does not take place in the core of the cyclone, where the pressure signal is larger, but it depends on the location of fronts and on the orographic features forcing air lift. Similarly the wave height reflects the effect of channelling and intensification of wind and not directly the depth of the pressure minimum. It is therefore required to further explore such connections in order to obtain a dynamically consistent picture of future climate scenarios. However, the analysis of these regional simulations suggests a milder and drier climate in future climate scenarios, with a consistent reduction of cyclone activity, precipitation and wave height during most of the year.

REFERENCES

Giorgi, F., M.R. Marinucci, and G.T. Bates, 1993: Development of a second generation regional climate model (REGCM2). Part I: Boundary layer and radiative transfer processes. Mon. Weather Rev., 121, 2794-2813.

Giorgi, F., M.R. Marinucci, G.T. Bates, and G. DeCanio, 1993: Development of a second generation regional climate model (REGCM2). Part II: Convective processes and assimilation of lateral boundary conditions. Mon. Weather Rev., 121, 2814-2832.

Giorgi, F., X. Bi and J.S. Pal, 2004: Mean, interannual variability and trends in a regional climate change experiment over Europe. Part I: Present day climate (1961-1990). Clim. Dyn., 22, 733-756.

Giorgi, F., X. Bi and J.S. Pal, 2004: Mean, interannual variability and trends in a regional climate change experiment over Europe. Part II: Future climate scenarios (2071-2100). Clim. Dyn., 23, 839-858.

Jones RG, Murphy JM, Hassell D, Taylor R, 2001: Ensemble mean changes in a simulation of the European mean climate of 2071-2100 using the new Hadley Centre regional modeling system HadAM3H/HadRM3H. Hadley Centre report, 19 pp.

Lionello P. and A.Sanna, 2005; Mediterranean wave climate variability and its links with NAO and Indian Monsoon Clim.Dyn. DOI: 10.1007/s00382-005-0025-4

Lionello P, F.Dalan, E.Elvini, 2002: Cyclones in the Mediterranean Region: the present and the doubled CO2 climate scenarios, Clim. Res.,22, 147-159
Lionello P., Bhend J., Buzzi A., Della-Marta P.M., Krichak S., JansÃ A., Maheras P., Sanna A., Trigo I.F., Trigo R., 2006a: Cyclones in the Mediterranean region: climatology and effects on the environment. In P.Lionello, P.Malanotte-Rizzoli, R.Boscolo (eds) Mediterranean Climate Variability. Amsterdam: Elsevier (NETHERLANDS) 324-372.
Lionello P., P.Malanotte-Rizzoli, R.Boscolo,P. Alpert, V.Artale, L Li, J.Luterbacher, W.May, R.Trigo, M.Tsimplis, U.Ulbrich, E.Xoplaki, 2006b; The Mediterranean climate: an overview of the main characteristics and issues In P.Lionello, P.Malanotte-Rizzoli, R.Boscolo (eds) Mediterranean Climate Variability.
Pinto J.G., T. Spangehl, U.Ulbrich and P.Speth (2006): Assessment of winter cyclone activity in a transient ECHAM4-OPYC3 GHG experiment. Meteorol. Zeitschrift, in press
WAMDI group, Hasselmann S, Hasselmann K, Bauer E, Janssen PAEM, Komen G, Bertotti L, Lionello P, Guillaume A, Cardone VC, Greenwood JA, Reistad M, Zambresky L, Ewing JA ,1988: The WAM model—a third generation ocean wave prediction model. J Phys Oceanogr 18:1776–1810

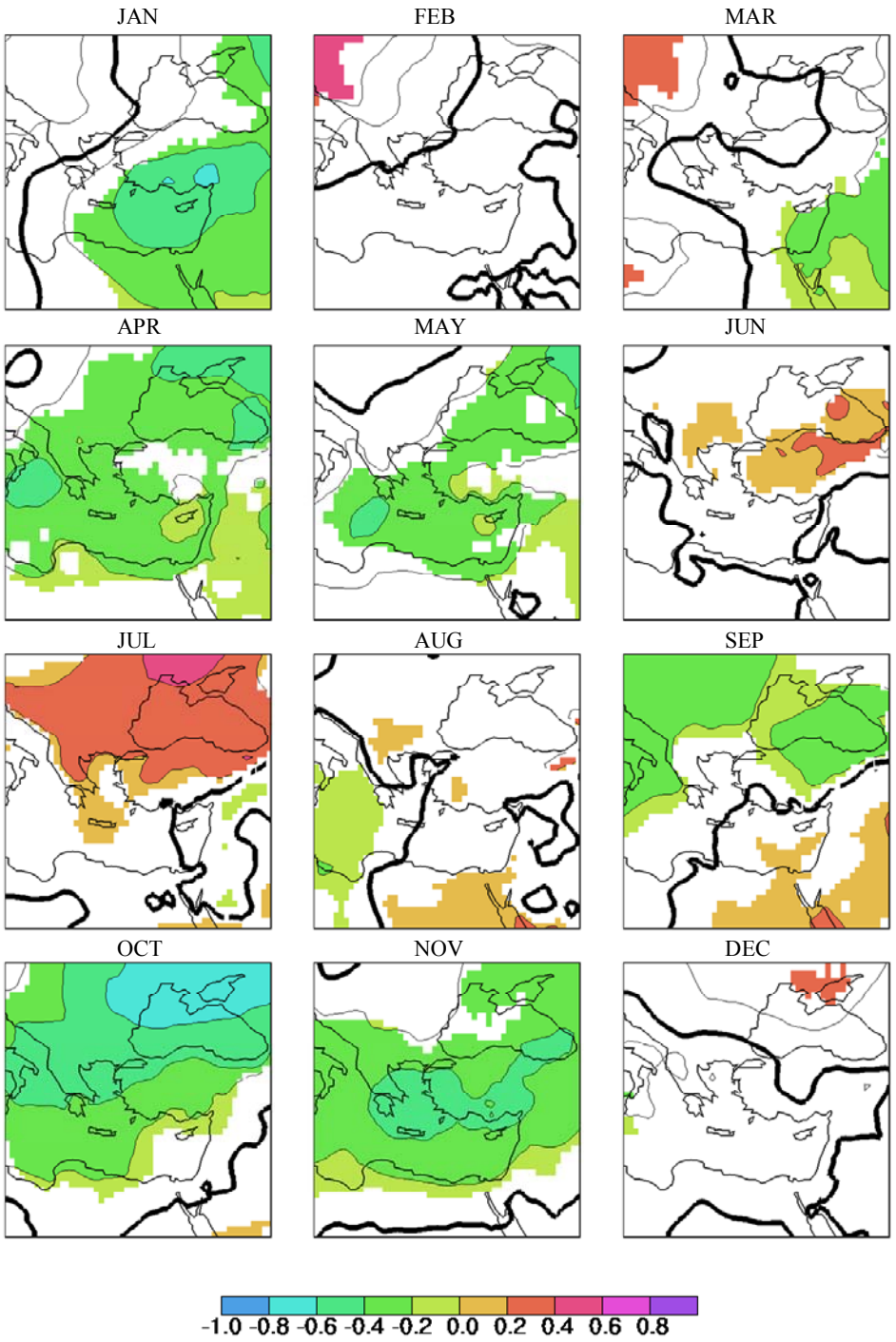

Figure 1. Change of monthly synoptic signal (values in hPa). Positive values denote areas where the A2 scenario has higher values than CTR. Only areas where the differences are statistically significant at the 95% confidence level are coloured. The thick black line denote the 0 level contour.

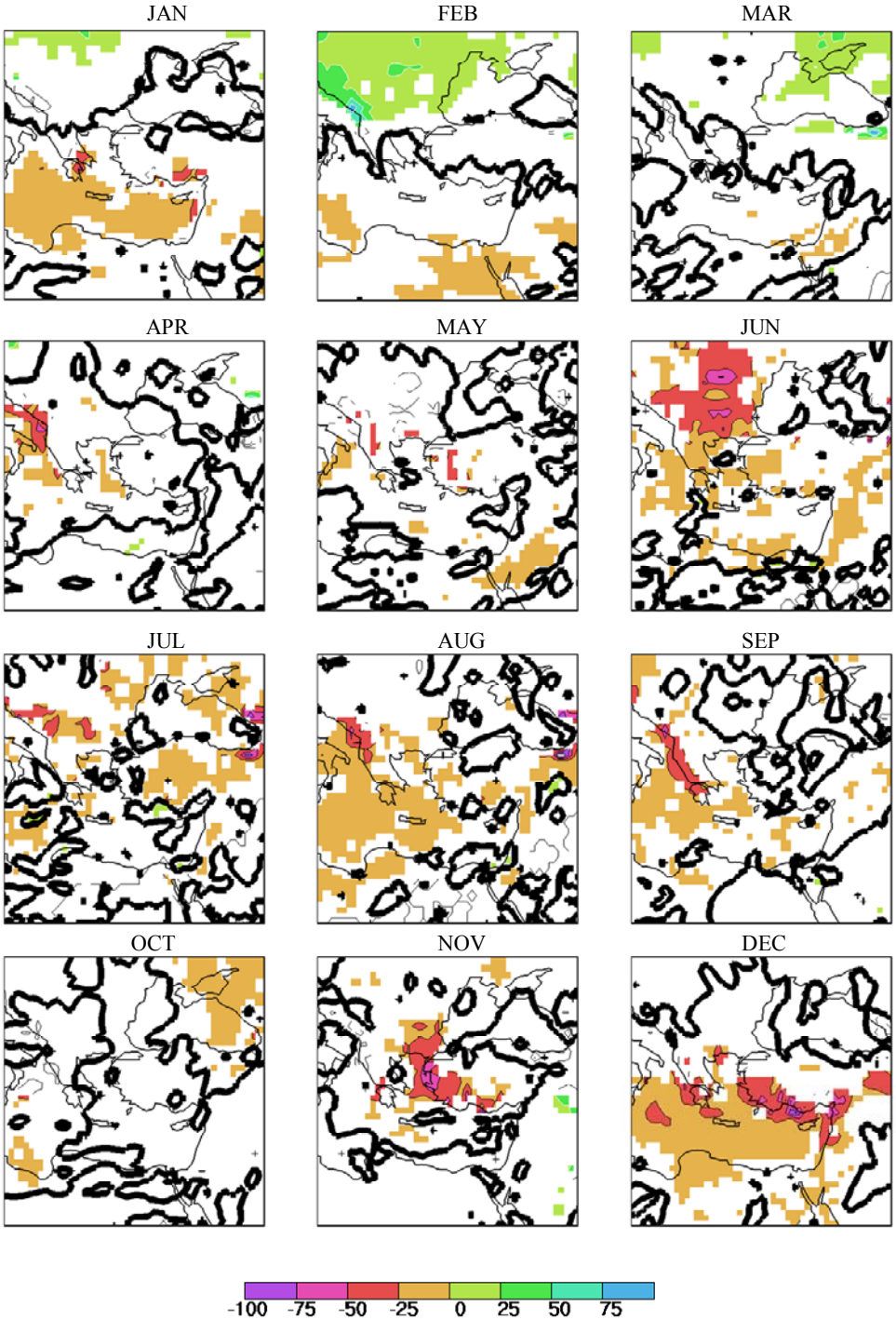

Figure 2. As Figure 1 but for the monthly accumulated precipitation (mm.)

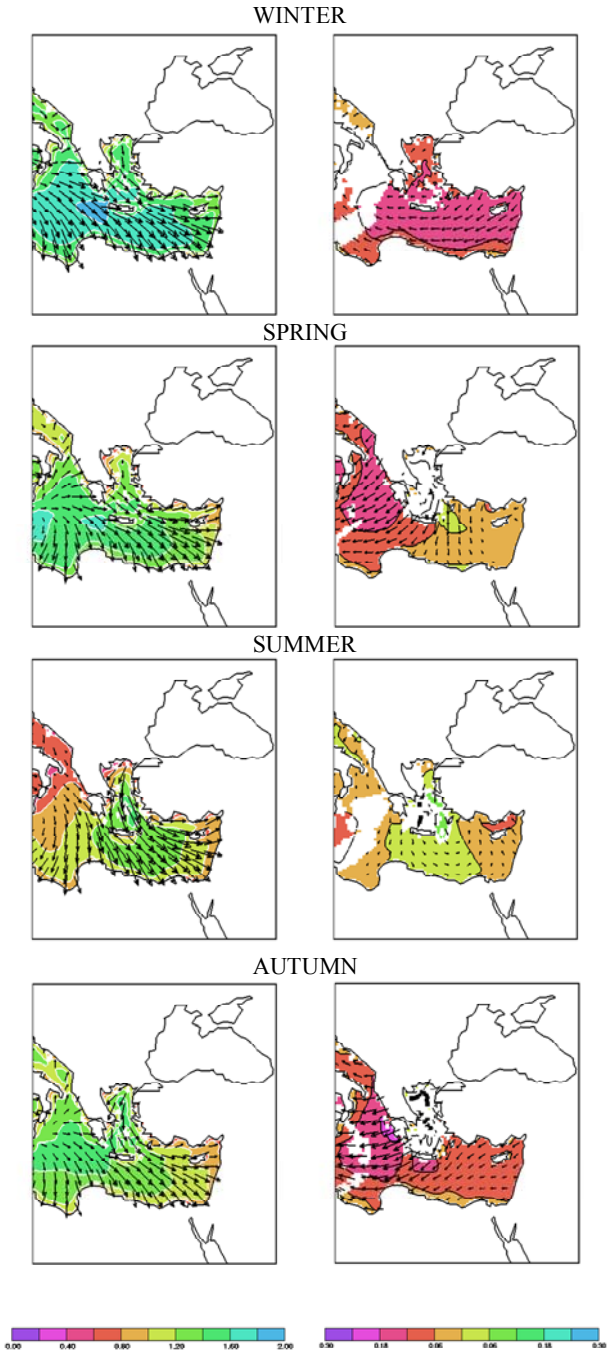

Figure 3. SWH average seasonal fields (left column) and differences between A2 and CTR simulations (values in metres). Negative values denote areas where the A2 fields have lower SWH. Arrows denote the mean wave direction.

THE IMPACT OF THE NORTH ATLANTIC OSCILLATION ON MIDDLE EAST RAINFALL

Emily Black

NCAS-Climate, Department of Meteorology, University of Reading; E.C.L.Black@reading.ac.uk

ABSTRACT

Understanding the impact of the North Atlantic Oscillation (NAO) is crucial to our understanding of both climate change and decadal variability in the Middle East. It is well known that winter precipitation and temperature over Europe are modulated by the NAO. Previous work has also demonstrated that the influence of the NAO extends as far east as Turkey. The impact of the NAO further south is, however, less clear. In order to clarify this issue, this study uses a combination of observed and reanalysis data to assess the effect of the NAO on rainfall in the Middle East.

Comparison between the time series of the NAO index and that of rainfall at several stations in the Middle East shows that the distribution of rainfall is different for NAO positive and NAO negative years. During NAO positive years, there is greater variability, which is reflected by a greater proportion of very rainy years. The relationship between NAO positive years and high rainfall is not universal - during some positive NAO years, rainfall is well below average. Moreover, there is no converse relationship between NAO-negative years and very low rainfall.

The strength of the relationship between the NAO and Middle Eastern rainfall varies within the rainy season, being strongest in November, December, January and February, and weak in October and March.

In recent years the NAO has tended to be increasingly positive - a trend that some climate modelling studies suggest will continue as greenhouse gas concentrations increase. The results of this study raise the question of what impact these projected changes in the NAO will have on interannual rainfall variability in the Middle East.

INTRODUCTION

Understanding the large scale controls on present day Middle East climate is essential if we are to predict how rainfall variability in the region will change in the medium and long term. This study investigates the controls on interannual variability in Middle East rainfall - in particular the role of the North Atlantic Oscillation (NAO).

In boreal winter, the NAO is a dominant pattern of circulation variability over the North Atlantic (see for example Hurrell, et al. 2003). The NAO can be thought of as an oscillation in atmospheric mass, and hence sea level pressure, between the northern and subtropical Atlantic (centres of action near Iceland and the Azores). During its positive (negative) phase, there is low (high) pressure in the Icelandic region and high (low) pressure in the Azores. The increased north-south pressure gradient during the positive phase of the NAO causes storms to move across the Atlantic on a more northerly track, leading to wet winters in northern

Europe and dry winters in southern Europe. In contrast, when the NAO is negative, the reduced north-south pressure gradient causes storms to move across the Atlantic on a more west-east track, leading to dry winters in northern Europe and wet winters in southern Europe (see for example Wallace and Gutzler 1981) .

Cullen, et al. 2002 and Cullen and Demenocal 2000 showed that the influence of the NAO extends as far east as Turkey. The impact of the NAO further south on rainfall in the Levant is, however, less clear. This study aims to tackle this issue by comparing time series of the NAO and rainfall.

DATA AND METHODOLOGY

This study uses observations of SLP, the NAO index and precipitation. The SLP data were taken from the NCEP reanalysis (see Kalnay, et al. 1996) and rain gauge data were extracted from the Global Historical Climate Network version 2 data archive (www.lwf.ncdc.noaa.gov/oa/pub/data/ghcn). The NAO index used is based on station measurements of sea-level pressure in Iceland, and the Iberian Peninsula. Details of how the index was calculated can be found in Jones, et al. 1997 and www.cru.uea.ac.uk/cru/data/nao.htm.

It can be seen from Figure 1 that there is a good density of rainfall stations in Levant region. Although the time period considered in this article is 1950-1999, data from a few gauges are available from 1845. The region bounded by the box 34^0-36^0 longitude and 31^0-33^0 latitude was selected as a study area because it contains is a particularly good density of stations, and because the rainfall within it is reasonably spatially coherent on an interannual timescale (mean January cross-correlation between stations of 0.67). A 1950-1999 time series of rainfall within the study area was calculated (see
Figure 3), and used as a basis for composites of atmospheric variables in wet and dry years. In order to avoid biases the data were standardised then gridded on a 1-degree scale before the time series or composites were derived.

Although the analysis was performed for the whole November - February rainy season, in most cases, only January plots are shown. Unless otherwise indicated similar results were obtained for November, December and February.

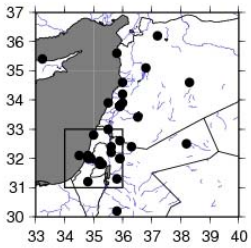

Figure 1. Location of rain gauges. The box is the area used for calculating the rainfall time series used in this study.

CLIMATE VARIABILITY ON SEASONAL-INTERANNUAL TIME SCALES

Figure 2 shows the mean seasonal cycle in rainfall between 1961-1990 for the region highlighted in Figure 1. It can be seen that the Middle East experiences most precipitation between November and March, and that the summer is completely dry. Rainfall in the Levant originates from mid-latitude cyclones during their eastward migration over the Mediterranean. Because these cyclones have a relatively large synoptic scale the seasonal-interannual variability of rainfall is spatially coherent within the area of interest (highlighted on Figure 1). It is evident from both Figure 2 and
Figure 3 that there is considerable interannual variability in rainfall.

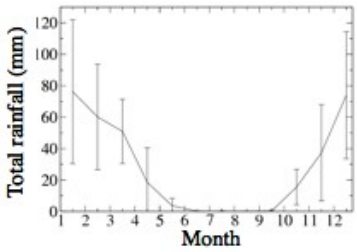

Figure 2. Seasonal cycle of rainfall for in the box shown in Figure 1. The error bars represent one standard deviation from the mean

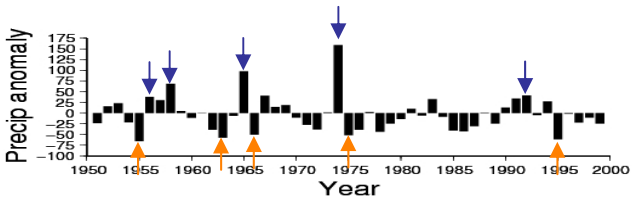

Figure 3. A time series of January precipitation anomalies in the box shown in Figure 1. The brown arrows show the five driest years, and the blue arrows show the five driest years.

OBSERVED TELECONNECTIONS

The large scale controls on interannual variability were investigated by constructing composites of atmospheric fields for the five wettest and the five driest years in the box shown in Figure 1. These years are highlighted in
Figure 3. The differences in precipitation, sea-level pressure (SLP) and storm track density between the wet and dry years are shown in Figure 4.

Figure 4a shows that during wet years, rainfall is low in western Europe and high throughout the Middle East. This is consistent with the SLP patterns shown in Figure 4b, which indicate that high rainfall in the study area is associated with high pressure over Europe. The storm track density composites shown in Figure 4c also fit in with this picture, with high rainfall in the study area associated with fewer storms over Europe and the Mediterranean, and more storms entering the Middle East.

On a larger scale, during rainy years, there is tendency to high pressure in the sub-tropical Atlantic and low pressure in the North Atlantic, although many of the anomalies are not significant at the 95% level (see Figure 4b). Figure 4c indicates a northward shift of the storm

track. To some extent these patterns of SLP and storm tracks resemble the NAO. The next section examines the relationship between the NAO and rainfall in the area of interest in more detail.

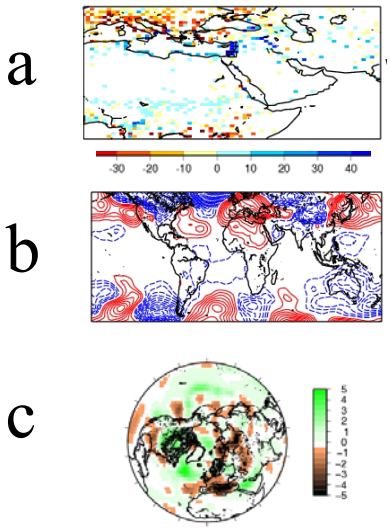

Figure 4. Difference in a) precipitation b) SLP (contour interval 0.5mb) and c) storm track density between the five wettest and five driest Januaries. The years included are shown in Figure 3

ANALYSIS OF RAINFALL AND NAO TIME SERIES

Figure 5 compares the time series of the NAO with that of rainfall in the area of interest for January. It is evident from Figure 5c that the distribution of rainfall is different for NAO positive and NAO negative years although the linear correlation between the NAO index and rainfall is low. During NAO positive years, there is greater variability, which is reflected by a greater proportion of very rainy years. In fact, nine out of the ten rainiest Decembers occur when the NAO is in its positive phase (see Table 1). The relationship between NAO-positive years and high rainfall is not universal - during some positive NAO years, rainfall is well below average. Moreover, there is no converse relationship between NAO-negative years and very low rainfall.

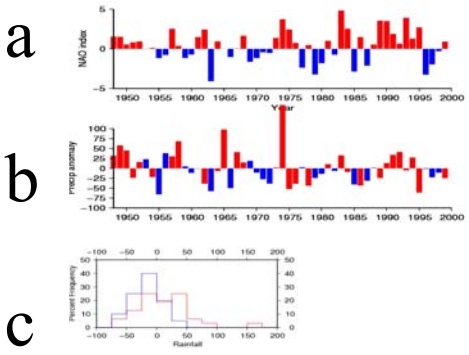

Figure 5. a) Time series of the January NAO index b) A time series of precipitation anomalies. NAO+ years are red and NAO- years are blue; c) Histogram of precipitation in NAO+ (red) and NAO- (blue) years.

In order to quantify these changes of distribution and estimate their significance, the rainfall was ranked and divided into five bins (quints). The numbers of NAO positive and NAO negative years falling into each quint is shown in Table 1. It can be seen that the strength of the relationship between the NAO and Middle Eastern rainfall varies within the rainy season, being strongest in November, December, January and February, and weak in October and March.

Table 1. Distribution of rainfall quintiles for NAO positive and negative years. Red bold numbers indicate that there are significantly more NAO-positive years than NAO-negative years in the rainiest quintile (assessed using the method described in Mason and Goddard 2001).

October

Quint	1	2	3	4	5
NAO -	5	4	4	6	4
NAO+	5	6	6	4	6

November

Quint	1	2	3	4	5
NAO -	5	6	6	6	**2**
NAO+	5	4	4	4	**8**

December

Quint	1	2	3	4	5
NAO -	6	6	5	6	**1**
NAO+	4	4	5	4	**9**

January

Quint	1	2	3	4	5
NAO -	4	5	6	4	**1**
NAO+	5	5	4	6	**9**

February

Quint	1	2	3	4	5
NAO -	7	4	4	4	**1**
NAO+	2	6	6	6	**9**

March

Quint	1	2	3	4	5
NAO -	4	6	1	3	4
NAO+	5	4	9	7	6

CONCLUSIONS

It has been shown that rainfall in the Middle East is highly variable on interannual time scales, and that this variability is driven to some extent by the large-scale atmospheric circulation. Although the linear correlation between the NAO and Middle Eastern rainfall is relatively low, the NAO has been shown to be significantly associated with the distribution of rainfall. In particular, the positive phase of the NAO is associated with increased variability, which is reflected by more extremely high rainfall years.

Future work will investigate the mechanism for the observed link between the NAO and Middle East rainfall, and will explore the implications for future and past climate variability in the Middle East.

REFERENCES

Wallace, J. M. and Gutzler, D. S. (1981) Teleconnections in the geopotential height field during the Northern Hemisphere Winter Monthly Weather Review 109: 784-812

Cullen, H. M., Kaplan, A., Arkin, P. A. and Demenocal, P. B. (2002) Impact of the North Atlantic Oscillation on Middle Eastern climate and streamflow Climatic Change 55: 315-338

Cullen, H. M. and Demenocal, P. B. (2000) North Atlantic influence on Trigris-Euphrates streamflow International Journal of Climatology 20: 853-863

Kalnay, E., Kanamitsu, M., Kistler, R., Collins, W., Deaven, D., Gandin, L., Iredell, M., Saha, S., White, G., Woollen, J., Zhu, Y., Chelliah, M., Ebisuzaki, W., Higgins, W., Janowiak, J., Mo, K. C., Ropelewski, C., Wang, J., Leetmaa, A., Reynolds, R., Jenne, R. and Joseph, D. (1996) The NCEP/NCAR 40-year reanalysis project Bulletin of the American Meteorological Society 77: 437-471

Jones, P. D., Jonsson, T. and Wheeler, D. (1997) Extension to the North Atlantic oscillation using early instrumental pressure observations from Gibraltar and south-west Iceland International Journal of Climatology 17: 1433-1450
Mason, S. J. and Goddard, L. (2001) Probabilistic Precipitation Anomalies Associated with ENSO Bulletin of the American Meteorological Society 81: 619-638

IMPACTS OF GLOBAL CLIMATE CHANGES ON LAKE ECOSYSTEMS IN TURKEY

Onur Kerimoglu[1], Temel Oguz[2], Meryem Beklioglu[1]

Middle East Technical University, Biology Department, 06531, Ankara, onurkerim@gmail.com
Middle East Technical University, Institute of Marine Sciences, PO Box 28, Erdemli

ABSTRACT

Impact of global climate change on lake ecosystems have not been explored widely. Most of Turkey being located in semi-dry to dry Mediterrenean climatic region, inland water bodies are prone to suffer major hydrological alterations initatiated through global climate change. In this study, we investigated impacts of global climate changes on the hydrological and ecological characteristics of the naturally formed large lakes including Lakes Beyşehir, Tuz and Van, and the Dam Lakes Keban and Atatürk in Turkey. First, the interannual and longer time scale variabilities of their hydrological parameters were obtained from the available data, and then their correlation with those of the hemi-spherical atmospheric teleconnection patterns were investigated. Correlations bertween the water level fluctuations of the study lakes and the North Atlantic Oscillation (NAO) were determined. The degree of correlations between natural climatic variabilities and local hydrological and ecological properties were disccussed for providing a basis for decision makers taking more appropriate measures for sustainable use of the resources at the face of global warming.

TENDENCIES OF STABLE ISOTOPIC CONTENT OF RAINFALL IN CENTRAL AND EASTERN MEDITERRANEAN.

Spyros P. Lykoudis[1], Athanassios A. Argiriou[2]

[1]National Observatory of Athens and University of Patras, Patras, Greece, slykoud@yahoo.com
[2]University of Patras, Patras, Greece

ABSTRACT

Rainfall is the basic source of surface and ground water bodies. The composition of rainfall in stable isotopes (^{18}O and ^{2}H) is now accepted as a major tool for tracking the origin of water bodies. The isotopic composition of rainfall is, however, highly variable and the accurate determination of the water budget at a given area requires a rather dense network of isotopic rainfall measurement stations, which does not exist at the major part of the globe. Many recent papers deal with the creation of gridded data maps of the isotopic composition of rainfall, using various statistical methods. These methods are combined in a way so as to minimize any interpolation errors yet they do not account for the possible influence of tendencies that might be present in the isotopic data. In the present work we investigate the existence of tendencies of the isotopic composition of rainfall in Central and Eastern Mediterranean (05° E - 45° E and 20° N – 55° N), based on the IAEA – GNIP database. We demonstrate that even though there may be some statistically significant trends, these do not form coherent spatial and temporal patterns. Consequently, the data can be used for the development of simplified models for estimating time series of isotopic characteristics of rainfall. Finally, we present some of these models and discuss the performance of their independent variables.

INTRODUCTION

Precipitation is the main source of surface as well as of ground water replenishment and its stable isotope composition has long been established as a valuable tool for the determination of the origin of a water body. A significant problem is the high variability of isotopic composition that results from its strong dependence on the meteorological conditions prevailing along the course of an air mass from the time of its formation till the time when this mass yields precipitation. This means that in order to obtain adequate information regarding the isotopic signature of the waters that form the input of the hydrological budget of an area, a dense network of isotopic precipitation measurements would be necessary, but no such network exists today, at least in the largest part of the globe.

An obvious solution is the use of models to estimate the isotopic composition of precipitation with a spatial resolution higher than that offered by the existing measurement network. Several recent studies have dealt with the generation of maps and gridded data sets of the isotopic composition of precipitation using a combination of statistical methods so as to minimize interpolation errors [1], [2], [3], [4], [5].

The procedure for creating these gridded data starts with the development of an empirical model that calculates the isotopic composition from other available data, such as meteorological, that are selected to be the independent parameters. Then the residuals,

calculated as the difference between isotopic model estimations and observations [3], [4], [5], or even the measurements themselves [2], [6], are used to generate a grid by applying interpolation methods such as the objective analysis [7], triangulation, and kriging. Finally, using the gridded independent parameters, the isotopic composition is calculated at each grid point by the empirical model, and to this result the gridded residual value is added to yield the final estimation.

Geographical variables such as latitude and altitude, well correlated to the variation of air temperature as well as other meteorological parameters, have been long recognized as factors affecting the isotopic composition of precipitation as well [8], [9]. These geographical variables are available in very high spatial resolution, becoming thus ideal candidates for independent parameters in empirical isotopic models. An improvement of such models is to include the meteorological parameters as variables [6].

Isotopic mapping efforts so far concentrated on climatologies, i.e. on average values, long term or not. These climatologies may be monthly, seasonal or even annual, and can refer to arithmetic or weighted means. In order to improve the density of the available measurement network it is commonplace to use stations even with just one year of isotopic data, regardless of the time period these measurements refer to. Spatial data quality considerations have clearly overcome temporal ones [4]. The use of mean values improves to a certain extent the lack of temporal homogeneity of the data, under some conditions though. More specifically, should there exist trends in the isotopic composition of precipitation then mean values calculated from data referring to different time periods are, by no means, directly comparable. In order to obtain comparable mean values one should either use data of the same time period from all stations, or to compensate for the contribution of the observed trends. Both approaches allow for significant errors for stations with limited time series, probably comparable to those introduced by the use of inadequate climatologies.

From another point of view, the empirical models are based solely on parameters referring to the place where precipitation occurs. The lack of any reference to the conditions pertaining to the place of origin or along the trajectory of the water vapor, suggests that the contribution of these parameters remains unchanged over the time period covered by the model. This means that there are no inter-annual variations either of the temperature of the water bodies from which the water vapor originates, or of the atmospheric circulations affecting the various areas, a clearly invalid assumption.

A possible alternative is the generation of gridded data time series. The simplest approach would be to introduce time (year) as an independent variable in the empirical isotopic models while, at a higher level, time series of gridded meteorological data along with circulation indices could be used. Using time series instead of climatologies should provide useful information to the mechanisms that shape the spatial and temporal distribution of the isotopic composition of precipitation.

This work focuses on the detection of possible trends in the isotopic composition of precipitation across the Central and Eastern Mediterranean, an important area from the hydrological and meteorological point of view. Based on these findings, some simple empirical models for estimating isotopic data time series are developed and assessed. In order

to smooth out any abrupt short-term variations, monthly data were aggregated, according to four calendar seasons and, according to the rainfall regime, into a wet and a dry period. The categories of this second aggregation were selected so as to reflect the rainfall regime of the majority of the area under study.

DATA – INITIAL PROCESSING

The main data source was the ISOHIS-GNIP database (version 12/2005) that apart from the stable isotope data contains all the necessary meteorological data (temperature, precipitation amount and vapor pressure) as well. The data used cover the area between 20°N–55°N latitude and 05°E-45°E longitude. Data from the works of d'Alessandro [10] and Kita [11] were also included in the previously mentioned database. Most data refer to monthly values, whereas some recent data refer to precipitation episodes. All data were adjusted so as to refer to standard monthly periods.

In all, 173 stations contained $\delta^{18}O$ data (15316 records) and 155 stations had data for $\delta^{2}H$ (12883 records). In order to avoid problems that could be caused by extreme values both during the detection of trends and during the development of the empirical models, all data were passed filtered by an outlier detection routine according to [12]:

$$abs(x_i - X_{50}) < f^*(X_{75} - X_{25}) \quad (1)$$

where x_i is the value of the examined variable X. The symbols X_{25}, X_{50}, and X_{75} denote the 25^{th}, 50^{th} (median) and 75^{th} percentiles of X. The parameter f is a dispersion factor equal to 4 [13]. Values not complying with equation (1) are considered as outliers and removed from the data set.

Table 1 presents the percentage of available data corresponding to each 5° ×5° area. The non-homogeneous geographical distribution of the available data is obvious. The whole Northern Balkans are not represented in the dataset, while Southern Russia and the Black Sea area have only a few stations. The same applies to the Northern African coast while inland North African stations are even fewer. On the contrary the coast of the Middle East and the northwestern part of the studied area have many stations operating for several decades.

Table 1. Percentage distribution of the available $\delta^{18}O$ data.

LON/LAT (°)	5	10	15	20	25	30	35	40	Total
55	5	2	0	0	0	0	0	0	7
50	8	29	7	4	1	0	0	0	48
45	3	9	13	0	0	0	0	0	25
40	0	0	1	0	1	0	3	1	6
35	0	2	0	0	0	3	3	0	9
30	0	0	0	0	1	1	3	0	5
25	0	0	0	0	0	0	0	0	0
Total	16	42	21	4	3	4	9	1	100

Despite the existence of significant gaps, the monthly distribution of the available data illustrates the climatic characteristics of the examined areas. Northern regions present a more or less homogeneous rainfall distribution throughout the year that gradually becomes diversified with drier summers occurring as one moves southward. The southernmost regions

present a monsoonal character with precipitation occurring mainly during the warm period. On the other hand, the western and eastern regions present relative homogeneous distribution of rainfall throughout the year, while at the central region, between 25°E and 35°E, there is an intense annual variation, with less precipitation occurring during summer. An overall assessment of the climatic characteristics of the regions based on the number of available data (precipitation samples) suggests that a definition of the period from April to September as dry is fairly representative of the southern regions while the northern regions do not have a dry period at all.

In order to create the seasonal time series it was deemed necessary to introduce some completeness criteria, thus avoiding the possibility of non-representative seasonal values to be included in the analysis. Obviously, these criteria had to be set in accordance to the season and the area under study. The area of interest was divided into three zones according to latitude: Zone 1 (25°N-30°N), Zone 2 (30°N–45°N) and Zone 3 (45°N–55°N) that have different seasonal characteristics. Table 2 presents a summary of the completeness criteria. Zone 3 has a uniform annual distribution of precipitation therefore all months are considered as equally possible to produce rain and thus represented in the dataset. An "at least 2/3" approach is adopted for this zone both in terms of the number of available monthly values and in terms of sampled precipitation amount ratio, that is the ratio of precipitation amount represented in the available isotopic sample of a given period to the total precipitation amount of that period. On the other hand the dry period of Zones 1 and 2 is allowed to have fewer monthly samples, but an increased sampled precipitation ratio is required.

Table 2. Completeness criteria: number of monthly samples, N, and sampled precipitation amount ratio, SPR, per period.

	Zone 3		**Zone 2**		**Zone 1**	
	N	**SPR**	**N**	**SPR**	**N**	**SPR**
4 seasons	>1	>66%	>=1	100%	>=1	100%
2 seasons	>4	>66%	Dry: >1 Wet: >4	Dry: >75% Wet: >66%	Dry: >1 Wet: >4	Dry: >75% Wet: >66%
Annual		>9	>66%	>90%	>5	>90%

After the application of the above criteria, seasonal and annual values of the isotopic parameters were calculated. Less than 10% of the originally available data were rejected by the quality control procedures.

Trend detection requires that the time series under investigation extend over a substantial number of years. Setting a minimum requirement of 9 years of data, leads to a reduction of the available stations down to 1/3 of their initial number. Only 57 stations had enough data for annual $\delta^{18}O$ trend testing, and 52 stations for $\delta^{2}H$. Similar figures apply for seasonal data set as well. Figure 1 presents the geographical distribution of the initially available stations as well as the stations eligible for trend detection according to the 9-year criterion.

Given that the available data are widely and inconsistently spread across the period from 1960 to 2002, the estimated trends are not comparable, at least in a spatial context. Thus it was deemed as useful to estimate trends corresponding to a period common for all the selected stations. This was 1981-2000, so as to provide as recent information as possible, while at the

same time, several stations with sparse yet quite long time series would be eliminated from the analysis, e.g. there were stations measuring back in the '60s or'70s that re-started their operation after 2000. In order to avoid over-elimination of stations, a 5-year window at both ends of the period was allowed. This means that selected stations should have data at least for the period 1986 – 1995.

Also, since northern stations were the majority in the selection list threatening to mask our intention for an assessment focusing on the Mediterranean, all stations above 50°N were also eliminated except of that of Krakow (50.07°N), being on the suggested limit. This reduced the number of examined stations to 22 and 21 for annual $\delta^{18}O$ and $\delta^{2}H$ respectively. Eastern Mediterranean is rather poorly represented in this data set (Figure 1).

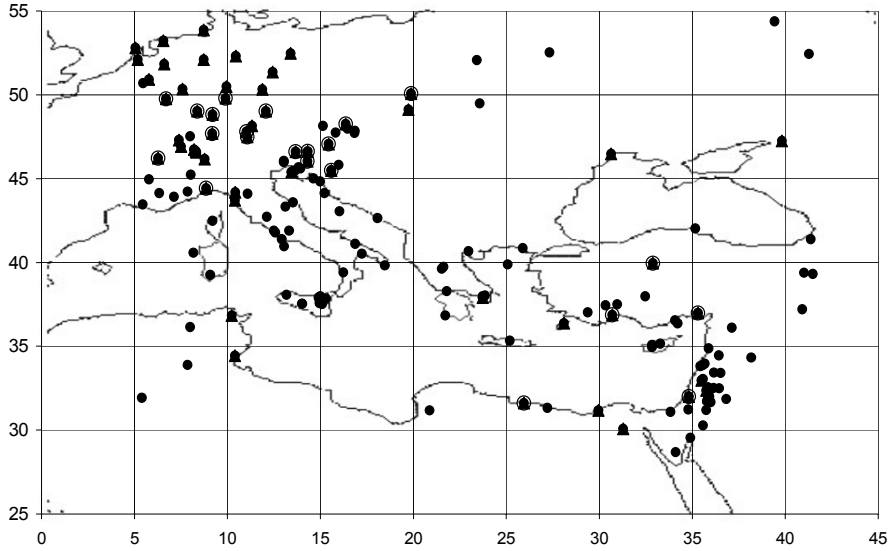

Figure 1. Stations with annual isotopic composition of precipitation: initially available (●), with at least 9 years of data (▲), and with enough data for the common period 1981-2000 (○).

TREND DETECTION

Two methodologies were used for trend detection. The maximum likelihood estimation was used in order to investigate the existence of linear trends in the isotopic compositions of stations having at least 9 years of data. All seasonal and annual datasets were tested. Furthermore, 2nd and 3rd order trends were also examined but the resulting polynomial fits were not statistically different from the corresponding linear ones. Hence, the common period time series (1981-2000) where tested only for linear trends. In addition the meteorological parameters were also tested. Finally, the common period time series were tested for the existence of trends using the nonparametric Mann-Kendall test [14]. Table 3 presents the percentage of statistically significant trends for each parameter and period examined.

Trends appear to be more significant during the transitional seasons, and on an annual basis rather than during winter and summer. Furthermore, significant trends in $\delta^{18}O$ are not consistently associated with significant trends in $\delta^{2}H$. The stations with 9 or more years of data present high rates (57-100%) of concurrently significant trends when four season data are considered, except for autumn (SON) when there is no concurrency at all. This rate, though,

falls when 2 seasons are considered (37 and 50%). The common period (1981-2000) data set on the other hand presents markedly lower concurrency rates either for four season data when only spring (MAM) has 100% and the other three have no concurrency, or for the two seasons (33 and 0%). Significant trend concurrency rates between isotopic data and temperature are very low, due to the fact that significant temperature trends are rather common while significant isotopic trends are relatively scarce.

Table 3. Percentage of statistically significant maximum likelihood (ML) and Mann-Kendall (MK) trends for the time series of the stations with a minimum of 9 years of data (9yr) and the common period (1981-2000).

	Significance Level **0.05**									***Significance Level*** **0.10**								
	δ^2H			**$\delta^{18}O$**			**d**			**δ^2H**			**$\delta^{18}O$**			**d**		
	9yr	1981-2000		9yr	1981-2000		9yr	1981-2000		9yr	1981-2000		9yr	1981-2000		9yr	1981-2000	
	ML	ML	MK	ML	ML	MK	ML	ML	MK	ML	ML	MK	ML	ML	MK	ML	ML	MK
Annual	13	10	18	19	14	14	19	14	5	19	19	18	26	23	18	25	38	18
DJF	7	0	0	13	9	4	21	18	14	9	0	9	16	9	4	26	27	18
MAM	16	14	9	18	17	9	19	9	5	26	14	13	31	22	22	25	9	9
JJA	7	5	0	8	0	0	24	10	5	9	10	10	20	0	5	35	25	10
SON	4	9	4	5	4	13	15	18	18	8	9	9	10	17	17	26	23	23
O-M	12	18	9	16	9	13	24	27	18	14	23	17	30	22	13	28	32	27
A-S	12	0	0	11	9	9	16	5	0	16	9	18	27	17	18	24	14	0

Setting the statistical significance aside, the estimated trends of $\delta^{18}O$ and δ^2H are very well correlated either on a seasonal or on an annual basis, irrespectively of the dataset used: the calculated correlation coefficient (r^2) is higher than 87% for the common period data set (1981-2000), for the four seasons period and also for the wet period trends. The correlation for the dry period is lower (r^2=70%), leading to an annual correlation with an r^2=79% (Figure 2a).

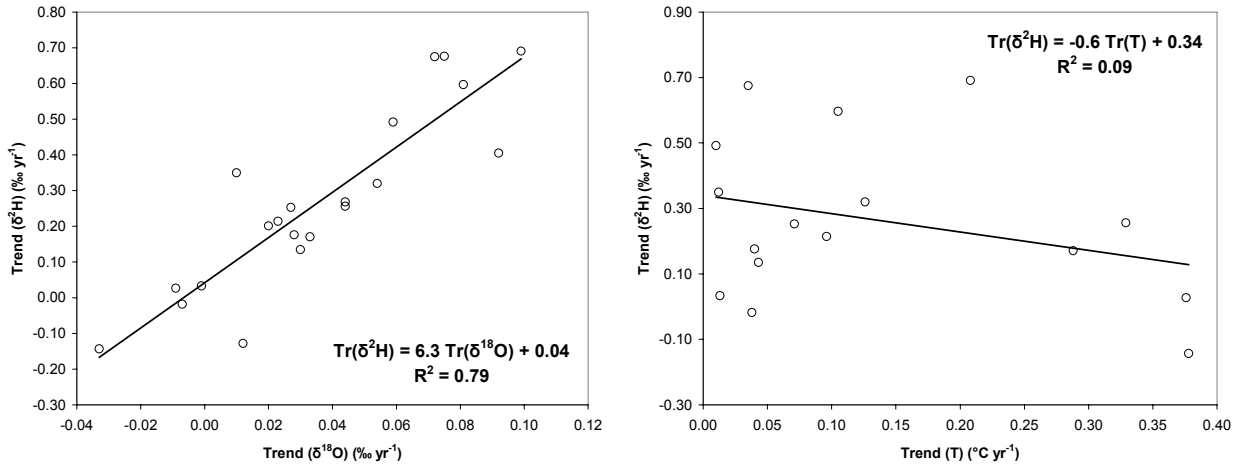

(a) (b)

Figure 2. Correlation between: (a) δ^2H and $\delta^{18}O$ trends and (b) δ^2H and air temperature (T) trends, for the annual data of the common period (1981-2000).

On the contrary neither air temperature nor precipitation trends seem to be correlated to the isotopic composition trends on any temporal scale (Figure 2b). This means that widely observed and well-documented temperature and/or precipitation trends are not necessarily accompanied or reflected to isotopic composition trends.

So far the estimated isotopic composition trends, even though well correlated between them, have been found to be spuriously significant and uncorrelated with other well established trends. Another point worthy of investigation would be the presence of possible organized spatial patterns. As mentioned before only data from the common period (1981-2000) might be considered comparable within this context, since data from the 9-year data set correspond to widely varying time periods. Figure 3 presents maps of the estimated linear trends of $\delta^{18}O$.

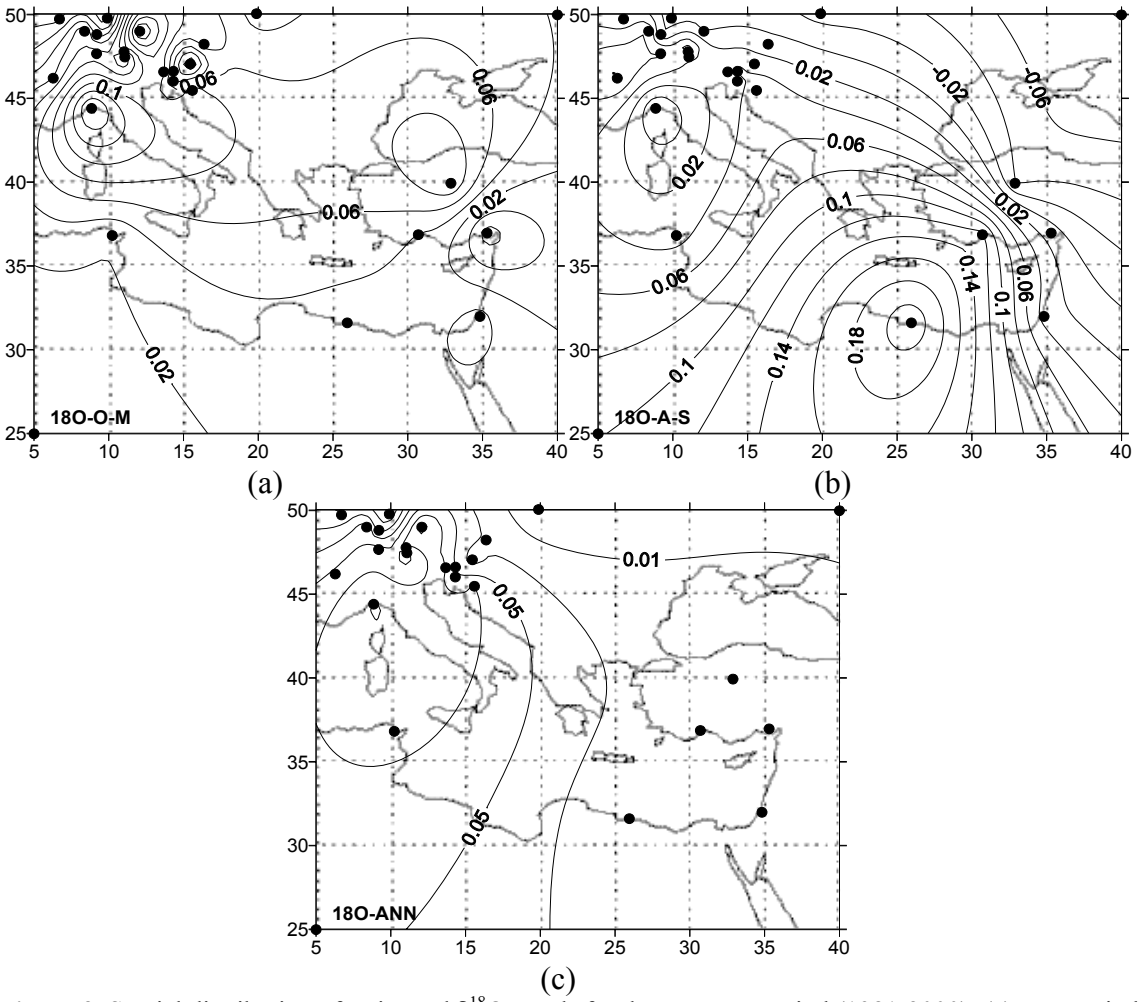

Figure 3. Spatial distribution of estimated $\delta^{18}O$ trends for the common period (1981-2000): (a) Wet period (October-March), (b) Dry period (April-September) & (c) Annual.

MODELS

As discussed in the introduction section of this paper, the most recent methodologies for generating an isotopic gridded set is to develop a model able to estimate isotopic parameters

from other, known and already available in gridded form parameters, such as latitude, longitude, altitude, temperature, precipitation amount etc.

All the relevant works so far have been using climatologies, monthly, seasonal or annual, yielding very high correlation coefficients with relatively simple models [3], [4] such as:

$$\delta^{18}O = \alpha_0 + \alpha_1 * Lat + \alpha_2 * Lat^2 + \alpha_3 * Alt \quad (2)$$

with Lat the latitude and Alt the altitude of the station.

In this work an attempt was made to obtain simple models that could produce time series of the isotopic parameters. In other works these models would either include time as an independent parameter or implicitly, using as independent variables time series instead of climatologies.

Three models were fitted to the data:

$$\begin{aligned} M_1 &: \delta = f(\text{Lat, Lon, Alt, Year}) \\ M_2 &: \delta = f(\text{Lat, Lon, Alt, Prec, T}) \\ M_3 &: \delta = f(\text{Lat, Lon, Alt, Prec, T, Vp}) \end{aligned} \quad (3)$$

with Lon the longitude, Prec the precipitation amount, T the air temperature, Vp the vapor pressure for the respective period, and Year the year at which each observation corresponds. All independent variables, except of "Year", are included in the models as mononyms up to 3rd order and stepwise linear regression was used to sort out the statistically significant parameters in each case.

All data that passed the quality control procedure were used for the development of the models. Table 4 presents the obtained correlation coefficients, r^2-adj. The δ^2H correlations are slightly better than those of $\delta^{18}O$, while deuterium excess, d, is clearly more difficult to be modeled using geographical and meteorological parameters. The model performance follows the annual cycle of temperature and, probably of precipitations with a maximum performance during winter and a minimum during summer.

Table 4. Correlation coefficients (r^2-adj) for isotopic composition models.

R^2-adj		**DJF**	**MAM**	**JJA**	**SON**	**O-M**	**A-S**	**Annual**
M_1	**$\delta^{18}O$**	0.67	0.60	0.52	0.64	0.63	0.61	0.71
	δ^2H	0.72	0.61	0.52	0.67	0.77	0.68	0.78
	D	0.51	0.34	0.11	0.26	0.48	0.14	0.53
M_2	**$\delta^{18}O$**	0.69	0.63	0.61	0.68	0.62	0.69	0.71
	δ^2H	0.74	0.66	0.56	0.68	0.77	0.68	0.78
	D	0.53	0.37	0.16	0.32	0.54	0.16	0.61
M_3	**$\delta^{18}O$**	0.71	0.67	0.61	0.66	0.74	0.67	0.74
	δ^2H	0.75	0.65	0.56	0.65	0.78	0.69	0.78
	D	0.55	0.37	0.16	0.32	0.54	0.16	0.59

The models performed comparably well for any specific parameter and period. In order to identify the dominating input parameters, the occurrence percentage of each parameter in the seven realizations of each model were computed. The results are presented in Table 5, where a value of e.g. 57% of the cases for Alt in model M_1 for $\delta^{18}O$ means that Alt is significant parameter in 4 out of 7 (4 seasons+2 periods + Annual) realizations of the M_1 model for $\delta^{18}O$. Altitude and latitude are very important parameters for isotopic variables. Longitude and Year follow but not for deuterium excess. Finally the air temperature, T, and vapor pressure, Vp, seem to be important only for $\delta^{18}O$, while precipitation steps in when Vp is not used.

Table 5. Parameter occurrence percentage for models M_1, M_2 and M_3. Cases with more than 5 occurrences out of 7 are in bold.

		Alt	**Alt^2**	**Alt^3**	**Lat**	**Lat^2**	**Lat^3**	**Lon**	**Lon^2**	**Lon^3**	**Year**	**Pr**	**Pr^2**	**Pr^3**	**T**	**T^2**	**T^3**	**Vp**	**Vp^2**	**Vp^3**
M_1	**$\delta^{18}O$**	**100**	**100**	57	**100**	57	57	57	14	14	**100**									
	δ^2H	**100**	**100**	**100**	**100**	**86**	**86**	**86**	**86**	**86**	**86**									
	D	**100**	57	**71**	**100**	29	29	14	57	43	57									
M_2	**$\delta^{18}O$**	**100**	**86**	**71**	**100**	**86**	**86**	**86**	0	43		43	57	**71**	**71**	**71**	43			
	δ^2H	**100**	**100**	**86**	**86**	**100**	**86**	**100**	**100**	**71**		**86**	57	57	**71**	57	57			
	D	**86**	43	43	**100**	57	57	**71**	**100**	**71**		**86**	**86**	29	29	29	**71**			
M_3	**$\delta^{18}O$**	**100**	**100**	57	**86**	57	43	57	**71**	14		**86**	**71**	43	**71**	57	57	**86**	**71**	**71**
	δ^2H	**86**	**71**	**71**	**100**	**71**	**71**	**86**	**100**	**86**		57	57	29	29	43	57	43	14	14
	D	29	14	14	43	29	29	29	43	29		29	43	29	0	0	14	14	0	0

CONCLUSIONS

In this paper we investigated the existence of tendencies of the isotopic composition of rainfall based on the IAEA – GNIP database for stations located in the Central and Eastern Mediterranean (05° E - 45° E and 20° N – 55° N). Our analysis showed that statistically significant tendencies occur more often during spring and autumn. The 80% of the isotopic tendencies are positive, while less than 20% are statistically significant. These percentages change from season to season and also vary depending on the time period covered by the analysis. One or two stations only present temporally consistent statistically significant tendencies.

The observed tendencies for $\delta^{18}O$ correlate well with the tendencies of δ^2H denoting their common dependence on the weather and other conditions. However, statistically significant tendencies for $\delta^{18}O$ often do not coincidewith statistically significant tendencies of δ^2H of the same station, denoting their different degree of dependence on the above-mentioned conditions. This is confirmed by the higher dependence between the $\delta^{18}O$ and δ^2H tendency, when this is calculated on a four-season basis rather on an annual basis. The spatial distribution of the tendencies shows a seasonal preference. During the wet period we observe relatively higher tendencies in the northwestern stations, while during the dry period a maximum occurs in the southeast.

The fact that the tendencies of the isotopic values are not statistically significant in most of the cases and also that in the few cases when such statistical significance is observed the tendencies do not show any temporal and spatial consistency or at least defined patterns, supports our argument that we can calculate gridded climatologies (i.e. long term averages) from short and of unequal duration time series, which in addition may not refer to the same

time period. This method however is not error free but the errors and uncertainties introduced are not expected to be higher that those introduced by the interpolation methods.
Concerning the models, the introduction of time as an independent parameter is a necessary step if we want to generate time series (instead of climatologies) of gridded data, which constitute a much better basis for comparison with the estimations emanating from global or regional climatic models compared to climatologies. Furthermore, the gridded time series would allow for a much better link between the isotopic content of rainfall and the atmospheric circulation patterns and would enhance the performance of hydrological applications.

Acknowledgements
The authors would like to thank the International Atomic Energy Agency (I.A.E.A.), Dept. of Nuclear Sciences and Applications, Isotope Hydrology Section, for providing the GNIP-ISOHIS data.

REFERENCES

[1] IAEA, GNIP Maps and Animations, International Atomic Energy Agency, Vienna. Accessible at http://isohis.iaea.org/, 2001.
[2] Birks S.J., Gibson J.J., Gourcy L., Aggarwal P. K., & Edwards T.W.D., Maps and animations offer new opportunities for studying the global water cycle, *Eos Transactions, AGU Electronic Supplement*, 83, 37, 2002 (http://www.agu.org/eos_elec/020082e.html)
[3] Bowen G.J., & Wilkinson B., Spatial distribution of delta O-18 in meteoric precipitation, *Geology*, 30, 4, 315-318, 2002.
[4] Bowen G.J., & Revenaugh J., Interpolating the isotopic composition of modern meteoric precipitation, *Water Resources Research*, 39, 10, art. 1299, 2003.
[5] Meehan T.D., Giermakowski T.J., & Cryan P.M., GIS model of stable hydrogen isotope ratios in North American growing-season precipitation for use in animal movement studies, *Isotopes in Environmental and Health Studies*, 40,4, 291-300, 2004
[6] Liebminger A., Haberhauer G., Varmuza K., Papesch W., & Heiss G., Modeling the oxygen 18 concentration in precipitation with ambient climatic and geographic parameters, *Geophysical Research Letters*, 33, 5, L05808, 2006
[7] Cressman G.P., An operational objective analysis system, *Monthly Weather Review*, 87, 10, 367-374, 1959
[8] Dansgaard W., Stable isotopes in precipitation, *Tellus*, 16, 4, 436-468, 1964.
[9] Siegenthaler U., & Oeschger H., Correlation of 18O in precipitation with temperature and altitude, *Nature*, 285, 314-317, 1980.
[10] d' Alessandro W., Federico C., Longo M., & Parello F., Oxygen isotope composition of natural waters in the Mt. Etna area, *J. of Hydrology*, 296, 1-4, 282-299, 2004.
[11] Kita I., Sato T., Kase Y., & Mitropoulos P., Neutral rains at Athens, Greece: A natural safeguard against acidification of rains, *Science of the Total Environment*, 327, 1, 285-294, 2004.
[12] Beck C., Grieser J., & Rudolf B., *A New Monthly Precipitation Climatology for the Global Land Areas for the Period 1951 to 2000*, DWD, Klimastatusbericht 2004, 2005.

[13] Eischeid J.K., Baker C.B., Karl T.R. & Diaz H.F., The quality control of long-term climatological data using objective data analysis, *J. of Applied Meteorology*, 34, 2787-2795, 1995.
[14] Libiseller C., MULTMK/PARTMK A Program for the Computation of Multivariate and Partial Mann-Kendall Test, downloaded on 17/07/2006 from: http://www.mai.liu.se/~cllib/welcome/PMKtest.html2002, 2002

LARGE-SCALE CHANGES IN PRECIPITATION AND RUNOFF IN THE MIDDLE EAST UNDER CLIMATE CHANGE – ENSEMBLE CLIMATE MODEL PREDICTIONS AND UNCERTAINTIES.

Debbie L Hemming

Hadley Centre for Climate Prediction and Research, Met Office. Fitzroy Road. Exeter. U.K. EX1 3PB.
debbie.hemming@metoffice.gov.uk

ABSTRACT

This paper examines the large-scale changes in modelled precipitation and runoff across the Middle-East region that occur in response to doubling atmospheric CO_2 concentration from 389ppm (control) to 778ppm (doubled CO_2). Results are compared from an ensemble of 81 model runs made using the Hadley Centre's computationally efficient Global Climate Model (GCM), HadSM3. Each ensemble member was run under the control and doubled CO_2 concentrations, with different combinations of plausible values for 34 key model parameters. This allows the uncertainties in future climate change projections that are associated with model parameterisations to be examined.

The Middle-East region as a whole shows ensemble-average increases in precipitation (11.6 mm/yr, 5.6 %) and runoff (7.8 mm/yr, 19 %) under doubled CO_2 concentrations. Over 90 % of the ensemble members show increases in the regional average run off: precipitation ratio, which suggests that more precipitation would be directed into runoff under doubled CO_2. However, these ensemble average values are significantly smaller than the range in values across the ensemble, which vary between -117.7 mm/yr and 138.8 mm/yr for precipitation and -8.1 mm/yr and 68 mm/yr for runoff, with standard deviations of 36.9 mm/yr and 11.5 mm/yr for precipitation and runoff, respectively.

Spatially, precipitation and runoff changes vary significantly between the control and doubled CO_2 runs. Decreases of up to -120 mm/yr are noted in the north-west of the region (northern Syria, Turkey and Greece), and increases of up to 80 mm/yr in are noted in southern areas; western Yemen, Eritrea, southern Sudan and northern Ethiopia. For some countries, the standard deviation across all ensemble members is smaller than the ensemble-average changes. This is most prominent for Turkey, where the ensemble-average precipitation and runoff are projected to decrease by -83.5 mm/yr and -40.1 mm/yr, and the ensemble standard deviations are 44.9 mm/yr and 28.1 mm/yr, respectively. The relatively large change in the ratio of runoff to precipitation in Turkey indicates that a greater proportion of precipitation is translated to runoff under doubled CO_2 conditions.

While considerable uncertainties have been noted in the projections of precipitation and runoff across the Middle-East region under doubled CO_2, in some locations, such as Turkey, the direction of change is more certain than in most other locations where the ensemble of model simulations span a wide range of positive and negative changes.

INTRODUCTION

Climate changes could have large impacts on freshwater availability, particularly in regions that already experience water stress [1]. Many parts of the Middle-East are vulnerable to water shortages under existing climate conditions, and understanding how this could change in future climates is of key socio-economic and political importance in this region.

Future climate model projections of precipitation and runoff changes in the Middle-East region under climate change scenarios have shown significant variation [2]. In order to adequately assess the possible impacts and national vulnerabilities of climate changes, full consideration of the uncertainties in climate models is of vital importance. One of the key uncertainties in these models relates to the choice of parameterisations.

In this paper, a large ensemble of global climate model (GCM) simulations, where each ensemble member has been forced by different but plausible parameterisations, is used to assess the potential impact of doubling atmospheric CO_2 concentration on precipitation and runoff in the Middle-East region and explore the uncertainties associated with model parameterisations.

METHODS

Model description

Model runs were conducted using a computationally efficient GCM, HadSM3, which consists of a fully-dynamic atmospheric GCM, HadAM3 [3], coupled to a 50m mixed layer ocean model. It has a regular horizontal grid resolution of 2.5° latitude by 3.75° longitude, 19 vertical levels, and is run on a 30 minute time-step. While HadSM3 retains the full atmospheric complexity, explicit ocean dynamics are not included in the simplified ocean model, instead spatial and seasonal variations in ocean heat transport are prescribed [4]. Ocean circulation and associated biogeochemical feedbacks to the atmosphere are therefore not accounted for. Land surface processes are modelled interactively using the Met Office Surface Exchange Scheme (MOSES) [5]. This utilises leaf-level physiological models for C_3 and C_4 plants to account for exchanges of carbon and water vapour by photosynthesis and stomatal conductance [6]. Soil respiration rate is assumed to double with every 10 K temperature increase [7], and a prescribed observation field describes the terrestrial vegetation distribution [8].

As with all GCMs, HadSM3 requires the specification of parameters which constrain those processes that cannot be modelled explicitly. For standard model runs, specific values for parameters are assigned according to suitable literature, and the results are verified against contemporary climatology. However, a range of plausible settings exist for all parameters, and these would likely result in different climate model results. To test the uncertainties involved in assigning specific parameter values, an ensemble of model runs were performed, each with slightly perturbed parameter settings.

Generation of ensemble

Experts were asked to select 34 parameters, and their plausible value ranges, which would encompass the major uncertainties in model processes and parameterisations (Table 1).

Using different combinations of parameter values, an ensemble of 81 model runs was generated. Two runs were made for each member, one with the 'present day' atmospheric CO_2 concentration (control) where CO_2 was fixed at 389 ppmv, and the other with doubled CO_2 (double CO_2). All runs were continued for at least 20 model years after equilibrium had been reached (see [9] for details), and the average values over a 20-year equilibrium period were used in the following analyses.

Table 1. Details of parameters perturbed in ensemble.

Scheme/Parameter	Description/Process Affected	Range of values	Units
Large Scale Cloud			
V_{fi}	**Ice particle fall speed**	0.5 to 2.0	ms^{-1}
C_t	**Cloud droplet to rain conversion rate**	$5.0x10^{-5}$ to $4.0x10^{-4}$	s^{-1}
C_w land	**Cloud droplet to rain conversion threshold**	$1.0x10^{-4}$ to $2.0x10^{-3}$	kgm^{-3}
C_w sea	**Cloud droplet to rain conversion threshold**	$2.0x10^{-5}$ to $5.0x10^{-4}$	kgm^{-3}
Rh_{crit}	**Threshold relative humidity for cloud formation**	0, 1	
Rhparam	**Flow dependent Rh_{crit}** Rh_{crit} in terms of local variance of grid box average Rh	0, 1	
Eacfbl	**Cloud fraction at saturation in boundary layer** Calculation of cloud cover in layers 5 or below	0.5 to 0.8	
Eacftrp	**Cloud fraction at saturation in free troposphere** Calculation of cloud cover in layers 8 to 19	0.5 to 0.7	
Vertcld	**Vertical gradient of cloud water in grid box** Influence of vertical cloud water gradients on cloud cover	0, 1	
Convection			
Ent	**Entrainment rate coefficient** Rate of mixing between environment air & convective plume	0.6 to 9.0	
Cape	**Time scale for destruction of CAPE** Intensity of convective mass flux	1 to 4	
Cnv_upd	**Convective anvils: updraft factor** Fraction of convective cloud containing updraft	0.1 to 1.0	
Anvil	**Convective anvils: shape factor** Shape of convective cloud	1 to 3	
Sea ice			
MinSIA	**Sea ice albedo at 0°C** Dependence of sea ice albedo on temperature	0.65 to 0.50	
Ice_tr	**Sea ice minimum temperature** For calculating sea ice albedo	-10 to -2	°C
Oi_diff	**Ocean-ice diffusion coefficient** Ocean to ice heat transfer	$2.5x10^{-5}$ to $3.75x10^{-4}$	m^2s^{-1}
Radiation			
Icesize	**Ice particle size** Effective radius of cloud ice spheres	25 to 40	μm
S_sphsw, C_sphsw, S_sphlw, C_sphlw	**Non-spherical ice particles** Short and long wave radiation properties which take account of non-spherical ice particles	0, 1	
Sw_absn	**Shortwave water vapour absorption** Shortwave absorption due to self-broadened continuum of water vapour	0, 1	
Dynamics			
Dyndel	**Order of diffusion operator** Spatial diffusive damping of heat, momentum & moisture	4, 6	
Dyndiff	**Diffusion e-folding time** Diffusion coefficients for heat, momentum & moisture	6, 12, 24	hrs
Gw_lev	**Starting level for gravity wave drag** Lowest model level at which drag is applied	3, 4, 5	
K_gwd	**Surface gravity wave constant** Magnitude of hydrostatic surface gravity wave stress	$1.0x10^4$, $1.5x10^4$, $2.0x10^4$	m
K_lee	**Trapped lee wave constant** Magnitude of non-hydrostatic surface gravity wave stress	$1.5x10^5$, $2.25x10^5$, $3.0x10^5$	$m^{-3/2}$
Land surface			
Canopy	**Surface-canopy energy exchange** Effect of vegetation canopy on surface energy balance	0, 1	
Soillev	**No. of soil levels accessed for evaoptranspiration** Varies with rooting depths	1, 2, 3, 4	
F_rough	**Forest roughness lengths** Surface fluxes over areas containing forest	0, 1, 2, 3	m
Boundary layer			
Charnoc	**Charnock constant** Roughness lengths and surface fluxes over sea	0.012 to 0.016	
Cnv_rl	**Free convective roughness length over sea** Surface fluxes over tropical oceans	$2.0x10^{-4}$ to $5.0x10^{-3}$	m
Flux_g0	**Boundary layer flux profile parameter** Stability dependence of turbulent mixing coefficients	5 to 20	
Lambda	**Asymptotic neutral mixing length** Calculation of turbulent mixing coefficients	0.05 to 0.5	

RESULTS AND DISCUSSION

Middle-East regional averages

The average precipitation (over land) and total runoff of all ensemble members increase by an average of 11.6 mm/yr and 7.8 mm/yr, respectively, across the whole Middle-East region (Table 2). While the volume of precipitation increase across the region is larger than that of runoff, the percentage change in runoff is over 3 times larger (19%) than the corresponding change in runoff (5.6%). Consequently, the average ratio of runoff to precipitation, which indicates the proportion of precipitation that translates directly into runoff, increases from 0.18 for the control climate runs to 0.2 for the doubled CO_2 runs. This is comparable to other runoff:precipitation ratios noted in arid and semi-arid regions [10, 11].

Table 2. Average precipitation (over land) and runoff (total, surface and sub-surface) across the Middle-East region under Control and Double CO_2 conditions, and the Change (absolute and %) between these two. The Standard Deviation (SD) of the changes noted across ensemble members are shown.

	Control (mm/yr)	Double CO_2 (mm/yr)	Change (mm/yr)	Change (%)	SD Change (mm/yr)	SD Change (%)
Precipitation	228.5	240.1	11.6	5.6	36.9	14.4
Total Runoff	40.8	48.5	7.8	19.0	11.5	24.3

The range of regional average precipitation and runoff changes recorded across the ensemble is represented by the standard deviations shown in Table 2. It is clear from these that for precipitation and total runoff the ensemble SD's are larger than the ensemble average changes. In both cases, the full range of values covers positive and negative changes; between -117.7 mm/yr and 138.8 mm/yr for precipitation and -8.1 mm/yr and 68 mm/yr for runoff.

Figures 1a and b show the frequency distributions for the regional average changes in precipitation and runoff of all ensemble members. Although the ensemble average precipitation and runoff have both increased, it is also clear from these figures that the uncertainty from different plausible parameterisations is considerably larger than the average changes. Importantly, the uncertainty ranges for both precipitation and runoff span positive and negative changes, making it impossible to specify the likely direction of future changes in average precipitation and runoff across the whole Middle-East region.

A frequency distribution of changes in the regional average ratios of runoff to precipitation for all ensemble members (Figure 2) shows that doubling CO_2 results in an increase in this ratio for 94% of the ensemble members. Although the uncertainty range is again large, between -0.04 and 0.12, this indicates that for most model parameterisations climate changes associated with doubling CO_2 will result in a larger portion of precipitation directed into runoff across the region. In a similar study, increases of 0.023 were noted in the modelled global average runoff:precipitation ratio under doubled CO_2 [12]. In that study, about 60% of the increase in this ratio was attributed to the direct impact of doubled CO_2 acting to reduce stomatal conductance and plant transpiration (see [6]), and therefore increase soil moisture and runoff. The remaining increase in this ratio was attributed to other influences of climate change, possibly more intense precipitation exceeding the infiltration rate.

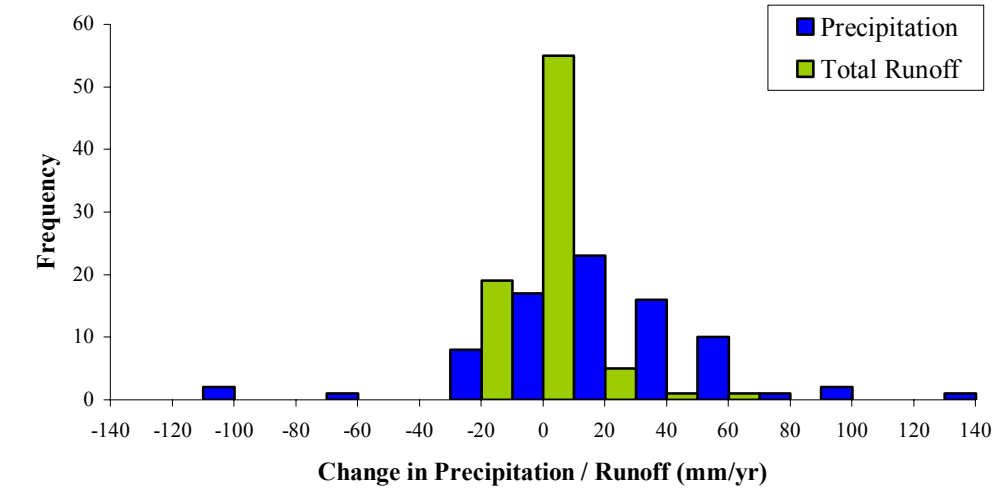

a)

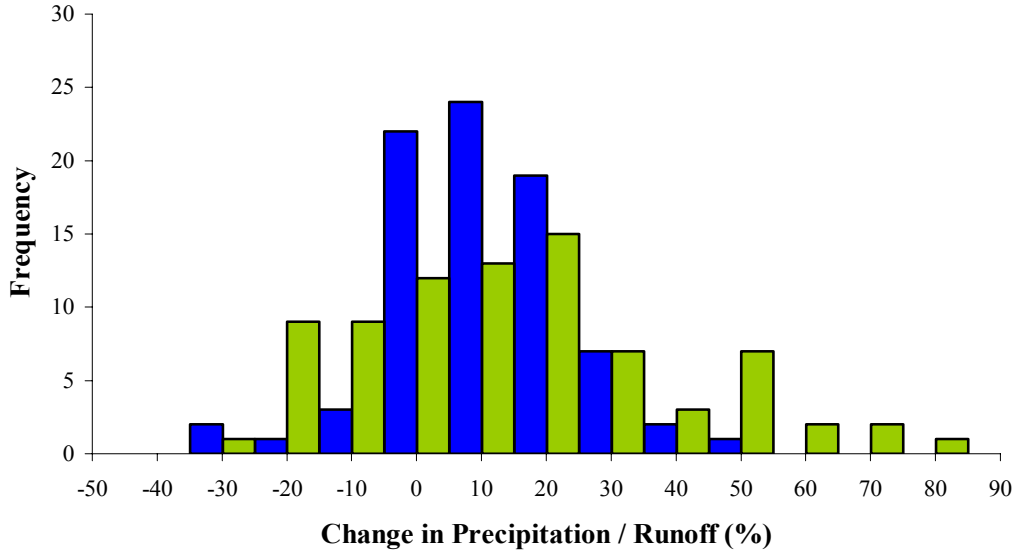

b)

Figure 1. Changes in a) volume and b) % Precipitation and Total Runoff in the Middle East region between the control and doubled CO_2 runs of the full 81 member ensemble.

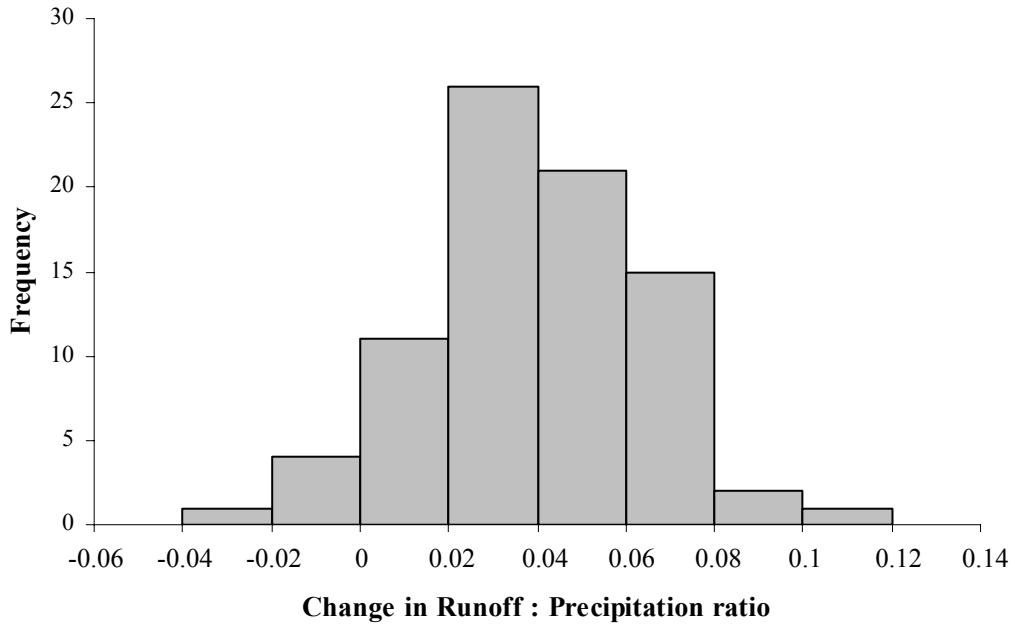

Figure 2. Changes in the Runoff : Precipitation ratios for the whole Middle East region between the control and doubled CO_2 runs of the full 81 member ensemble.

Spatial variations

Figures 3a and b show the spatial changes in average precipitation and runoff over the Middle-East region under doubled CO_2. It is clear from these that there are large spatial differences in the projected changes in precipitation and runoff across the region, although as would be expected, these spatial trends are similar for precipitation and runoff. Both of these parameters show decreases in a band spreading from Turkey in the north-west of the region, through Syria, northern Iraq, Iran and Afghanistan in the east of the region.

The most intense decreases in precipitation and runoff, of up to -120 mm/yr, are projected for the north-west of the region (northern Syria, Turkey and Greece), and the main increases are projected in the south of the region; encompassing most of the Arabian peninsula, Egypt, Sudan, Eritrea and northern Ethiopia. The largest increases, of up to 80 mm/yr, occur in western Yemen, Eritrea, southern Sudan and northern Ethiopia, and smaller increases, less than 40 mm/yr, are noted in the north-east of the region.

Figure 4 summarises the country average changes in precipitation and runoff between the control and doubled CO_2 runs, and the ensemble SD's for each country. As with the regional averages (Table 2), most of the country average changes in precipitation and runoff are smaller than the associated SD across the ensemble members. Therefore, both the direction and magnitude of changes are uncertain for most countries in this region. The only instances where the average changes are larger than the ensemble SD's are for both precipitation and runoff in Turkey, and for precipitation in Syria and Yemen. For these cases, Turkey is projected to experience the largest average decreases in precipitation (-83.5 mm/yr ± 44.9 SD) and runoff (-40.1 mm/yr ± 28.1 SD), Syria is projected decreases in precipitation (-32.8 mm/yr ± 26.1 SD) and Yemen is projected increases in precipitation (67.3 mm/yr ± 63.7 SD). Turkey also shows the most significant changes in the runoff : precipitation ratio (see Figure 5), indicating that a larger proportion of the increase in precipitation will runoff.

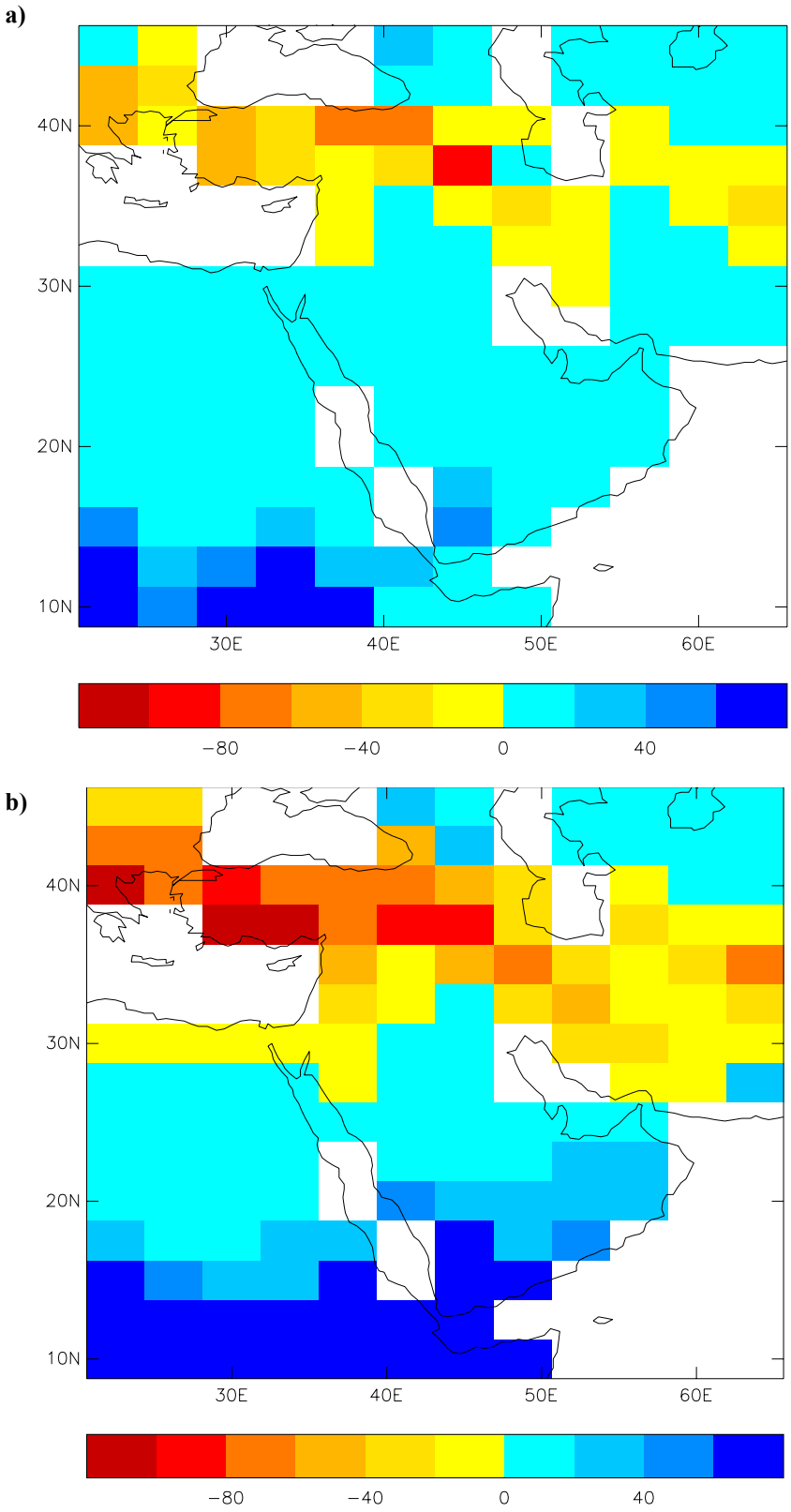

Figure 3. Ensemble average change in a) precipitation and b) runoff between the control and doubled CO_2 runs.

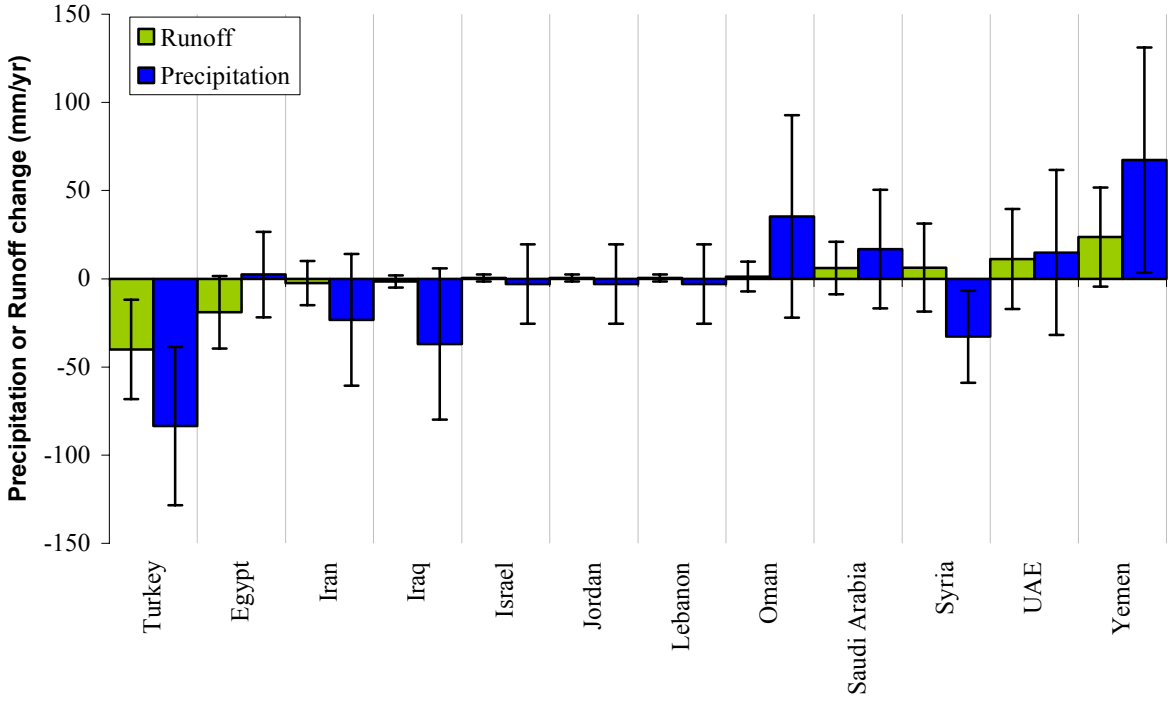

Figure 4. Ensemble average changes in precipitation and runoff for each country. The error bars are the standard deviations of these averages across the ensemble.

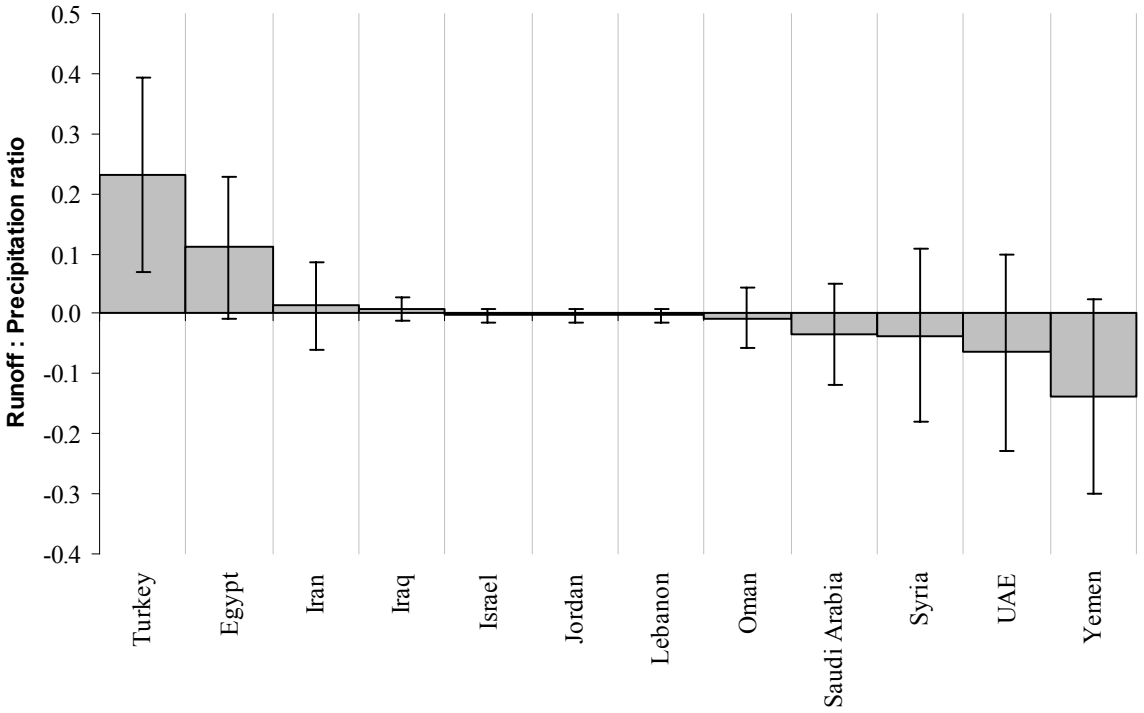

Figure 5. Ensemble average runoff : precipitation ratios for each country. The error bars are the standard deviations of these averages across the ensemble.

CONCLUSIONS

This paper has used an ensemble of 81 GCM runs to examine future projections of precipitation and runoff across the Middle-East region. Each ensemble member is set with different plausible parameterisations, which has also enabled the uncertainties involved with these to be assessed.

Under doubled CO_2, precipitation and runoff show average region-wide increases, although spatially this varies significantly, from decreases of up to -120 mm/yr in the north-west of the region (northern Syria, Turkey and Greece), to increases of up to 80 mm/yr in southern areas; western Yemen, Eritrea, southern Sudan and northern Ethiopia. For most model parameterisations climate changes associated with doubling CO_2 are projected to result in a larger portion of precipitation directed into runoff across the region.

The uncertainty ranges for regional average precipitation and runoff are considerably larger the ensemble average changes, and these ranges span both positive and negative changes. This is also the case for most of the country average changes. In these cases, the uncertainty in the precipitation and runoff response to doubled CO_2 is too large to project with confidence the direction of these changes under doubled CO_2 conditions. However, for specific countries; Turkey, Syria and Yemen, the SD across all ensemble members is smaller than the ensemble-average changes, and more confidence can be attached to the projected precipitation, runoff and runoff : precipitation ratio changes. This is most prominent for Turkey, where the ensemble-average precipitation and runoff are projected to decrease by -83.4 mm/yr and -40.1 mm/yr, and the ensemble SD's are 44.9 mm/yr and 28.1 mm/yr, respectively.

REFERENCES

[1] Ravenga et al, 2000
[2] IPCC 1998 The regional impacts of climate change: An assessment of vulnerability. CUP.
[3] Pope VD, Gallani M, Rowntree PR, Stratton RA 2000 The impact of new physical parameterisations in the Hadley Centre climate model – HADAM3. Climate Dynamics 16, 123-146.
[4] Hewitt C & Mitchell J 1997 Radiative forcing and response of a GCM to ice age boundary conditions: cloud feedback and climate sensitivity. Climate Dynamics 13, 821-834.
[5] Cox PM, Betts RA, Bunton CB, Essery RLH, Rowntree PR & Smith J 1999 The impact of new land surface physics on the GCM simulation of climate and climate sensitivity. Climate Dynamics 15, 183-203.
[6] Collatz, G.J., J.T. Ball, C. Grivet, and J.A. Berry (1991). Physiological and environmental regulation of stomatal conductance, photosynthesis and transpiration: A model that includes a laminar boundary layer. Agric. And Forest Meteorol., 54, 107-136
[7] Raich J and Schlesinger W 1992 The global carbon dioxide flux in soil respiration and its relationship to vegetation and climate. Tellus 44B, 81-99.
[8] Wilson MF & Henderson-Sellers A 1985 A global archive of land cover and soils data for use in general circulation climate models. Journal of Climatology 5, 119-143.
[9] Barnett DN, Brown SJ, Murphy JM, Sexton DMH & Webb MJ 2005 Quantifying uncertainty in changes in extreme event frequency in response to doubled CO_2 using a large ensemble of GCM simulations Climate Dynamics.
[10] Candela A, Aronica G, Santoro M 2005. Effects of forest fires on flood frequency curves in a Mediterranean catchment. Hydrological Sciences 50 (2), 193-206.

[11] Mohamed YA, van den Hurk BJJM, Savenihe HHG, Bastlaanssen WGM 2005. Hydroclimatology of the Nile: results from a regional climate model. Hydrol. Earth Syst. Sci. Discuss. 2, 319-364.
[12] Betts RA, Boucher O, Collins M, Cox PM, Falloon P, Gedney N, Hemming DL, Huntingford C, Jones CD, Sexton D & Webb M Submitted. Future runoff changes due to climate and plant responses to increasing carbon dioxide. Nature.

TEMPORAL AND SPATIAL VARIATION OF RAINFALL RATE IN MARMARA REGION

Zafer Aslan[1], Bahar Oğuzhan[2], Zehra Nevin Caglar[2] Nail Yeniceri[2]

[1]Anadolu BIL Professional School of Higher Education, Bahçelievler/Florya, İstanbul, Turkey, zaferaslan@anadolubil.edu.tr
[2]Bogaziçi University, Kandilli Observatory and Earthquake Research Institute, Meteorological Laboratory, Çengelkoy, İstanbul, Turkey

ABSTRACT

The fact that the climate parameters, in particular the rainfall data are depending on geography can be explained by considering various effects. In Turkey, most important of these factors are the topography and the synoptic scale of air masses. Rainfall variability that is caused by these effects is calculated by taking into account the spatial coherence of the rainfall in Marmara Region. The calculations are carried out for each month. Cross and distant correlation tables based on long term data are presented in this paper. Rainfall is subject to significant temporal and spatial variability, and analysis of time series is more complex. During the last few decades precipitation has tended to increase in the mid-latitudes, but decrease in the Northern Hemisphere subtropics and generally increase through out the Southern Hemisphere. The accuracy of other precipitation records should be treated with caution. Precipitation is more difficult to monitor than temperature due to its greater temporal and spatial variability Other uncertainties in the data set may be due to the collection efficiency of rain gauges. Results of the presented paper indicate that for regions of geographical proximity, the high spatial coherence exhibits variations depending on motion of the local factors. Variance analysis show significant correlation between rainfall rate values on coastal area.

Keywords: Rainfall variability, Climate parameters, Variance analysis

INTRODUCTIONS

Turkey is under the effect of different climatological conditions. The complex topographical structure and different air masses cause the important variability of meteorological parameter, (Shukla 1993; Oduro-Afriye 1989). This study presents some results of rainfall rate values in Marmara Region.

MATERIAL AND METHODS

Study Area and Data

To study temporal and spatial variations of annual total rainfall rate in Marmara Region 10 different climatological stations have been considered. Data recorded in 10 station (Adapazari: λ: 41.00, φ: 30.50; Balikesir: λ: 39.50, φ: 28.00; Bandirma: λ: 40.00, φ: 28.00; Bilecik: λ: 40.0, φ: 30.00; Bursa: λ: 40.00, φ: 29.00; Canakkale: λ: 40.0, φ: 26.50; Edirne: λ: 41.50, φ: 26.50; Istanbul: λ: 41.00, φ: 29.00; Kocaeli: λ: 41.00, φ: 30.00; Tekirdag: λ: 41.00, φ: 27.50) between 1901 and 2001 have been statistically analysed.

Methods

In this paper long time rainfall values and oceanic nino index (ONI) have been statistical analysis by using SSPS and surfer.

ANALYSIS

Spatial variations of rainfall rate values increase in near vicinity of İstanbul, Kocaeli, Bandırma and Bursa (Fig.1), (New at all. 1999, 2000; Barry at all. 1992).

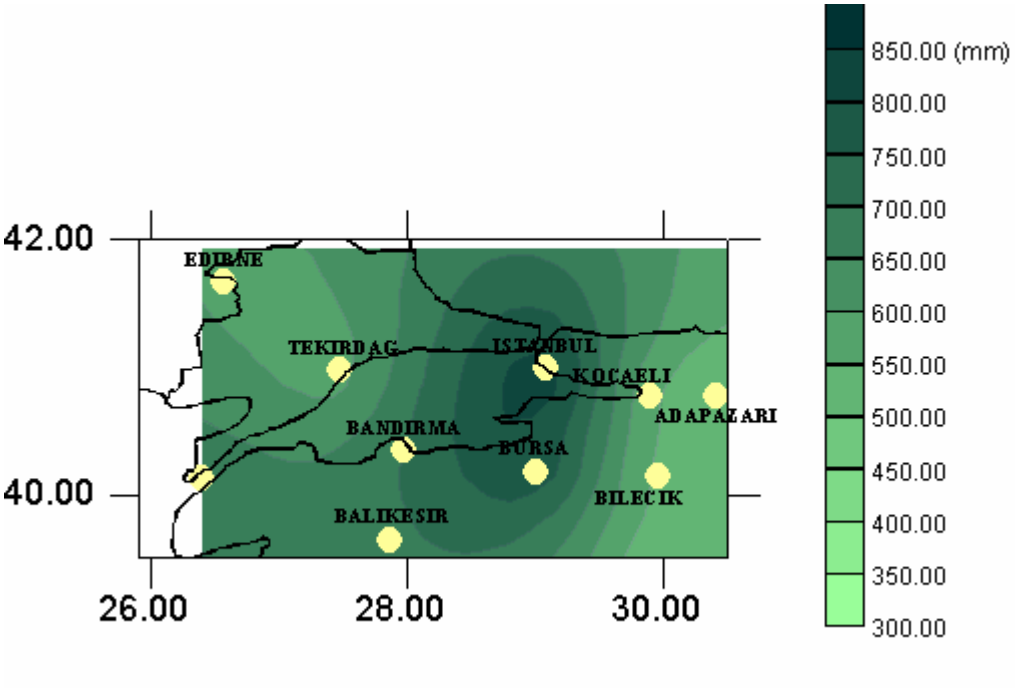

Figure 1. Spatial variation of mean annual rainfall rate in Marmara Region, (1901-2001)

Table 1. Annual total rainfall rate values in Marmara Region, between (1901-2001)

Station N.	Stations	R(mm)
1	Adapazarı	509,3
2	Balıkesir	687,6
3	Bandırma	703,2
4	Bilecik	531,1
5	Bursa	791,4
6	Çanakkale	691,3
7	Edirne	589,5
8	İstanbul	836,2
9	Kocaeli	551,9
10	Tekirdağ	572,3

Long time mean and rainfall rate values are lower (R < 600mm) in Adapazarı, Bilecik, Kocaeli and Edirne.

Figure 2 (a,b,c,d,e,f,g,h,i,j) shows linear trend analysis of long time rainfall rate values.

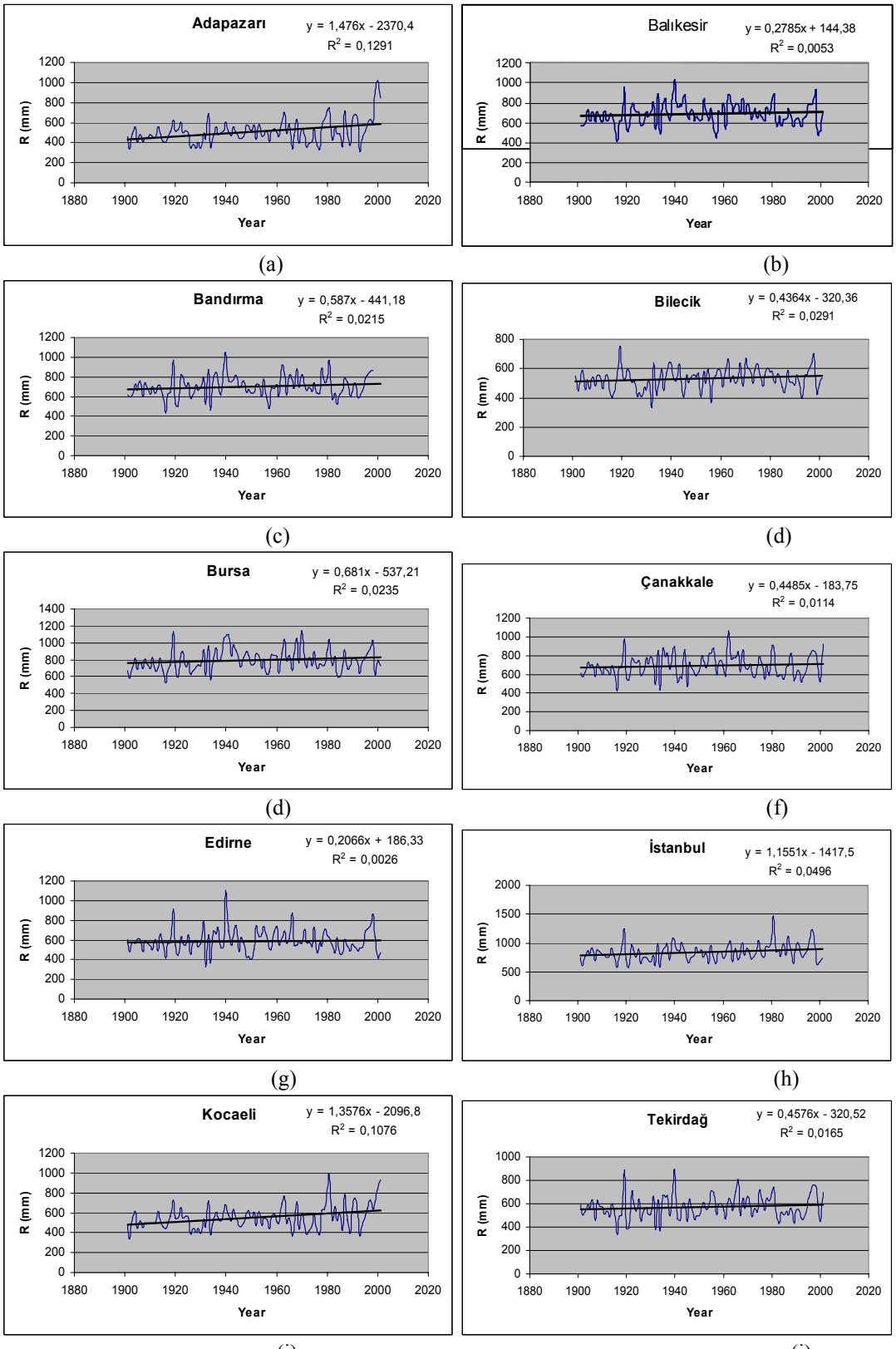

Figure 2. Temporal variation of rainfall rate values in Marmara Region (1901-2001) (a)-Adapazarı,(b)-Balıkesir,(c)-Bandırma,(d)-Bilecik(e)-Bursa,(f)-Çanakkale (g)-Edirne, (h)-İstanbul, (i)-Kocaeli,(j)-Tekirdağ

In Marmara Region, rainfall rate values show increasing trends in all stations between 1901 and 2001, Figure 2. In Adapazarı, Kocaeli and İstanbul increasing ratio of rainfall rate values are higher than the other stations. The minimum increasing trend has been observed in and near vicinity of Edirne.

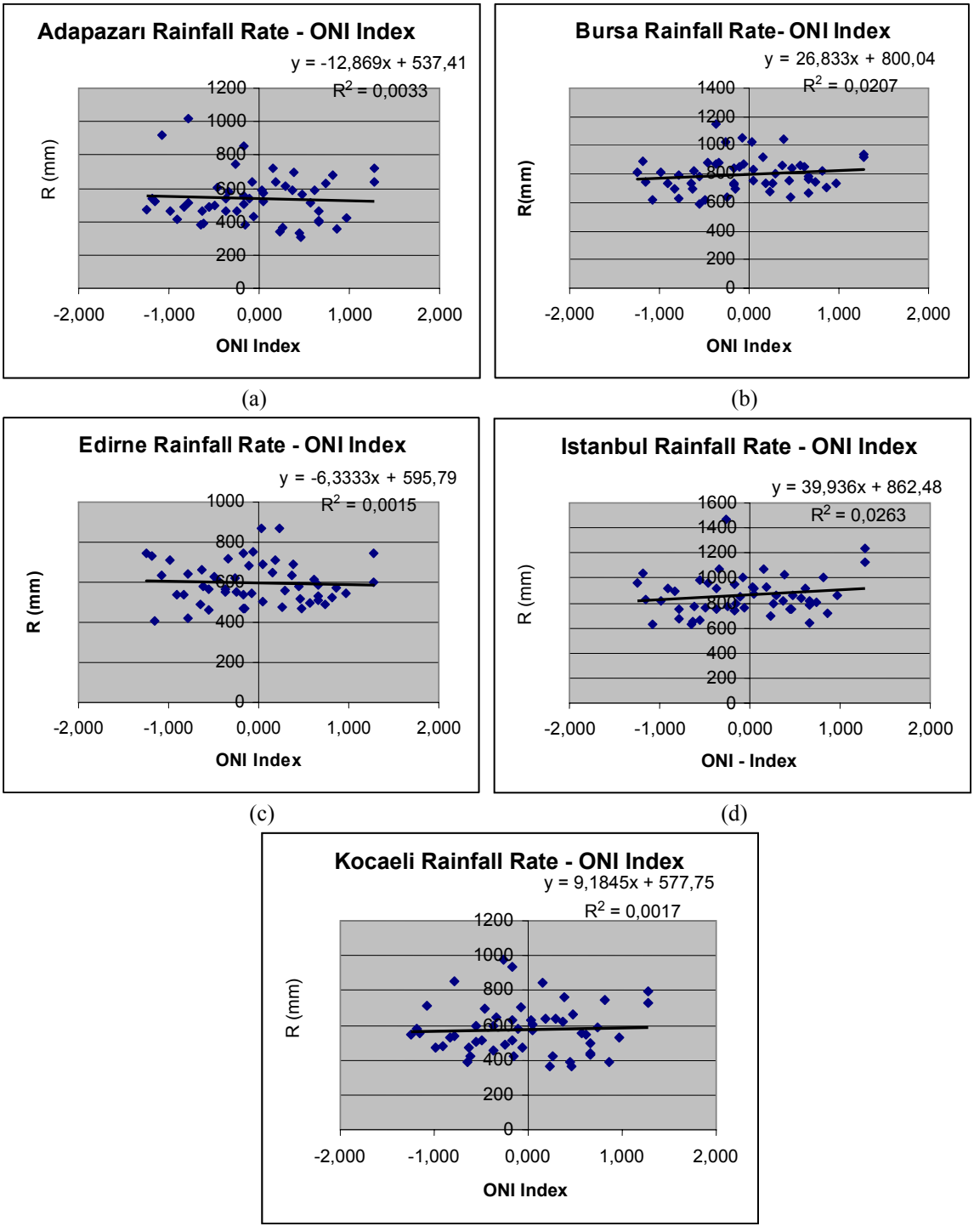

Figure 3. Correlation between ONI and rainfall rate in Marmara Region

ONI Index (ONI) shows a positive relation between rainfall rate values in Bursa, İstanbul and Kocaeli, Figure 3.(b,d and e)

Oceanic Nino Index (ONI), 3 monthly running mean of SST anomalies in the Nino 3.4 region (5º N-5 ºC,120º-170ºW) based on the 1971-2000 period have been compared with rainfall value in figure 3,(NOAA,2006).

Table 2. Similarity matrix (Distance Correlation) of rainfall rate values in Marmara Region.

Stations	VAR00001	VAR00002	VAR00003	VAR00004	VAR00005	VAR00006	VAR00007	VAR00008	VAR00009	VAR00010
Adapazarı		,248	,469	,434	,426	,300	,141	,448	,926	,306
Balıkesir	,248		,907	,613	,824	,693	,672	,692	,419	,732
Bandırma	,469	,907		,622	,798	,708	,632	,758	,582	,783
Bilecik	,434	,613	,622		,733	,431	,449	,645	,531	,528
Bursa	,426	,824	,798	,733		,463	,512	,706	,550	,552
Çanakkale	,300	,693	,708	,431	,463		,593	,549	,426	,823
Edirne	,141	,672	,632	,449	,512	,593		,454	,200	,768
İstanbul	,448	,692	,758	,645	,706	,549	,454		,673	,636
Kocaeli	,926	,419	,582	,531	,550	,426	,200	,673		,408
Tekirdağ	,306	,732	,783	,528	,552	,823	,768	,636	,408	

The highest correlation has been observed between Balıkesir and Kocaeli (Station Numbers 2 and 9). The lowest has been observed in between Adapazarı and Edirne (Station Numbers 1 and 7).

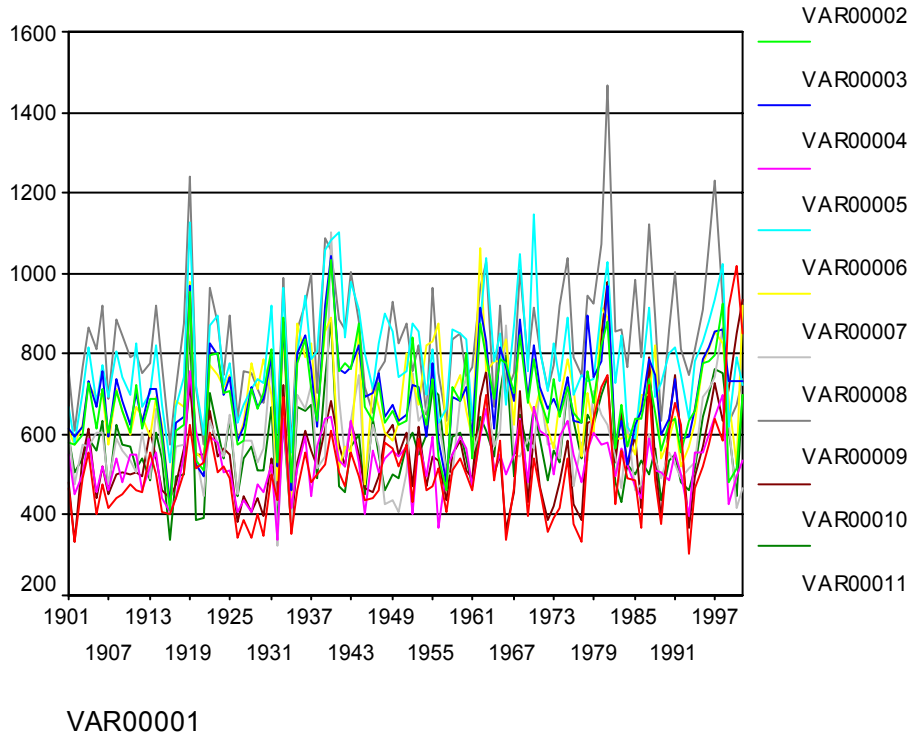

Figure 4. Time variation of annual total rainfall rate in all stations in Marmara Region.

Increasing trend of rainfall rate in strong El Nino years (1982,1986 and 1998) have been observed in Figure 4.

RESULTS AND CONCLUSIONS

Annual total rainfall rate values increases in all stations based on long term data between 1901 and 2001, (Aslan at all. 1997). Composition of oceanic Nino Index with rainfall rate values has a negative effect on rainfall rate values observed in Adapazarı and Edirne increasing ONI value shows an increasing trend in rainfall rate in Kocaeli, Bursa and İstanbul.

REFERENCES

Aslan, Z. and D. Okçu (1997),‘’Analysis at large, meso and small scale effects on pressure, relative humidity, temperature, precipitation and wind speed variations’’, ICTP preprint, IC/IR/96/49, March..

Aslan, Z., D. Okcu and S. Kartal,(1997), "Harmonic Analysis of Precipitation, Pressure and Temperature Over Turkey", Il Nuovo Cimento, Vo.20 C, N.4, p. 595-605, 1997.

Barry, R.G., and R.J. Chorley, (1992): Atmosphere, Weather and Climate, p. 392, The Chaucer Press Ltd., Bungay.

New, M. G., M. Hulme and P.D. Jones., (1999), Representing 20th century space–time climate variability I: Development of 1961-1990 mean monthly terrestrial climatology, J. Climate,12, 829-856.

New, M. G., M.Hulme, and P. D. Jones., 2000, Representing 20th.century space-time climate variability II: Development of 1901-1996 monthly terrestrial climate fields, J. Climate, 13, 2217-2238.

NOAA; ONI (2006), National Weather Service for Environmental Prediction, Climate Prediction Center, USA

Oduro-Afriye, K., (1989) , “On The Mean Monthly Equivalent Temperature and Rainfall in West Africa”, Theo. Appl. Climatol., Vol. 39, pp. 188-193.

Shukla J.,(1993), ‘‘Prediction of Inter-annual Climate Variations’’ (Springer-Verlag, New-York) 1993, pp. 217-231.

ANALYSIS OF PERCENTILE BASED PRECIPITATION INDICES OVER IRAN

Ahmad Asgari, Fatemeh Rahimzadeh and Ebrahim Fattahi

Atmospheric Science and Meteorological Research Center (ASMERC),
P.O.Box: 14965-114, Tehran, Iran, rahim_f@irimet.net

ABSTRACT

Analysis of extreme precipitation has received too much attention during recent years. Indices like R95p (very wet days) and R99p (extremely wet days) are among robust extreme indices that compare extreme values of daily precipitations of a given place with their own values from standard normal period of 1961-1990. R95p and R99p are those days that daily precipitation exceeds thresholds of 95th and 99th percentile respectively.

Although Islamic Republic of Iran Meteorological Organization currently operates more than 160 synoptic stations, but we had to select only 33 out of them. Limiting factors for selection of the stations were reliability and continuity of precipitation data, and coverage of 1961-1990 periods.

We found non-zero values for very wet days index for all individual years in stations like Babolsar, Bandar Anzali, Gorgan, and Rasht (located in littoral provinces of Caspian Sea), but other stations experienced at least one year without very wet days. Highest R95P of the country is from Bandar Anzali with value of 1096 mm in 1975. If we divide the country into 3 regions, we almost observe negative trends for R95p index over eastern and western regions, and positive trend over central region. Strongest positive and negative trends were found in Babolsar (slope of +3.2 mm/yr) and Bandar Anzali (slope of -1.46 mm/yr).
Our results also show that every station has experienced at least one year without extremely wet days. We clearly observe negative trends for most of the country. Some 3 small regions show positive trends. Highest R99p of the country is again from Bandar Anzali with value of 655 mm in 1997. Strongest positive and negative trends were found in Babolsar (slope of +2.14 mm/yr) and Bandar Anzali (slope of –2.49 mm/yr.
If we didn't take into account drought years of late 1990's and early 2000's, trends for both indices would modify significantly.

Keywords*:* Extreme precipitation indices, Very wet days, Extremely wet days, Iran, and trend

INTRODUCTION

Changes in several components of the hydrological cycle such as increase and decrease of precipitation, heavy and very heavy precipitation, have been documented over the world during the last few decades. According to the third assessment report of the Intergovernmental Panel on Climate Change [7] there has been likely a statistically significant 2 to 4% increase in the frequency of heavy and extreme precipitation events. The first global studies of daily temperature and precipitation extremes over land showed the fraction of annual total precipitation from events wetter than 95th percentile of wet days(>=1mm) for 1961-90 have increased in many parts of the USA, central Europe and southern Australia and there are a few coherent areas of decrease too [4].

Alexander et al., [1] prepared maps of changes of extreme precipitation over different land areas of the world with sufficient data and found positive trends of the precipitation contribution of very wet days to total precipitation during recent decades.

Of course, many studies have been done for different regions and countries during last decades. For example, Hennessy et al., [6] showed significant changes in upper percentiles in their study of long term precipitations over Australia. They found significant changes of frequency of extreme precipitation events based on using fixed threshold. Suppiah and Hennessy [6] found increasing trends in 90^{th} and 95^{th} percentiles over most of Australia. Plummer et al., [9] proved that the variation of percentiles depends on the region and season. Klein Tank and Können, [8] found increasing trend in the number of very wet days during the second half of the 20th century over Europe. Groisman et al., [5] found statistically significant increases in heavy and very heavy precipitation over the United State of America.

Zhang et al., [14] collected the Middle East daily precipitation data and found that precipitation climatology of the region varies considerably from one place to another. There are few stations in the region with significant positive and negative trends. Generally, analyses of precipitation anomaly represent wetter region. There have been a few studies on averages and daily precipitation data at national level. One of first efforts in this area is work of samiee and his colleagues, in 1989. These researchers, on their comprehensive study of precipitation over Iranian territory found many features of the country precipitation including probable maximum 24- hour precipitations.

ASMERC, [2] studied changes of climatic elements averages like precipitation over country on a project entitled "Statistical detection of climate change over Iran". In another project, ASMERC in 2006 [3] according to most recent methods, fully examined extreme precipitations and temperatures over Iran.

In this work, we present studies done on two indices of extreme precipitation i.e., R95p (very wet days) and R99p (extremely wet days).

DATA ISSUSES AND EXTREME PRECIPITATION INDICES

It is noteworthy that reliable data could provide us a suitable background to study collective behaviors of climate. Although there are more than 160 operating synoptic stations in the country, we used daily precipitation data from synoptic stations' network of Islamic Republic of Iran Meteorological Organization (IRIMO) Which its first stations were officially started their systematic observations in 1951. The main reasons for the application of synoptic stations' data are easy access to their meta data, daily precipitation data and also our knowledge about their data quality and homogeneity [10].

In this work, we had to choose a smaller subset of 27 stations' data due to avoiding of problems like inhomogeneity of the data, and missing data [10] and covering standard normal period 1961-1990. Geographical locations of used stations are shown in Table 1.

Table 1. Geographocal characteristics of the selected stations

No.	Station	Geographical Coordinates		Height (m)	WMO No.	Period
		Longitude (N)	Latitude (E)			
1	Abadan	30° 22′	48° 15′	6.6	40831	1951-03
2	Arak	36° 06′	49° 46′	1708.0	40769	1961-03
3	Babolsar	36° 43′	52° 39′	-21	40736	1951-00
4	Bam	26° 09′	58° 21′	1066.9	40854	1956-03
5	Bandar Abbas	27° 13′	56° 22′	10.0	40895	1960-03
6	Bandar Anzali	37° 28′	49° 28′	-26.2	40718	1961-03
7	Birjand	32° 52′	59° 12′	1491.0	40809	1955-03
8	Bushehr	28° 59′	50° 50′	19.6	40858	1951-03
9	Esfahan	32° 40′	51° 52′	1600.7	40800	1961-03
10	Ghazvin	36° 15′	50° 00′	1278.3	40731	1960-03
11	Gorgan	36° 51′	54° 16′	13.3	40738	1960-03
12	Kerman	30° 15′	56° 58′	1753.8	40841	1961-03
13	Kermanshah	34° 19′	47° 7′	1322	40766	1951-03
14	Mashhad	36° 16′	59° 38′	990	40745	1951-03
15	Oroomieh	37° 32′	45° 5′	1312.5	40712	1961-03
16	Ramsar	36° 54′	50° 40′	-20.0	40732	1955-03
17	Rasht	37° 12′	49° 39′	36.7	40719	1956-03
18	Sabzevar	36° 12	57° 43′	977.6	40743	1954-03
19	Sanandaj	35° 20	47° 00′	1373.4	40747	1959-03
20	Shahrekord	32° 20′	50° 51′	2061.4	40798	1955-03
21	Shiraz	29° 33′	52° 36′	1488	40848	1951-03
22	Tabriz	38° 5′	46° 17′	1361.0	40706	1951-03
23	Tehran-Mehrabad	35° 41′	51° 19′	1190.8	40754	1956-03
24	Yazd	31° 54	54° 24	1230.2	40821	1952-03
25	Zabol	31° 13′	61° 29′	489.2	40829	1961-03
26	Zahedan	29° 28′	60° 53′	1369.0	40856	1951-03
27	Zanjan	36° 41	48° 41′	1663.0	40729	1955-03

In our study, we selected R95p and R99p indices out of some large selections [4; 13]. R95p (very wet days) and R99p (extremely wet days) represent amount of precipitation falling above 95^{th} and 99^{th} percentiles of standard normal period 1961-1990. We used Rclimdex software (in R language) to analyze the two indices and Mann-Kendall test as a powerful non-parametric test to examine trend for the selected indices.

RESULTS

Indices of R95p and R99p that are based on comparison of daily intense precipitations and values of 95th and 99th percentiles are more robust than fixed threshold indices like R20mm (Number of days with precipitation more than 20 mm).

Very wet days

Our results show that we have experienced daily precipitations more than 95th percentile in each year of the period in stations like Babolsar, Bandar Anzali, Gorgan, and Rasht in Caspian region. Ramsar located in the same region, has only experienced one year with no very wet days. Bandar Anzali and Ramsar got total precipitation more than 1000 mm for their very wet days in 3 and 1 year(s) respectively. The former has recorded 1096 mm total precipitation for its very wet days in 1975 that is highest value for such days among the Iranian stations under study (Fig. 3). The rest of studied stations have experienced some years with no very wet days. In southern stations of Abadan, Bam, and Bandar Abbas, the index of R95p have been zero in most years of the period.

If we divide country into 3 bands in N-S orientation, we observe negative trends for eastern and western bands, and positive trends for central one (Fig. 1). Strongest positive trends for R95p index have been found in Babolsar (slope of +3.2 mm per year) and Bandar Abbas (slope of +0.83 mm per year) respectively. Strongest negative trends for the index have been found in Bandar Anzali (slope of -1.46 mm per year) and Gorgan (slope of -1.44 mm per year) respectively. It is noteworthy that Babolsar and Bandar Anzali with such contradictory trends are not very far from each other.

Statistically speaking, we don't expect compatible results obtained from using Mann-Kendall and least square methods. This is due to repeat of zeros in the time series of the index. As least square method accepts significance of trends for stations of Babolsar, Tabriz, and Zahedan, but Mann-Kendall method rejects it for Babolsar.

Extremely wet days

Each station has experienced at least one year with zero value for the index of R99p. since we have diverse precipitation regimes over the country, thresholds of 99th percentiles are very different from a point to another. The thresholds are 109 and 31 mm in Bandar Anzali, and Zabol respectively. Ramsar has recorded 797 mm total precipitation for its extremely wet days in 1976 that is highest value for such days among the Iranian stations under study. The highest total precipitations for such days in Bandar Anzali and Zabol are 655 mm in 1997 and 45 mm in 1994 respectively (Fig. 4).

Most of the country experiences negative trends for the index of R99p.There are some small regions in Hormozgan province (adjacent to Strait of Hormoz), north, west of the country that show positive trend for the index (Fig. 2). Strongest positive trends for R99p index have been found in Babolsar (slope of +2.14 mm per year) and Ramsar (slope of +2.11 mm per year) respectively. Strongest negative trends for the index have been found in Bandar Anzali (slope of -2.49 mm per year) and Shiraz (slope of -1.56 mm per year) respectively. Two contradictory trends in two close locations in Caspian region are again remarkable.

We again didn't find same results from using Mann-Kendall and least square methods. As P-values accept significance of trends only for Abadan, Babolsar, Tabriz, Shiraz, and Zahedan, Mann-Kendall method rejects significance of trends in all stations except Babolsar, Gorgan, oroomieh, Ramsar, and Rasht.

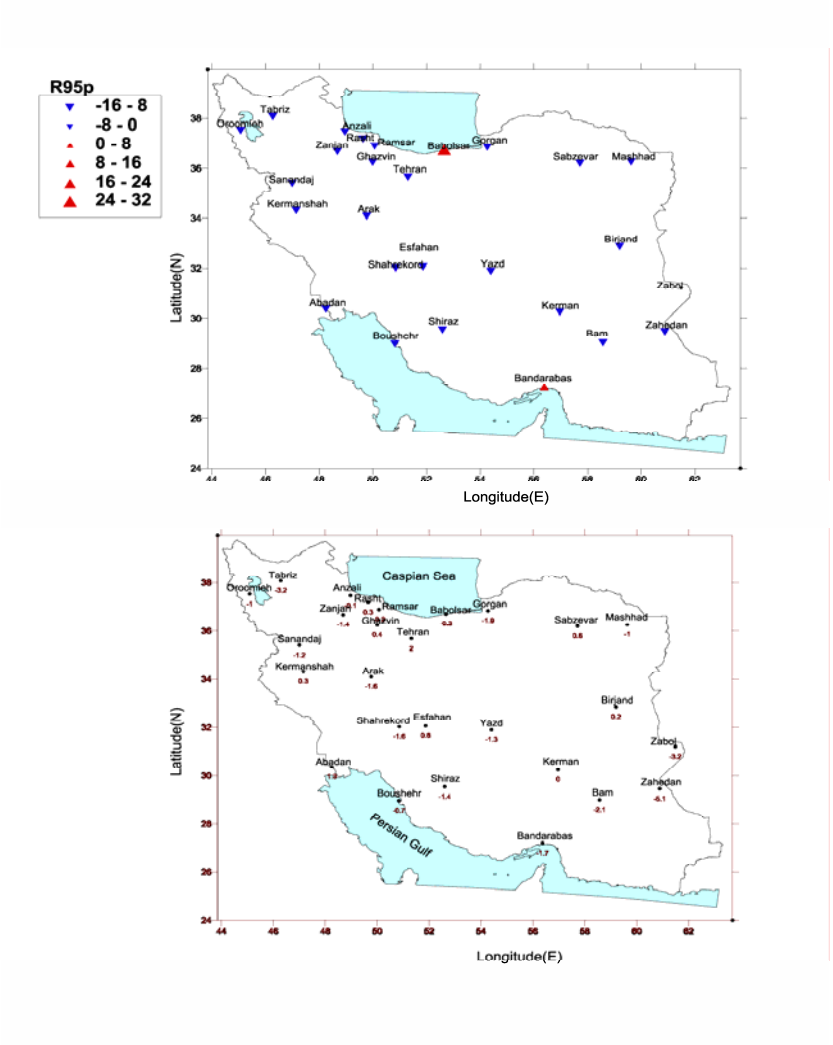

Figure 1. Decadal trends for R95p index in selected Iranian synoptic stations for period 1951-2003.

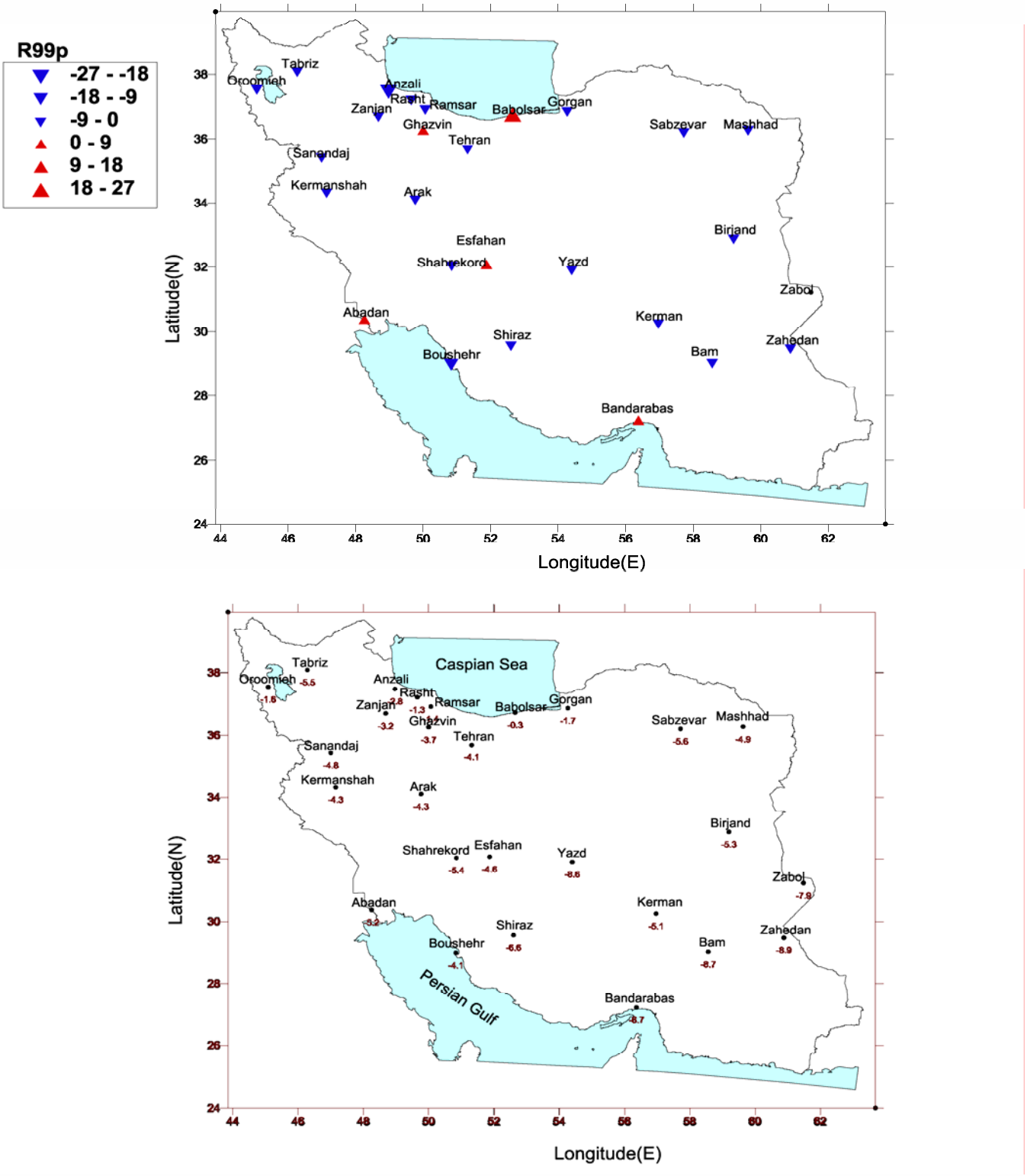

Figure 2. Decadal trends for R99p index in selected Iranian synoptic stations for period 1951-2003.

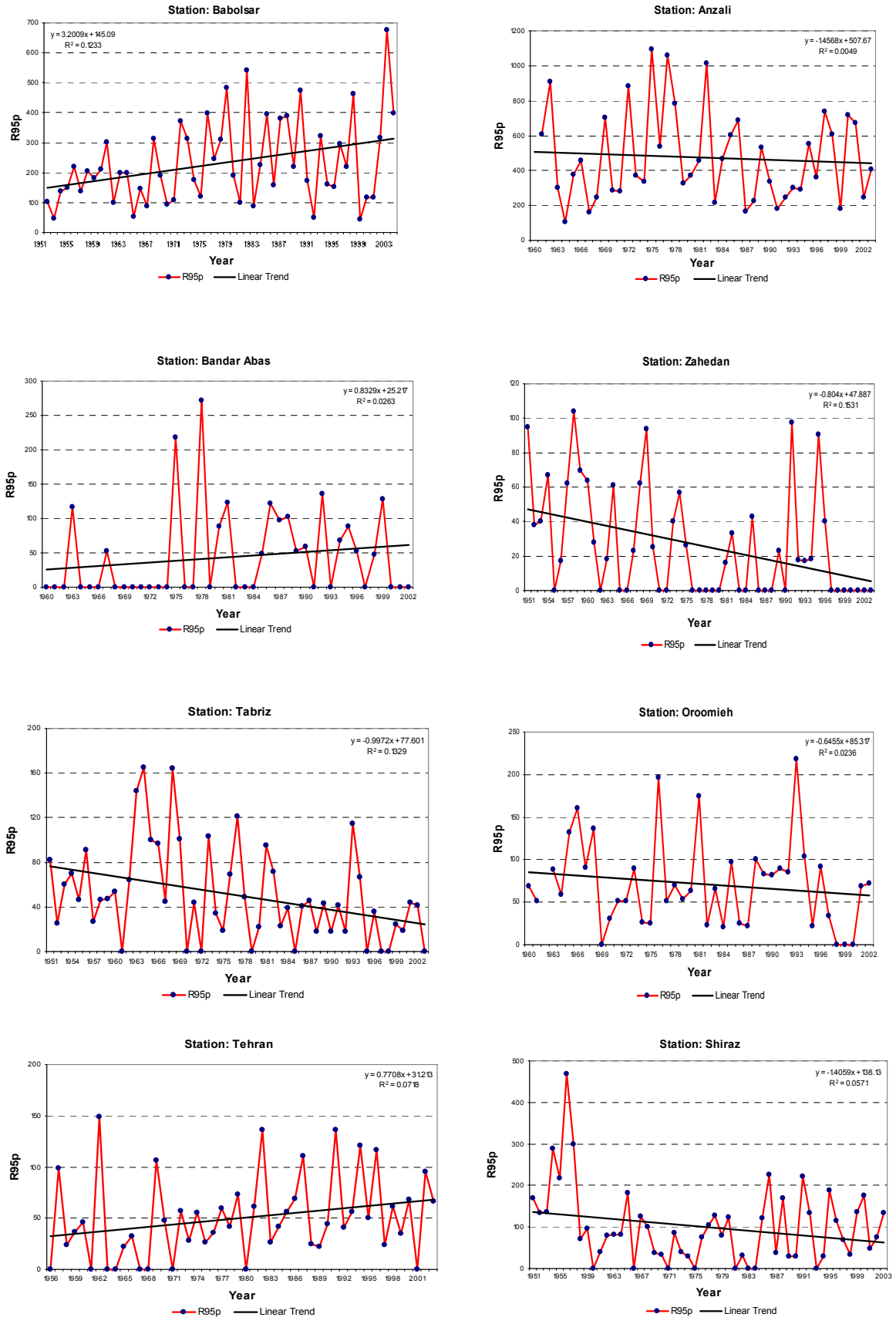

Figure 3. Some selected cases for their negative trends, large values, and positive trends of R95p over Iran.

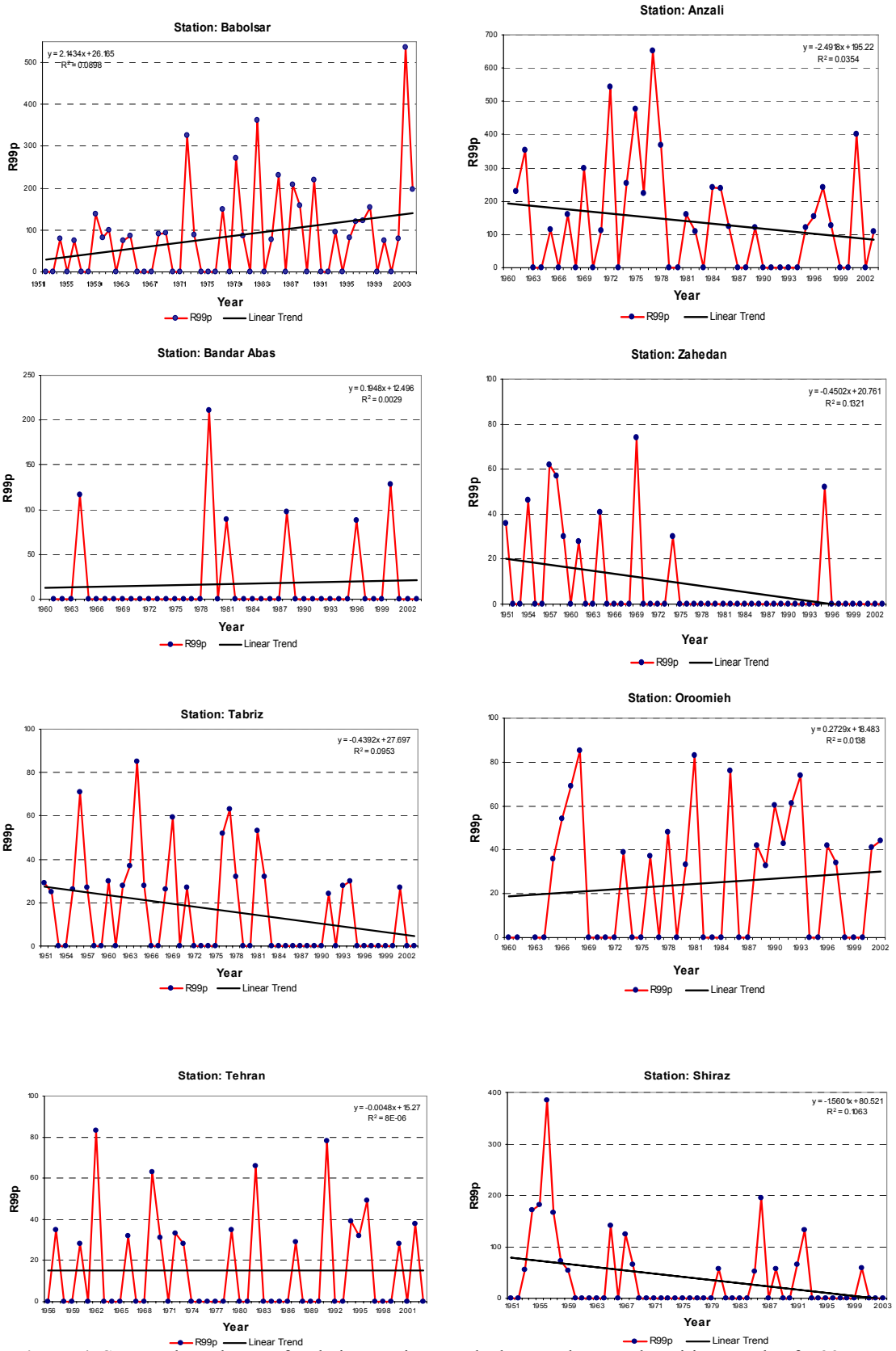

Figure 4. Some selected cases for their negative trends, large values, and positive trends of R99p over Iran.

REFERENCES

1. Alexander, L., X. Zhang, T. C. Peterson, J. Caesar, B. Gleason, A. Klein Tank, M. Haylock, D. Collins, B. Trewin, F. Rahimzadeh, A. Taghipour, K. Rupa Kumar, J. Revadekar, G. Griffiths, L. Vincent, D. Stephenson, J. Burn, E. Aguilar, M. Brunet, M. Taylor, M. New, P. Zhai, M. Rusticucci, J. L. Vazquez-Aguirre., 2006: Global observed changes in daily climate extremes of temperature and precipitation. J. Geophys. Res., D05109, doi:10.1029/2005JD006290.
2. ASMERC, 2003: National report of project on "statistical detection of climate change over Iran" , ASMERC publications (In Farsi).
3. SMERC, 2006: Final Report of project on study of extreme climatic indices over Iran, ASMERC publications (in Farsi).
4. Frich, P., L.V. Alexander, P. Della- Marta, B. Gleason, M. Haylock, A.M. G. Klein Tank, T. Peterson, 2002: Observed coherent changes in climatic extremes during the second half of the twentieth century. Climate Res., 19, 193–212.
5. Groisman, P.Ya., et al., 2004: Contemporary changes of the hydrological cycle over the contiguous United States: Trends derived from in situ observations. J. Hydrometeorology., 5, 64–85.
6. Hennssey KJ, Suppiah R, Page CM. 1999: Australian rainfall change, 1910-1995. Australian Meteorology Magazine 48: 1-13.
7. Houghton JT, Ding Y, Griggs DJ, Noguer M, Van der Linden Pj, Dai x, Maskel K. Johnson CA (eds), 2001: Climate Change 2001:The Scientific Basis, Cambridge University Press: Cambridge, UK
8. Klein Tank, A.M.G. and G.P. Können, 2003: Trends in indices of daily temperature and precipitation extremes in Europe, 1946–1999. J. Climate, 16, 3665–3680
9. Plummer, N. Salinger MJ, Nicholls N.Suppiah R. Hennessy Kj Leighton RM, Trewin BC, page CM, Lough JM, 1999: Changes in climate extremes over the Australian region and New Zealand during the twentieth century, Climate Change 42:183-202.
10. Rahimzadeh, F., and A. Asgari, 2003: A Survey on Recent climate change over IRAN. Proceeding of 14th Global Warming international conference & expo (27-30 May, Boston, USA).
11. Samiee, M., M. Askari, and K. Bastani, 1989: Technical Report on statistical analysis of 24-hour precipitations over Iran , IRIMO publications (in Farsi).
12. Suppiah R. and Hennessy KJ. (1998): Trend in total rainfall, heavy-rain events and number of dry days in Australia. 1910-1990. International Journal of Climatology 10: 1141-1164.
13. URL1: http://cccma.seos.uvic.ca/ETCCDMI/list_27_indices.html
14. Zhang, X., E. Aguilar, S. Sensoy, H. Melkonyan, U. Tagiyeva, N. Ahmed, N. Kutaladze, F. Rahimzadeh, A. Taghipour, T.H. Hantosh, P. Albert, M. Semawi, M. Karam Ali, M. Halal Said Al-Shabibi, Z. Al-Oulan,Taha Zatari, I. Al Dean Khelet, S. Hammoud, M. Demircan, M. Eken, M. Adiguzel, L. Alexander, T. Peterson and Trevor Wallis, 2006: Trends in Middle East Climate Extremes Indices during 1930-2003. J. Geophys. Res., 110, D22104, doi:10.1029/2005JD006181

REGIONAL CLIMATIC IMPACTS OF GLOBAL WARMING OVER THE EASTERN MEDITERRANEAN

Barış Onol[1], Fredrick H. M. Semazzi[2], Yurdanur S. Unal[1], H. Nuzhet Dalfes[1]

[1]İstanbul Technical University, İstanbul, Turkey (onolba@itu.edu.tr)
[2]North Carolina State University, Raleigh, USA (fred_semazzi@ncsu.edu)

ABSTRACT

Social-economic preparations for future climate change require geographically more detailed projections than global climate models can provide. Therefore, regional climate model based climate change projections are needed and they have been successfully used for many different regions of the world especially North America and Europe.

In this study, we used the regional climate model (ICTP-RegCM3) to downscale present and future scenario output simulated by the NASA-Finite Volume General Climate Model (fvGCM). Our climate model domain is 10E:50E; 28N:50N. It is centered over Turkey and it includes the Black Sea and the eastern Mediterranean Sea. The present day simulations (1961-1990) are based on the IPCC RF GHG forcing and the future climate change simulation (2071-2100) is based on the A2 IPCC A2 GHG emissions. Relatively high resolution of 30 km is adopted to resolve the complex topography of the domain.

RegCM3 results show that the difference in winter precipitation between the present and the future scenarios are very dramatic. The results also show projections of significant increase in rainfall along the east coast of the Black Sea and over the Kaçkar and the Caucasus Mountains. There is also large decrease of rainfall over the southern and eastern regions of Turkey, and along the eastern coast of the Mediterranean. We have ascertained that this winter climate change precipitation pattern is related to the strengthening of NAO based on EOF analysis for both RegCM3 and fvGCM simulation data. We envisage that the combined effect of the projected reduction in rainfall over the southern and eastern regions of Turkey and, snow cover over the eastern Turkey mountains could have a devastating impact on the regional water resources in the future.

During summer, temperature increase is as large as 6 °C over the region of interested. However, it is not as large (approximately 2 °C) during winter. Our results further show that temperatures increase due to global warming will be associated with enhanced evaporation which may negatively impact reservoirs and irrigation schemes through out the region.

INTRODUCTION

Regional climate change studies have been conducted for many different applications such as agriculture, seasonal forecasting, hydrological applications and paleoclimate. Because of its ability to resolve sharp gradients and contrasts in the surface conditions, the regional climate modeling approach yields more accurate and spatially detailed information.

Numerous climate change studies have been carried out for many different regions: Over North America [1, 2, 3, 4], Europe, [5, 6, 7], Eastern Asia [8], Australia [9] and these regional

climate simulations have been driven by general climate models double-CO_2 simulation outputs at the boundaries. The results of these studies have shown that temperature differences between control and future climate simulations range between 1^oC and 10^oC. The corresponding projections in the precipitation are less consistent among different models and they exhibit positive and negative changes, depending on the region of interest and model.

A few European Union projects have investigated the climate change of Europe. According to these studies, Europe will be much more affected by the human-induced climate change compared to the many other parts of the world. However none of these studies has focused directly on the Eastern Mediterranean (EM) region. Also studies related to the region of our interested have not been done for future climate change scenarios. Climatic variability of synoptic systems has been analyzed by using reanalysis [10; 11]. In addition, rainfall variability over EM and its teleconnection to North Atlantic variability has been investigated by examining reanalysis and station data [12]. Evans [14] has used a regional climate model for investigating precipitation patterns over the Middle East covering the eastern part of our domain and validated the results using extensive station data but the simulation only covered 5 recent years for the present climate.

The purpose of our research is to investigate possible changes in future climate using the dynamical downscaling method over EM and to provide useful information that decision makers may need for the assessment of climate change. To achieve this objective, we used IPCC (Intergovernmental Panel on Climate Change), present and future climate scenarios which are discussed in greater details in the subsequent sections of this paper.

METHODS AND DATA

Dynamic downscaling reduces the scale gap and produces physically based simulations at smaller spatial scales than GCMs. This approach results in more realistic simulations for topographically driven climate such as over EM.

We adopted the IPCC A2 scenario for our future climate change simulation covering the period of 2071 to 2100. A2 is one of the extreme IPCC scenarios which is useful to understand the upper limits of human induced global warming. Our control simulation (RF) is based on the period, 1961-1990, which has been defined by IPCC as the standard control simulations period.

Regional Climate Model Version 3: RegCM3

To perform dynamical downscaling, the RegCM3 has been used for both RF and A2 simulations. It is a three-dimensional hydrostatic atmospheric model. It uses a sigma-pressure based vertical coordinate system and we adopted 18 vertical levels in this study. The radiation transfer package is based on the NCAR-CCM3 scheme. IPCC SRES greenhouse gases forcing has been adapted into the code and anthropogenic emissions changes, CO_2, CH_4, N_2O, CFC11 and CFC12, have been taken into account in the RegCM3 A2 simulation. The atmospheric component of the model is coupled to the Biosphere-Atmosphere Transfer Scheme called BATS [14]. For large scale precipitation the model uses the SUBEX scheme [15]. The model has three options for the convective precipitation scheme for the computation of cumulus convection. After many tests over EM domain, we adopted the Grell [16]

convective scheme with the Arakawa-Schubert [17] closure assumption. Further details about RegCM3 are given in Pal et al.[18].

Since the model performance is sensitive to the choice of the model domain the evolution of mesoscale features over the region has been considered to define the model domain (28N-50N, 10E-50E). Also appropriate selection of model resolution is important because EM has very complicated terrain. To resolve the sharp topographic gradient over EM the and large contrasts in vegetation, we run RegCM3 at 30 km resolution, which is relatively high considering expensive computation for the 60 years total simulation that we carried out.

NASA-Finite Volume GCM: fvGCM

NASA-fvGCM model output has been used to construct the lateral boundary conditions for the RF and A2 RegCM3 simulations. This model uses a terrain-following Lagrangian control volume for vertical coordinate system [19]. The horizontal resolution of the model is 1°x1.25° which is considerably high for GCMS and beneficial for the RegCM3 simulations. For RF simulation, observed sea surface temperature, sea ice distribution and GHG have been used. For the A2 simulation, the Hadley Centre coupled model HADCM3 output perturbations were calculated and added to the observed SST after applying a linear trend [20].

Observations

CRU (Climate Research Unit TS 2.1), GCN (Global Climate Normals-NCDC) and GHCN2 (Global Historical Climate Network Version 2-NCDC) data sets have been used to validate the RF monthly climatology of precipitation and temperature results. RF simulation time period (1961-1990) has been taken to define climate normal for the all data set. CRU is a 0.5° gridded monthly data set. We used the GCN and GHCN data sets for the country area averages.

RESULTS

Present-Day Simulation (RF)

The RegCM3 mean climatological temperature distribution agrees very well with the observed climatology for all the seasons. However, there is a 2-4 °C warm bias over the Caucasus Mountains and over the northern sector of the model domain during winter (Figure 1) and over the south part of the model domain in summer. The autumn and spring temperature means were reproduced almost perfectly by RegCM3. The annual mean is 2 °C warmer than CRU over the domain (Figure 1). The GCM contribution to this warm bias is about 1°C which is partially corrected in RegCM3. In terms of annual temperature variability, model representation is poor since the RCM multi-annual variability depends on the GCM variability, which is a well-known deficiency inherited by limited are model from GCMs.

Precipitation results for RF compare well with the CRU observations (Figure 2). RegCM3 realistically reproduced the general precipitation pattern for all the seasons. RF results are consistent with the fact that most of precipitation over the model domain occurs along the coastal areas and mountainous regions. However in winter and spring time, the model produced too much precipitation over these regions, especially over the Dalmatian coast, east of Black Sea coast and southwest of Turkey coast, there is too much precipitation. Similar results are also noted for the countries of Albania, Montenegro, Slovenia and Georgia. Their

area averages have been calculated by using station data. However, this can be a sampling problem since there are not enough stations in the datasets we used. All these regions have the same characteristics in terms of precipitation and with very steep topography along the coast. Moisture availability over the coastal regions and the effect of steep topography results in exaggerated orographic precipitation by model. Model resolution should be higher to solve such complexity but this is not practical for multi-decadal climate simulations because of the prohibitive computational cost.

Climatological mean conditions for autumn precipitation has been reproduced better than for the winter and spring seasons. Model precipitation in summer season is drier than observations. The reason for these dry conditions is associated with the GCM moisture availability. The fvGCM simulation used to construct the boundary conditions for RegCM3 is also very dry during summer. This deficiency is passed over to RegCM3 through the boundary conditions.

Overall, RegCM3 produced annual mean precipitation and temperature very well compared to the CRU observations. Using 30 km resolution in RegCM3 brought significant improvement for both variables considering the complex topography but the resolution of observations is not high enough to validate the model result, especially over mountainous regions.

Future Simulation (A2)

The future simulation based on the IPCC A2 scenario covers the period of 2071-2100. The standard RegCM3 radiation scheme was modified and IPCC SRES greenhouse gases forcing has been adapted into the RCM. The climate change calculations are based on the difference, A2 minus RF simulation results.

Temperature changes in summer (Figure 2) reach up to 7°C over the Balkan States. The western region of Turkey is dominated by the same heat wave with temperatures exceeding 6°C. Area average and spatial distribution changes for temperature are also highly consistent with each other. Temperature increase over the eastern part of Turkey is not large as the region over the west of the country, but it is still very high, typically around as 4°C. Because of the extension of the summer season, autumn temperature change is still very high and it is around 4-5 °C (not shown). Winter and spring increases are not as high as autumn and they are around 2-3°C (not shown). Annual increase over the domain fluctuates between 2 and 5°C (Figure 2) and temperature pattern change is still dominated by robust summer increase. The model results show that the least increase occurs over the coast of the Iskenderun Gulf and the surrounding region. The weak SST changes may cause this effect.

The 30 year daily mean temperature evolution in A2 also shows significant changes which can be seen in a seasonal transition periods of the projected climate. The A2 simulation shows that 2°C abrupt temperature increase occurs around mid-February over Turkey. This abrupt change implies that the spring season starts early which may result in significant negative impacts on many different social-economic sectors such as, agriculture and the environment. We strongly urge that the implications of this finding recommend to be evaluated for adaptation. The A2 scenario simulation also shows that the summer season is much longer than for the current conditions. In particular, the magnitude of temperature is much higher for

the entire domain. Clearly, there is need for extensive heat wave analyses to understand the impact of these changes.

In the A2 simulation, the precipitation pattern changes distinctively in winter season. The results show significant increase (10%-50%, Figure 2) in rainfall along the east coast of the Black Sea, over the Kaçkar and the Caucasus Mountains. There is also large decrease (20%-60%) for rainfall over the south and southeastern regions of Turkey, and the eastern coast of the Mediterranean (Figure 2). Winter precipitation decrease over Greece is very significant (32%). Over the east of Turkey, Syria and Iraq, there is significant increase of precipitation in autumn which is related to the flow pattern change and moisture availability increase (Figure 2). Annual change of precipitation is dominated by winter season change (Figure 2). The P-values were calculated for all the regions, and they show that all the dominant changes we have identified above are statistically significant. This pattern change in precipitation appears to be part of the northern hemisphere change. The poleward change in intensity, and upward shift of the storm tracks in the GCM ensemble climate scenario simulations have been discussed by Yin[21]. This shift and intensity change was also found in fvGCM and it directly affects the RegCM3 simulations through the lateral boundaries.

CONCLUSION

We analyzed climate change simulations produced by the regional climate model (RegCM3) based on the RF and A2 IPCC scenarios. RegCM3's ability to simulate the present climate over the EM domain, with such a complex topography and surface contrasts, is very realistic which gives us the confidence in our climate change simulations. Temperature change in the future scenario simulation, especially during the summer season over the Balkan region and Western Turkey, is 3-4°C higher than the eastern part of the domain. In the winter season, temperature change for all these countries is less than 3°C thus resulting in very large temperature range between the winter and summer seasons. The 4°C additional intra-seasonal difference can affect transition seasons.

Precipitation pattern changes are the most important aspect in the future climate. This is particularly important regarding the availability of water resources in the future. Winter precipitation change over EM is related to the change in the anticyclonic circulation in the A2 case which is also in good agreement with the previous study of Giorgi[7]. We note the strong resemblance of our simulated climate change pattern (A2 minus RF) over EM and the results obtained by Eshel[12] which was based on the analysis of the NCEP reanalysis and stations data. They demonstrated that this pattern is associated with North Atlantic variability. We therefore infer that climate change over EM is in response to the modulation of the North Atlantic variability by global warming. The precipitation decreases by 24% in A2 over southeastern Turkey (upstream of Euphrates and Tigris basin) in winter. These two rivers are the main water resources of the region. Thus our results indicate the potential for major reduction in water availability under the projected climate change conditions.

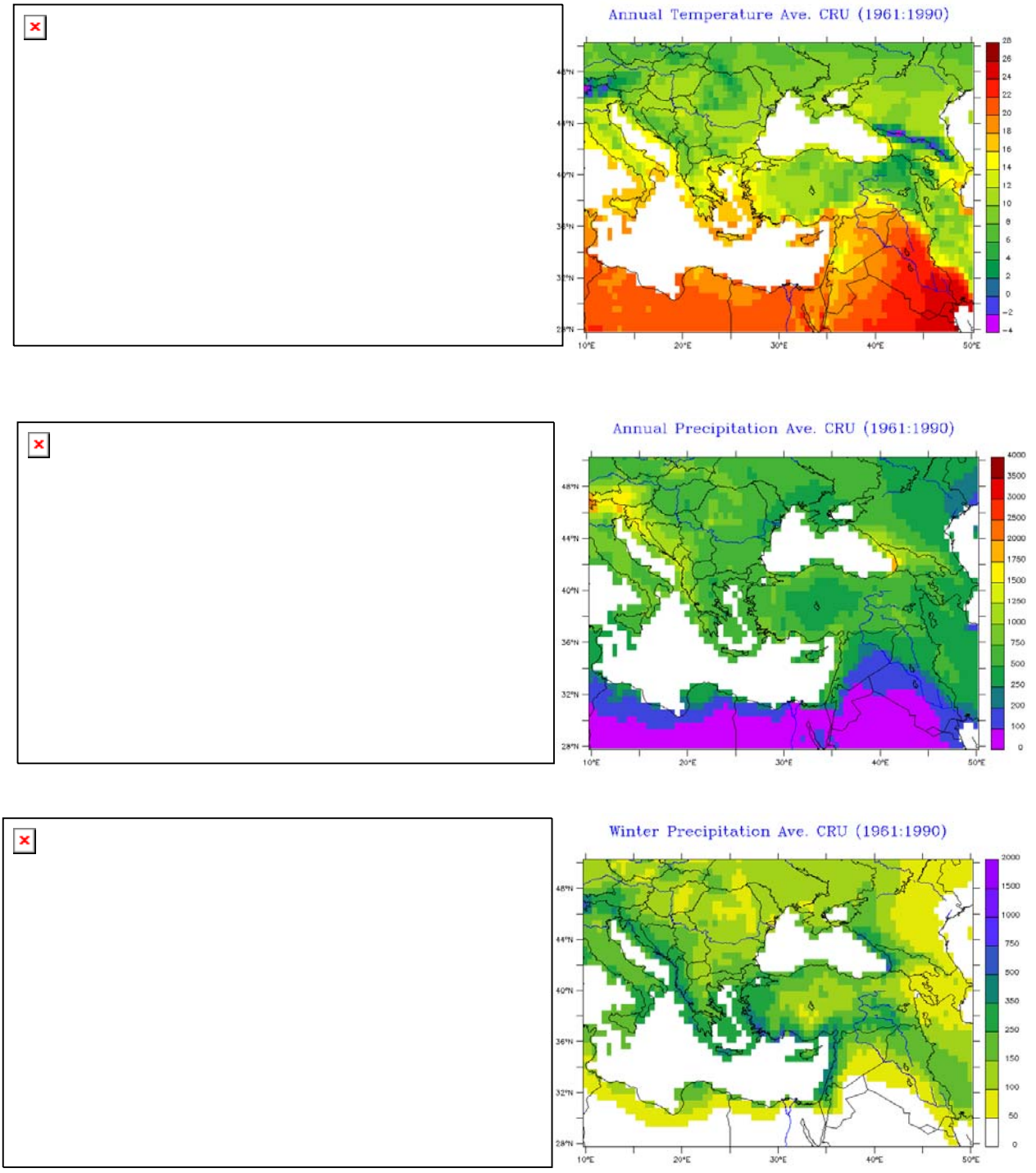

Figure 1. Compare to RegCM3 RF (left side) versus observation (right side) results. 30 years (1961-1990) temperature mean (upper), precipitation mean (middle) and winter precipitation mean (lower).

Considering the social economic diversity of the EM region, our climate change projections indicate considerable increased strain on the future water-dependant social-economic activities of the region. . We believe that the results of our regionalized study could have important implications in the development of strategies for dealing with the climate change problem for the EM region.

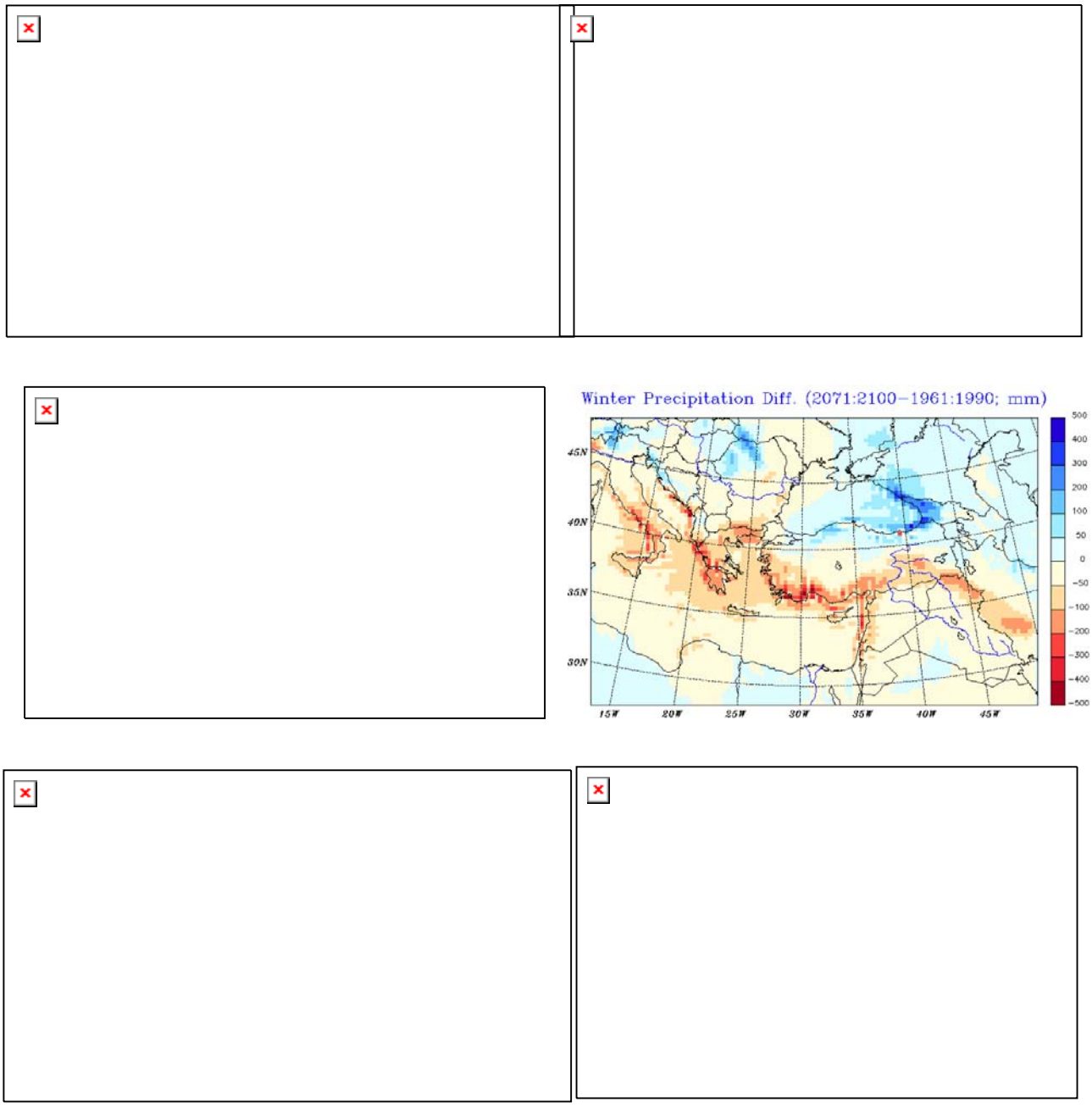

Figure 2. Temperature A2 minus RF (annual: upper left; summer: upper right), Precipitation A2 minus RF (annual: middle left; Winter: middle right; Autumn: lower left), Winter precipitation percent change (lower right)

REFERENCES

[1] Giorgi, F., C. Shields, and G. T. Bates, Regional climate change scenario over the United States predicted with a nested regional climate model, *J. Clim*., 7, 375-399, 1994.
[2] Giorgi, F., L. O. Mearns, C. Shields, and L. McDaniel, Regional nested model simulations of present day and 2 CO2 climate over the central plains of the U. S., *Clim. Change*, 40, 457 493, 1998.
[3] Leung, L.R.,, Qian, Y., Bian X., Washington, W.M., Han J, and Roads J.O., 2004, Mid-Century Ensemble Regional Climate Change Scenarios for the Western United States, C*limatic Change,* 62, 75-113.
[4] Chen M., D. Pollard, and E. J. Barron, 2003, Comparison of future climate change over North America simulated by two regional models, *J. Geophys. Res,* 108, D12,4348.
[5] Murphy J, 2000, Predictions of Climate Change Over Europe Using Statistical and Dynamical Downscaling Techniques, *Int. J. Climatol*. 20: 489-501.
[6] Giorgi F., B. Xunquiang, J. S. Pal, 2004, Mean, interannual variability and trends in a regional climate change experiment over Europe. I. Present-day climate (1961-1990), *Cl. Dyn*., 22, 733-756.
[7] Giorgi F., B. Xunquiang, J. S. Pal, 2004, Mean interannual variability and trends in a regional climate change experiment over Europe. II: Climate change scenarios (2071-2100), *Cl. Dyn*., 23, 839-858.
[8] Hirakuchi, H., and F. Giorgi, 1995, Multi-year present and 2xCO2 simulations of monsoon climate over Asia and Japan with a regional climate model nested in a general circulation model, *J. Geophys. Res*., 100, 21,105 21,126.
[9] McGregor, J.L. and K. Walsh, 1994, Climate change simulations of Tasmanian precipitation using multiple nesting, *Journal of Geophysical Research,* 99, D10, 20,889-20,905.
[10] Alpert P., I. Osetinsky, B. Zivb and H. Shafir, 2004, Semi-objective classification for daily synoptic systems: Application to the Eastern Mediterranean climate change, *Int. J. Climatol.* 24: 1001–1011.
[11] Krichak S. O., M. Tsidulko, and P. Alpert, 2000, Monthly Synoptic Patterns Associated with Wet/Dry Conditions in the Eastern Mediterranean, Theor. Appl. Climatol. 65, 215±229.
[12] Eshel G, B. F. Farrell, 2000, Mechanisms of Eastern Mediterranean Rainfall Variability, *J. Atmos. Sc.*, Vol. **57** (19), pp. 3219-3232, October 1 2000.
[13] Evans J. P., R. B. smith and R J. Oglesby, 2004, Middle East climate simulation and dominant precipitation processes, Int. J. Climatol. 24: 1671–1694.
[14] Dickinson, R. E., A. Henderson-Sellers, and P. J. Kennedy, 1993: Biosphere-Atmosphere Transfer Scheme (BATS) version 1E as coupled to the NCAR Community Climate Model, Tech. Rep. TN-387+STR, NCAR, Boulder, Colorado, pp. 72.
[15] Pal, J. S., E. E. Small, and E. A. B. Eltahir, 2000: Simulation of regional scale water and energy budgets: Influence of a new moist physics scheme within RegCM, J. Geophys. Res., 105, 29,579–29,594.
[16] Grell, G. A., 1993: Prognostic evaluation of assumptions used by cumulus parameterizations, Mon. Wea. Rev., 121, 764–787
[17] Arakawa, A., and W. H. Schubert, 1974: Interaction of a cumulus cloud ensemble with the large-scale environment, Part I, J. Atmos. Sci., 31, 674–701.
[18] Pal J.S., F. Giorgi, X. Bi, Nellie Elguindi, F. Solmon, X. Gao, R. Francisco, A. Zakey4 J. Winter, M. Ashfaq, F. Syed, J. L. Bell, N. S. Diffenbaugh, J. Karmacharya, A. Konar, D.

Martinez, R. P. da Rocha1, L. C. Sloan, A. Steiner, 2005, The ICTP RegCM3 and RegCNET: Regional Climate Modeling for the Developing World. BAMS, Submitted.
[19] Lin, S.-J., 2004: A vertically Lagrangian finite-volume dynamical core for global models. *Mon. Wea. Rev*., 132, 2293-2307.
[20] E. Coppola, F. Giorgi, 2005, Climate change in tropical regions from high resolution time slice AGCM experiments, Quarterly Journal (Royal Meteorological Society), 131 (612): 3123-3145 Part B
[21] Yin, J. H., 2005, A consistent poleward shift of the storm tracks in simulations of 21st century climate, *Geo. Res. Let.* , VOL. 32, L18701, doi:10.1029/2005GL023684

CLIMATE CHANGE IN CENTRAL EUROPE IN CORRELATION WITH CHANGES OF SUN ACTIVITIES

Horst Borchert

Johannes-Gutenberg University Mainz, Geographic Institute Westring 159, D-55120 Mainz, Germany, BCHT01@aol.com

ABSTRACT

Continuous measurements of air pollution and meteorological components in Central Europe within the last 30 years showed between 1987 and 1991 very strong changes of their values. As a consequence SO2-based winter-smog alert-systems were cancelled and Ozone-based summer-smog alert-systems were introduced. These changes of air pollution were accompanied with a strong increasing jump of the long time trend of global radiation of nearly 2 mW/cm2 (yearly averages) and of ground-near temperature of about 1,2 °C in Central Europe during this short time interval. These climatic changes were accompanied with the reduction of cloudiness which was in correlation with the reduction of cosmic rays (neutrons) especially strong within the 22nd sunspot period. Sun observations of NASA showed since this time stronger increase of eruptions of protons transporting solar winds, which were reducing cosmic radiation by magnetic deflections. This effect caused reductions of cloudiness partly till about 30 %. Therefore this "Climate Jump" with its increasing ground near temperature, causing the above mentioned changes, is sun made. Moreover the North Atlantic Oscillation (NAO) showed correlation with neutron flux, which stables the assumption, that there is a causal connection between sunspot controlled cosmic rays and cloudiness: The found correlations between these components give a causal chain which leads to the knowledge, that increasing sun activity causes the increase of global temperature and as a consequence also the observed prolongation of the growing season and further more increasing UVB-radiation, what means finally climate change in Central Europe,.

Keywords: Air pollution, Climate change, Global temperature, Global radiation, Cloudiness, Cosmic radiation, Sunspots, Neutron flux, 22nd Sunspot period, North Atlantic Oscillation, Growing Season, Stratospheric Ozone

INTRODUCTION

The widely forested German country Rhineland-Palatine with its industrialised towns Mainz and Ludwigshafen seems to be an area representative for Central Europe in geographic sense. Air Pollutions and meteorological components there are measured by the telemetrical controlled system ZIMEN with 31 measuring stations in forested regions and in towns (ZIMEN, 2005). Comparing long time trends of these components one can see remarkable coincidental changes between 1987 and 1991 (Fig.1). The strong decrease of SO2 and PMx was in earlier times seen mainly as a result of successful legal management to reduce emissions. The strong increase of anthropogenic O3-concentrations was first seen mainly as a result of the increase in traffic (Borchert, H., 1998). But these strong changes of pollutants since 1987 were accompanied with very strong increase of ground-near air temperature and of

intensity and duration of sunshine, caused by reductions of cloud cover. Further investigations lead to the knowledge that these sudden changes of anthropogenic air pollutions in this short time interval were also caused by strong changes of meteorological components which were relative strongly controlled by extraterrestrial influences (Borchert H., 2004). In the following paper is shown by correlations the causes of this knowledge.

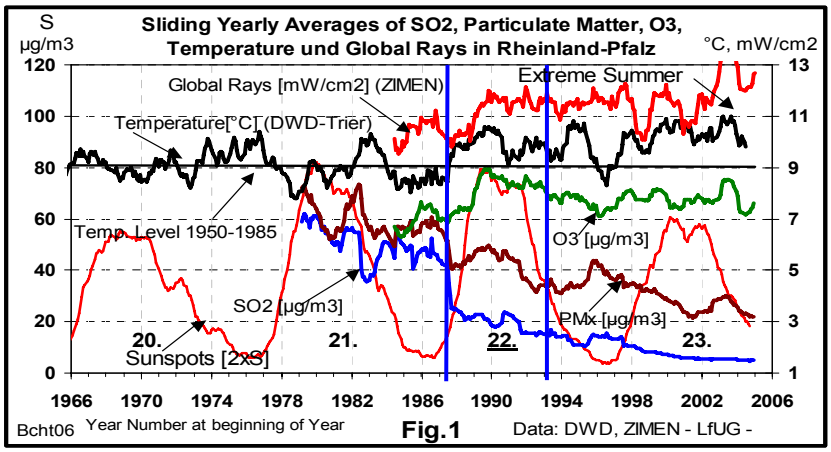

Figure 1. Air-pollution and meteorological components in West Germany

Climate Change in Central Europe

The simplest method to describe climate is to study temperature (Figure 2).

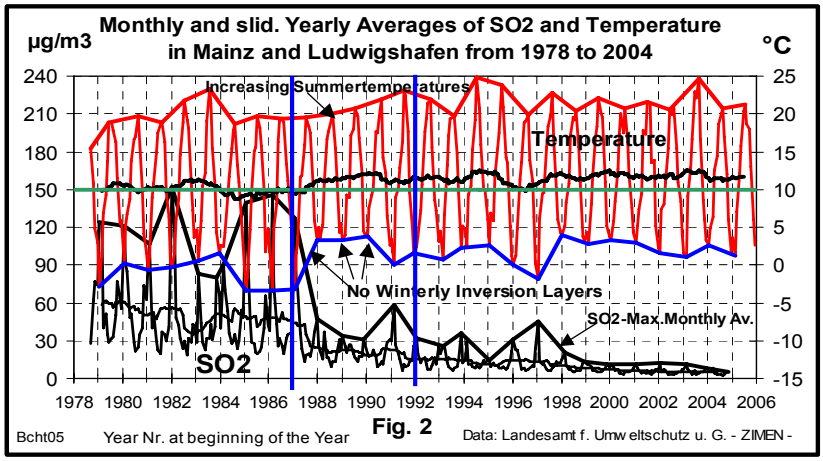

Figure 2. Monthly and sliding Yearly Averages of SO2 and Temperature in Mainz and Ludwigshafen from 1978 to 2004

Yearly averages of temperatures in the west of Germany show since 1988 a relative strong increase of about 1.2 °C and remain with this higher value until now (Fig. 2). Before this jump the monthly averages in wintertime were relatively low (~ 0°C). SO2 showed high values. It came partly from power plants of the eastern COMECON countries, transported by cold and dry north eastern winds beneath inversion layers of about 800 m height. After 1988 these cold eastern winds vanished. Since 1990 the monthly temperature in wintertime was higher than 2 °C before. SO2 and dust decreased very strong. After 1991 these emissions were stopped by legal reductions of emissions of power-plants and also by collapse of the emitting industries in the eastern countries. In summer time the temperatures were

continuously increasing from 1987 to 1991 of about 3 °C. After this "**jump of temperature"** the long time trend of the warmest monthly temperatures was almost constant until now.

Looking for longer time measurements of meteorological components than ZIMEN we used data of the Deutsche Wetterdienst (www.dwd.de). The long time trend of temperature at all measuring stations does not show any significant increase between about 1940 and 1986. **The main increase of the temperature in Central Europe happened between 1988 and 1990.** From 1991 on until now the sliding yearly averages of the ground near temperatures (measured 2m above ground) are oscillating around a level which is between 0.8 °C and 1.5 °C higher than the level before. Sliding yearly averages of the temperature show an oscillation period of about three years. Therefore the sliding three years averages demonstrate the jump of temperature between 1987 and 1992 much clearly (Figure 3).

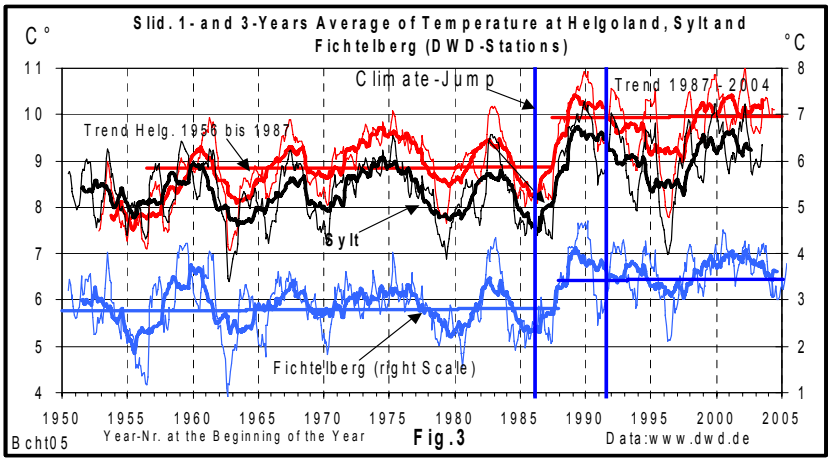

Figure 3. Temperature at Helgoland Sylt and Fichtelberg

This Jump of the temperatures occurs at all sites in Central Europe. At higher positioned stations the jump is smaller than in valleys. But all stations show the same trend (Figure 4).

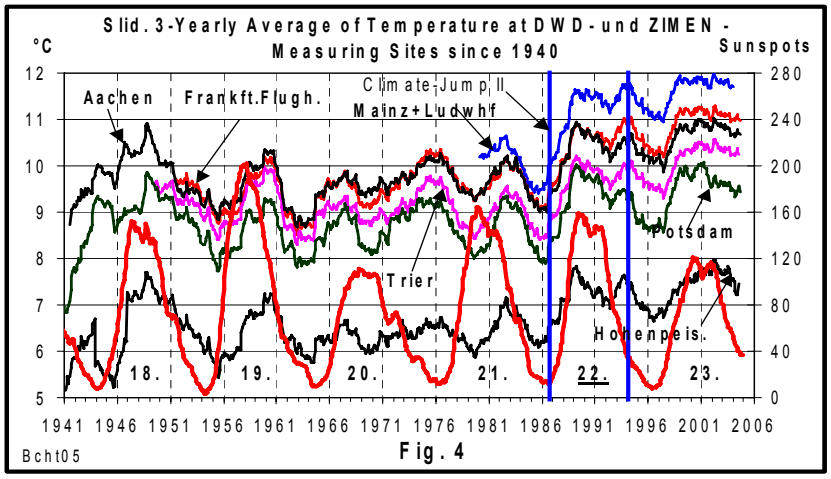

Figure 4. Temperature since 1940 in comparison with Sunspot-Frequencies

The jump of the temperature at all stations, we call it “Climate Jump II”, happens with in the 22nd Sun spot period, which appeared between 1986 and 1996. During this time Earth was influenced by a lot of very strong extraterrestrial events (Thompson R., 2004), (STEDATA 22, 2003). Therefore we ask for any possible causal connections between changes of sun activity and observed climate changes. Researches in this direction have already been done in earlier times until now (Karin Labitzke, 1987, 2005).Sun intensity (Global radiation) was continuously measured to study anthropogenic O3-formation. Between1987 and 1990 Global Rays were relatively strong increasing of about more than 1,5 mW/cm2 (Yearly Average) (Fig.5). It was found agreement between global rays and sunshine duration (Fig.6). Further more there was a plausible agreement between O3 - development and global radiation. O3 is mainly produced by photolysis of the anthropogenic precursor NO2 in presence of Hydrocarbons in traffic regions and towns. It is transported into the forested regions far away from these anthropogenic precursors. O3 shows a strong increase between 1987 and 1990 too.

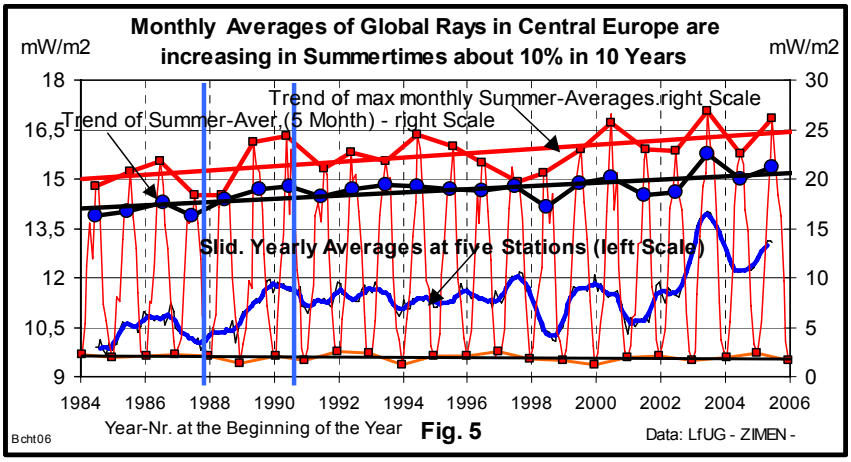

Figure 5. Increasing Global Radiation, measured at 5 sides in Central Europe

The yearly averages of Global Radiation were also increasing during this short time about 1.8 mW/cm3 and caused an increase of the yearly averages of temperature of 1.2 +- 0.3 °C.

..

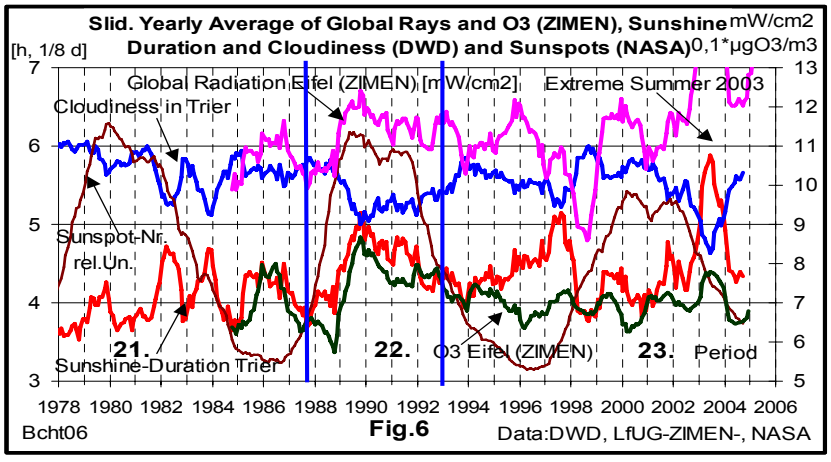

Figure 6. Sliding Yearly Averages of Global Rays and O3 (ZIMEN), Sunshine-Duration and Cloudiness (DWD) and Sunspot-Frequencies (NASA)

It is obvious that global radiation is strongly modulated by Cloudiness (see extreme summer 2003). The measurements of Global Radiation at 10 sites showed a strong increase of Sunshine intensity between 1987 and 1992, sorted by the geographical altitude. This phenomena pointed to strong influence of cloudiness which modulates temperature. **Therefore one must look for possible influences on Cloudiness, which controls Sunshine and in consequence anthropogenic O3 and ground near Temperature.**

These strong changes of all components were lying in the time range of the 22nd Sunspot period with its already mentioned extreme terrestrial influences. Therefore one should seek for possible links between Sunspot frequencies and terrestrial meteorological components.

Sunspots and Cosmic Rays

According to a theory of Marsh and Svensmark (1998), (Eur. Org. for Nucl. Res. CERN, 2000) secondary particles of the extragalactic cosmic rays produce clouds in air which is saturated with water like in a **Wilson Fog Chamber** (1911). To study the production of these secondary particles of cosmic rays several physical institutes worldwide are measuring the neutron rates since 1958 (World Data Centre C2, 2005). Besides other particles Neutrons are formed through nuclear collisions of extra galactic cosmic radiation (mostly protons) interacting with the atmosphere. Structure and percentage of the reduction of neutrons depend only from their geographic altitude (Figure 7)

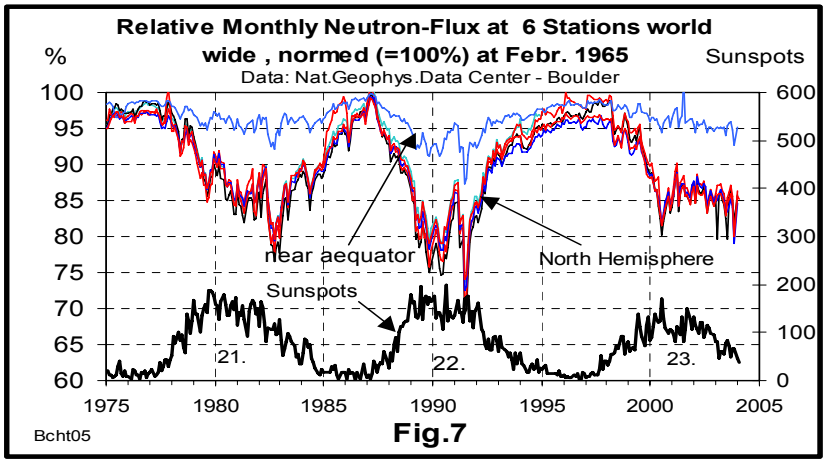

Figure 7. Relative Monthly Neutron-Flux at 6 Stations world wide, normalized (=100%) to February 1965

Sunspots are accompanied by soft Röntgen - Rays of 0,01 to 1 nm (Flares), which are produced by magnetic deflection of sunspot emitted protons and electrons. They are reaching the Earth after 8 minutes and mark the starting point of the current of protons and electrons (sun wind), which have velocities of more than 300 km/sec and reach the Earth several hours later (www.spaceweather.com). The "Sun wind" deflects the cosmic rays, which are high energetic protons, coming from extragalactic sources (so far as we know), and reduces the secondary particles in the lower atmosphere. There is a good correlation between reduction of neutron flux and sun spot frequency that means Sun spots are controlling the intensity of secondary particles of the cosmic rays in the atmosphere (Figure 8)

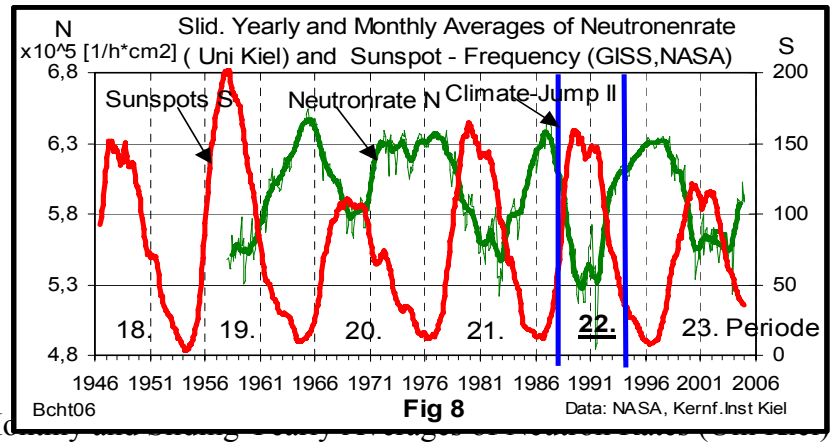

Figure 8. Mo and Sunspot-Frequencies (NASA)

If the secondary particles of cosmic rays would produce clouds, then there exists a link between sun activity and terrestrial climate change. Data collected from satellites have shown that the amount of low clouds over the earth closely follows the amount of secondary particles of extra galactic cosmic radiation. This effect (max 30 %) depends not only on the number of sunspots but especially of their energetic efficiency. **With this method the Sun opens its way to the earth and produces more direct global radiation.** This process works always und modulates the terrestrial climate. One can find harmonic correlations between the sun periods and the oscillating global temperatures (Labitzke, K. et al., 1988), (Scafetta and West, 2003). During the 22nd and actual 23rd period relative often extremely high energetic mass ejections from the sun were observed, especially in Spring and Autumn of 1989.

The time rows of the Neutron rates, measured by the Institute of Physics of the University in Kiel, are in a very good correspondence with all measurements of cosmic rays world wide.

They are very good negative correlated with the time rows of the sunspot frequency (Roehrs, 2005) (Fig.8). Stations in the north of the 40th Latitude have nearly the same loss of cosmic rays and more than twice of equatorial places (Huancayo): Therefore it seems to be plausible that the averaged increase of global temperature is smaller in the equatorial region (0.5 to 1 Degree C/100 Years) than in the northern hemisphere (2 to 4 Degrees/100 Years) (Gray, V.R., 2003).

Neutron Rates and Cloudiness

To prove the thesis of Svensmark, there are in the following Figures time rows of cloudiness compared with Neutron-flux. in Central Europe. .

.

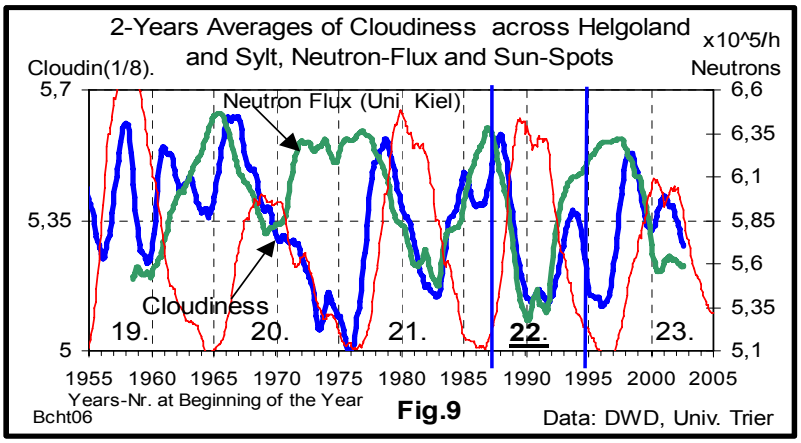

Figure 9. Cloudiness, averaged over **Helgoland and Sylt** (DWD), and Neutron Flux (Uni Kiel)

The sliding 2-Years Averages of the Islands Helgoland and Sylt in the eastern part of the North-Sea show a lot of resonance with the alternations of Neutron-flux. Especially during the 22nd Period there is a good correlation between the reduction of cosmic rays and clouds.

A rough estimation gives, that the reduction of the Cosmic Rays of about 17 % may lead to a reduction of Cloudiness of about 13 %. This effect causes an increase of the averaged yearly ground near temperature of about 1.2 +- 0.3 °C in Central Europe.

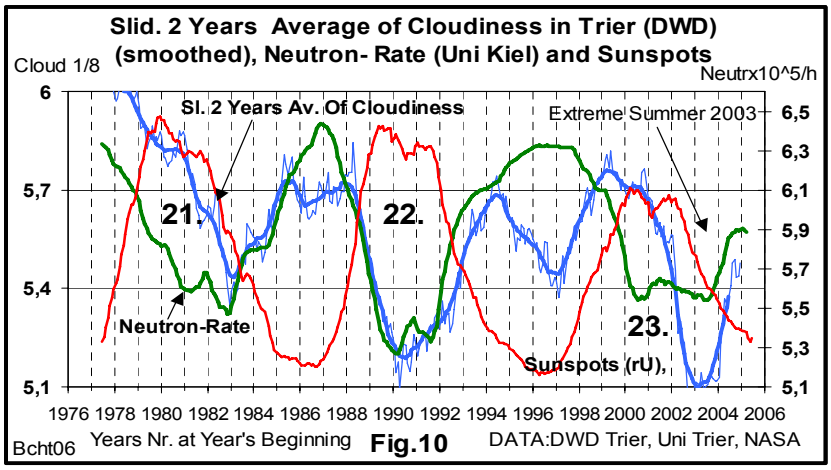

Figure 10. Sliding 2-Yearly Averages of Cloudiness at **Trier** (DWD), Neutron Rate (Uni Kiel) and Sunspot-Frequencies (NASA)

One finds this correlation at all measuring sites of the DWD from the North-Sea (Figure 9) and to the south of Germany near the Alps and it seems to sustain the postulation of Svensmark.

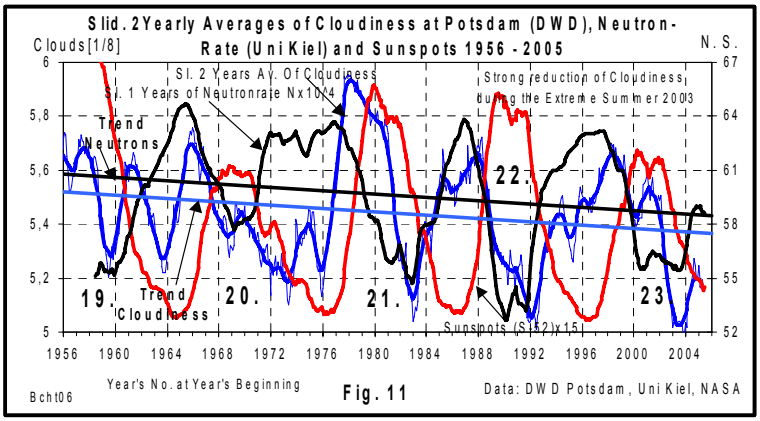

Figure 11. Cloudiness at Potsdam (DWD) and Neutron-Rates (UNI-Kiel)

Therefore one can suppose, that clouds periodically in the range till nearly 30 % are really produced by drops which are produced by cosmic rays as micro aerosols. This supposition seems to be stabilised by similar behaviour of the long time trends of neutron flux and cloudiness (Fig.11)

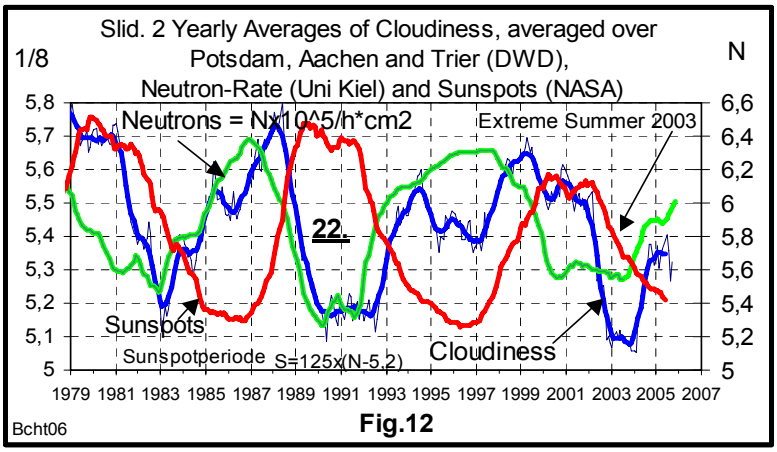

Figure 12. Comparison of Neutron-Rate with delayed Cloudiness

If there is a causal connection between cloudiness and cosmic rays, than there exists a link of the controlling connection between sun activity and terrestrial climate change.

One gets best correlations (K~0,75, values between 1980 and 2005, 2Yearly averages) between Cloudiness and Neutrons by using a delaying time of cloudiness of about 10 month in relation to time rows of Neutron rates.. This effect seems to be caused by the delaying inertia of the ocean. Furthermore there is another systematic destruction of the general correlation: After every new increase of by reduction of cosmic rays reduced cloudiness there

exists systematic a certain "intermediate reduction" of cloudiness, which is modulated by sunspot frequency too. This systematic effect is not yet understood.

North Atlantic Oscillation (NAO) and Sun Activity

There exists a good known correlation between the North - Atlantic- Oscillation and the behaviour of the weather in Central Europe, for instance the cloudiness (Fig. 13). The NAO-Index shows the time rows of the Difference of Air Pressure measured at Azore - Islands and at Iceland.

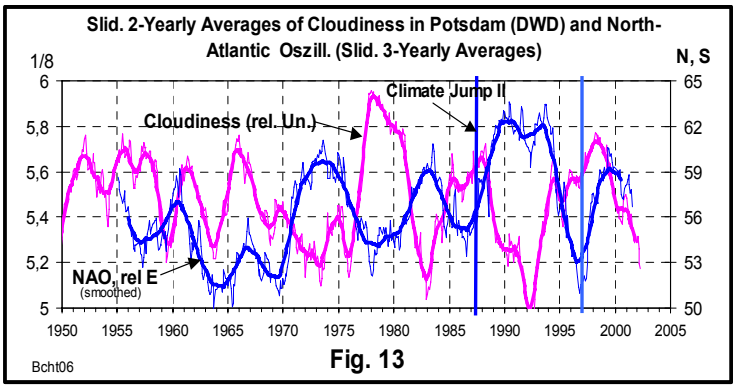

Figure 13. Cloudiness in Potsdam (DWD) and North- Atlantic Oscillation Index

As a consequence there exists an anti correlation between changes of the NAO-index. and Neutron rates (Fig.14)

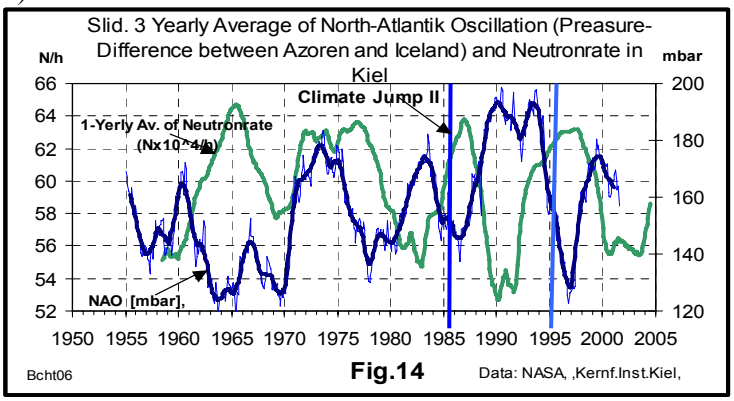

Figure 14. North-Atlantic Oscillation Index and Neutron Rate (Uni Kiel)

The opposite correlation between the NAO-index and Neutron rate in Fig. 14 gives rise to the opinion, that cosmic radiation controls via "Swensmark-Effect" the NAO-Index and the climate in Central Europe. Between the periodic changing sun activity and its influence on the earth's meteorology one can observe a certain delay-time of a half to one year, possibly caused by the inertia of the ocean.

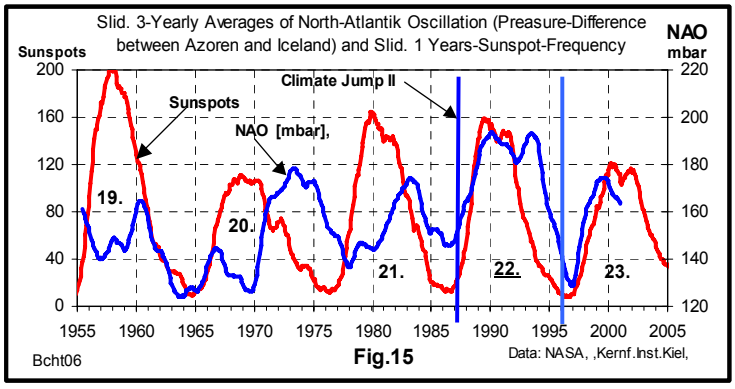

Figure 15. North-Atlantic Oscillation Index and Sunspot-Frequencies

Cosmic Rays, Temperature and Growing Season

On this way there is a causal chain between sun activity and development of terrestrial temperature: Strong changes of climate components between 1987 and 1991 seem to be a consequence of a not normal increase of sun activities with strong reducing cloudiness and increasing sun shine. During this climate jump ground level temperature increases relatively strong (about 1,2 °C +- 0,3 °C) and remains at higher long time level up to now.

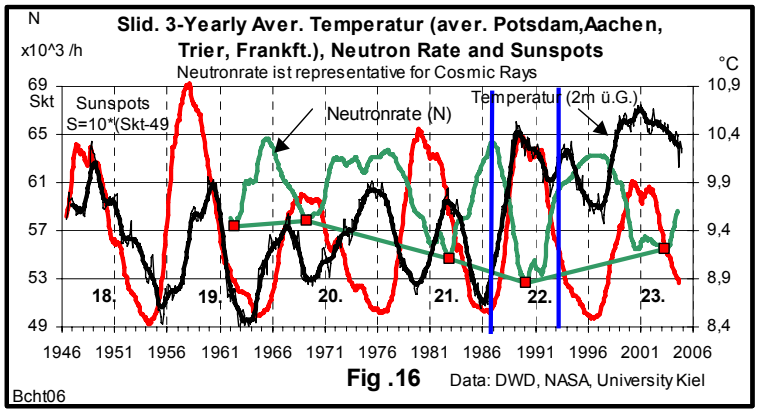

Figure 16. Temperature, Neutron-Rates and Sunspot Frequencies

As a consequence of this Climate Change at the end of the eighties one can observe a strong influence into biological systems: Fig.16 shows a correlation between the reduction of starting time of growing season in Central Europe and decreasing Neutron rates. The prolongation of the greening time of plants (Chmielewski, F.-M. and Rötzer, T.) starts just with the strong reduction of Neutron Rates with beginning of the 22. Sunspot period**. Finally the length of growing season seems to be controlled by sun activities too.**

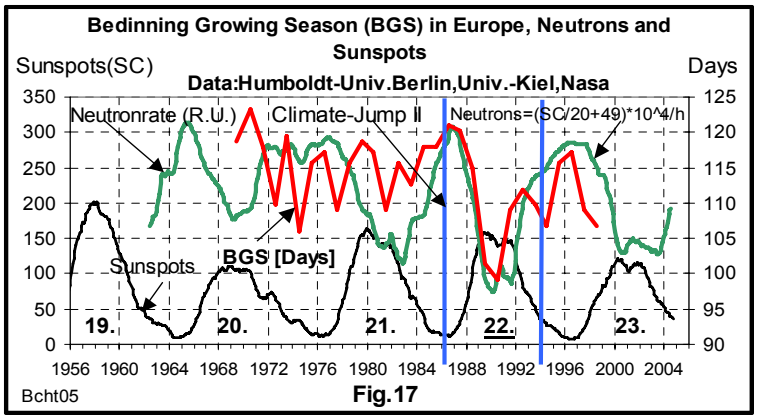

Figure 17. Beginning Growing Season (BGS) in Europe, Neutron Rates and Sunspot Frequencies

Sun Activity, Cosmic Rays, O3-tot-Thikness and terrestrial UVB

Looking for further possible connections between changes of Sun activities and terrestrial climatic effects one can see correlation between changes of sun controlled cosmic radiation and ground near UVB-Radiation. There exists a very good known anti correlative change of the thickness of the stratospheric Ozone layer and ground near UVB-Radiation (DWD Hohenpeisenberg). The reduction of O3 tot - thickness mostly is seen to be caused by volcano emissions of dust, SO2 and NOx and by anthropogenic Cl, disturbing the Chapman-Cycle.

But there is an anti cyclic behaviour between O3-tot-thikness and Cosmic Rays..Further more there starts the reduction of O3-tot-thickness with the end of 21. sun spot period in correlation with the reduction of Cosmic rays too (Fig. 18). That leads to the question for an influence of

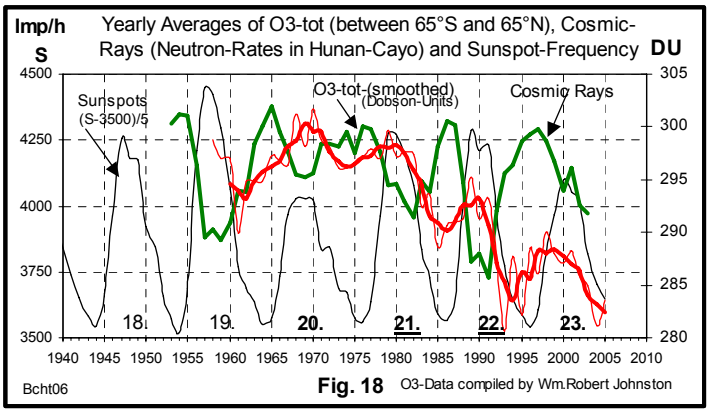

Figure 18 . Time rows of Ozone- Layer in comparison with sun spot frequency

the changing sun activity in to the increase of UVB-radiation. The reduction of Neutron-flux is the real degree of force of sun activity in direction to the earth (sun wind). The time rows of stratospheric O3 - layer in the earth's range between 65°South and 65°North show to be in correlation with cosmic radiation (Neutron-Flux). It leads to the supposition, that the reduction of the stratospheric O3tot-layer may be caused by influencing the Chapman Cycle by increasing solar radiation (protons of the solar wind) as a consequence of increasing sun

activity, not only by increasing anthropogenic Cl-Production. It follows, that the increasing UVB-Radiation in the last twenty years seems to be naturally caused too.

Sun Emissions of Protons

To look for further observations to stabilise the sun made climate change during the eighties we studied by NASA published satellite measurement values. Fig 19 shows the monthly satellite-measured sums of Protons with energies higher than 10 MeV These strong "Sun Winds" started with the 22nd Period 1989 with an extremely large sunspot in March and continued in October with great solar mass ejections.

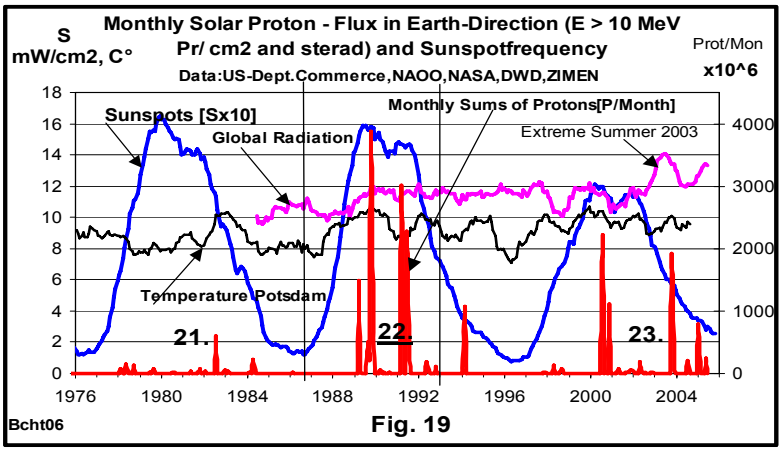

Figure 19. Monthly Solar Proton-Flux in Earth Direction, Sunspot Frequencies, Terrestrial Global Rays and ground near Temperature since 1976

These proton currents produced blackouts at electric power plants in the northern hemisphere and disturbed wireless contacts between earth and aeroplanes and satellites, they produced auroras seen at the Equator. Such strong solar mass ejections occurred repeatedly during the 22nd and in the 23rd period until now. The NASA comments this behaviour "The Sun Goes Haywire". One of the last great sun wind events influencing earth occurred at 15 January 2005 from a sunspot Nr. NOAA 720. This behaviour of the sun makes the fact plausible that terrestrial temperatures remains in tendency at a higher level than before 1988.

Global Temperature and Sunspots

This work deals with the question of the global warming: The time rows of global temperature show two jumps since 1900, no continuous increasing as often postulated: The first "Climate-Jump I" happens between approximately 1920 and 1935, the second "Climate Jump II" starts about 1987 (Fig. 20). The second jump seems to be mainly caused by special solar activities like described in this paper.

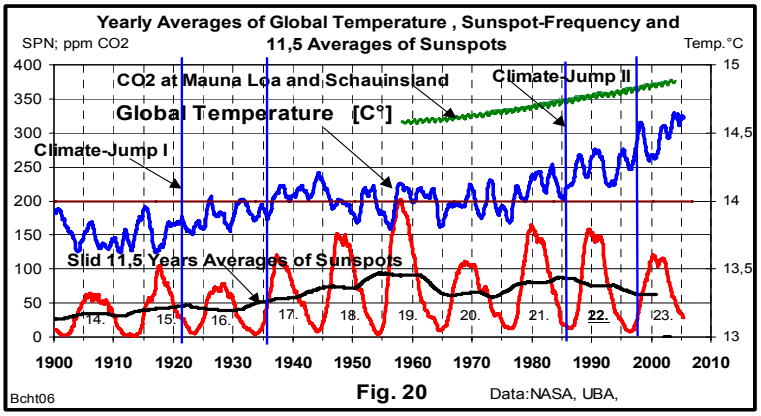

Figure 20. Global Temperature, Sunspot Frequencies and CO2.

Also other observations point to extraterrestrial influences causing climate change: The trend of global temperature increases with decreasing length of the basis of sunspot periods (K~0,8). Continuous reduction of Be10 and C14 since about 1880 points to decreasing cosmic radiation, caused by increasing Sun activity. That leads via Svensmark-effect to reduction of cloudiness and increasing global temperature. The increase of CO2 is continuous and shows no jump. There is a modulation of the increasing averages of the CO2-concentration of Hawaii by the 22nd Sun spot period. The Increase of CO2 concentrations seem to be mainly powered by increasing temperature and finally by increasing Sun activity. The main cause of the sudden climate change during the eighties was the sudden increasing number of extreme height energetic mass ejections of the sun, possibly caused by a close nearby constellation of the torques of the Sun and Sun System (Landscheidt Th., 2004). Further studying of these phenomena with further measured data may lead also to answer the question, why the global warming seems to tend today to lag behind the increase of some greenhouse gases without Methan.

CONCLUSION

In the last thirty years the main increase of temperature in Central Europe happened within the short period of 4 years between 1987 and 1991. This event was coincidental with increasing sun activities, increasing intensities of sun winds and with decreasing cosmic radiation (neutron rates) with the consequences of reducing cloudiness, increasing global radiation and increasing ground near temperature. It leads to the opinion that Climate Change in the past century in Central Europe seems to be mainly Sun made.

REFERENCES

Borchert, H., 1998. The Trend of Air Pollution in Western Germany in the past Twenty Years as a Result of Clean Air Management, 11th World Clean Air Congress IUAPPA, Durban, S.Africa, ISBN 0-620-23064-9. www.UMAD.de

Borchert, H., 2004. Changes of Air Pollution in Central Europe in Correlation with

Changes of Climate and Sun Activities, 13th World Clean Air Congress, London, August 2004, Nr.39, CD, www.UMAD.de.
Chmielewski F.M.; Rötzer, T., 2000. Phenological Trends in Europe in Relation to Climate Change, Agr.Met. 07,2000, www.agrar.hu-berlin.de/pflanzenbau/agrarmet
Cugnon, P. et al., 2005. Online catalogue of the sunspot index, sidc.oma.be
Deutscher Wetterdienst, 2005: Data of temp., cloudiness, sunshine: www.dwd.de.
European Organisation for Nuclear Research, 2000, A Study of the Link between Cosmic Rays and Clouds with a Cloud Chamber at the CERN PS, CERN/ SPSC 2000-021,P317, Apr. 24. 2000, xxx.lanl.gov/abs/physics/0104048.
Gray V. R., 2003. Regional Temperature Change.www.john-daly.com/guests/regional.htm.
Labitzke, K. et al (2005).:"Sunspot, theQBO, and the Stratosphere in the North Polar Region,,." Meteor. Z., http://strat-www.met.fu-berlin.de/abstracts/langematz2003.html
Marsh, N. and Svensmark, 2000.Cosmic Rays, Clouds, and Climate. Space and Science Reviews. pp 1-16, Kluver Acad. Publishers. www.dsri.dk.
NASA, 2004. Record-setting Solar Flares"; www.spaceweather.com/solarflares.
Roehrs, 2005 : Kieler Neutronen-Monitor-Messung. ifkki.kernphysik.uni-kiel.de.
STEDATA 22, 2003. Database for 22nd Solar Activity, Dep. of Earth Science, Baraki University: shnet1.stelab.nagoya-u.ac.jp/omosaic/step/stedata.htm.
Scafetta, N., West, B. J., 2003. Solar Flare Intermittency and the Earth's Temperature Anomalies. Phys. Rev. Lett. 90,248701
Landscheidt, Th. 2004. Klimavorhersage mit astronomischen Mitteln?
Schroeter Institut, Research in Cycles of Solar Activity, Nova Scotia, Canada, www.solidarität.com
Thompson, R. 2003. Solar Cycle Number 22 (1986 – 1996) in Review, Australian Government, IPS Radio and Space Services: www.ips.gov.au/Educational/2/3/2
World Data Centre C2 for Cosmic Rays, www.env.sci.ibaraki.ao.jp/data
Zentrales Immissionsmeßnetz (ZIMEN): Data from 1978-2000: Monthly bulletins ISSN 0720-3934; Since 2001: www.UMAD.de

GENERATION OF WIND STORM IN THE MOUNTAINOUS COAST

Hyo Choi

Kangnung National University Kangnung, Korea, choihyo@kangnung.ac.kr

ABSTRACT

The evolution of internal gravity waves was investigated under the development of katabatic wind, when mountain-land breeze associated with westerly synoptic wind blowing over the top of the mountain in the west toward the East Sea of Korea (called Japan Sea) from August 13, 2004 through August 16, 1995 and March 9, 2004 through March 11, using three dimensional non-hydrostatic numerical models such as both Local Wind Model and MM5 model. As westerly synoptic wind blowing over the top of the mountain toward the coastal sea in the east, during the day was hindered from the strong intrusion of upslope wind associated with sea-valley wind from the East Sea toward the top of the mountain, two different kinds of wind regimes confront each other in the mid of eastern slope of the mountain and the upslope wind goes up to the height of 1700m over the ground, becoming an easterly return flow in the upper level of the sea. Below sea-breeze front, two kinds of circulations were detected with a small circulation over the coast and a large one from the coast to the open sea. Then, katabatic wind did not exist in the lee side of the mountain. Near the sunset, synoptic westerly wind blowing over the top of the mountain in the west toward the sea side in the east became katabatic wind under the weaken sea-valley breeze. As nighttime went on, synoptic westerly wind became a strong downslope wind (katabatic wind), which was under the change of sea-valley wind into mountain-land breeze, due the cooling of the ground surface at night, but the sea-valley circulation still existed in the coastal sea. Thus, katabatic wind in the inland basin of the coast and sea-valley wind circulation in the coastal sea produced the development of internal gravity waves over the coastal sea. After midnight, katabatic wind should be intensified by both westerly synoptic wind and mountain-land breeze induced by more nighttime radiative cooling of the ground surfaces, resulting in the formation of a strong downslope windstorm. The wind storm caused the development of internal gravity waves with hydraulic jump motion in the eastern side of the mountain from the ground surface of the coast bounding up toward the upper level of the sea, while relatively moderate wind on the sea surface.

This research may be applicable to the prevention of forest fire and to the management of winter water supply. This work was funded by the Korea Meteorological Administration Research and Development Program under Grant CATER 2006-2308.

SHALLOW LAKE ECOSYSTEMS OF SEMI-ARID TO ARID MEDITERRENEAN REGION AND GLOBAL WARMING: PREDICTIONS FROM PRESENT

Meryem Beklioglu

Middle East Technical University, the Department of Biology, TR-06531, Ankara, Turkey, e-mail: meryem@metu.edu.tr

ABSTRACT

Shallow lakes are the most diverse with high ecological and conservation values among the other inland aquatic ecosystem. How changes in climate will affect the ecological state of shallow lakes is debatable. Few studies have experimentally tested the effects of increased temperature and nutrient enrichement. Long-term field data show that effects of warming on water quality can be contradictory and the net effect therefore difficult to predict. In Turkish shallow lakes located in a semi-arid to arid Mediterranean climate, where the hydrological changes are common phenomenones, are presumably very sensitive to water level fluctuations (WLF). Investigation on the relationships between WLF and submerged macrophyte development in five Turkish shallow lakes revaled that in all lakes, WLF emerged as a major factor determining submerged plant development. High submerged plant coverage was observed when the water level was low. Water level fluctutation is expected to be severe through global warming that lake levels are expected to go down. Consequently, more vegetation growth was expected of. However, warmer water temperature, low dissolved oxygen availability associated with longer hydraulic residence stimulated internal phosphorus loading and suppression of denitrification. These processes are likely to increase nitrogen and phosphorus availability and in turn, increased turbid water condition through global warming. Unders such turbid conditions submerged plant development were supressed. Furthermore, warmer conditions stimulated anoxic water that led to major fish kill that enhanced top-down control of turbid conditions and in turn stimulating submerged plant development. These two processess are likely to take place as common phenomenon uder warmer and drier condition, therefore, aquatic vegetation development and water clarity would depend on which of the processes would override the other.

Moreover, in semi-arid or arid Mediterranean freshwater lakes, sensitivity to hydrological conditions also has significant consequences for the in-lake concentration major ions, especially for determining the salinity. Current drier conditions increased salinity of freshwater lakes. Hydrological extremes (floods and dry periods) are predicted to follow from global climatic changes. Therefore, freshwater lakes in the region are predicted become more saline in the future. Increased salinity would likely to change species composition and diversity of shallow lakes.

WAVELET – BASED ANALYSIS OF RAINFALL RATE AND EROSIVITY

Zafer Aslan[1], Deniz Okcu[2], Ayfer Serap Sogut[2]

[1]Anadolu BIL Professional School of Higher Education, Florya, Istanbul, Turkey, zaferaslan@anadolubil.edu.tr
[2]Bogazici University, Kandilli Observatory and Earthquake Research Institute, Meteorological Laboratuary, Çengelkoy, Istanbul, Turkey

ABSTRACT

The purpose of wavelet analysis is to find out the cluster pattern of smooth versions of variables. Wavelet techniques which have been commonly used in the engineering problems in recent years are an alternative method to FFT algorithm. Functions can be approximated to any prescribed accuracy with a finite sum of wavelet transforms. The wavelet transform decompose a signal into a set of special basis functions that are wavelet functions. The wavelet expansion gives a time – frequency localization of the signal. This specification means that the most of the energy of the signal is well represented by a few set of wavelet basis functions. This can help in signal identification. After several introductions to apply wavelet in monthly variations of rainfall rate and water erosivity data in Marmara Region, small, meso and large scale effects on fluctuations are being demonstrated. Wavelet analyses helps to explain cross interactions between two variables. Results of this paper can be used to determine changes in climate and phenomenon such as ENSO and annual solar cycle.

Keywords: Wavelet, water erosivity, rainfall rate.

INTRODUCTION

Everywhere in the world where people change a natural ecosystem into agriculture, the land degrades (Pla Sentis, 1998). The visible part is erosion, when soil particles leave the land, transported by gravity, water or wind. Some erosion is natural but present rates are more than worrying (Aslan, 1997; Aslan et all, 2006).

Forests are a dominant biome of the earth and have a vital importance on environmental well-being. Leaves of the trees intercept and filter out dust particles from the air. Forests are regulator of climate and water flow, effective in releasing oxygen into the atmosphere and help reduce the extremes of heat during the day and cold at night (Aslan. and Tokgözlü, 2000; Skidmore, 2000).

In addition to vital contributions to the environment, forests provide many products and services. To encourage sustainable development, all renewable natural resources and forests have to be managed in a point of view based on the ecosystem principles. We can share there main groups the importance of soil as agricultural, industrial and economical. Studies show that soil is used by the first people, plant to grow started at least 8000 years ago. It has been since primary ages the industrial importance of soil (Türkeş, 1999).

Erosion which modern science gives importance and creates great problems in the world is the worldwide matter. In order to solve these problems, people are charged of great deal of responsibilities (Flanagen and Livingston, 1995).

MATERIAL AND METHODS

Study area

Monthly total rainfall rate values were considered in remote locations of Western Turkey (İstanbul, Edirne, Tekirdağ, Bilecik, Kocaeli, Bandırma, Çanakkale, Balıkesir, Bursa, and Adapazarı) between the years of 1901 and 2001 (New et al,1999; New et al, 2000), Table 1.

Table 1. Study area

Station	Latitude (λ)	Longitude (φ)
ADAPAZARI	41,00	30,50
BALIKESİR	39,50	28,00
BANDIRMA	40,00	28,00
BİLECİK	40,00	30,00
BURSA	40,00	29,00
ÇANAKKALE	40,00	26,50
EDİRNE	41,50	26,50
İSTANBUL	41,00	29,00
KOCAELİ	41,00	30,00
TEKİRDAĞ	41,00	27,50

Methods

Modified Fournier Index (MFI): The definition of these indices and risk classes are defined as below (Michiels and Gabriels, 1996). Modified Fournier Index (MFI):

$$MFI = \sum_{i=1}^{12} p_i^2 / P \qquad (1)$$

Where, p_i is monthly rainfall rate and P is annual rainfall rate.

Tablo 2. Description of MFI classes

MFI (range)	Description	Class
<60	Very low	1
60-90	Low	2
90-120	Moderate	3
120-160	High	4
>160	Very high	5

Wavelet Techniques: Wavelet is families of small waves generated from a single functions f(t) which is called mother wavelet. A sufficient condition for a function f(t) to qualify as a mother wavelet is given as (Siddiqi et all, 2002):

$$\int_{-\infty}^{\infty} |\ f(t)\ |^2\ dt < \infty \qquad (2)$$

The Fourier transform F of f(t) is defined as

$$F(w) = \int_{-\infty}^{\infty} f(t) e^{iwt}\, dt \qquad (3)$$

A function ψ(t) satisfying the following condition is called a continuous wavelet:

$$\int_{-\infty}^{\infty} |\ \psi(t)\ |^2\ dt = 1 \qquad (4)$$

and

$$\int_{-\infty}^{\infty} |\ \psi(t)\ |\ \ dt = 0 \qquad (5)$$

Higher order moments may be zero, that is,

$$\int_{-\infty}^{\infty} t^k \psi(t) dt = 0 \qquad \text{for} \quad k=0,\ldots,N-1$$

The wavelet transform of f(t) denoted by W_f (a,b) is defined as:

$$W_f(a,b) = \frac{1}{\sqrt{a}} \int_{-\infty}^{\infty} \Psi((u-b)/a)\, f(u) du = \int_{-\infty}^{\infty} f(u) \psi_{a,b}^{(u)} du \qquad (6)$$

where $\psi_{a,b}^{(u)} = \frac{1}{\sqrt{a}} \psi((u-b)/a)$ **(7)**

Here "a" is a scaling parameter, b is a location parameter and $\psi_{a,b}^{(u)}$ is often called continuous wavelet (or daughter wavelet) while ψ(u) is the mother wavelet.

$\left|W_f(a,b)\right|^2$ is called the scalogram of the function *f* and it can also be interpreted as energy density (Can et all, 2005),

$$\int_{-\infty}^{\infty} \left|W_f(a,b)\right|^2 db = W(a) \qquad (8)$$

which is called the wavelet variance or wavelet spectrum. It may be observed that the scalogram can be represented either as three-dimensional plot or as a 2-dimensional grey scale image. Here parameters a and b represent respectively the scaling factor and the location in time, (Siddiqi et all, 2002). In the following sections f(t) will be considered as rainfall rate values in Marmara Region.

ANALYSIS

Temporal and spatial variations of variables

The mean annual rainfall rate and Modified Fournier Index (MFI) values are presented in Tables 3 and 4 respectively.

Table 3. Mean annual rainfall rate values

	1901-1930	1931-1960	1961-1990	1991-1998	1999-2001	Mean (1901-2001)
ADAPAZARI	461	505	510	548	927	509
BALIKESİR	653	714	699	721	531	687
BANDIRMA	667	716	718	739	733	703
BİLECİK	510	529	550	564	486	531
BURSA	732	834	805	832	712	791
ÇANAKKALE	668	700	701	704	631	689
EDİRNE	567	611	587	635	507	589
İSTANBUL	789	825	882	939	680	836
KOCAELİ	507	547	562	597	833	552
TEKİRDAĞ	547	578	581	609	574	572

Table 4. Variaton of MFI values

	1901-1930	1931-1960	1961-1990	1991-1998	1999-2001	Mean (1901-2001)
ADAPAZARI	47.44	46.61	58.06	65.96	108.76	65.37
BALIKESİR	75.61	78.23	72.69	77.31	83.01	77.37
BANDIRMA	74.14	75.06	77.16	76.51	76.00	75.77
BİLECİK	55.64	52.17	51.30	58.48	71.65	57.85
BURSA	82.15	85.63	87.66	84.66	98.01	87.62
ÇANAKKALE	73.95	80.70	75.75	78.81	118.97	85.64
EDİRNE	61.40	68.83	62.45	69.97	52.13	62.96
İSTANBUL	92.19	87.55	89.97	99.99	91.14	92.17
KOCAELİ	55.00	52.08	62.83	69.33	101.22	68.09
TEKİRDAĞ	63.14	65.02	62.02	65.47	80.40	67.21

Spatial variation of annual total rainfall rate values show the maximum rainfall rate values (836 mm in İstanbul) were observed in the Northeastern part of Marmara region. The lowest value is 509 mm (Adapazarı).

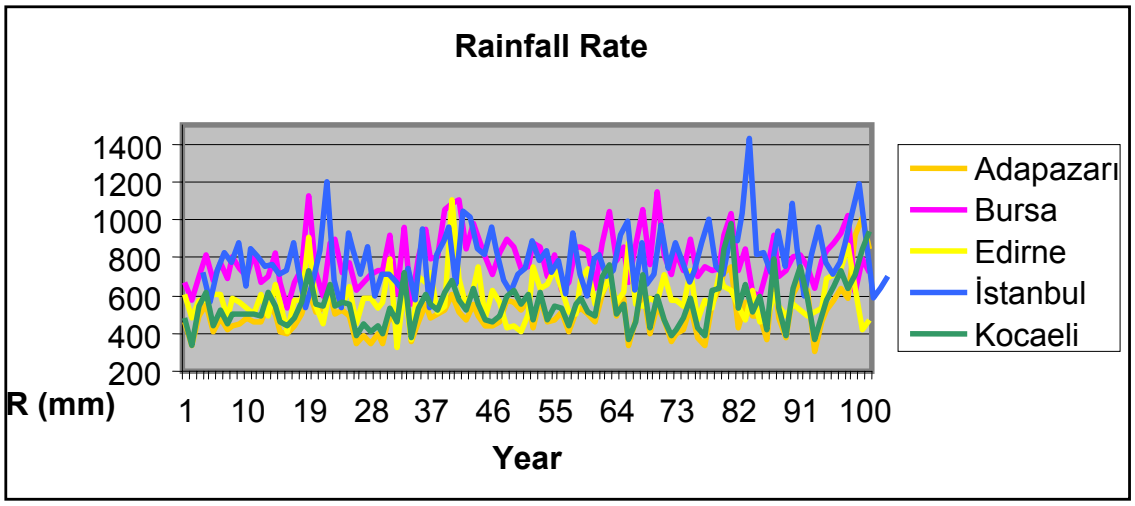

Figure 1. Temporal variation of rainfall rate, (mm).

Wavelet Analysis

1D-Continious wavelet analyses of annual total rainfall value have been presented in figures 2(a-e). Wavelet analysis explain small, meso and large scale effects on rainfall rate values.

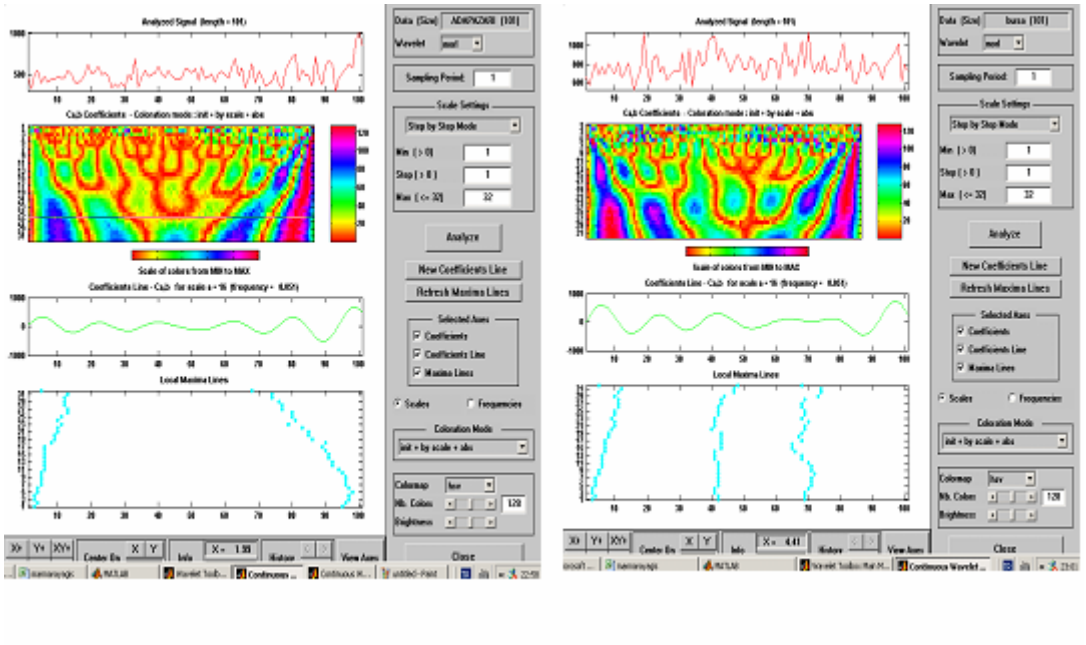

2(a-b). 1D Wavelet analysis (Morlet) in Adapazarı and Bursa

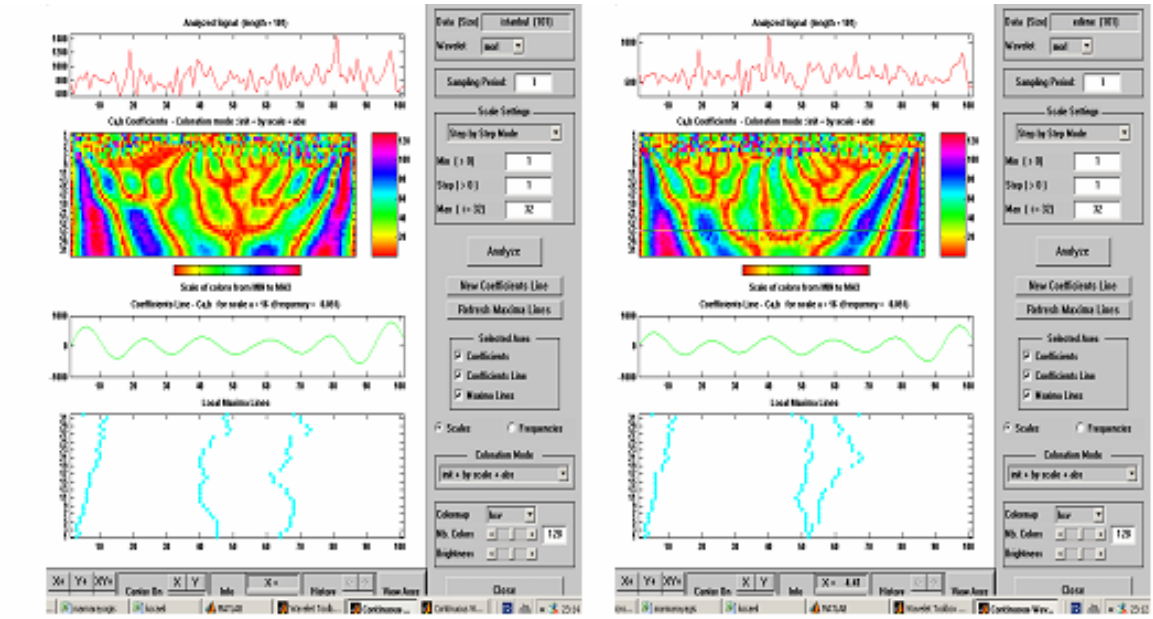

Figure 2(c-d). 1D Wavelet analysis (Morlet) in İstanbul and Edirne.

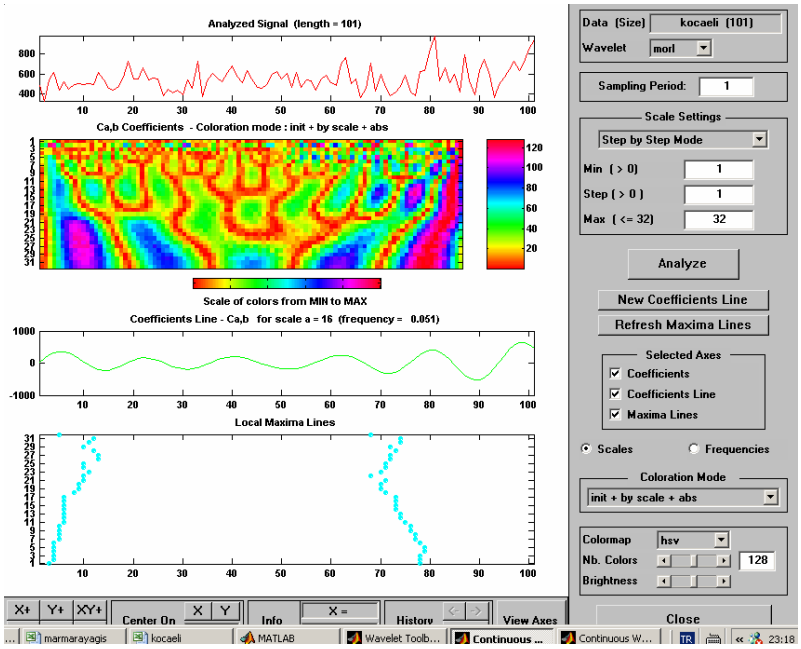

Figure 2(e). 1D Wavelet analysis (Morlet) in Kocaeli.

RESULTS AND CONCLUSIONS

Comparison of El Nino 3.4 variations with rainfall rate and water erosion risk values have been analyzed by using 1D-Continious wavelet methodology. Higher effects of El Nino and La Nina on rainfall rate and water erosion have been observed in İstanbul and Kocaeli than the other stations.

The relationship between past solar flare and climatological parameters is complex (Foukal et all, 2006). Indeed some signatures of solar activity have been accompanied by increasing rainfall rate values.

REFERENCES

Aslan, Z., A. S. Söğüt and D. Okçu (2006): "Water Erosion Risk Analysis", AGROENVIRON2006, Proceedings of the Int. Symposium, 2-7 September, Ghent, Belgium, p.7-14.

Aslan, Z., (1997): "Analysis of rainfall Erosivity and Climatic Factor of Wind Erosion", ICTP Pre-print, IC/97/135, Trieste, Italy.

Aslan, Z., and A. Tokgözlü, (2000): "Climatological Changing Effects on rainfall Erosivity and Wind Erosion", AGROENVIRON2000: 2nd. International Symposium on New Technologies for Environmental Monitoring and Agro-Applications", p.265-273

Can, Z., Z. Aslan, O. Oguz and A. H. Siddiqi, (2005): "Wavelet transforms of meteorological parameters and gravity waves", Annales Geophysicae, Vol. 23, p. 650-663.

Flanagen, D.C and J. Livingston, (1995): USDA-Water Erosion Prediction Project (WEPP), Soil and Water Conservation Society, pp.131 Iowa.

Foukal, P., C. Fröhlich, H. Spruit and T.M.L. Wigley, (2006): Variations in solar luminosity and effect on the Earth's climate, nature05072, vol.443/14 (review article), p. 161-166.

Micheles, P. and D. Gabriels, (1996): Rain variability indices for the assessment of rainfall erosivity in the Mediterranean region, Soil degradation and Desertification in Mediterranean Environments, J. L., Rubio and A. Calvo (Eds.) Geoforma Editions, Logrono''.

New, M. G., M. Hulme and P.D. Jones., (1999): Representing 20th century space–time climate variability I: Development of 1961-1990 mean monthly terrestrial climatology, J. Climate,12, 829-856.

New, M. G., M.Hulme, and P. D. Jones., (2000): Representing 20th.century space-time climate variability II: Development of 1901-1996 monthly terrestrial climate fields, J. Climate, 13, 2217-2238.

Pla Sentis, I., (1998): "Modeling the Influence of Soil Sealing and Soil Compaction on Soil Erosion Processes", College on Soil Physics, ICTP/SMR.pp1065-9, Trieste.

Skidmore, E., L., (2000): "Air, Soil, and Water Quality as Influenced by Wind Erosion and Strategies for Mitigation", AGROENVIRON2000: 2nd. International Symposium on New Technologies for Environmental Monitoring and Agro-Applications", p.216-221.

Siddiqi, A. H., Z. Aslan and A. Tokgozlu, (2002): "Wavelet based computer simulation of some meteorological parameters: Case Study in Turkey", Trends in Industrial and Applied Mathemadics., Eds. A. H. Siddiqi and M. Kocvara, p. 95-105, Kluwer Academic Publishers, London.

Türkeş, M., (1999): Vulnerability of Turkey to desertification with respect to precipitation and aridity conditions, Tr.J. of Engineering and Environmental Science, 23: 363-380.

CONTEMPORARY CLIMATE CHANGE IN JORDAN

Muwaffaq Freiwan[1] and Mikdat Kadioglu[2]

[1] Jordan Meteorological Department, P.O.Box: 341011, Amman 11134, Jordan
mfreiwan@yahoo.com
[2] Istanbul Technical University, Faculty of Aeronautics and Astronautics, Department of Meteorological Engineering, Maslak, 34469 Istanbul, Turkey.
kadioglu@itu.edu.tr

ABSTRACT

Climate change in Jordan is very sensitive to water resources, which are at the verge of depletion because annual per capita water is at one of the lowest levels in the world. In order to address such sensitivity, it is necessary to examine effective meteorological factors such as annual and monthly precipitation and temperature time series. Sixteen representative meteorological stations were chosen for the study of contemporary climate change calculations in Jordan. Annual and monthly time series of precipitation, maximum temperature and minimum temperature were tested by the runs (Swed-Eisenhart) homogeneity test. Consequently, the sequential version of the Mann-Kendall rank and the linear trend tests were applied to available data. On the other hand, the sequential version of the Mann-Kendall rank trend test was applied to the inter-annual means, coefficient of variation and skewness parameters. Signals of climate trends such as warming in maximum temperature, more statistically significant warming in minimum temperature, decreasing trends in daily temperature range and statistically insignificant decreasing precipitation trends were detected, which may be enhanced by heat island, urbanization, pollution and aerosols effects. Two spells are recognized in the time series, where the first spell started in the early 1970's and the second beyond the year 1992 with warming trend in maximum temperature and farther warming in minimum temperature resulting in a decreasing trend in the diurnal temperature range that are associated with a slight decrease in precipitation. The inter-annual coefficient of variation of maximum and minimum temperatures reveals increasing trends in the majority of the stations while they exhibit an apparent decreasing trend in diurnal temperature range and a general, but insignificant decreasing trend in precipitation is observed.

INTRODUCTION

Continuously increasing human activities especially in the second half of the 20th century started to affect the composition of the atmosphere to a significant extent. Emission of pollutant increases the concentration of the long-lived greenhouse gases in the atmosphere and leads to global warming [1, 2]. Trend becomes the most commonly used technique to detect climate change in regional and local basis {3, 4, 5]. Global surface temperature has increased by about 0.3 – 0.6°C since the late 19th century and about 0.2 – 0.3°C over the last 40 years in the 20th century [6]. The recent warming has been greatest over the continents between latitudes 40°N and 70°N. Temperature range has decreased globally in the second half of the 20th century [7]. Since nights became warmer more than days, minimum temperature increases have been about twice compared to maximum temperature. On the other hand, there has been a small positive (1%) global trend in precipitation over land during

the 20th century. Precipitation has increased over lands in high latitudes in the northern hemisphere especially during the cold season concomitant with temperature increases.

Local and regional long-term temperature and precipitation records are used in climate variability investigations. In climate assessment studies, trends are statistical fundamental tools in the detection of climate variability.

In a regional basis, [8] investigated the trends and periodicity of surface air temperature series from eight meteorological stations in the east Mediterranean using different correlation tests. He found a significant positive trend at 99% confidence in Malta, Jerusalem and Tripoli, and negative trend at 95% confidence level in Amman. The trends exhibit an increase (decrease) around 2°C (1°C) in minimum (maximum) temperature at Amman.
In the light of increasing population growth and continuous depletion of the available water resources in a country located at the fringe of the desert, the studies of climatology and climate change are important. There are few comprehensive studies in Jordan about vulnerability and adaptation to climate variability for investigating climate change, environment, water resources, housing and settlement constructions, economy, agricultural and industrial issues [9, 10].

[11] studied the climate change in Jordan Valley by analysing the daily records of maximum and minimum temperatures, rainfall and global irradiance at three stations located in the northern, central and southern parts of the valley. They found no significant trends in annual rainfall, but maximum temperature and diurnal temperature ranges have decreased significantly in the three stations, while trends in minimum temperature were not always consistent and significant.

The climate change scenarios expect a reduction of precipitation about 20 – 25% in the dry season (April – September) and 10 – 15% in wintertime with temperature decrease about 1.5°C in Jordan during the current half of the century [12].

In this study, the number of investigated stations is more than in the previous works, to represent all the topographic and climatic regions and to cover as larger as possible of Jordan. As an effective technique, the sequential version of the Mann-Kendall rank trend test was applied not only to time series themselves, but also to their statistical moments in order to detect climate variability in the statistical parameters, such as the means, coefficient of variation and skewness. The homogeneity of the monthly and yearly precipitation, maximum and minimum temperature time series have been tested by the runs (Swed – Eisenhart) test. Linear trend and the sequential version of the Mann-Kendall rank trend tests were also applied to the time series of precipitation and maximum, minimum as well as daily temperature range in addition to their inter-annual statistical parameters. In order to discuss the spatial and temporal distribution of the trends, the seasonal and annual Mann-Kendall statistics of the 16 stations were also illustrated in maps using Kriging method.

DESCRIPTION OF THE STUDY AREA

Jordan is located about 80 km to the east of the Mediterranean Sea, between 29°10'- 33°45'N and 34°55'–39°20'E with an area of 89,329 km^2 and population of 5,5 millions. It has a

unique topography that might not be found anywhere else. The western part of the country is the world lowest valley that lies along north – south direction between two mountain ranges with a length of about 400 km and its width varies from 10 km in the north to 30 km in the south. Its elevation varies between 170 – 400 m below mean sea level (m.s.l.). Jordan River passes through this valley from north to south down to the Dead Sea and comprises approximately one third of the border between Jordan, Palestinian and Israel territories. Jordan River is the main source of irrigation in Jordan Valley. Just to the east of the Jordan Valley the north – south mountain range reaches about 1,150 m above m.s.l in the northern parts and about 1,500 m above m.s.l in the southern parts of the Kingdom (Fig. 1). To the east of this mountain range is a semi-desert plateau that extends to cover approximately 80% of the country.

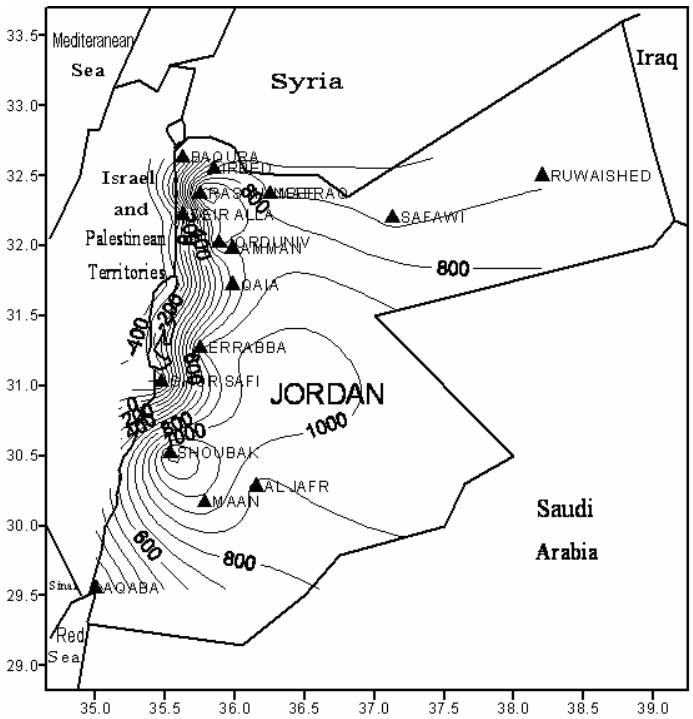

Figure 1. Location and elevation (meter above MSL) of the selected stations.

DATA DESCRIPTION AND HOMOGENITY ANALYSIS

Among nearly 50 observation stations of Jordan Meteorological Department 16 representative stations were chosen to study their trends and climate variability. In such a selection, reliable and long-term record properties were considered in addition to rather representative scatter of station locations and elevations in the west, with two stations in the eastern desert (see Figure 1). The length of the data records vary between 30 and 78 years.

The data are subject to quality control procedures in the climate division of Jordan Meteorological Department (JMD). The data must be tested to avoid spurious variabilities and trends that may appear and lead to mistakes in various studies, such as the climate variability. Many researchers have shown ways of eliminating such problems in their studies [13, 5, 14]. For instance, [15] studied the discontinuous inhomogeneity of the time series by comparing

the data of a particular station to another one that has a great similarity in weather conditions by calculating the ratio of rainfall and differences in temperature between the two stations. They consider absolute homogeneity if the data compared to a third station have similar climatological characteristics. [16] applied the short-cut Bartlet test to examine the homogeneity in seasonal and annual temperature time series in six stations in the southern Mediterranean including Amman station. Especially, in spring time series some exceptions of homogeneity are found for Alger and Amman in Jordan. The results of Mann-Kendall trend test for Amman match with those that have been found in this study.

Despite of the persuasive history of the selected stations in this study, and of the satisfactory common sense about the homogeneity of the data, the runs test for randomness is applied to the monthly and annual data of precipitation, maximum temperature and minimum temperature at all the stations. Details about this test (which is also called Swed-Eisenhart test) can be found in many publications such as [17].

It is found that all time series fulfill the 95% confidence level of annual precipitation homogeneity except at Jordan University station with run value as 2.69. This station is excluded from the study. In general, the seasonal and monthly rainfall data are homogeneous. Few individual months, mainly September and October in some stations are exceptional, which may experience no rain in successive several years and receive great amounts of precipitation in other several years and probably frequent extreme values may affect the run number in the test. Annual maximum and minimum temperature time series fulfill the 90% confidence level of homogeneity except Jordan University and Ghor Safi. The both stations have been excluded from the study. Some stations show randomness in monthly temperature time series in the summer months. This may be explained by the extreme temperature values that are frequently recorded in summer months in several successive years, which may appear as a jump. Furthermore, in summer months, maximum and minimum temperatures have an apparent increase, which is identical to the global and regional warming that has been mentioned by [7].

METHODOLOGY

Probably the most common approach is to estimate trends by linear regression as well as two-phase regression methods [18]. Such parametric methods require the variable to be normally distributed in addition to temporal and spatial independence [19, 20, 21]. In order to avoid disadvantages of the parametric methods, nonparametric approaches such as the sequential Mann-Kendall rank trend test [22, 23, 24, 5] is employed in this study.

The climatic trend is defined as a monotonic increase or decrease in the average value between the beginning and the end of an available time series [25]. Among some nonparametric trend tests, the sequential version of the Mann-Kendall rank test has the ability to detect the beginning and/or the end of the trend. The Mann-Kendall test is widely used for trend testing, particularly when many time series are analyzed at the same time. It has many advantages among others, the following points are significant.

i. It is free from normal distribution assumptions,
ii. It is resistant to effects of outliers and gross data errors,

iii. It allows missing and censored data (as only ranks are used), and
iv. It also gives the point in time of the beginning of a developed trend.

The Mann-Kendall test is, therefore, directly applicable to climatological data for a given month or season [26].

In this study, the time series of monthly mean precipitation, and maximum, minimum and monthly average of daily temperatures are analyzed in order to identify meaningful long-term trends by making use of the Mann-Kendall statistics. Details about sequential Mann-Kendall rank trend test can be found in many publications such as [5, 22, 23, 24, 27, and 28].

The values ± 1.96 ($\approx \pm 2$) of the test are statistically significant at 5% and the values ± 2.54 ($\approx \pm 2.5$) are statistically significant at 1% confidence level.

Annual and seasonal sequential Mann-Kendall rank statistics application results to 20 time series in addition to the Mann-Kendall trend statistics of the inter-annual mean, standard deviation (SD), coefficient of variation (CV), skewness (SK) and kurtosis (KR) of maximum temperature, minimum temperature, daily temperature range and precipitation time series are calculated. In order to identify the spatial variation of annual and seasonal Mann-Kendall statistics, their inter-annual statistical moments, the regional variations are calculated through the Kriging technique and the end products are given in more than 40 maps. Because of the limited area allocated for each paper, we will not be able to show all these illustrations and will very few figures as samples of the results.

DISCUSSION

Spatial variability of the annual Mann-Kendall trend statistics

As mentioned in section 4, the values outside the range ± 2 are considered significant trends at 95% confidence level, and similarly the values those are outside the range ± 2.5 are considered significant trends at 99% confidence level. For instance Figure 2 indicates that some stations expose obvious significant warming maximum temperatures trends, where as some others have cooling trends, but it is significant at the 95% level only in Amman, which may be due to the heat island effect. The minimum temperature increasing trend is significant at 99% confidence level in many stations. This may be explained also by the heat island effect due to the intense urbanization [29]. The daily temperature range exhibited an apparent significant decrease in the majority of the stations while no significant trends have been found in the annual rainfall time series (Figure 2).

The seasonality of the Mann-Kendall trend statistics

In winter season, no significant maximum temperature trends have been found except in Aqaba. Increasing trends have appeared in winter minimum temperature in the arid region (at Jafr) and in the Jordan Valley (Deir Alla). Generally, decreasing trends of the diurnal temperature range in winter season are also obvious in several stations. From the same figure, it is clearly seen that none of the stations show a significant trend in winter season precipitation. According to [30] the decrease of maximum temperature cannot be explained by greenhouse gases and aerosols only, but other factors such as the increase in precipitation results from the increase of water vapor and cloud cover in the atmosphere causing decrease in the sunshine duration. Warming trends in minimum temperature appears at the majority of

the stations, which may be according to the recently remarkable increase of urbanization and heat island resulting in an apparent decrease in diurnal temperature range.
The general trend of spring and autumn precipitation appears in the form of decreasing trend. However, it is significant only in few stations in spring season namely Q.A.I.A., Shoubak and Wadi Duleil stations.

In summer season, some stations show a slightly insignificant increasing trend in maximum temperature, but significant warming trends appear in many other stations. All stations reveal obvious warming trends in minimum temperatures with remarkable significance. Accordingly, the summer diurnal temperature range reveals a clear decreasing significant trend in most stations.

Mann-Kendall Statistics of the Moments

The sequential version of Mann-Kendall trend statistics of the inter-annual mean, standard deviation, coefficient of variation, skewness and kurtosis of maximum temperature time series are calculated and the spatial variations of these statistics are illustrated in contouring maps. The inter-annual maximum temperature shows a significant warming trend in many sites, but a significant cooling trend has appeared only in Amman.

The standard deviation measures the degree of variability or dispersion of a variate. Therefore, the largest is the standard deviation the greater is the departure from the mean value, and accordingly a higher probability of recording extreme values.In order to compare the variations at two or more time series, it is convenient to use a dimensionless magnitude such as coefficient of variation. The highest increasing trends of the coefficient of variation are apparent in the southern and eastern arid areas, which explain the high probability of recording extreme values.

The inter-annual maximum temperature is negatively skewed, because autumn season is 3 – 4°C warmer than spring season. The Mann-Kendall trend values of skewness are around zero. Accordingly, no important change is expected to occur in inter-annual skewness, and consequently, in inter-annual maximum temperature distribution. The inter-annual kurtosis coefficient of maximum temperature is generally negative, because the distribution has a smaller concentration probability near the mean. The Mann-Kendall statistics of inter-annual kurtosis exhibit insignificantly decreasing trends. This implies an increase in the inter-annual maximum temperature departures from the inter-annual mean value, which may be attributed to the obvious increase in the maximum temperature in summer more than in other seasons.

The inter-annual minimum temperature reveals increasing trends at most of the sites. The increasing coefficient of variation trends implies more inter-annual variability of the minimum temperature, which may amplify the minimum temperature difference between the warm part (summer and autumn) and the cold part (winter and spring) of the year. The obvious significant increase in minimum temperature in summer and autumn versus the slight increase in winter and spring may prove this allegation. The inter-annual skewness of minimum temperature is very close to symmetric normal distribution. The Mann-Kendall trend statistics exhibit an insignificant increasing trend in most stations. It may increase the concentration of probability below the mean, and increases the chance of extreme record occurrences. Due to the smaller concentration of probability near the mean, the inter-annual

kurtosis is platykurtic (negative). Negative or insignificantly decreasing trends of the inter-annual kurtosis coefficient are detected by the Mann-Kendall trend test. That means the probability is going to concentrate far away from the mean value. This can be attributed by the different rates of increasing minimum temperatures during different seasons. The inter-annual diurnal temperature range reveals decreasing trends in most of stations, which is the natural result of the increasing inter-annual minimum temperature and the increasing (but in a smaller rate) of the inter-annual maximum temperature.

The inter-annual coefficient of variation of the daily temperature range is near zero at all sites except at Irbed and Amman in the north and at Deir Alla in the Jordan Valley. The decreasing coefficient of variation of the daily temperature range results from the decrease in maximum temperature, and the obvious significant increase in minimum occurs at the largest two cities of Jordan; namely, Amman and Irbed. Such an increase may be attributed by the heat island and urbanization, pollution and greenhouse gases.

The inter-annual skewness of the diurnal temperature range shows some increasing trends. The increasing skewness means more concentration of the diurnal temperature range near lower values (below the inter-annual mean) that emphasizes the decrease of the diurnal temperature range, which is a logical result in the light of the previous discussion related to the maximum and minimum temperatures.

The Mann-Kendall trends of the inter-annual kurtosis of diurnal temperature range are near zero. However, the majority of them are insignificantly negative trend values. The decreasing negative kurtosis implies less concentration of probability near the mean, and consequently, a wide band of variation for the diurnal temperature range is expected to be enhanced. The inter-annual mean of precipitation reveals insignificantly decreasing Mann-Kendall trends in most stations. It is significant at 90% level only in Shoubak. No significant trend has been detected in coefficient of variation of the inter-annual precipitation, thus the large coefficient of variation of precipitation is expected to prevail the eastern and southern parts, and low coefficient of variation of precipitation is expected to dominate the high lands. In other words, the aridity or drought is expected to remain as a characteristic of the southern and eastern regions of the country. Both skewness and kurtosis of the inter-annual precipitation have not revealed any significant Mann-Kendall trend. There are some decreasing insignificant trends in skewness in the central and southern arid regions that probably may increase the drought [31] in these regions such as Q.A.I.A., Jafr and Rabba. There are some insignificantly increasing trends in skewness that probably may cause extreme precipitation and floods in areas such as Wadi Duleil.

The kurtosis coefficient of the inter-annual precipitation has the same pattern of skewness and the same properties that emphasize the above explanation for the related stations. The high kurtosis values coincide with higher positive skewness values, and the lower or negative kurtosis values coincide with negative skewness leading to the same influence.

Climate variability investigations in selected locations

Six stations are chosen from different topographic and climatic regions in order to illustrate their sequences of forward and backward [u (t_i) and u' (t_i)] values, and to compare these statistics with linear trends of the related climatological variables and to discuss their local

climatic variability. These stations are Irbed (northwest), Amman Airport (eastern city Centrum), Shoubak (from the southern heights), Deir Alla (from the middle part of Jordan valley), Aqaba (a coastal city from the extreme south) and finally Ruwaished (from the eastern desert area) (Figure 1).

The parametric linear trend methods require the data to be normally distributed. Otherwise, such methods are not suitable to detect trends. To reveal the advantages of the nonparametric sequential version of the Mann-Kendall trend test, which is free from the normal distribution assumption, sequential version of the Mann-Kendall trend values of precipitation, maximum temperature, minimum temperature and diurnal temperature range time series, and consequently, the linear trends of the same time series during the same period are plotted in figures. One of these figures will be shown as a sample.

Figure 3 shows that precipitation and maximum temperature exhibit decreasing trends, but minimum temperature exhibits a clear increasing trend, and consequently, the daily temperature range reveals an obvious decreasing trend. Since the linear trend is not able to detect the beginning of the trends, the Mann-Kendall test apparently detects the beginning and end of the trends. Fig. 3 also shows that the precipitation in Irbed exhibits a decreasing trend along the whole period (1938 – 2000). It is significant from 1941 to 1963 and another decreasing trend is seen beyond 1992. Maximum temperature time series of Irbed exhibits a general decrease along the record period (1955 – 2000), but it is significant beyond 1975 and the cooling trend becomes less significant beyond 1992. This can be seen from Fig. 3 by the warm spell in the maximum and minimum temperature time series. The minimum temperature in Irbed shows an obvious warming trend starting by the year 1975, and consequently the daily temperature range reveals an apparent decreasing trend beyond 1975. This may be considered as a result of urbanization and heat island effect in Irbed, the second largest city in the country.

The linear trend shows a slight decrease in Amman precipitation. The Mann-Kendall test shows some increasing and decreasing trends in various periods, but the general pattern of Amman precipitation trend has slightly decreasing trend from 1955, and a further decreasing trend takes place beyond 1992. The same figure also shows that both maximum and minimum temperatures have a complex behavior. Maximum temperature has a cooling linear trend. Mann-Kendall test shows several cooling and warming trend patterns, the last trend pattern starts in 1965. There is a significant cooling trend beyond the year 1982, and a slightly increasing trend started beyond 1992. Minimum temperature linear trend shows a slight increase, but Mann-Kendall test detects several cooling and warming trend patterns of which the most important is the warming trend that started in 1975. The diurnal temperature range has a general decreasing that started to be significant by the year 1992.

Both linear and Mann-Kendall trend tests reveal a clear decreasing trend in Shoubak precipitation time series. The Mann-Kendall test has detected the beginning of the trend as 1946 and it is more significant during the period 1954 – 1967. Maximum temperature time series shows an obvious linear warming trend and the Mann-Kendall test has detected the start of the trend in 1972. Slightly increasing linear trend has been detected in minimum temperature time series, while Mann-Kendall test shows an insignificant cooling trend. Consequently, the diurnal temperature range in Shoubak reveals an increasing trend by 1973

and becomes significant gradually beyond 1987. The increasing trend of diurnal temperature range is contradictory to all other sites, where the range is obviously decreasing.

The precipitation time series shows a slightly increasing linear trend. The Mann-Kendall has detected decreasing trends since the beginning of the record up to the year 1967 then the precipitation series has a monotonic pattern up to 2000.In maximum temperature, it is clearly seen that the warming trends started to appear beyond 1986, but further warming trends in minimum temperature are also started to appear since the beginning of the record. Daily temperature range exhibits an obvious significant decreasing trend that starts by the year 1964. This implies that the days are becoming somewhat warmer, and the nights are becoming warmer and warmer in the Jordan valley.

Neither by linear nor by the Mann-Kendall trend test, a consistent significant trend in Aqaba precipitation time series has been detected. Maximum temperature reveals an obvious cooling trend along the entire time series. While the minimum temperature has an insignificant warming trend from 1975, and consequently, the daily temperature range has a decreasing trend that start with the onset of the record.

Finally, at Ruwaished, which is a station from the arid area, no significantly consistent trend in precipitation time series has been detected. A slightly cooling trend in maximum temperature and more significant and apparent warming trends have occurred in minimum temperature especially beyond 1976, and consequently, a significantly obviously decreasing diurnal temperature range trend has been detected especially beyond the year 1970.

CONCLUSION

Consequent to the homogeneity testing of the annual and monthly precipitation, maximum temperature, and minimum temperature time series of the selected stations for the study, the sequential version of the Mann-Kendall rank trend test and the linear trend test have been applied to the available representative data in order to detect any trend or climate change in the country. As a new approach, the sequential version of the Mann-Kendall rank trend test has been applied to the inter-annual mean, coefficient of variation, skewness and kurtosis of maximum temperature, minimum temperature, diurnal temperature range and precipitation time series. The trends are discussed in yearly and seasonal basis. The most important conclusions can be given as follows.

- The yearly precipitation time series are homogeneous with 95% confidence level except in Jordan University station. Maximum and minimum temperature time series are homogeneous with 90% confidence level except in Jordan University and Ghor Safi. Accordingly, these two stations were excluded from the study.
- The cooling or slightly warming trends in annual maximum temperature with accompaniment of the obvious warming trends in the annual minimum temperature result in an apparent decrease in the diurnal temperature range in the majority of the stations.
- No significant trends have been detected in annual precipitation except a decreasing trend at 95% confidence level in Shoubak station.

- In winter season, no significant trends have been detected in precipitation and maximum temperature time series. While a general, but insignificant warming trends are obvious in minimum temperature and a general decrease in the diurnal temperature range.
- In spring, autumn and summer seasons, a slight warming is exhibited in maximum temperature, but the minimum temperature reveals a significant apparent warming trend in the majority of the sites, resulting in a decreasing diurnal temperature range.
- The general trend in spring and autumn precipitation time series is decreasing, but it is significant in few sites such as Q.A.I.A., Shoubak and Wadi Duleil stations.
- The plot of Mann-Kendall statistics for some stations shows that an evidence of cooling trend in maximum temperature and an obvious warming in minimum temperature have started in the beginning of 1970's. This matches with the global issues, where 1990's is the warmest decade in the 20th century.
- Another spell of probable climate variability is evident in the last decade of the 20th century, where a slight decreasing trend in precipitation accompaniment with warming trend in maximum temperature and more significantly warming trends in minimum temperature and decreasing daily temperature range are obvious beyond the year 1992.

The natural variability of climate could be as large as the changes have been actually observed. In the case of Jordan, the time series are usually too short to define a definite long-term climatic trend. It might be a good indication to a signal of the recent climate variability. These behaviors of climate variability in Jordan could be summarized by the statement: "the days are becoming little bit warmer while the nights are becoming warmer and warmer in Jordan with accompaniment of slightly decreasing precipitation".

The following recommendations shed light on the possible future development of this and related studies.

- The beginning and end of the real seasons are usually not coincident with the astronomical or meteorological seasons. Therefore, it should be more realistic to discuss the statistical moments and their variability on monthly basis,
- Water harvesting projects could be intensified in the eastern and southern parts of the country, because of the higher probability of recording extreme precipitation values by heavy showers of rain in short periods of time, and the lack of water sources in those regions,
- In order to detect the real causes of warming in minimum temperature and cooling in maximum temperature the cloud cover, sunshine duration, evaporation and solar irradiance variability might be the appropriate study in the near future, and
- The impacts of increasing temperatures and decreasing diurnal temperature range on cooling and heating degree-days in different seasons, and consequently, the energy consumption in the country deserves more attention and detailed investigations.

REFERENCES

[1] Friedly, H., Lotscher, H., Oeschger, H., Siegenthaler, U. and Stauffer, B., 1986: Ice core record of the $^{13}C/^{12}C$ ratio of atmospheric CO_2 in the past two centuries. *Nature*, 324, 237 – 238.

[2] Lorius, C., Jouzel, J., Raynaud, D., Hansen, J. and Le Treut, C., 1990: The ice core record: Climate sensitivity and future greenhouse warming. *Nature*, 347, 139 – 145.

[3] Dickinson, R. E., 1989: uncertainties of estimates of climatic change: A review. *Climate Change*, 15, 5 – 13.

[4] Balling, R. C. Jr., 1992: The heated debate: greenhouse prediction versus climate reality. *Pacific Research Institute for Public Policy*, San Francisco, 1955 pp.

[5] Kadıoğlu, M., 1997: Trends in surface air temperature data over Turkey. *Int. J. of Climatol.*, 17, 511 – 520.

[6] Houghton, J. T., Meira Filho, L.G., Callander, B. A, Katenberg, A. and Markell, K., 1995: Climate Change 1995, The science of climate change, *Cambridge University Press*, Cambridge, UK.

[7] Houghton, J. T., Callander, B. A. and Varney, S. K., 1992: The supplementary report of the IPCC scientific assessment, *Cambridge University Press*, Cambridge, UK, p. 198.

[8] Hasanean, H. M., 2001: Fluctuations of surface air temperature in the east Mediterranean. *Theo. Appl. Climatol*., 68, 1-2, 75 – 87.

[9] UNDP, 1999: Vulnerability and adaptation to climate change in Jordan. Vol. 1, Project No. JOR/95/G31/IG/99, *Al-Shamil Engineering*, Amman, Jordan.

[10] Abandeh, A., 1999: Climate trends and climate change scenarios, Vulnerability and adaptation to climate change in Jordan. Vol. 1, Project No. JOR/95/G31/IG/99, *Al-Shamil Engineering*, Amman, Jordan.

[11] Cohen, S. and Stunhill, G., 1996: Contemporary climate change in the Jordan Valley. *J. Appl. Meteorol*., 35, 1051 – 1058.

[12] Ragab, R. and Prudhomme, C., 2002: Climate change and water resources management in arid and semi-arid regions: prospective and challenges of the 21st century. *Biosystem Engineering*, 81, 1, 3 – 34.

[13] Rodhe, H. and Virji, H., 1976: Trends and periodicities in east African rainfall data. *Mon. Wea. Rev*., 104, 307 – 315.

[14] Ben-Gai, T., Bitan A., Manes, A., Alpert, P. and Rubin, S., 1999: Temporal and spatial trends of temperature patterns in Israel. *Theor. Appl. Climatol*., 64. 163 – 177.

[15] Karl, T. R. and Williams, C. N., 1987: An approach to adjusting climatology time series for discontinuous inhomogeneities. *J. Climate and Appl. Meteorol*., 26, 1744 – 1763.

[16] Aesawy, A. M. and Hasanean, H.M., 1998: Annual and seasonal climatic analysis of surface air temperature variations at six southern Mediterranean stations. *Theor. Appl. Climatol.*, 61, 55 – 68.

[17] Neave, H. R. and Worthington, P.L., 1992: Distribution-Free Tests. *Routledge press*, London, UK.

[18] Solow, A. R., 1987: Testing of climate change: An application of the two-phase regression model. *J. Clim. Appl. Meteorol*., 26, 1401 – 1405.

[19] Plantico, M. S., Karl, T.R., Kukla, G. and Gavin J., 1990: Is recent climate change across the United States related to rising levels of anthropogenic greenhouse gases. *J. Geophys. Res*., 95, 16617 – 16637.

[20] Cooter, E. J. and LeDuc, S. K., 1995: Recent frost date trends in the North-Eastern USA. *Int. J. Climatol*., 15, 65 – 75.
[21] Huth, R., 1999: Testing for trends in Data unevenly distributed in time. *Theor. Appl. Climatol.*, 64, 151 – 162.
[22] Sneyers, R., 1990: On the statistical analysis of series of observations. WMO, Technical Note 143, 415, TP. 103, Geneva, *World Meteorological Organization*. P. 192.
[23] DeGaetano, A. T., 1996: Recent trends in maximum and minimum temperature threshold exceedences in the North-Eastern United States. *J. Climate*, 9, 1646 – 1660.
[24] Türkeş, M., Sümer, U. M. and Kılıç, G., 1996: Observed changes in maximum and minimum temperatures in Turkey. *Int. J. Climatol*., 16, 463 – 477.
[25] Olaniran, O. J., 1991: 'Evidence of climate change in Nigeria based on annual series of rainfall of different daily amounts, 1919 – 1985'. *Climate Change*, 19, 319 – 341.
[26] Kadıoğlu, M. and Aslan, Z., 2000: Recent trends of growing season length in Turkey. *2nd International Symposium on New Technologies for Environmental Monitoring and Agro-Applications Proceedings,* 18-20 October 2000, Tekirdağ/Turkey, pp. 295-303.
[27] Kadıoğlu, M. and Şaylan, L. 2001: Trends in growing degree-days in Turkey. *Water Air and Soil Pollution*, 126, 83 – 96.
[28] Kadıoğlu, M., Şen, Z. and Gültekin, L., 2001: Variation and trends in Turkish seasonal heating and cooling degree-days. *Climatic Change*, 49, 209 – 223.
[29] Oke, T. R., 1973: City size and the urban heat island. *Atmospheric Environment Pergamon Press*, Vol. 7, pp. 769 – 779, UK.
[30] Henderson-Sellers, A., 1986: Increasing clouds in warmer world. *Climate Change*, 9, pp. 267 – 309.
[31] Şen, Z., 1998: Statistical meteorology. Istanbul Technical University*, Meteorological Engineering Department*, Istanbul, Turkey, p. 12. (In Turkish).

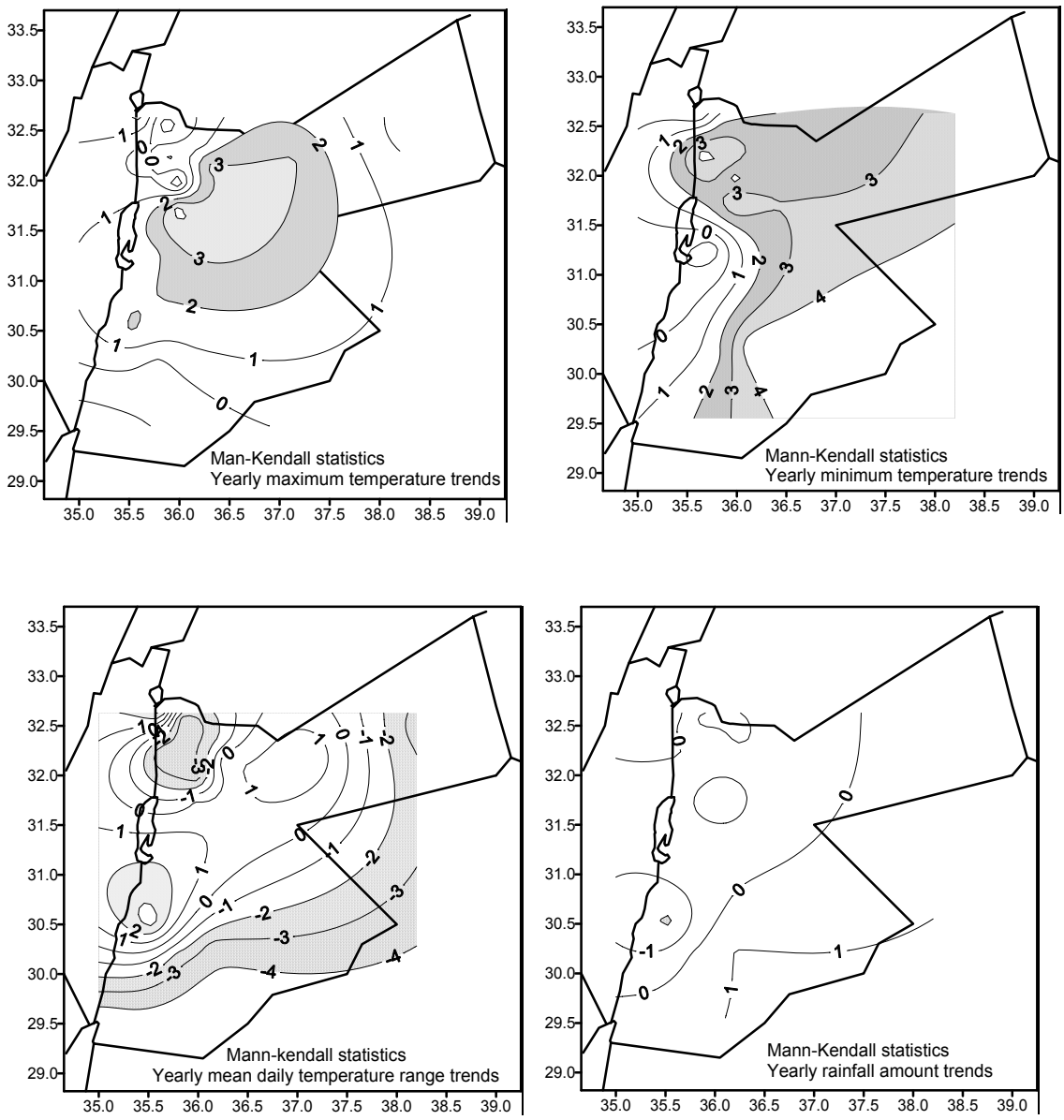

Figure 2: Mann-Kendall statistics of annual maximum and minimum temperatures, daily temperature range and rainfall. Dot and gray shading mark regions of cooling and warming (decreasing and increasing trends for temperature range and rainfall) respectively, with a significant occurrence (95% level).

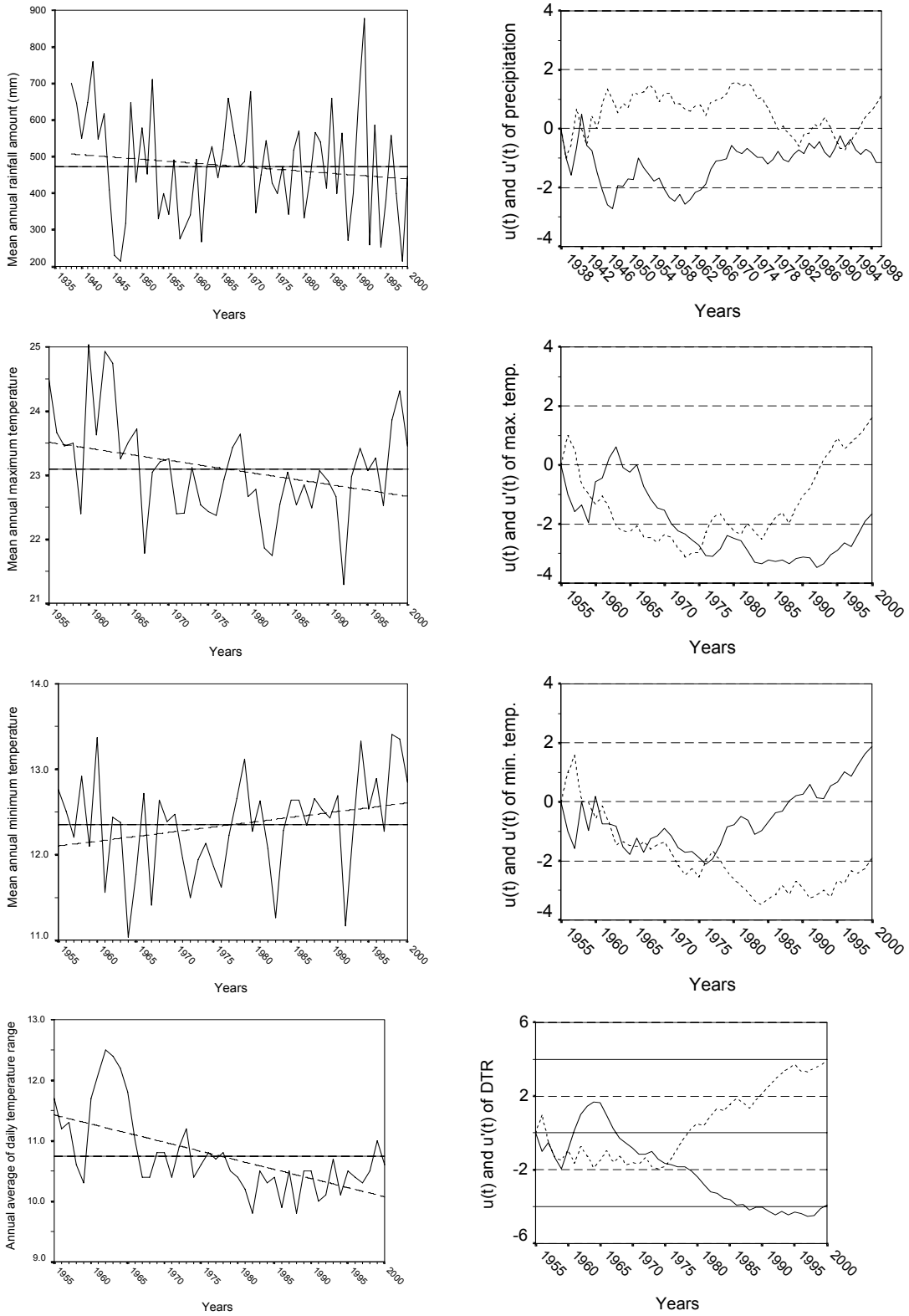

Figure 3: Linear trends (left) and the sequential version of the Mann-Kendall trend forward and backward statistics (right) of the mean annual precipitation (mm), maximum and minimum temperatures and daily temperature range (°C) at Irbed (1938 – 2000 for precipitation and 1955 – 2000 for temperature).

STUDY OF WARM NIGHTS OVER IRAN DURING LAST DECADES

Fatemeh-Rahimzadeh, Ahmad Asgari and Nooshin Mohammadian

Atmospheric Science and Meteorological Research Center (ASMERC), P.O.Box: 14965-114, Tehran, Iran,
phone No: 0098-21-44580651-9, rahim_f@irimet.net

ABSTRACT

Based on Intergovernmental Panel on Climate Change (IPCC) findings, it is expected to have higher probability of extreme temperature events especially for mid-latitude regions due to global warming. Warm nights indices can be considered as efficient indicators for detection of changes in distribution of extreme temperature events. It is expected to have increasing trends of warm nights in Iran too. To prove this, we analyzed results obtained using two indices including warm nights index (TN90P) and tropical nights index (TR20) over the country.

This paper describes the results of analysis of TN90P and TR20 indices, their natural sequences and trends for 33 of those Iranian synoptic stations with high quality and homogenous precipitation data over period starting from their establishment time up to 2003.

Significant positive trends have been found for TN90P and TR20 for almost the whole country, except for Bandar Abbas (Coastal port of Persian Gulf), Arak, and Ghazvin (Industrial cities located in west of central region of the country). Birjand (East of the country) is the only point that has almost stationarity. Strongest positive and negative trends for TN90P were found respectively in Shiraz (South of the country) with slope of +0.65 and Bandar Abbas with the slope of -0.085. Both least square and Man-Kendall methods confirm significance of trends in two above stations and also in most of the other stations.

Our results also show a few years with TR20 greater than 200 in stations like Bushehr and Bandar Abbas (Coastal ports of the Persian Gulf). Even Bandar Abbas experienced TR20 with value of 251 in 1962. This value is the highest one for the country.

Keywords *:* Warm nights, Warm nights index, Tropical nights index, Iran

INTRODUCTION

There is a strong need to understand variability of extreme events and changes of their frequencies. Most of the recently published papers were focused on the global and regional extremes, especially, extreme low temperatures [7; 8 and 12]. Based on the results of many studies on global and regional changes, increase in daily minimum is stronger than that for maximum temperature and there is a remarkable consistency between these research over the Northern USA [7], Canada [5], Australia and New Zealand [12], and China [18].

Collins [6] used a set of high quality Australian daily temperatures data and showed that the trends are particularly strong for indices based on minimum temperature that many of them are statistically significant at the 95 percent confidence level. The significant increases in TN90p have already been well documented in papers like Frich et al., [9], Kiktev et al., [11].

Zhang et al., [19] have examined trends in 27 indices including warm nights and tropical nights indices at 75 stations from 15 countries in the Middle East region for the period 1950-2003. The results showed statistically significant positive trends for these two indices almost in whole region. They mainly found that there is a significant decrease in number of days with extreme low temperatures e.g., warm nights and tropical nights.

Alexander et al., [1], recently showed that there are significant positive trends in the occurrence of warm nights and tropical nights in the latter half of the 20th century for many locations throughout the world. They showed positive trends for number of warm nights, over 70% of the land area under study for period 1951-2003.

At national level, several studies have examined trends in Iranian averages of minimum temperatures. For instance, Alijani [3], Jahaditoroghi [10], and Rasooli [13] have worked on some selected stations. Furthermore, Rahimzadeh and Asgari [14; 15] using a set of high-quality records showed significant trends for minimum and also maximum temperature over most of the Iranian territory for period 1951-97. They found increasing trends for minimum temperatures in all stations under study except Oroomieh located in northwest of the country. Such an exception for Oroomieh is confirmed by ASMERC [2] studies too.

As extremes like warm nights and tropical nights that relate to variability of minimum temperature have great economic and social impacts [16], they are to be fully examined. The main purpose of this paper is to show the behavior of the two indices of minimum temperature including warm nights (TN90P) and tropical nights (TR20) over Iran during last decades.

DATA AND METHODOLOGY

We initially used data of daily minimum temperatures of more than 150 stations received from the data archives of the Islamic Republic of Iran Meteorological Organization (IRIMO). Most of the initially established stations contain inhomogeneity and uncertainty in their data sets in the initial years. In this work, we had to limit presentation of results from only 27 stations due to problems like minimizing the effect of inhomogeneity, and to presence of wide data gaps and also to shortness of period. We tried to choose stations based on our knowledge of the recent analyses [14; 15]. Geographical locations of used stations are shown in Table 1. We had to reject to work on stations not covering period 1961-90 in spite of longevity of their dataset. These selected stations have almost no missing data. As we mentioned before, two indicators listed with their exact definitions available from the ETCCDMI/CRB Climate Change Indices Web Site were used.

We computed these indices using RClimDex [20], which was developed at the Climate Research Branch of Meteorological Service of Canada on behalf of the ETCCDMI. This software along with the documentation is available at http://cccma.seos.uvic.ca/ETCCDMI. To calculate the minimum temperature values corresponding to the 90th percentiles of each station record, initially long-term (1961-90) temperatures average were determined for every day of the calendar year. TN90p (warm nights represented by percent of time minimum temperature is greater than 90th percentile of the daily minimum temperature) and TR20

(annual number of tropical nights i.e., nights with minimum temperature >20º C), have been examined over the country.

Table 1. Geographocal characteristics of the selected stations

No.	Station	Geographical Coordinates		Height (m)	WMO No.	Period
		Longitude (N)	Latitude (E)			
1	Abadan	30˚ 22′	48˚ 15′	6.6	40831	1951-03
2	Arak	36˚ 06′	49˚ 46′	1708.0	40769	1961-03
3	Babolsar	36˚ 43′	52˚ 39′	-21	40736	1951-00
4	Bam	26˚ 09′	58˚ 21′	1066.9	40854	1956-03
5	Bandar Abbas	27° 13′	56˚ 22′	10.0	40895	1960-03
6	Bandar Anzali	37˚ 28′	49˚ 28′	-26.2	40718	1961-03
7	Birjand	32° 52′	59˚ 12′	1491.0	40809	1955-03
8	Bushehr	28° 59′	50˚ 50′	19.6	40858	1951-03
9	Esfahan	32˚ 40′	51˚ 52′	1600.7	40800	1961-03
10	Ghazvin	36° 15′	50˚ 00′	1278.3	40731	1960-03
11	Gorgan	36° 51′	54˚ 16′	13.3	40738	1960-03
12	Kerman	30° 15′	56˚ 58′	1753.8	40841	1961-03
13	Kermanshah	34° 19′	47˚ 7′	1322	40766	1951-03
14	Mashhad	36˚ 16′	59˚ 38′	990	40745	1951-03
15	Oroomieh	37˚ 32′	45˚ 5′	1312.5	40712	1961-03
16	Ramsar	36˚ 54′	50˚ 40′	-20.0	40732	1955-03
17	Rasht	37˚ 12′	49˚ 39′	36.7	40719	1956-03
18	Sabzevar	36˚ 12	57˚ 43′	977.6	40743	1954-03
19	Sanandaj	35˚ 20	47˚ 00′	1373.4	40747	1959-03
20	Shahrekord	32˚ 20′	50˚ 51′	2061.4	40798	1955-03
21	Shiraz	29˚ 33′	52˚ 36′	1488	40848	1951-03
22	Tabriz	38˚ 5′	46˚ 17′	1361.0	40706	1951-03
23	Tehran-Mehrabad	35˚ 41′	51˚ 19′	1190.8	40754	1956-03
24	Yazd	31˚ 54	54˚ 24	1230.2	40821	1952-03
25	Zabol	31˚ 13′	61˚ 29′	489.2	40829	1961-03
26	Zahedan	29˚ 28′	60˚ 53′	1369.0	40856	1951-03
27	Zanjan	36˚ 41	48˚ 41′	1663.0	40729	1955-03

Systematic long term changes of indices are calculated by linear trend analysis. Since normal frequency distribution is not fitted very well with the indices data, we used non–parametric Mann-Kendall statistics [17] to find whether trends are significant or not.

RESULTS

Highest values found for warm night index (TN90p) have been in accordance with one of most recent warm years of the earth. Years of 1998, 2005, 2002, 2003, and 2004 have been 5

warmest years of the earth since 1851(Brohan et al., 2006). Shiraz recorded highest percentage of 51.23 of warm nights in 1999. This corresponds to 194 nights. This city also experienced percentages of more than 30 percents in ten years during the study period. Such a high percentage (%30) has also been found in cities like Bandar Abbas, Bandar Anzali, Tehran, Mashhad, and Ramsar. Besides to Arak, Birjand, Sannandaj, and Zabol, other cities under study have so far experienced percentages greater than %20 (73 warm nights). We observed positive trends for TN90p index almost for the whole country (Figure 1). Exceptions were Arak, Ghazvin, and Bandar Abbas. Negative trend in Bandar Abbas, to some extent has been due to higher values of the index in the early period. Birjand also showed stationarity. Strongest positive and negative trends of the TN90p index were found in Shiraz and Bandar Abbas with slopes of +0.65 and -0.085 respectively.

More or less every location in the country has so far experienced tropical nights. The index of TR20 (Number of Tropical Nights) in southern and central regions were found very high in most of years. In littoral provinces of Caspian Sea, TR20 is almost in the range of 50-120. In Province of Sistan and Baluchestan located in SE of the country, TR20 has never exceeded 160 and Zahedan, center of the province has even had the index less than 10 in some years. Number of tropical nights was over 200 in some years in southern cities like Bandar Abbas and Bushehr. The former has a record of 251 nights in 1962. We found no tropical nights in some years in cities like Arak, Oroomieh, and Sharekord. It is noteworthy that Shahrekord has only experienced non-zero tropical nights in 9 years during period. We found positive trends of the TR20 index for most of the country that are mostly significant (Figure 2). Strongest positive and negative trends of the index were found in Sabzevar and Bandar Abbas with slopes of +1.59 and -0.12 nights per year respectively. Figures 3 and 4 also show natural sequences and trends of both indices for some selected station of the country.

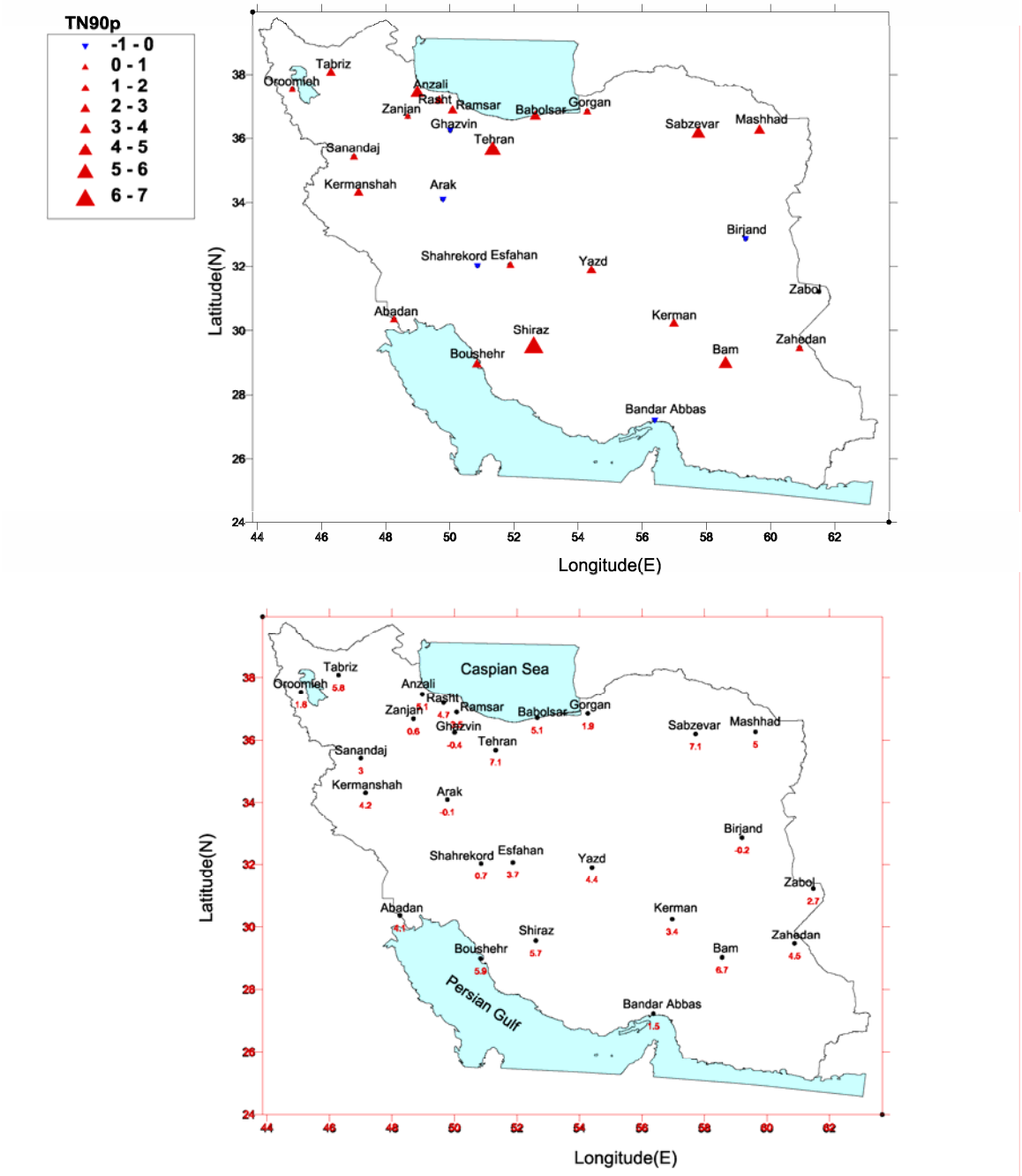

Figure 1. Decadal trends for TN90p index in selected Iranian synoptic stations for period 1951-2003.

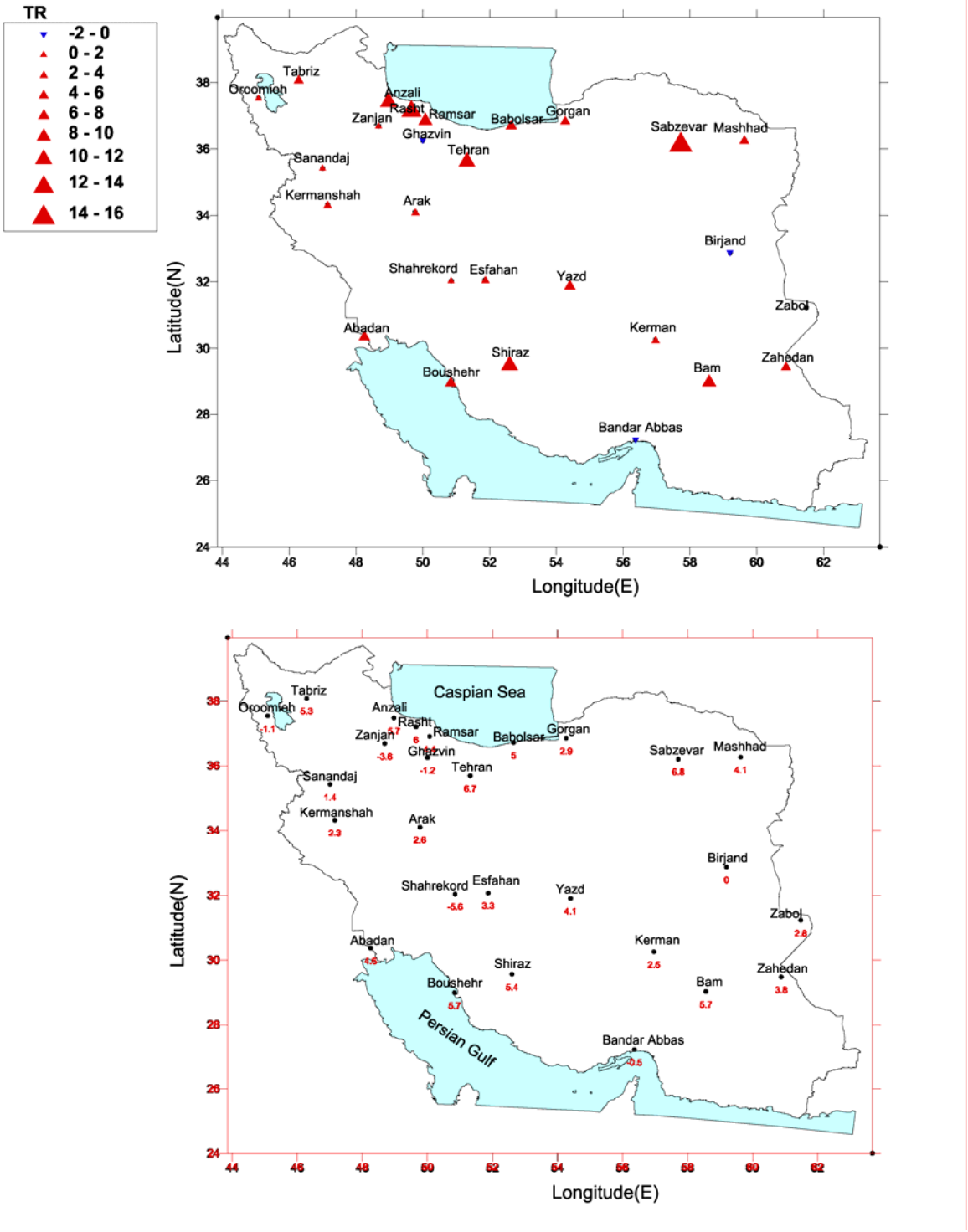

Figure 2. Decadal trends for TR20 index in selected Iranian synoptic stations for period 1951-2003.

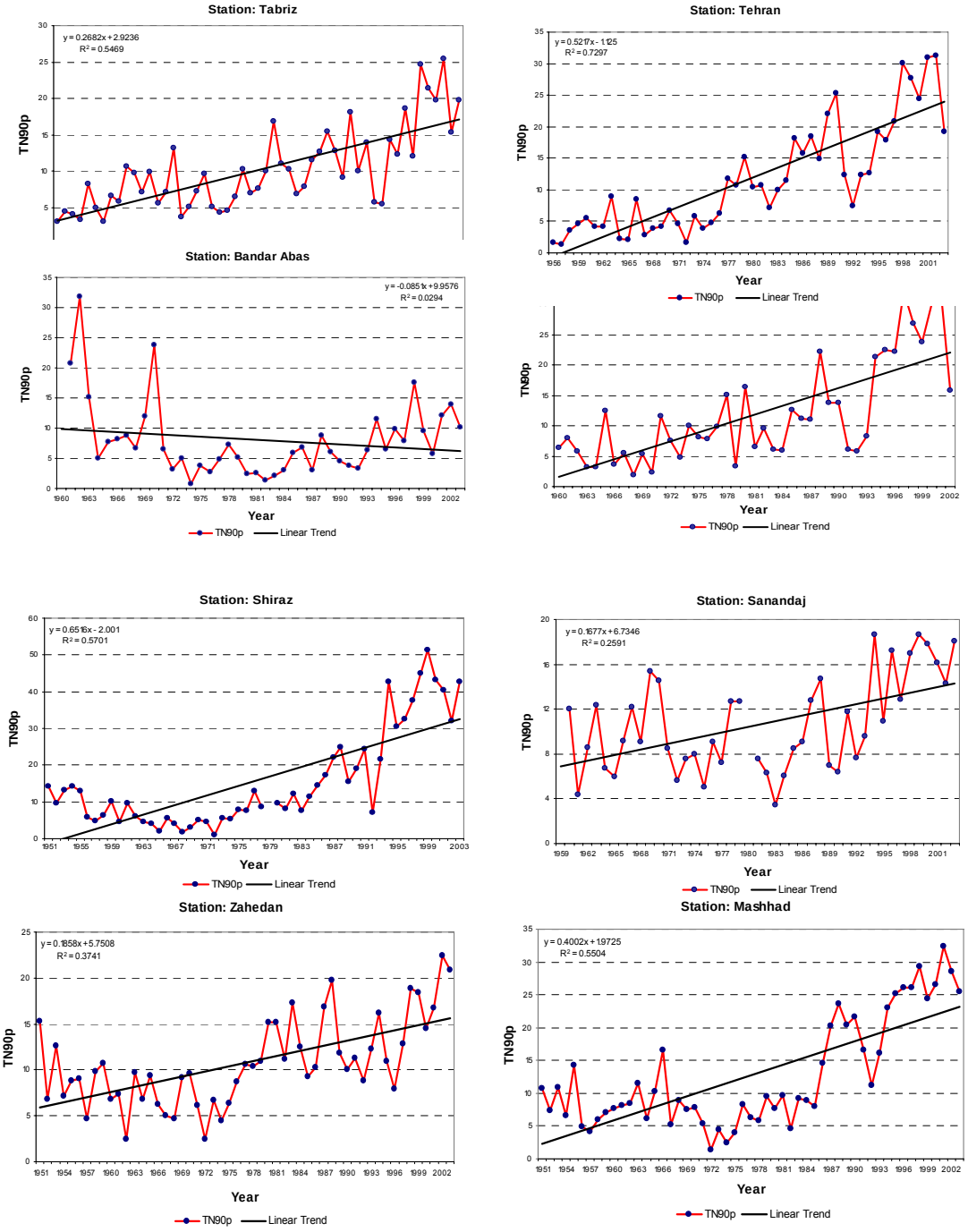

Figure 3. Some selected cases for their negative trends, large values, and positive trends of TN90p over Iran.

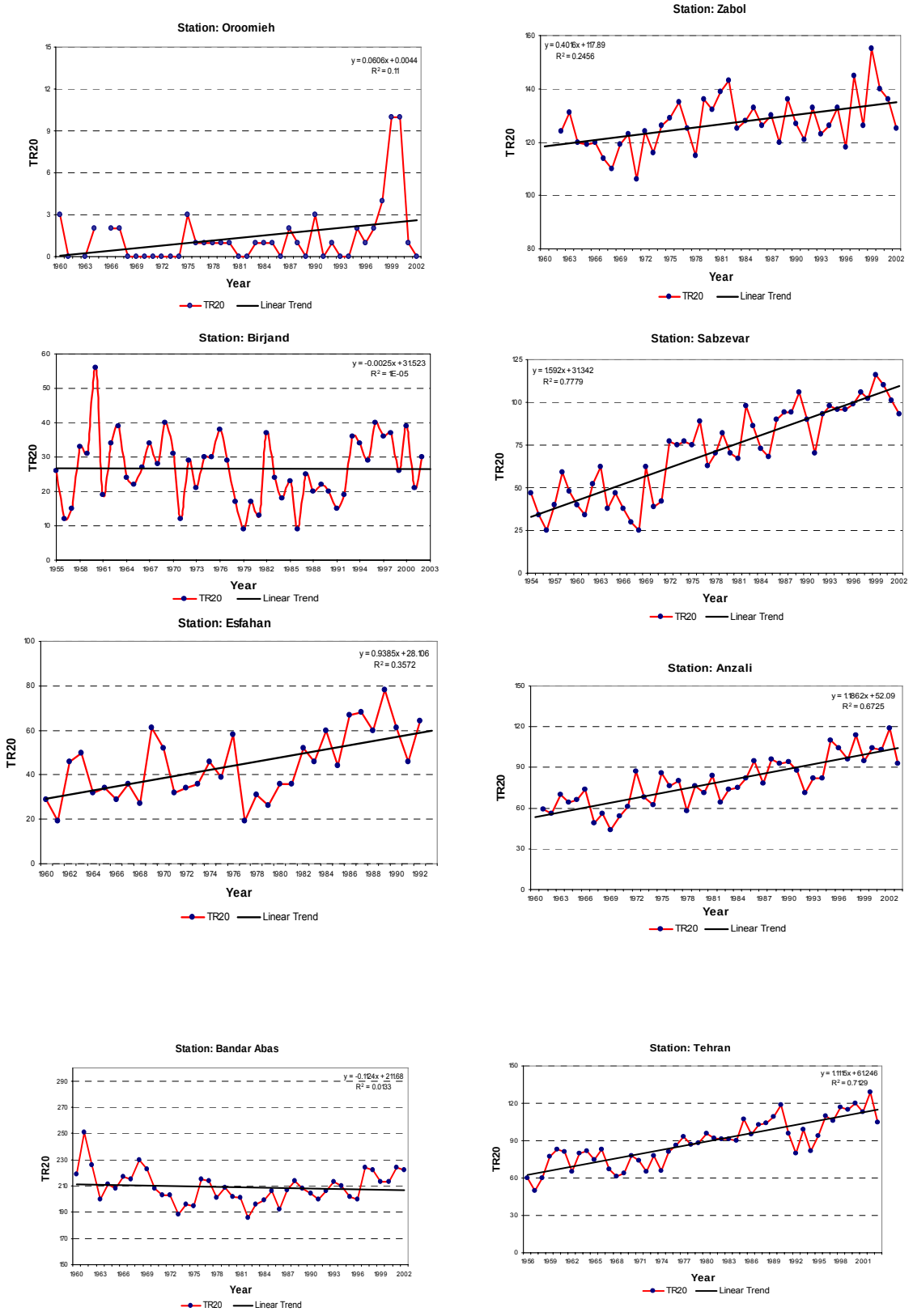

Figure 4. Some selected cases for their negative trends, large values, and positive trends of TR20 over Iran.

REFERENCES

1. Alexander, L., X. Zhang, T. C. Peterson, J. Caesar, B. Gleason, A. Klein Tank, M. Haylock, D. Collins, B. Trewin, F. Rahimzadeh, A. Taghipour, K. Rupa Kumar, J. Revadekar, G. Griffiths, L. Vincent, D. Stephenson, J. Burn, E. Aguilar, M. Brunet, M. Taylor, M. New, P. Zhai, M. Rusticucci, J. L. Vazquez-Aguirre., 2006: Global observed changes in daily climate extremes of temperature and precipitation. J. Geophys. Res., D05109, doi: 10.1029/2005JD006290.
2. ASMERC, 2005, National Project report on " reduction of chilling damage on agricultural products in provinces of east and west Azerbaijan (In Farsi)
3. Alijani, B., 1997 : Temporal variability of temperature over Tehran, First regional conference on climate change, Iran (In Farsi)
4. Brohan, P. et al., 2006: Uncertainty estimates in regional and global observed temperature changes: A new dataset from 1850, J. Geophys. Res., 111, D12106, doi: 10.1029/2005JD006548.
5. Bonsal, B. R., X. Zhang, L. A. Vincent, and W. D. hogg, 2001: Characteristics of daily and extreme temperature over Canada. J. Climate, 14, 1959-1976.
6. Collins, D.A., P.M. Della – Marta, N. Plummer and B.C. Trewin, 2000, Trends in annual Frequencies of Extreme Temperature events in Australia. Australian Meteorological Magazine, Vol. 49, PP. 277- 292.
7. Degaetano AT, 1996: Recent trends in Maximum and Minimum temperature threshold exceedences in Northern United States, Journal of climate 9:1646-1657.
8. Easterling, D.R., J.L. Evans, P.Ya. Groisman, T.R. Karl, K.E. Kunkel, and P. Ambenje, 2000: Observed variability and trends in extreme climate events: A brief review. Bulletin of the American Meteorological Society, 81(3), 417-425.
9. Frich, P., L.V. Alexander, P. Della- Marta, B. Gleason, M. Haylock, A.M. G. Klein Tank, T. Peterson, 2002, Observed coherent changes in climatic extremes during the second half of the twentieth century. Climate Res., 19, 193–212.
10. Jahaditoroghi , M. 2000, Determination of temperature and precipitation for Mashhad in period 1951-1994. Quarterly journal of Geographical Research, Nos. 54 and 55, 151-165(In Farsi)
11. Kiktev, D., D.M.H. Sexton, L. Alexander, and C.K. Folland (2003), Comparison of modeled and observed trends in indices of daily climate extremes, J. Climate., 16, 3560-3571.
12. Plummer, N. Salinger MJ, Nicholls N.Suppiah R. Hennessy Kj Leighton RM, Trewin BC, page CM, Lough JM, 1999. Changes in climate extremes over the Australian region and New Zealand during the twentieth century, Climate Change 42:183-202.
13. Rasooli, A., 2002:Analysis of time series of air temperature over Tabriz, Nivar, Nos.13-16, 7-15.
14. Rahimzadeh, F., and Asgari. A, 2003. A Survey on Recent climate change over IRAN. Proceeding of 14th Global Warming international conference & expo (27-30 May, Boston, USA).
15. Rahimzadeh, F., and Asgari. A, 2005. A look at difference of increasing rates of maximum and minimum temperatures and decreasing rate of DTR over Iran, Geographical Research, 73, 155-171 (In Farsi).
16. Ryoo, S. B., W.T. Kwon, and J.G. Jhun, 2004: Characteristics of Wintertime Daily and Extreme Minimum Temperature over South Korea. International Journal of Climatology, Vol. 24, PP. 145-160.
17. Sneyers, R., 1990. On the Statistical Analysis of Series of Observations, WMO Publ. No. 415, Geneva.
18. Zhai Pm. Sun A, Ren F Liu X, gao B. Zhang Q. 1999. Changes of climate extremes in China. Climate Change 42: 203-218e.
19. Zhang, X., E. Aguilar, S. Sensoy, H. Melkonyan, U. Tagiyeva, N. Ahmed, N. Kutaladze, F. Rahimzadeh, A. Taghipour, T.H. Hantosh, P. Albert, M. Semawi, M. Karam Ali, M. Halal Said Al-Shabibi, Z. Al-Oulan,Taha Zatari, I. Al Dean Khelet, S. Hammoud, M. Demircan, M. Eken, M. Adiguzel, L. Alexander, T. Peterson and Trevor Wallis, 2006: Trends in Middle East Climate Extremes Indices during 1930-2003. J. Geophys. Res., 110, D22104, doi: 10.1029/2005JD006181.
20. URL1: http://www.R-project.org

ANALYSIS OF THE DATES OF SPRING AND FALL FREEZING IN THE EAST AND WEST AZARBAIJAN PROVINCES

F.Sahraian, K.Noohi, M. Pedram, A.Sedaghatkerdar

Atmospheric Science and Meteorological Research Center
sahraian@irimet.net

ABSTRACT

From 1990 to 1999, 280 and 133 cases of freezing has been documented in the West and East Azarbaijan provinces, respectively. They rank the first and second among the other provinces in Iran. They are also the most important regions for entrance of cold systems to Iran.

In this study, we analyzed the dates of the first fall and late spring freezing , regardless the type of freezing for 26 meteorological stations from (1986 to 2000). The results show that the earliest mean date of first fall freezing is the second of October and the latest mean date of late spring freezing is the sixteenth of November. These freezing end from twenty seventh of March till sixth of May.

This study also showed that in the west and south west regions of the West Azarbaijan and east of East Azarbaijan, adjacent to Sabalan mountain and regions near to the Sahand mountain, the freezing comes earlier and end much later with longer duration. However, in the north regions of these two provinces, and the south regions of the lake of Oromeieh, the freezing comes later and end earlier with the shorter duration.

Keywords: Freezing, East and West Azarbaijan Provinces

INTRODUCTION

The dates of the beginning and the end of freezing period have an extra importance in agriculture. That is because farming products can grow in a special range of temperature and if the temperature outranges this temperature range, the products will have decrease in growing and even leads to termination of the product.

The first freezing that occurs in the freezing period is called "Early fall freezing". In fall, the freezing will harm the active growing branches sooner than normal time.

The last freezing that occurs during the freezing period is called "late spring freezing".
In spring freezing later than normal time will cause a kind of damage that depends on growing stages of fruit. The trees are very sensitive to cold air specially from blooming to fruit yielding.

In order to decrease the damage of freezing we need some information about frequency, duration and date of occurrence of freezing.

A frost day is a 24 hour of time in which the temperature of the meteorological shelter reaches to zero or less.

The average time of growing period is determined by the dates of the first and last freezing in fall and spring, and this information is used to determine the species of the plants for farming in that area. If probabilities and distribution of these dates around the average are determined, these data will be more useful for analyzing the early fall freezing & late spring freezing. Many studies has been done about freezing, rather theoretical or statistical methods. Frich and et. al (2002)studied on global changes in climatic extremes during the second half of the 20th century. He concluded that the No. of frost days has decreased in midlatituds regions and north part of north hemisphere[1]. Samiee (1997) has founded some tables of predicting the beginning & ending dates of fall & spring freezing by using the daily minimum temperature of meteorological stations. In this research, the period of free frost period was also determined for the first time[4]. Kamali (et all 2001) has researched on local freezing and the potential of return periods of freezing. The data of this study was the minimum temperature of 120 meteorological stations for the period of (1951-1998). The range of temperature was -4.4°C to -8.9°C. They concluded that the dates of chilling and freezing are random and obey normal distribution and they are independent of each other [2].

West and East Azerbaijan provinces with having 280 & 133 freezing occurrences within (1990-1999) have the first & second rank among other Iranian provinces[3].

The formal report of agriculture insurance shows that in a period of 16 years an amount of 122, 907, 421, 13 Rials has been paid for damage of both provinces wheat crop. Of course the damage is far more than mentioned. so the beginning and ending dates of freezing, the length of the period and the number of freezing days of these two provinces, which are the entrances to most of the cold weather systems to our country, is extremely important. In the mountainous regions such as East & west Azarbaijan provinces, prediction of the chilling and freezing dates is more complicated, because temperature inversion, increases the daily range temperature, and the roughness increases the problems due to analyzing the results of temperature data.. By predicting of freezing dates and early warning, the damage of farming crops can decrease significantly.

METHODS

In order to extract the first dates of freezing in fall and the last in spring, the minimum daily temperatures of at least 26 stations in these provinces were used in (1986-2000) period.
These stations were chosen based on spatial distribution and long length of records in this area. Because the statistical period of these stations are different from each other, a common period of 13 years was considered for all.

It's good to mention that the minimum daily temperatures in these stations are measured at 6:30 am & 6:30 pm local time.

After extracting and completing the minimum daily temperatures, the first dates in autumn and the last dates in spring in which temperature fell zero or less were determined by running a computer program .for calculating the probability of 25%, 50% and 75% for these freezing dates, all the dates must have been converted to numbers and in order to do so, the first of September was set to the starting point and all dates where given a number according to the

number of days away from the start. It's quite good to mention that the freezing starts in a year and ends at the beginning of the next year. Different statistical tests including homogeneity has done on the time series of first and last freezing dates.
The length of the freezing is the subtraction of the beginning and the end of freezing dates.
The number of freezing days were analyzed for better understanding of freezing in this area. After calculating the parameters of freezing with the probability of 25%, 50%, 75% by using of GIS software, the isovalues maps of freezing parameters were graphed, which are shown in fig.1 to fig.4.

CONCLUSION

-In the (1986-2000) period, on average, the first freezing has been occured on 2th October in "Sarab" station and the latest on 16th November in "Jolfa", "Maraghe", "Miyane" and "Pichek" stations..
-On average, the longest length of freezing is 216 days in "Sarab" station, and the shortest is 133 days in "Oshnavieh" station.
-The most No. of frost days is 175 days reported by "Khalkhal sofla" station and the least is 81 days reported by "Oshnavieh" station.
-The risk period of freezing in East and West Azerbaijan provinces, starts form 25th Sep. to 11th Nov. with probability of 25%, from 2th Oct. to 16th Nov. with probability of 50% and from 8th Oct. to 27th Nov. with probability of 75%.
-The risk period of freezing in East and West Azerbaijan provinces ends from 13th April. to17t May. with probability of 25%,from 27th Mars. to 6th May. with probability of 50% and from. 20th Mars to1th May. with probability of 25%.
-In the west and south west regions of the West Azarbaijan and east of East Azarbaijan provinces, adjacent to Sabalan mountain and regions near to the Sahand mountain, the freezing comes earlier and end much later with longer duration, However in the north regions of these two provinces, and the south regions of the lake of Oromeieh, the freezing comes later and ends earlier with the shorter duration.

REFERENCES

[1] Frich, P. L. V. Alexander, P. Della, Marta, B. Gleason, M. Haylock, A. Klein Tank, and T., Peterson, 2002," Global changes in climatic extremes during the 2nd half of the 20th century", Climate, Res., 19, 193 – 212.
[2] Kamali,GH.,2001, Review of chilling and freezing disasters on crop production in Iran ,Final Report of Research Project ,I.R. of Iran Meteorological Organization(IRIMO).
[3] Report of Research Project, 2002 ,Determination of potential of occurrence of weather and climate hazards in Iran, Report No.3,ASMERC, IRIMO.
[4] Samiee, M., M.,Askari,KH.,Bastani,1997,Begining and ending of frost in Iran, Report of Research Project, IRIMO.

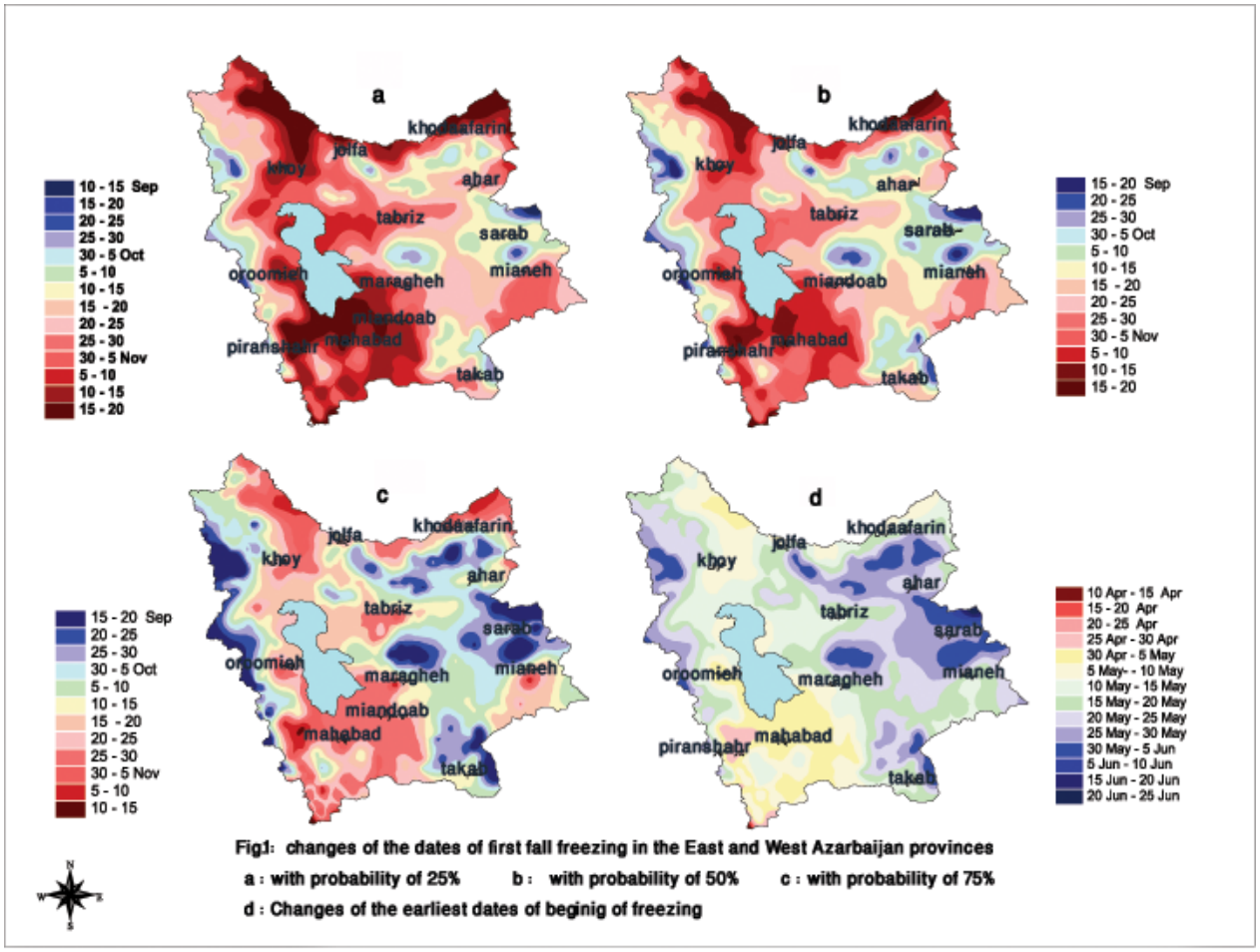

Fig1: changes of the dates of first fall freezing in the East and West Azarbaijan provinces

a : with probability of 25% b : with probability of 50% c : with probability of 75%

d : Changes of the earliest dates of beginig of freezing

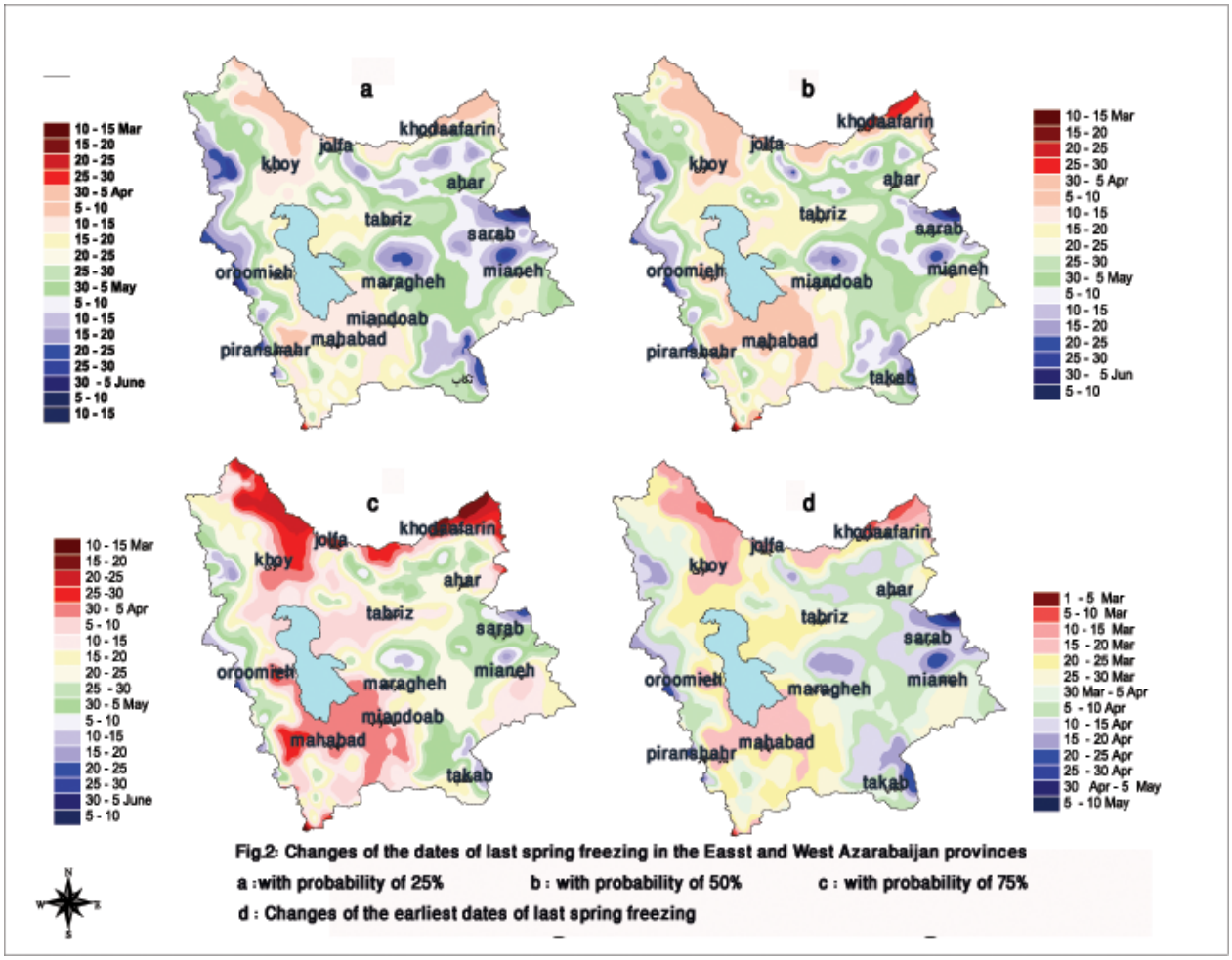

Fig.2: Changes of the dates of last spring freezing in the Easst and West Azarabaijan provinces

a :with probability of 25% b : with probability of 50% c : with probability of 75%

d : Changes of the earliest dates of last spring freezing

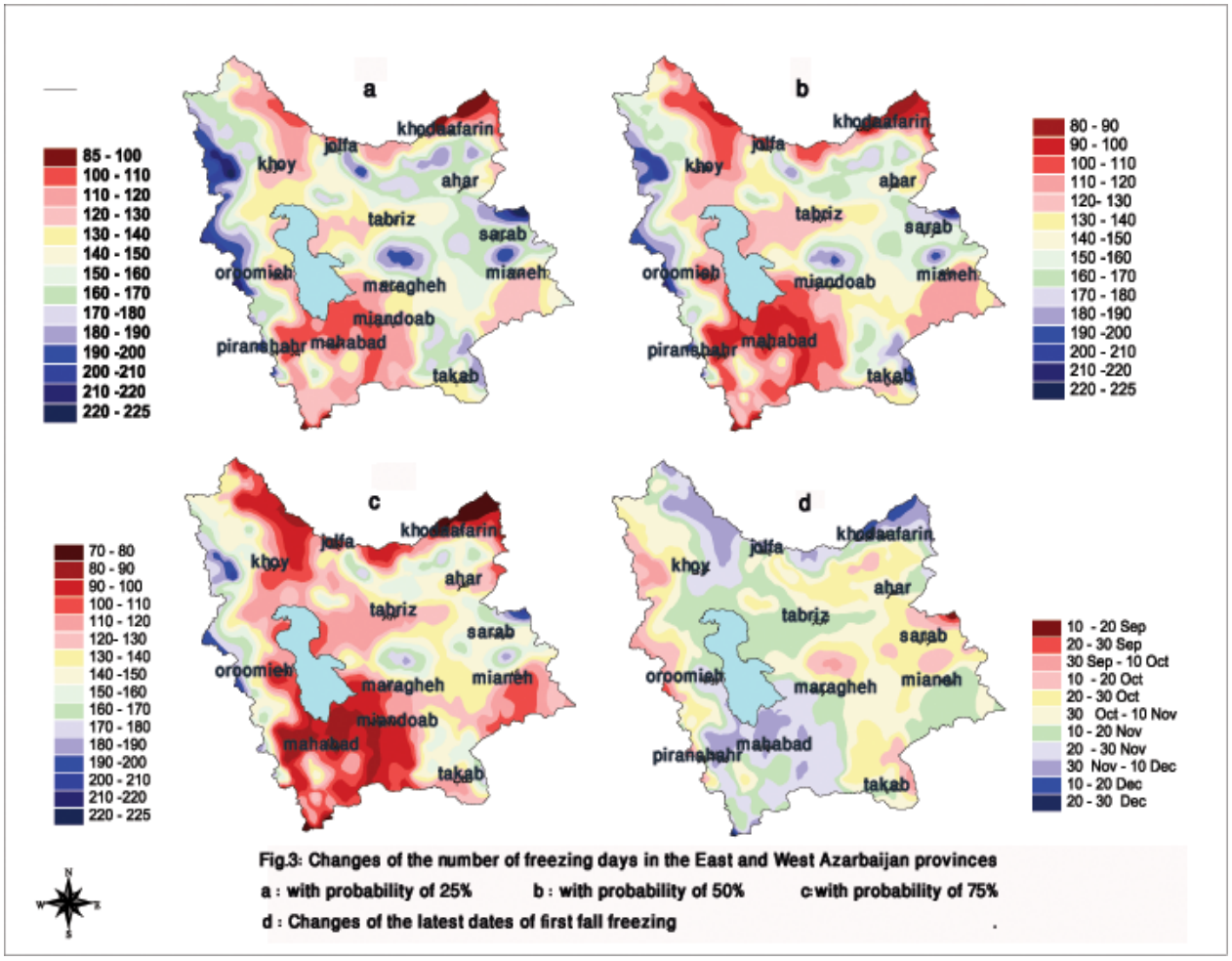

Fig.3: Changes of the number of freezing days in the East and West Azarbaijan provinces

a : with probability of 25% b : with probability of 50% c: with probability of 75%

d : Changes of the latest dates of first fall freezing

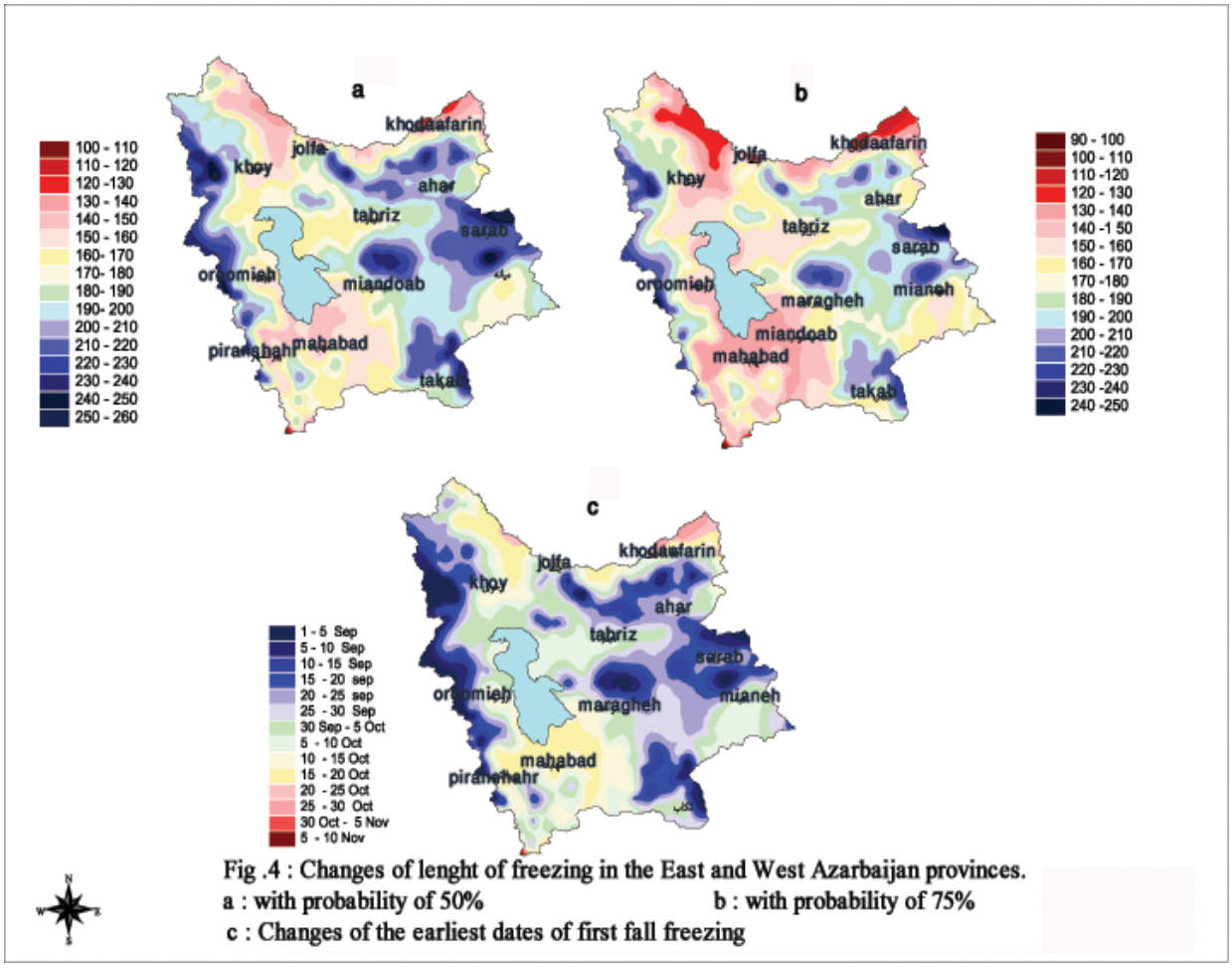

Fig .4 : Changes of lenght of freezing in the East and West Azarbaijan provinces.
a : with probability of 50% b : with probability of 75%
c : Changes of the earliest dates of first fall freezing

DROUGHT EVALUATION IN ISFAHAN PROVINCE USING STATISTICAL AND GEOSTATISTICAL METHODS

Mohammad Reza Yazdani, Morteza Khodagholi, Korosh Shirani, Sattar Chavoshi

Agriculture and Natural Resources Research Center, Isfahan, Iran,
moreya1@yahoo.com

ABSTRACT

Iran is one of the countries which has effected by Natural hazards such as flood, earthquake, drought and etc. These hazards create a lot of damages and changes natural conditions. Drought is one of the natural hazards that is more complicated compared with the others because of its slow affect. Desert in Isfahan province are extended especially in east part of it affected of drought progress. Drought evaluation is one of the most important approaches that can be used in drought management. For this goal it is necessary to define an index that indicates, intensity, duration and amount of the drought .In this study 85 rain gauges were selected in Isfahan province and around of it for 32 years period. Climatologic drought was evaluated using statistical indexes such as, percent of mean rainfall, rainfall deviation index and standard precipitation index. Then local distribution of drought was classified. Standard deviation index is used for drought area extension. Geostatistical methods were used for interpolation and best variogram was determined. Generally, spherical method has the best fitted model. Maps of drought extension were prepared using ILWIS 3 software and krigging method. Local and temporal pattern of drought was determined. Drought area extension is declined when rainfall is increased. Results showed that about 50 percent of Isfahan province had affected by drought in 1994, condition was normal in1974, but wet condition was occurred in 1990.

Keywords: Climatologic drought, Drought index, Geostatistics, Isfahan.

INTRODUCTION

Drought is one of the most important natural hazards that it can cause a lot of damages. Isfahan province is located in central dry part of Iran. Annual rainfall is low in this region and it has not Homogeneity in space and time. Drought has negative effects on crop yield. In this region this phenomenon has been accelerated due to climate changes. There is no common define for drought because of multiple factors influencing it. Therefore we can see a lot of indexes or definitions for drought regard to each geographical region. However intensity and duration of it is differs from everywhere. Generally, Hydrologic drought has been created with extension of climatologic drought [1,10,15] and this problem can causes water resources crisis in dry and semidry lands. Human has effective role on climate changes besides natural factors. Drought maybe cans not appearance due to unsuitable grazing, inaccurate land use and deforestation but these can increase hazard frequency of drought [17]. There are several definitions for climatologic drought. Usually, climatologists considered the occurrence of a drought when the rainfall is lower than longtime average. Indexes of drought is mainly on the basis of rainfall factor, such as, rainfall is less than 85 percent of average [9], annual or monthly rainfall is less than a special percent of average [6] and when annual rainfall is lower

than 75 percent of average or monthly rainfall is lower than 60 Percent of average monthly rainfall [3]. In this study were used three statistical indexes for temporal drought analysis.

Study area

The study region was Isfahan province with 105263km^2 area and it has longitude 49 30' to 55 50' and latitude form 31 26' to 34 30'. Isfahan province is located in central part of Iran. Annual average of rainfall is about 170 millimeters and has high coefficient variable. Generally amount of rainfall is decreasing from west to east sections. Figure 1 shows study area.

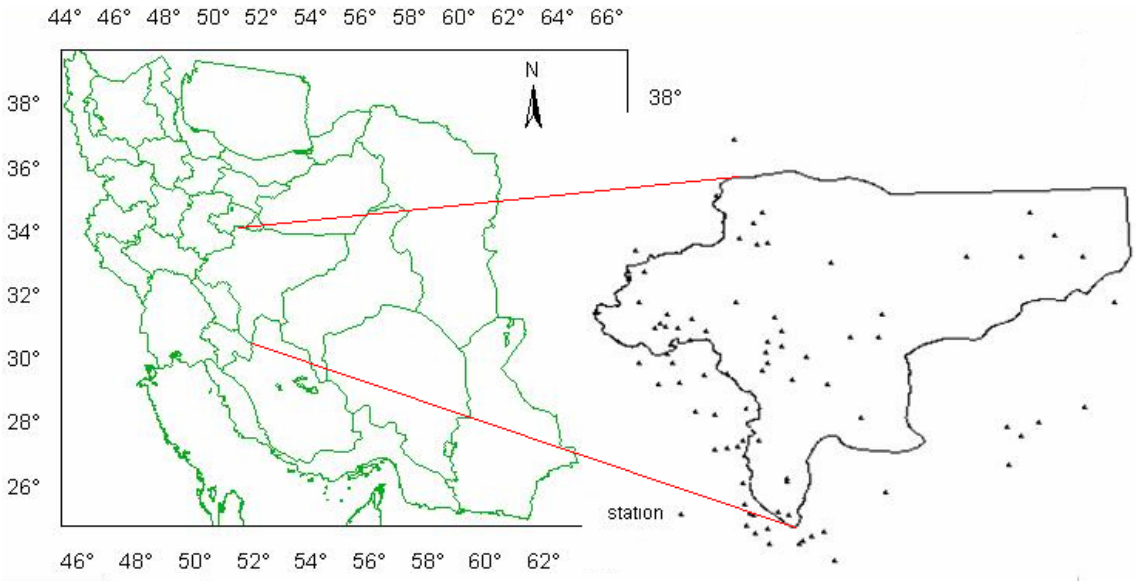

Figure 1. Location of study area

METHODS

In this study 85 rain gauges was selected during 1961-1998(figure 1).These years were selected based on water year that each year starts from October to September. Run test was used for Homogeneity control of data. Then missing data was completed using correlation method among stations [14].

Statistical methods

It is necessary to determination a suitable method for recognition, definition and evaluation of drought before get a decision about drought management. However three statistical indexes were selected in this survey that are following:

Percent of mean rainfall: it is define as rate of a rainfall to long time mean rainfall:

$$\%p = \frac{p_i}{p} \times 100 \qquad (1)$$

Where p_i is rainfall in a year and p is longtime mean rainfall in the station [6] .This method is simple and flexible and it mostly has been used by researcher. Classification of this method is presented in table 1.

Table 1. Drought classification based on percent of mean rainfall

Class	Drought description	Percent of mean rainfall
1	Poor	70-80
2	Moderate	55-70
3	Intensive	40-55
4	High intensive	<40

Standard deviation index: deviation from average can indicates rainfall variations form average, regard to below relation:

$$S = \sqrt{\frac{\sum (x_i - \bar{x})^2}{n-1}} \qquad (2)$$

Where S is standard deviation, x_i rainfall for ith samples, $\bar{x}$ is average rainfall and n is sample size. Table 2 has presented for drought classification using this index [11].

Table 2. Drought classification using standard deviation index

Class	Drought description	Standard deviation
1	Poor	<0.5S
2	Moderate	0.5S-S
3	Intensive	S-2S
4	High intensive	>2S

Standard precipitation Index: it has follow equation:

$$Z = \frac{x_i - \mu}{\sigma} = \frac{x_i - \bar{x}}{S} \qquad (3)$$

Where μ is mean of a society, $\bar{x}$ is sample mean, σ is standard deviation of the society and s is standard deviation of selected sample[4,13,16]. Indian researchers had used this index for Analyzing annual and seasonal rainfall data of Indian. Classification of this index are depicted in table 3 [6].

Table 3. Drought classification using standard precipitation index

class	Drought definition	Z
1	Very intensive wet (VIW)	>2
2	Intensive wet (IW)	1.5:1.99
3	Wet (w)	1:1.49
4	Normal (N)	0.99: -0.99
5	Drought (D)	-1: -1.49
6	Intensive Drought (ID)	-1.5:1.99
7	Very Intensive Drought(VID)	<-2

Interpolation method

It is require transferring point distribution to regional distribution. Therefore, interpolation methods have been used. One of these methods is geostatistical method. This method considers correlation and local structural of data. In geostatistical method data of a parameter in distinguish coordinate can have estimated with the same parameter in another distinguish coordinate. For this purpose, Krigging method was selected among geostatistical methods.

Table 4. Drought classification for two indexes.

Year	Percent of mean rainfall Index	Standard deviation Index	Year	Percent of mean rainfall Index	Standard deviation Index
	class			class	
1967-1968	-	2	1983-1984	-	2
1968-1969	-	2	1984-1985	3	1
1969-1970	2	2	1985-1986	-	2
1970-1971	3	2	1986-1987	-	3
1971-1972	1	3	1987-1988	-	3
1972-1973	2	2	1988-1989	2	2
1973-1974	-	2	1989-1990	-	2
1974-1975	-	3	1990-1991	1	2
1975-1976	-	3	1991-1992	-	3
1976-1977	-	2	1992-1993	-	3
1977-1978	2	3	1993-1994	2	2
1978-1979	-	2	1994-1995	-	3
1979-1980	-	3	1995-1996	-	3
1980-1981	1	2	1996-1997	2	2
1981-1982	1	2	1997-1998	-	3
1982-1983	-	2	1998-1999	-	2

This method is based on weighted moving averages and it has called the best unbias estimator. General equation of this method is following:

$$Z^*(x_i) = \sum_{i=1}^{n} \lambda_i . Z(x_i) \quad (4)$$

Where, $Z^*(x_i)$ is estimated parameter, λ_i is weight of ith sample, n; sample size and $z(x_i)$ is observed parameter[8,12]. If variable z has normal distribution we can use this method, other wise it is necessary using nonlinear Krigging or change distribution of the variable to normal distribution. A criterion of mean absolate error (MAE) was used for error evaluation and selection of the best model in this study. This criterion defines as:

$$MAE = \frac{1}{n} \sum_{i=1}^{n} \left| Z^*(x_i) - Z(x_i) \right| \quad (5)$$

Where, $Z^*(x_i)$ is estimated variable x_i, z (x_i); observed variable x_i and n is number of variable. The best method has lower MAE.

RESULTS

Data got normal distribution using logarithmic transformation. Then variography analysis was done using GS^+ software and sill, nugget and effective range was determined in each year. The errors were calculated for Gaussian and spherical methods considering similitary of them. Spherical model was used for interpolation because it had lower error. Interpolation was down using ILWIS software and annual rainfall maps were calculated with digital band of the study area. These maps were used in equations 1 to 3 and have calculated percent of mean annual and standard deviation of rainfall. Drought classifications are summarized in table 4 in each year.

Drought classification was calculated using standard precipitation index and table 3. Local distributions of droughts using this index are depicted for Isfahan province in the years of 1980 and 1995(figure 2 and 3).

Mean annual rainfall has high correlation with extension of drought area and these have linear relation (R^2= 0.89). This relation is:

$$P = -638.84A + 121188 \quad (6)$$

Where P is annual rainfall in mm and A is drought area in km^2.
Frequency analysis of annual rainfall indicated that the best distribution was log-Pearson type III. Rainfall with different return interval was calculated and the results are presented in table 5.

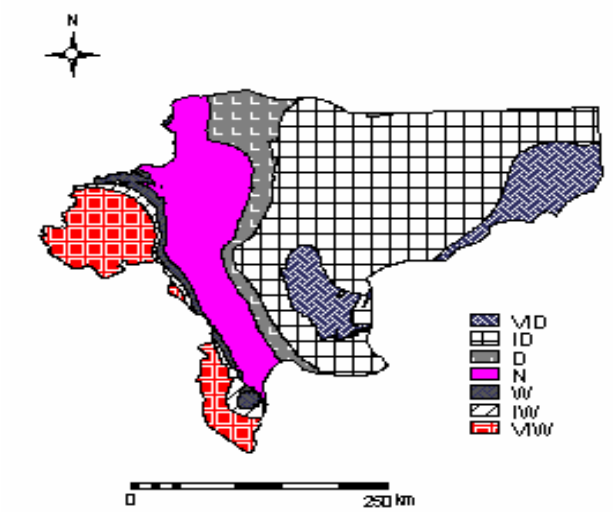

Figure 2. Local distribution of drought classification using standard precipitation index in 1986.

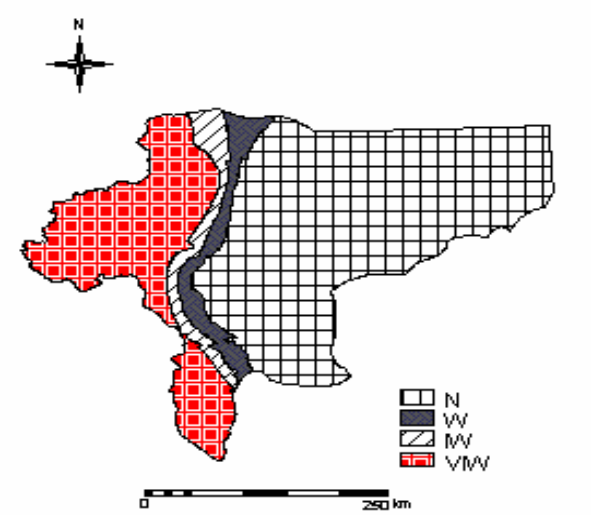

Figure 3. Local distribution of drought classification using standard precipitation index in 1986.

Table 5. Mean annual rainfall in different intervals

return interval	mean annual rainfall (mm)
2	136.54
5	177.7
10	200.39
20	219.4
25	224.9
50	240.8
100	255
200	267.7

CONCLUSION

In this study, climatologic drought had evaluated using 85 rain gauges for a 32 year period. After completing data, Interpolation was calculated for annual rainfall in study area. Variography analysis showed that nugget was changed from 0.001 to 0.025 and sill was changed from 0.012 to 0.23.Effective range varied 250000 to 300000 meters. Neighbor number of 26 had the lowest error. Result from percent of mean rainfall index showed that drought had a lot of changes and it had periodic pattern. In Isfahan province, 13 year had drought conditions based on this index. It varied from weak to intensive and remain years had wet conditions. Standard deviation Index showed drought condition in all years. Drought classification changed from moderate to intensive. But in standard precipitation index, droughts had local and temporal changes. For example, the most area of Isfahan province (73%) had affected by drought in 1984, in spite of this region had wet condition in the years of 1971 and 1995. Regard to this method, 30 percent of studied period had droughts conditions and this rate was 28 and 42 percent for wet and normal condition respectively. With attention to relation 6, the area of drought in Isfahan province was decreased due to increase of rainfall and this relation is linear. However wet limit was determined 189.7 millimeters rainfall. Therefore if the annual rainfall was lower than this amount, we could expected drought occurrence (the mean annual rainfall was calculated 139.5 in study area and selected period).

Rainfall frequency analysis indicates that if the annual rainfall is with 2-5 return intervals, drought occurrence will be high probable. Rainfalls with 2 return periods can causes a drought, that it covers 30 percent of region area. However this is probability estimation. Results indicate that percent of mean rainfall index is simple and it depend on normal condition in each rain gauge, but standard deviation index is not a suitable index for drought evaluation, however Index of annual standard precipitation not only considers mean rainfall but also it can determines rainfall change in a station. This index has the best capability compared with two other indexes. This index has average and standard deviation of 0 and1, so it can use same as comparable index among stations. Drought extension can be estimated using relation between rainfall and drought area. Results of this survey indicate better capability of standard precipitation Index compared with other selected indexes in Isfahan province and it can be used for evaluating time and space of droughts. However dry and wet conditions have periodic pattern in study area.

REFERENCES

1 Ahmad, Sh., et al, (2004) Drought mitigation in Pakistan: current status and option for future strategies, International Water Management Institute, Drought series, paper3.
2-Bearl, L.R. and Kubik ,H.K.(1972)Drought severity and water supply dependability, J. of Irrig. And Drain. Div., 98(3): 433-442.
3-Farajzadeh, M. (1995) Evaluation and prediction of drought in Iran, PhD thesis. Tarbiat Modarres University.
4-Ghayor, H. and masoodian,A.(1999) study on local and temporal pattern of drought in Isfahan province, 2th regional conference on climate change, Tehran.

5-Hajarizadeh, Z.and fatahi,E.(2003) Evaluation of drought in khorasan province indicating short terms drought, 3th regional conference and 1st national conference on climate change.
6- Hays, M.J. 1999.Drought indices, climate impacts, National Drought Mitigation Center, USA.
7-Hays, M.J., Suoboda, M.D., Wilhite, D.A. and Vanyavkho O.V.(1999) Monitoring the 1996 drought using the standardized precipitation index, BAMS 80,pp: 429-438.
8-Hosseini pak .A. (1998) Geostatistics, Tehran university publication, Iran.
9-Hoyt, J.C.(1936), Drought of 1930-1934, V S geography survey, water supply, paper No.68
10-International strategy for disaster reduction (2003) Drought: Living with risk, ISDR Ad Hog Discussion Group on drought.
11-LashaniZand, M.(2003) study on climatologic drought in Iran and the approaches to overcome it: a case study on 6 basins in west and northwest of Iran, PhD thesis, University of Isfahan, Iran.
12-Madani, H. (1998) the theory of Geostatistics, Amirkabir university of technology publication, Tehran.
13-Masoudian, A. (1998) study on time and space of precipitation changes in Iran, PhD thesis, University of Isfahan, Iran.
14-Mahdavi, M.(1999) Applied hydrology, Tehran university publication.
15-Razaei, T.and saghafian, B. (2004) Evaluation and management of drought risk, dry and drought journal, No, 2.
16-Smakhtin, V.U., Hughs, D.A. (2004).Review, automated estimation and analyses of drought indices in south Asia, Working paper 830, Colombo, Srilanka: International water management Institute.
17- UN Mission report. 2000. United nations technical mission on the drought situation in the Islamic Republic of Iran.

FREQUENCY OF THE HEAT WAVES IN ISTANBUL AND ITS RELATION TO CIRCULATION PATTERNS

Yurdanur Unal and Sibel Menteş[1]
[1]Istanbul Technical University, Department of Meteorology, Maslak, Istanbul, Turkey
sunal@itu.edu.tr

ABSTRACT

Many studies found significant increases in extreme temperature events within last few decades. Much attention has been given to events affecting the major metropolitan areas since ecosystems, human health and activities are very sensitive to these extremes. Extreme temperatures have been estimated to increase more than the mean temperature values. Long lasting extreme events such as heat waves, dry spells are harmful to the ecosystem and create danger on human health. Occurrence of heat waves is known to be influenced by atmospheric circulation and especially by certain flow patterns. Hence, it is important to determine the frequency of heat waves and their relation to circulation patterns.

In this study, we determined the heat waves and their frequencies for Istanbul from 1975 to 2005 for the months May to September (5months). Heat wave events are defined by the period of time in which temperatures are higher than a certain threshold for at least consecutive 3 days. Large scale circulation is characterized by 500hPa geopotential heights. Therefore, 2.5 degree NCEP re-analysis 500hPa geopotential heights covering the region of 10W-50E and 25N-60N are used to resolve the circulation patterns. Dominant modes of variability are identified in two time scales. First, Blackmon and Lau's (1980) low pass and band pass filters are applied to filter low frequency variability (longer than 10 days), and synoptic scale variability (2.5 to 6 days). Then, to find out the dominant circulation patterns, principal component analysis with VARIMAX rotation is applied to geopotential heights data in these time scales. Finally, we examined the relationship between dominant modes of time scales and circulation patterns of the days within the heat waves.

INTRODUCTION

World Health Organization for Europe states that heat waves have undesirable effects on human health. In 2003, it is estimated that heat wave related deaths all over Europe are more than 12000. Recent climate projection suggests that ongoing global warming by this century might increase the frequency, intensity and duration of heat waves.[1]

Climate variables on a local scale are influenced by large-scale circulation. Therefore, heat waves are closely related to circulation conditions, but their occurrence is favored by certain flow configurations[2]. Heat waves are generally associated with specific atmospheric circulation patterns represented by 500-hPa positive height anomalies that dynamically produce subsidence, clear skies, light winds, warm-air advection, and long lasting hot conditions at the surface. Predominant drought conditions also intensify the heat waves[3]. Relationship between circulation and occurrence of long lasting extreme events is thus an important component of a climate system.[2]

Changnon et al. (1996) compared the 1999 and 1995 heat waves, and concluded that especially the extreme nocturnal conditions of temperature and humidity during the peak of the 1999 and 1995 events were very similar. Reduction of the death poll from 700 to 114 in these two events was not due to different meteorological conditions but due to different responses[4]. Kunkel et al. (1996) examined the 1995 heat wave and the synoptic weather patterns associated with it and compared the conditions to the pervious heat wave events. They showed that high dew points due to limited vertical mixing from a subsidence inversion played a key role in the apparent temperature which is a quantity combining the effects of both temperature and humidity[5]. To answer the question whether the 1995 Chicago heat wave was an extreme anomaly or part of ongoing trend, Karl et al. (1997) analyzed the temperature records in the 26 Midwest stations of US and found that hourly temperatures increase moderately with no significant trend when 1995 event is excluded[6].

In this study, we defined heat waves by using maximum temperature data recorded in Göztepe meteorological station in Istanbul. The relationship of the heat waves experienced in Istanbul with the large scale circulation patterns is investigated for the months of May through September and the period of 1975-2005 by using the 500 hPa geopotential heights.

DATA

Data used in this study are daily maximum temperatures at Göztepe Meteorological Station obtained by Turkish State Meteorological Service and cover the periods between 1975 and 2005 for May through September. Göztepe meteorological station is located in Asian side of Istanbul. Data do not have any missing values within the period examined. Statistical summary of the data are presented in Table 1.

Table 1. Statistical description of daily maximum temperature data for Göztepe

	May	June	July	August	September
Average ^{o}C	21.3	26.2	28.5	28.3	24.9
Standard Deviation ^{o}C	3.8	3.3	2.8	2.7	3.1
Maximum ^{o}C	33	39.2	39.7	38.8	33.6
Minimum ^{o}C	9.9	13.6	19.5	19.8	13.4

Table 1 shows that highest temperatures in Istanbul are experienced in summer months and especially in the month of July, and lowest values are in May. Highest variability is seen during the transition month of May.

The second data set used in this study is daily averaged 500hPa geopotential height NCEP/NCAR re-analysis data covering the area of 10^{o}W-50^{o}E and 25^{o}N-60^{o}N. Data domain consists of 25x15 grid points. Data set comprises 31 years of daily averaged geopotential heights, and the observations span the same time interval of the station data, 1975-2005 for May – September.

PRINCIPAL COMPONENT ANALYSIS

In this study, we use the Principal Component Analysis (PCA) to determine the significant number of patterns from geopotential height of 500 hPa . PCA is well documented in the literature[9,10,11,12], and has been widely applied in meteorology to reduce a data set containing large number of variables to a data set containing fewer new variables with a large fraction of the variance of the original data. It is assumed that original data set consists of interrelated variables. After transformation, m original variables are represented by k new variables, where k is possibly less than m. Dimension of the new set of variables, k –called k principal components (PCs)– depends on the correlation among the variables. Usually data for atmospheric fields show large correlations among the variables. New variables (PCs) are linear combinations of the original variables, and the weighting functions are called the empirical orthogonal functions or eigenvectors.

In this paper, PCA is applied to 500 hPa geopotential height data for 1975-2005 warm months (May-September) to extract the significant atmospheric variability from noise, and data are filtered as low frequency variability (longer than 10 days) and high frequency variability components (between 3 to 7 days) prior to principal component analysis.

The PCA seeks dominant modes of variability and expresses the deterministic part of the original time series in the highest principal components. It simply filters out the noise part of the data by using the captured variance by each principal component. The resulting empirical orthogonal functions are normalized eigenvectors of the sample correlation (covariance) matrix. Eigenvectors are the solutions of the equation (1):

$$\mathbf{C}\,\mathbf{e}_i = \lambda_i\,\mathbf{e}_i \qquad (1)$$

Where $C = D^T D$ is m by m spatial correlation matrix and D is the data matrix with the dimension n by m. Here D^T is transpose of matrix D. In this study, each column of D includes 500 h Pa geopotential height at a specific location for n days. C corresponds to the cross-covariance matrix with diagonal elements corresponding to the variance at that geographical location. m is the number grid points. $\mathbf{e}_i$s are normalized eigenvectors satisfying equation 1, and λ_is are corresponding eigenvalues. Eigenvectors are defined to satisfy the relation of $\mathbf{e}_i\,\mathbf{e}_j = \delta_{ij}\,\lambda_i$. Here δ_{ij} is equal to one for i=j and zero for i≠j. Eigenvalues represent the variance associated with corresponding eigenvectors and principal components. Eigenvalues are indexed in the decreasing order of their values so that the first eigenvalue represents the variance captured by the first eigenmode or PC, and it is associated with the maximum variability. Second mode captures the second highest variance and so on. Therefore eigenvalue with the highest order has the minimum variance among all. The corresponding PC accounts for the temporal variability that represents original variables projected over each eigenmode. The PCs are defined by:

$$\mathbf{p}_i = \mathbf{D}\mathbf{e}_i \quad \text{for } i=1,\ldots,k, \qquad (2)$$

where $k \leq m$. Sum of the first k eigenvalues represent the captured variance by k principal components. Therefore, to reduce the dimension of the large data set, one can seek possible ks to account for most of the variance in the original data set by keeping k as small as possible. Therefore, it is possible to capture most of the significant information in the original data set by including some smaller number of principal components. Thus, there is a trade off between number of new variables and amount of captured variance. The question is how few principal

components can be retained without discarding important information included in the original data set. There are several methods to determine k reported in the literature, and it is a subjective choice, which depends on the data and the purpose of the analysis. Preisendorfer (1988) investigates many principal component selection rules[11]. One of the simplest methods, the scree-test, is adopted in this study. The method is based on viewing eigenvalues in a logarithmic scale in relation to their orders. This subjective judgment seeks a break point (k) on the plotted curve in which slope of the curve is steep on the left of the break point and shallow on the right of the break point. The sum of the first k (breaking point) eigenvalues gives the portion of the total variance captured by the new set of k variables. Hence, sum of all eigenvalues corresponds to the total variance of the original data set.

HEAT WAVES

In this study, the heat waves are defined as the prolonged extreme events lasting at least for three consecutive days and within this period maximum temperatures exceed a certain threshold. Threshold values are determined by frequency distribution of maximum temperatures for warm months (May-September) for 31 years of observations in Göztepe. Huth et al. (2000) and Meehl and Tebaldi (2004) define two threshold values in order to classify the heat waves as tropical days and summer days.[2,3] We use the same approach here. 97.5 and 81 percentiles of the maximum temperature distributions correspond to 32°C and 29°C, respectively. The heat spells in which temperatures are exceeding 32°C and 29°C are as called tropical days and summer days, respectively, by following Huth, et al., (2000)[7]. Figure 1a and 1b shows the number of heat waves and the number of days in each heat wave. Blue and red bars correspond to tropical days and summer days.

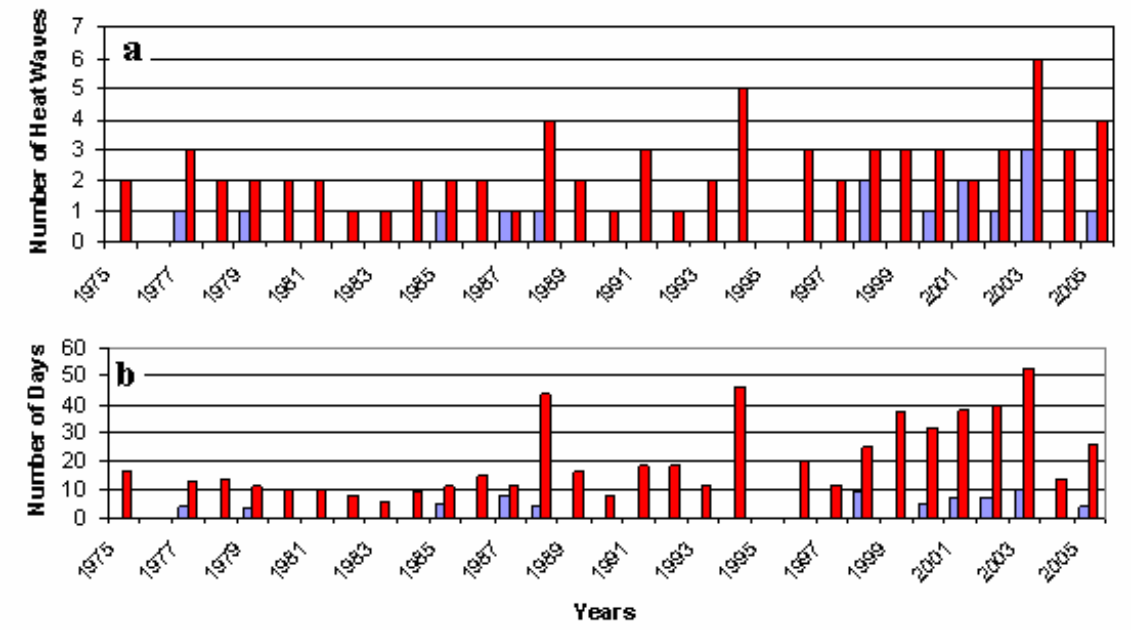

Figure 1. **a)** Number of heat waves defined by two threshold values of 32°C (blue) and 29°C (red). **b)** Number of days within the heat waves defined in a.

For the period of 1975 and 2005, it is striking that the number of heat waves and number of days within heat waves increase especially in late 1990s and in early 2000s. The most extreme case is experienced in 2003. Number of days in which temperatures exceed 32^{o}C and 29^{o}C are 10 and 53, respectively; and the number of heat wave events are 3 and 6 for both cases. Corresponding nocturnal temperatures are also high during these heat waves.

During June for the period of 1975-2005, duration of the heat waves defined by using the definition of summer days is generally 6 or 8 days. Especially, heat waves determined by using the lower threshold of 29^{o}C are common in June.

During July, heat waves between 2001 and 2002 continue for 22 days while in 2000 for 11 days with the peak value of 39.7^{o}C which is the highest recorded maximum temperature within the observation period. In July, number of heat waves in which temperatures exceed 32^{o}C is significantly higher compared to the other months.

During August, the third highest temperature value of 38.8^{o}C is experienced. Heat waves continuing for 15-19 days are observed. Most striking event is occurred in 1998. It starts in July and continues until 10th of August with the total of 21 days. Similarly heat waves started in July of 2002 and 2003 affected the region and continued in August. Durations of the heat waves are 28 days and 20 days, respectively.

During September, frequency and the duration of heat waves are significantly reduced. In 1994, there is only one heat wave (composed of summer days) lasted for 11 days.

DOMINANT CIRCULATION PATTERNS

Before searching for a relationship between the circulation and heat waves, we examined the dominant circulation patterns over Europe and Western Asia for two different time scales. First is the low frequency variability, longer than 10 days, and the second is the high frequency variability, variability within the period of 3 to 5 days, or in synoptic scale. Synoptic scale pressure formations such as cyclones and anticyclones, their movements affect the instantaneous weather conditions in midlatitudes, and also daily variability, and low frequency variability such as blocking events affect weather conditions over large areas for relatively long period of time. For this purpose, 500hPa heights were filtered using Blackmon and Lau's (1980) low-pass and band-pass filters[5,6], which retain the variability of the periods longer than 10 days (low frequencies) and 2.5 to 6 days (synoptic frequencies), respectively. Principal component analysis (PCA) is applied to the filtered data and significant patterns are rotated by using the VARIMAX rotation to reduce the domain dependency, to obtain physically meaningful patterns and to simplify the interpretation. The simple idea of VARIMAX rotation is that for each factor, high loadings (correlations) are associated with a few variables; the rest becomes near zero.

For the low frequency variability, scree-test reveals that first 9 eigenmodes are significant. They capture 95% of the original variability. First three modes explain 39%, 19% and 15% of the total variance, respectively. The first three modes after VARIMAX rotation is illustrated in Figure 2 a-c.

The first mode represents three anomaly centers which are located over Scandinavia, north of Italy and Saudi Arabia. Northwestern part of Turkey is under the influence of cyclonic or anticyclonic flow. The second mode shows a strong gradient over eastern Russia trough the northwest of Black Sea, negative/positive anomalies over eastern Black Sea and positive/negative anomalies over central Mediterranean. The third represents a strong negative/positive anomaly centered Aegean Sea influencing the western part of Turkey.

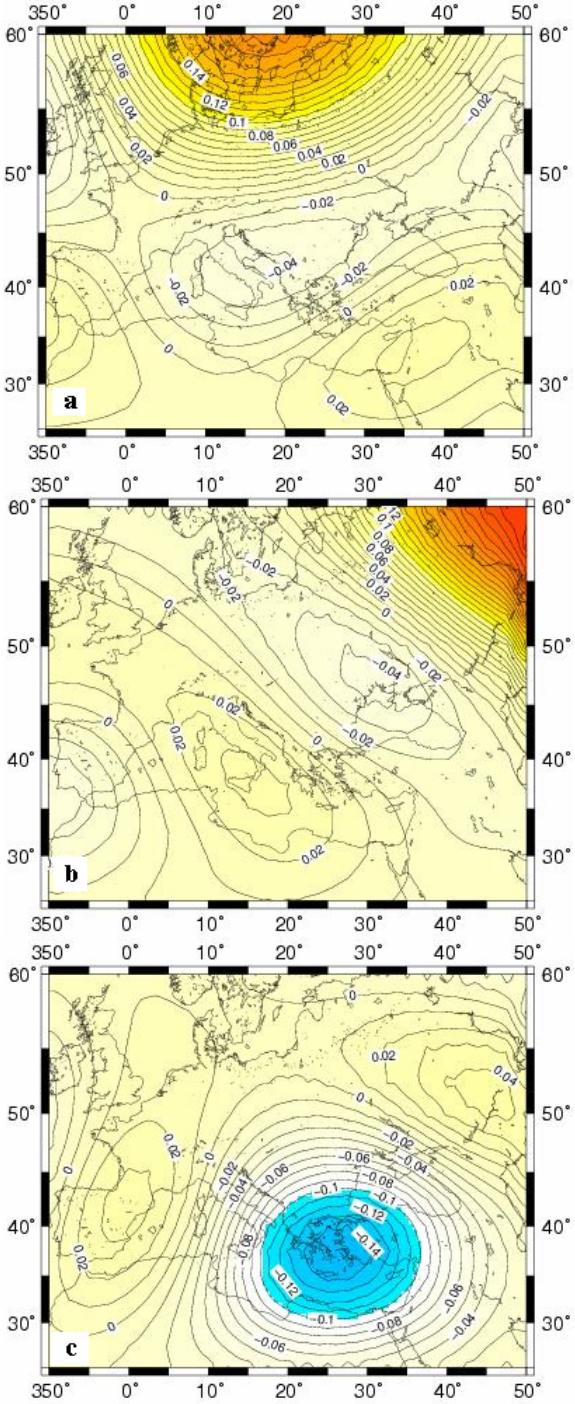

Figure 2. First three dominant patterns of 500hPa geopotential heights for low frequency variability.

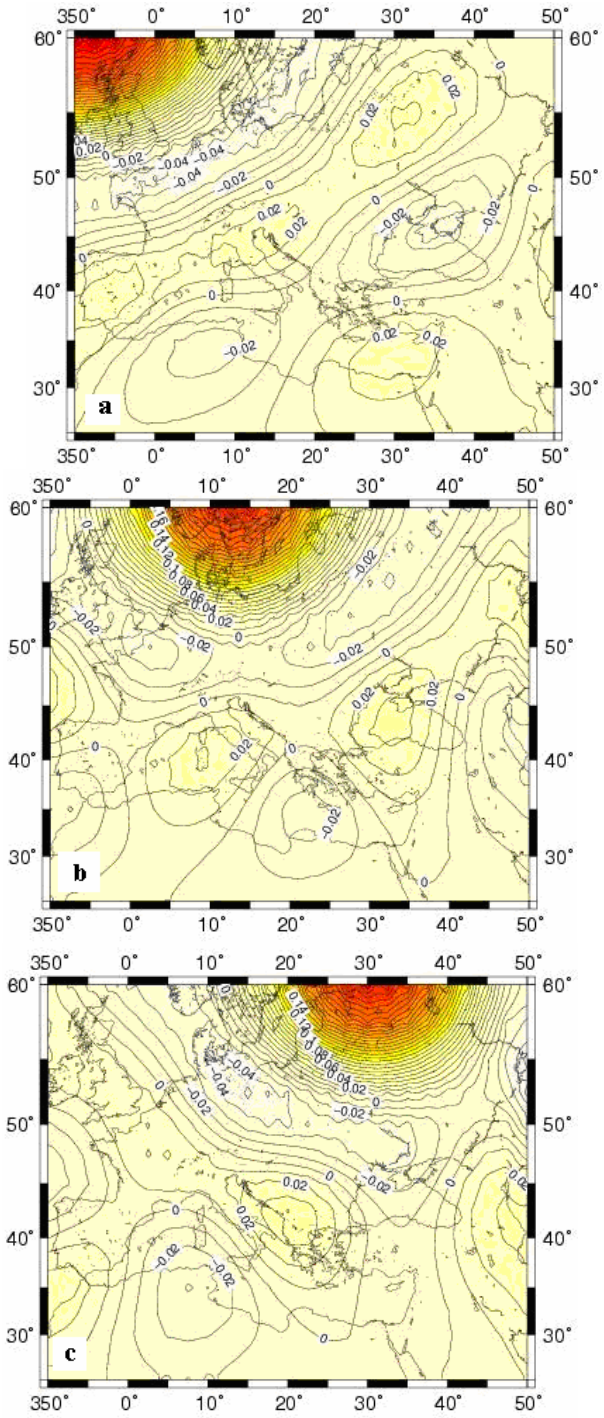

Figure 3. First three dominant patterns of 500hPa geopotential heights for high frequency variability.

For the synoptic frequency modes, first 3 modes account 16%, 13% and 10% of the total variance associated with the synoptic frequency variability. The first three modes after VARIMAX rotation is illustrated in Figure 3 a-c.

The first mode consists of trough and ridge systems extended from southwest to northwest over central Europe and over Istanbul, positive/negative height anomalies over England and

eastern Mediterranean. The second mode shows a structure of confluence centered in eastern Europe. Positive/negative anomalies are located over central Black Sea and southeast of Italy and negative/positive anomalies are over northern Europe and north of Libya. The third mode corresponds to a seesaw structure of positive and negative anomalies over southeastern Europe and northern Africa.

RELATIONSHIP OF HEAT WAVES WITH CIRCULATION PATTERNS

Heat waves form in two different frequency modes. First, low frequency modes such as blocking anticyclone affect large areas, provoke heat waves, and are generally associated with sub-continental or planetary scale motions. The second is the synoptic frequency motions such as cyclones and anticyclones which are effective especially in the midlatitudes. Amplitude and duration of heat waves are different in both modes.

In this study, each circulation pattern for both low frequency and synoptic frequencies is correlated with the observed 500hPa geopotential heights. For each heat wave, one of the patterns is assigned to those days by considering the highest correlation between the patterns and 500hPa geopotential heights. Table 2 summarizes the frequency of the assigned most similar patterns associated with the heat waves.

Table 2. Frequency of the patterns associated with the heat waves in Istanbul.

	Low Frequency			Synoptic frequency		
	Pattern 1 %	**Pattern 2 %**	**Pattern 3 %**	**Pattern 1 %**	**Pattern 2 %**	**Pattern 3 %**
June	93.0	7.0		16.0	77.0	7.0
July	98.0	2.0		41.0	57.0	2.0
August	97.7	2.3		38.5	58.8	2.7
September	96.0	4.0		17.4	82.6	

For the low frequency patterns, most of the heat waves occurre when the first low frequency pattern dominates the region. The correlations between this pattern and the heights are negative in all cases. Therefore negative geopotential height anomalies located over Scandinavia and Saudi Arabia, and positive anomalies centered over southern Europe create favorable conditions for heat waves to occur in Istanbul (Fig. 2.a). These conditions are due to anticyclone over Azores extending through southern Europe during summer months and existence of warm Arabian cyclone in the southeast of Turkey. Second favorable condition develops when positive 500hPa height anomalies are present and located over northeastern Black Sea and Eastern Europe, and negative 500hPa anomalies are over southern Europe and central Mediterranean (Fig.2.b). These conditions are supported by an inflow of warm air from warm Anatolia plate, by existence of a cyclone over southern Europe or trough and anticyclone over Black Sea and east Europe. Influence of low frequency third circulation mode becomes negligible.

For the synoptic frequency patterns, negative correlation with the first mode indicates that favorable conditions for the heat waves in Istanbul show a pattern consisting of positive 500hPa height anomalies over northwestern Anatolia, Black Sea and northern Africa which form a ridge over Istanbul, and negative anomalies over Arabia, southern and northeastern Europe. Easterly warm airflow from Anatolia plate connected to African anticyclone and ridge control the surface weather in the northwestern part of Turkey. Especially during July and August, 41% and 38.5% of the observed heat waves within the period of 1975-2005 are connected to this pattern. The second synoptic-frequency mode is related mostly with the heat wave occurrences in Istanbul for all months (June-September), and more than 58% of the heat waves for each month are controlled by this pattern. In this pattern, negative height anomalies exist over Scandinavia and positive anomalies over eastern Europe, northern Europe and central Mediterranean. Heat waves are linked to the ridge system with African origin and centered over central Mediterranean (Fig.3.b). The weak relation between heat waves and synoptic frequency circulation pattern is found with the third mode which corresponds to a seesaw structure of negative and positive height anomalies over southeastern Europe and northern Africa. This structure supports the warm southerly or southwesterly airflow originating from Africa.

CONCLUSIONS

Heat waves in Istanbul are investigated by using the daily maximum temperature data observed between 1975 and 2005 for the months of April-September in Göztepe meteorological Station. Highest temperature monitored within the study period is 39.7^{o}C during the 7-day heat wave of July, 2000. The second highest maximum temperature is on 28th of June in 1982. This heat wave is started on 22nd and persisted for eight days. Number of the heat wave events peak in 2003 with six heat waves. Total number of days with temperatures at least 29^{o}C, is 53. WMO states that during July and August 2003, significantly above-average temperatures were observed throughout Europe, Scandinavia, and western Russia, with monthly mean temperatures exceeding the 90th percentile in each region. On August 15 through 17, a few days after the highest temperatures since 1873 were recorded in Paris, maximum temperatures in Istanbul were above 33^{o}C and minimum temperatures were around 22^{o}C.

Duration of heat waves changes depending on the planetary and synoptic scale events. Therefore, in this study relationship between the heat waves and both low and synoptic frequency modes affecting the development of the systems near the surface is investigated. In the low frequency mode, two patterns show significant correlation with the 500hPa height on days in which heat wave is observed. In the synoptic frequencies, three modes are linked significantly to the heat waves. Flow patterns for both modes reveal that heat waves in Istanbul generally occur when ridge or trough systems are positioned over the region to support the warm air flow from Africa and Mediterranean.

REFERENCES

1. World Health Organization (WHO), “The health impacts of 2003 summer heat waves,” WHO Briefing Note for the Delegations of the 53rd session of the WHO Regional

Committee for Europe, Vienna, Austria,8 to 11 September 2003; available at www.euro.who.int/document/Gch/HEAT-WAVES%20RC3.pdf.
2. Huth R., J. Kysely and L. Pokorna, 2000, 'A GCM Simulation of Heat Waves, Dry Spells, and Their Relationships to Circulation', *Climatic Change* **46:** 29–60.
3. Meehl, G. A. and C. Tebaldi, ,2004, 'More Intense, More Frequent, and Longer Lasting Heat Waves in the 21st Century', *Science* **305**, 994–997
4. Chagnon, S.A., K.E. Kunkel, and B. C Reinke, 1996,'Impact and responses to the 1995 Heat Wave: A call to action', *Bull. Amer. Meteor. Soc*., **77**,1497,1506
5. Kunkel, K. E., S.A. Chagnon, B.C. Reinke. and R.W. Arritt,.1996, 'The July 1995 Heat Wave in the Midwest: A climatic perspective and critical weather factors', *Bull. Amer. Meteor. Soc*., **77**,1507,1518.
6. Karl, T. R., and R. W. Knight, 1997: The Chicago heat wave: How likely is a recurrence? *Bull. Amer. Meteor. Soc.,* **78,** 1107–1119.
7. Blackmon, M. L., 1976,'A Climatological Spectral Study of the 500 mb Geopotential Height of the Northern Hemisphere Wintertime Circulation', *J. Atmos. Sci.* **34**, 1040–1053.
8. Blackmon, M. L. and N.C. Lau,.1980, 'Regional Characteristics of the Northern Hemisphere Wintertime Circulation: A Comparison of the Simulation of a GFDL General Circulation Model with Observations', *J. Atmos. Sci.* **37**, 497–514.
9. Harman, . H.H., 1976, 'Modern factor analysis', University of Chicago Press, Chicago.
10. Jolliffe, I.T, 1986 'Principal component analysis', Springer-Verlag, New York.
11. Preisendorfer R.W,1988, 'Principal component analysis in meteorology and oceanography', Developments in atmospheric science, 17, Mobley and Curtis (Eds) Elsevier.
12. Anderson, T.W., 1984, 'An introduction to multivariate statistical analysis', John Wiley&Sons, New York.

CHANGE IN THE FROST FREE SEASON LENGTH AND NUMBER OF FROST DAYS IN THE WEST AND EAST AZERBAIJAN PROVINCES

M. Pedram, F. Rahimzadeh, F. Sahraian, K. Noohi

Atmospheric Science and Meteorological Research Center (ASMERC), pedram@irimet.net

ABSTRACT

One of the most important impacts of recent global warming is decreasing number of frost days and increasing frost free season length. Positive and negative impacts of changes in planting patterns, due to changing of planting and harvesting dates have been paid too much attention by experts and policy makers. To detect these changes in Azerbaijan provinces, where produce many agricultural products in Iran, 8 meteorological stations with more than 30 years and high quality data were selected in that region. Using daily minimum temperature, the number of frost days and frost free season length were calculated. The linear trend and their significance, in association with significant changes in decadal means and variances of those parameters were determined by statistical methods. The results show that, the number of frost days has decreased in the most of stations except, Oroomieh and Jolfa. There are no significant changes in decadal mean for Tabriz, Oroomieh, Miyandoab, Sarab and Maragheh stations. Changes in decadal variance for Miyandoab are significant. Increasing trends of the length of frost free season were observed in Oroomieh, Jolfa, Sarab and Ahar. On the contrary, decreasing trend was observed in Tabriz, Maragheh and khoy. Stationarity was also observed in Miyandoab. Further more no significant changes in decadal means have been experienced. In general, the obtained results are not consistence with the pattern of global changes for number of frost days and frost free season length.

Key words: Length of frost free season, Number of frost days, Planting pattern, Iran

INTRODUCTION

Global warming, a gradual increase in planet-wide temperatures, is now well documented and accepted by scientists as fact. Studies indicate that the average global surface temperature has increased by approximately 0.3-0.6°C over the last century. This is the largest increase in surface temperature in the last 1,000 years and scientists are predicting an even greater increase over this century [12]. Global climate change influences early and late frost events, which inhibit growth and possibly damage many plants. It has been found decreasing frost days across northern Europe during the twentieth century [7] and similarly, in Canada [2]. Schartz and Reiter [9] found phonological evidence of a move to an earlier spring in parts of North American, and Cayan et al. [3] also indicated a change toward earlier spring in the western United States. Furthermore recent observed warming in that country has resulted in a decrease in the number of frost days, an earlier date of last spring freeze, a later date of the first fall frost, and a lengthening of the frost free season, for the 1948-1999 period [4]. Furthermore Frich et al. [5] found evidence of longer growing seasons and fewer frost days in much of mid- and high latitudes in Northern Hemisphere in the last 50 years. Alexander et al. [1] updated the results of Frich et al. and provided an unprecedented global picture of changes in daily temperature extremes and found decreasing trend in number of frost days in most part of the world. This result has been found by Zhang et al. [13] for Middle East in the 1950-2003

periods. These negative trends are robust and all of them are significant. Rahimzadeh & Asgari [8] studied the occurrence of recent climate change for our country, Iran. They indicated the surface temperature has increased during the second half of the twentieth century for most of the stations under study. Also, they found abrupt increase of minimum temperature in the late 1970s for most of the stations.

East and West Azerbijan provinces with 89000 km^2 area lie in the northwest of Iran. They are one of the most important providers of agricultural products in the country. Regarding the effects of global warming and the observed impacts of climate changes throughout the world, one would expect that changes have occurred on the annual frost days and frost free season length in this region, during the last few decades. So, the purpose of this study is to examine changes in number of frost days and free frost season length for that region for the latter near half of the twentieth century.

DATA SET & METHODS

In the base on WMO documents [6], frost day is a day on which the minimum air temperature in the thermometer shelter falls below 0°C temperature. Also, frost-free season is the period, usually expressed in days, between the last observed occurrence of frost in the spring and the first observed occurrence of frost in the autumn. So, we needed the long term records of daily air minimum temperature association with the date of their occurrence. The data used here comes from the Islamic Republic of Iran Meteorological Organization (IRIMO) observation network. At present, there are 19 synoptic stations and 15 climatology stations in the East and West Azerbaijan provinces which are operational and observe the meteorological parameters. The stations in the network were chosen based on the length of the record and by considering their metadata. The length of the records of those stations varies from 4 to more than 50 years. As from 26 stations in that region which are located between 45º 05' and 48º 22' eastern longitude and 35º 58' and 39º 26' northern latitude, 15 stations have more than 10 years records (Fig.1). So, we have limited our study on Golfa, Ahar, Khoy, Tabriz, Sarab, Oroomieh, Maragheh and Miyandoab which have records for at least 30 years. Table 1 shows the characteristic of those 8 selected stations.

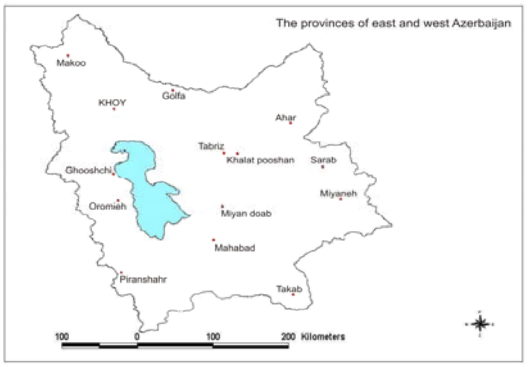

Figure 1. Geographical position of the synoptic & climatology stations in East and West Azerbaijan provinces (record length >= 10 years).

Table 1. Characteristics of the selected Synoptic and climatology stations in East and west Azerbaijan provinces

Establishment Year	Elevation(m)	Latitude	Longitude	Station	No.
1960	1103	38° 33′	44° 58′	Khoy	1
1951	1313	37° 32′	45° 05′	Oroomieh	2
1952	1314	36° 58′	46° 09′	Miyandoab	3
1984	736	38° 45′	45° 40′	Golfa	4
1983	1477	37° 24′	46° 16′	Maragheh	5
1948	1361	38° 05′	46° 17′	Tabriz	6
1985	1157	38° 29′	47° 04′	Ahar	7
1986	1651	38° 56′	47° 32′	Sarab	8

The dates of the first autumn and last spring freezes, found and converted to Julian dates. Due to the cold climate of Azerbaijan region, some stations could potentially have a freeze date at the last of summer. So, for the purposes of this analysis spring and autumn were arbitrarily divided at 1 September. Length of frost free season resulted from the spring date to the fall date, too.

In order to detect and distinguish the behavior of number of frost days and frost free season length, we looked at the long term tendency of those time series, throughout the determination of linear trends by using Least Square method. Furthermore, we examined the changes in their distribution, including change in mean and variance, by using nonparametric tests. We used Kendal' Tau test [11] to calculate the significance level of number of frost days and frost free season length trends. Also, Kruskal-Walis and Hartly tests [10] were applied for determination of significance of the equality 10 years period Means, and homogeneity 10 years period variance, respectively.

Figures 2 and 3 show the linear trends of frost free season length and number of frost days associated with their smoothed series. The used filter is designed to remove less than decadal fluctuations and has 13 weights [14]. The linear trend of frost days is negative in most of the stations except in Oroomieh and Golfa. The trends are significance in Tabriz, Oroomieh, Maragheh and Khoy. For other stations, the trend lines only show the long term tendency of the time series. It is noticeable that the resultant trends in most of stations are consistent with the results shown in other researchers such as Frich et al. (2002). In the Base on Kruskal-Walis test, mean of number of frost days has only significance changes in Tabriz, Oroomieh, Miyandoab, Sarab and Maragheh. Hartly test Indicated non significance changes of variance, except in Miyandoab station. The frost free season length is stationary in Miyandoab, and has decreasing trend in Tabriz, Maragheh and Khoy stations. Kendal' Tau test showed those trends are significance only in Tabriz, Maragheh and Oroomieh. There are no significance changes in decadal means of this parameter. The changes in decadal variances are only significance in Sarab.

In this study, the first and last frost dates have been determined without considering the causes of occurrence, either radiational or advectional. But, since the region is opposed to the warm air displaced from the equator to the north, it seems that the radiation does not have such an expected role in occurrence of the frosts. So if the advectional types could be determined separately, the obtained results might have more trust and homogeneity.

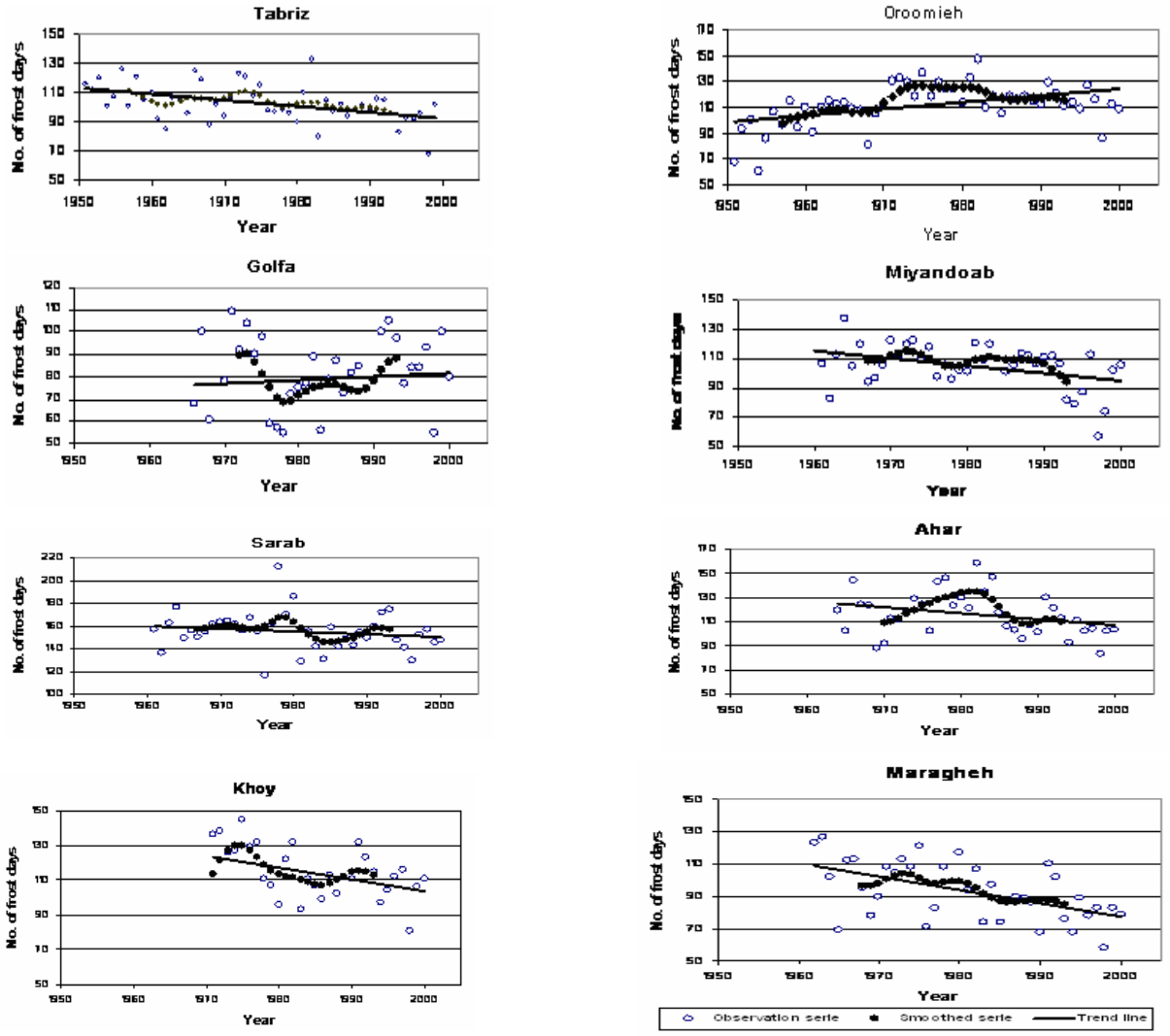

Figure 2. Trends of the length of frost free season in 8 selected stations in Azerbaijan region.

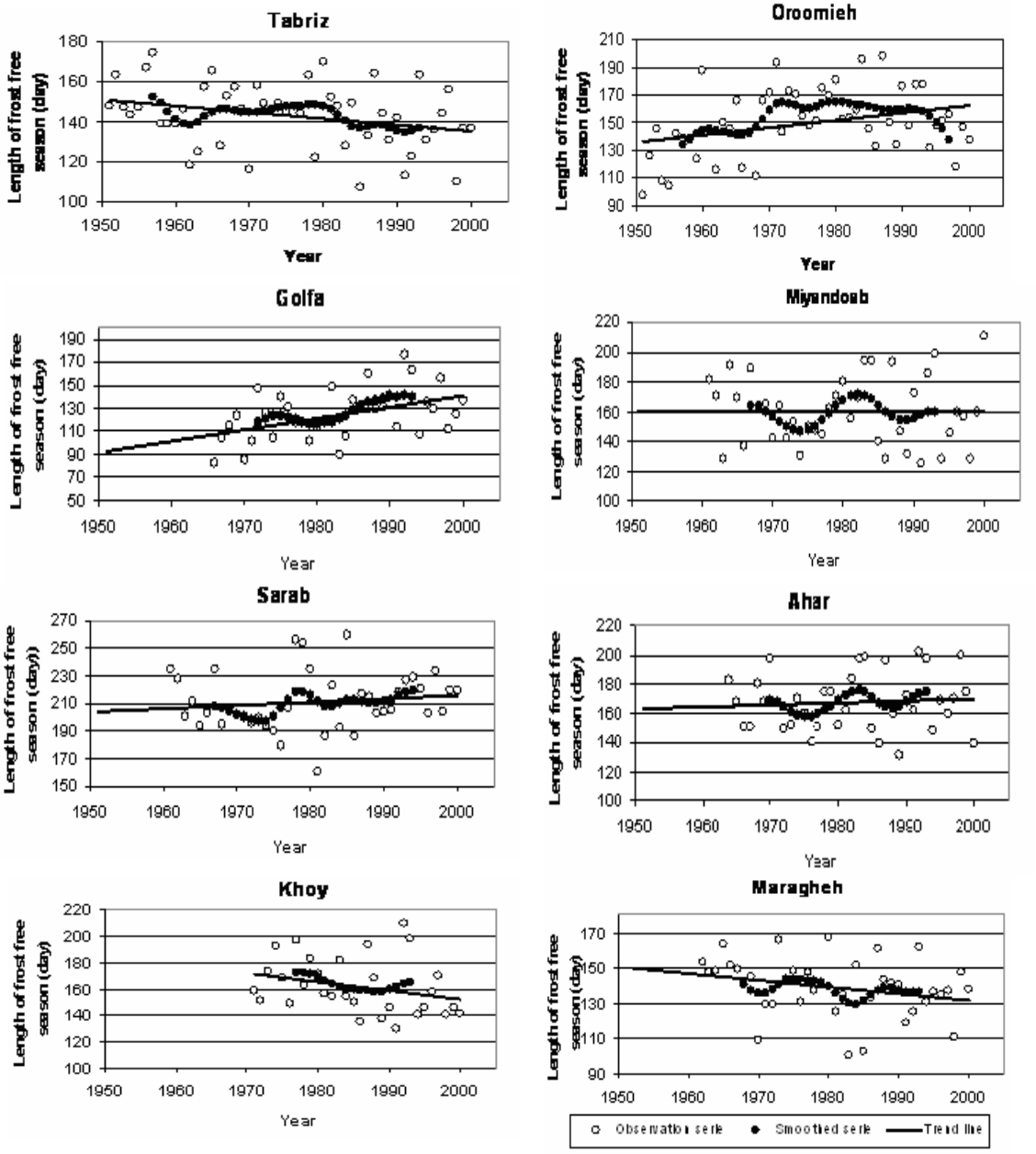

Figure 3. Trends of number of frost days in 8 selected stations in Azerbaijan region.

REFERENCES

[1] Alexander, L., X, Zhang, T.C. Peterson, J. Caesar, B. Gleason, A. Klein Tank, M. Haylock, D. Collins, B. Trewin, F. Rahimzadeh, A. Tagipour, P. Ambenje, K. Rupa Kumar, J. Revadekar, G. Griffiths, L. Vincent, D. Stephenson, J. Burn, E. Aguilar, M. Brunet, M. Taylor, M. New, P. Zhai, M. Rusticucci and J.L. Vazquez-Aguirre, 2006, Global observed changes in daily climate extremes of temperature and precipitation. J. Geophys. Res., D05109, doi, 1029/2005JD006290.

[2]. Bonsal, B. R., X. Zhang, L. A. Vincent, and W. D. Hogg, 2001, characteristics of daily and extreme temperatures Canada, J. climate, 14, 1959-1976.

[3]. Cayan, D. R., S Kammerdiener, M. Designer, J. Caprio, and D. Peterson, 2001, changes in the onset of spring in the western united state, Bull, Amer. Meteor. Soc. 82, 399-415.
[4]. Easterling, D. R., 2002, Recent Changes in frost days and the frost in the United States, Bull. Amer. Meteor. Soc., 83, 1327-1332.
[5] Frich, P., L. V. Alexander, P. Della Marta, B. Gleason, M. Hay lock, A. Klein Tank, and T. Peterson, 2002, Global Changes in Climatic extremes during the 2th half of the 20th century, climate, Res., 19, 193-212.
[6]. Gloyne, R. W., Lomas, J., 1980, Lecture notes for training class II and class III agricultural meteorological personnel, WMO, 551, Geneva.
[7]. Heino, R., and Coauthors, 1999, progress in the study of climate extremes in northern and central Europe, climate change, 42, 151- 181.
[8]. Rahimzadeh, F., and Asgari. A., 2003, A survey on Recent climate change over Iran. Proceeding of 14th Global Warming international conference & expo (27-30 May, Boston, USA).
[9]. Schwartz, M. D., and B. Reiter, 2000, Changes in North American Spring, Int. Climatol., 20, 929-932.
[10]. Sheskin, D. J., 2000, Handbook of Parametric & nonparametric statistical procedures,Chapman & Hall/CRC.
[11]. Sneyeres, R., 1990. On the Statistical Analysis of Observations,WMO Publ. NO. 415, Geneva.
[12].URL1:http://earthoservatory.nasa.gov/Library/Global warming
[13]. Zhang, X., E. Aguilar, S. Sensoy, H. Melkonyan, U. Tagiyeva, N. Ahmed, N. Kutaladze, F. Rahimzadeh, A. Taghipour, T.H. Hantosh, P. Albert, M. Semawi, M. Karem Ali, A. Halal Said Al-Shabibi, Z. Al-Oulan, Taha Zatari, I. Al Dean Khelet, S. Hammond, M. Demircan, M.Eken, M. Adiguzel, L. Alexander, T. C. Peterson and T. Wallis, 2005, Trends in Middle East climate extremes indices during 1930-2003, J. Geophys. Res., D22104, doi, 10. 1029/2005JD006181.
[14]. Zheng, X., and R. E. Basher, 1999: Structural time series models and trend detection in global and regional temperature series. *J. Climate,* 12, 2347-2358.

GAS HYDRATE AND FREE GAS OCCURRENCE VS CLIMATE CHANGES AND INSTABILITY SLOPES FROM SEISMIC DATA ANALYSIS. THE SOUTH SHETLAND MARGIN CASE

Maria F. Loreto, Umberta Tinivella and Flavio Accaino

Istituto Nazionale di Oceanografia e Geofisica Sperimentale (OGS), Borgo Grotta Gigante, 42/C, Sgonico – Trieste (Italy). mfloreto@ogs.trieste.it

ABSTRACT

Over the last 30 years, several study on gas hydrate have been performed to define the major related issues. The potential effects of natural gas hydrates, such as (i) potential energy resource, (ii) factor in global climatic change and (iii) submarine geo-hazard, are not completely understood.

Gas hydrates are a solid phase composed of fresh water and low-molecular-weight gases (predominantly methane), which form under conditions of low temperature, high pressure, and adequate gas concentrations. These conditions are common in the upper few hundred meters of marine sediments accumulated along continental slopes. Gas hydrates in marine environments have been mostly detected from the analysis of seismic reflection profiles, in which they produce a remarkable Bottom Simulating Reflector (BSR). This reflector is associated to sediments extensively filled by gas hydrates, above, and free gas below. Gas hydrates are present onshore and offshore (along all continental margins) and close to mud volcanoes in the Eastern Mediterranean Sea.

The gas hydrate layer is affected by strong instability that could be related to the pressure, associated with sea-level changes, and to the temperature changes. Climate changes, realizing trough temperature and consequently pressure variations, determine the destabilization of the Bottom Simulating Reflector. This destabilization can create a weak zone, located close to the former hydrate stability depth that could favour sediment failures and submarine slumps. Considering that 1 m^3 of hydrate is composed approximately by 0.8 m^3 of fresh water and 163 m^3 of gas, consequently a huge methane volume is realised in the ocean reaching in some part the atmosphere (greenhouse effect). Unfortunately, neither the volumes of gas that are involved nor their dynamics are well enough understood to asses whether or to what degree marine gas hydrates act as a buffer in accentuate to climatic changes. Moreover where the gas hydrate miss or is destabilized, gas escape can be related to tectonic and intense erosional events, as speed turbiditic currents and instability slopes.

Thus, to study the climate changes and instability slopes related to gas escapes, the quantitative evaluation of gas hydrate and free gas is essential. Analysis of seismic data using iteratively the tomographic inversion and pre-stack depth migration can produce the regional velocity field, which can be translated in gas hydrate and free gas concentration terms. This method was applied on seismic data acquired offshore of the Antarctic Peninsula. A preliminary analysis of these data suggest that a feedback between environmental changes and gas realising exist.

Keywords: Gas hydrates, Fluid escape, Instability slope, South Shetland Margin.

INTRODUCTION

Huge gas quantities of natural gas are stored in the form of gas hydrate within the pore space of marine sediments along continental margins worldwide. Gas hydrates consist of solid water molecules that encage gas molecules and forming a crystalline structure like ice. Gas hydrates are composed in most part by methane and in minor part by other gas such as ethane, butane, propane. On seismic data, the gas hydrate layer is geophysical inferred from the presence of a reflection that simulates the sea-bottom trend called Bottom Simulating Reflector (BSR), which is characterized by a reverse polarity compared to the sea-bottom signal and can cross-cut the sediment stratification and tectonic structures [1, 2]. The BSR is a reflection cased by acoustic impedance contrast due to the presence of gas hydrate above and free gas accumulated below [1, 3, 4]. The amplitude of this reflection is controlled by gas concentration of two phases, this means that hydrate may be present, even if the BSR miss, in low concentrations [5, 6].

Hydrates presence prevent sediment compaction, their in situ dissociation due to pressure and temperature changes, that in turn are related to global changes, could be an important factor in creating weak sediment layers, along which sediment failure could be triggered [7] and collapse of the structure of the host sediment giving the potential for slumping [8]. During these events huge gas quantities are released from hydrate reservoir into the water column contributing to acidification of oceans and in some case to climate change if the gas reaches the atmosphere [9, 10]. The releasing of gas within water column is well documented, but only a few percentage of this gas can reach the atmosphere contributing to the climate warming [11]. Greinert et al. [12] have demonstrated that the gas normally released by sediments, seepage, or mud volcano usually does not reach the atmosphere, being completely oxidized by the water. The gas could reach the sea-level contributing to climate warming if abrupt and huge gas quantities have released in the water column [13-16], triggered by slumps or tectonic activity.

GEOLOGICAL SETTING

The South Shetland margin is a convergent plate boundary where the Phoenix oceanic plate is subducted beneath the continental block of the Antarctic plate, generating a trench-accretionary prism sequence [17, 18]. The extension at the spreading ridge ceased about 2.3-3.3 Ma, therefore the subduction take place as a consequence of sinking and roll-back of the oceanic lithosphere [18, 19]. The passive subduction favours the formation of the Bransfield back-arc basin, a narrow accretionary prism and a complex plate subduction [20, 17, 21]. The margin is laterally confined by two major oceanic fracture zones: the Hero, located to SW, and the Shackleton located to NE, that intersecting the continental lithosphere delimitate the block of the Antarctic Peninsula [22].

The accretionary prism large in a range of 20 – 30 km is characterized by a complex deformational style represented by thrusts and reverse faults [17, 18] on which a normal fault system is over-imposed, related to the extensional regime. The passive subduction favor the activity of left-lateral Shackleton Fracture Zone and associated array of extensional faulting, approximately orthogonal to the strike slip system [23]. Within the accretionary prism, the recognised BSR [24] is very continuous and with high amplitude, in a restricted area

(indicated with yellow in Fig. 1), and becomes more discontinuous in the southern part of the investigated area; the median depth from the seafloor is about 700 ms [25].

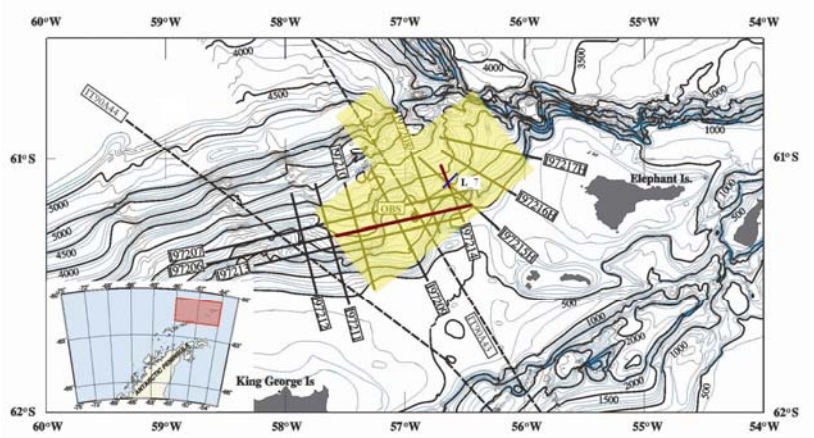

Figure 1. Location map of seismic data set (solid and dashed lines), and bathymetry (yellow area) acquired during the Austral summers 1996/97 and 2003/04. The red dashed line indicates the analysed seismic lines. The location of the analysed chirp line is indicated with blue line (L_7).

The presence of a strong BSR suggested the idea to acquire new date in the area where it was more continuous. The preliminary analysis of new acquired data (Multibeam, Chirp and OBS) highlight the presence of fluid escape zones, mud volcanoes and slumps localized around this area [26]. Slope instability, local fluid escape and gas hydrate instability suggest that possible relation can exist among them.

The focus of this work is to estimate hydrate and free gas amounts, trapped within the pore space of sediments along the South Shetland margin. This estimate that can give an idea about the gas that could be released. The quantification of gas contents is performed producing a velocity field with pre-stack depth migration and focusing velocity analysis.

GEOPHYSICAL DATA

A strong BSR was identified on multichannel seismic reflection profiles acquired during the Austral summers 1996/1997 (Fig. 1), and Multibean and chirp profiles acquired during the Austral summer 2003/2004 (Fig. 1) along the South Shetland margin [24, 23]. The seismic data were acquired using as energy source two GI guns with a total volume of 4 l firing every 25 m. The streamer length is 3000 m with a group interval of 25 m sampling rate is 1 ms. The high-resolution bathymetry (Multibeam data) was acquired using the new *Seabat* 8150 Multibeam system, with a nominal depth range of 0.5 – 15 km and a frequency of 12 kHz. Data acquisition and processing of Multibeam was performed using the PDS2000 software, the swath coverage is about 12 km, which corresponds to 2.5 times the water depth. The sea water velocity was measured by 4 CTD probes in the water column. Editing of the navigation and filtering on raw data were applied to remove noise. Sub-bottom Chirp data were acquired with CAP-6600 Chirp II, with 16 transducer and 2-7 kHz of sweep. The sonar operating frequency is 7 kHz and the sample rate is 0.533 ms.

VELOCITY FIELD AND PRE-STACK DEPTH MIGRATION

The estimation of gas hydrate and free gas concentrations is based on the P-wave velocity, which can propagate within the matrix and the fluid filling the pore space of sediments, corresponding to the velocity used to migrate seismic sections. The method uses the pre-stack depth migration to determine, iteratively and with a layer stripping approach, the velocity field and a satisfactory seismic image in depth. The approach, based on semblance analysis, is described in details in [30]. The velocity filed was verified by the flatness of reflectors recognized in the Common Image Gathers (CIGs) depth migrated. The first step of the pre-stack depth migration, performed used the Seismic Unix (SU) software [27], is done using a uniform velocity field of 1470 m/s (water velocity) and updated every iteration by the picking on semblances (see example in [37]). The final velocity filed (Fig. 2a), smoothed to attenuate strong lateral variations, is used to produce a final pre-stack depth migration section (Fig. 2b). This method is applied to determine an accurate velocity field to the depth of the BSR or, when possible, to the depth of the BGR (free gas layer). The depth part of seismic section is migrated with a velocity gradient.

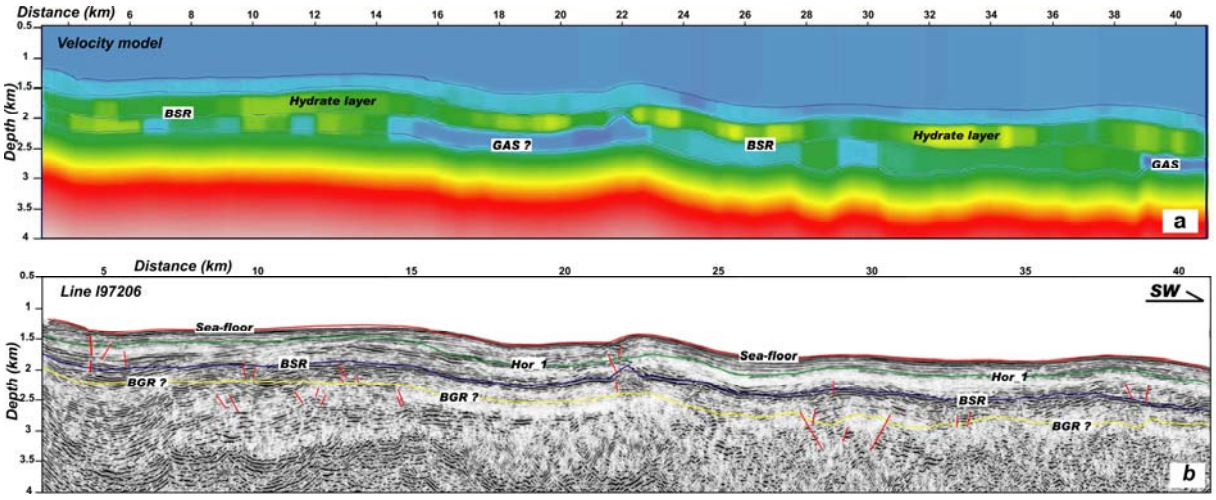

Figure 2. Velocity field of line I97206 (a), which is located parallel to the continental margin (red line in Figure 1), constructed with the described method and used to perform the pre-stack depth migration section (b). The horizon picked under the sea-floor is indicated with Hor_1 (green line). Some faults are also indicated with red solid segments.

DISCUSSION

The analysis of some pre-stack depth migrated seismic profiles highlight the presence of tectonic structures and morphology of sea-floor that could be correlate to gas hydrate instability. Integrated analysis of seismic sections and velocity fields make be able to analyse relations among tectonics, slope instabilities and fluid escapes. Using the procedure developed by Tinivella [29], it is possible to translate the velocity section into gas concentration section.

Fluid and tectonics

The seismic section I97206, acquired in the accretionary prism area and parallel to the continental margin (Fig. 1), shows an evident furrow (at the distance of 4 km) that affects the sea floor where stratified sediments result interrupted (Fig. 3, left). In the deeper part, the stratified sediments show local interruption and downward shifting that on the opposite site close in on-lap on the top of folded sediments. Based on geometries, this stratified sedimentary unit is interpreted as a sedimentary basin, which can thickness thanks to the upward movement of folded sediments and to fault activities. The velocity field (Fig. 3, right), used to perform the pre-stack depth migration of this part of line, is characterized by velocity values, varying in a range of 2100 – 2400 m/s, associate to a gas hydrate layer. Immediately below the hydrate layer is present a low velocity layer, varying in a range of 2400 – 1320 m/s, thick about 0.2 km. These very low velocity are associated to free gas filling sediments and trapped by the gas hydrate layer. The high velocity characterizing deeper sediments of basin, around 5 km of distance (Fig. 3, left), correspond to the area affected by faults; one of that cut sediments from the deeper part to the sea-floor. This high velocity zone suggests that the fault can act as conduit trough which the fluids move upward and released in the ocean. This fault is located in correspondence of a channel that cross-cut the accretionary prism about orthogonal to the margin (Fig. 1), suggesting that the channel is tectonically controlled.

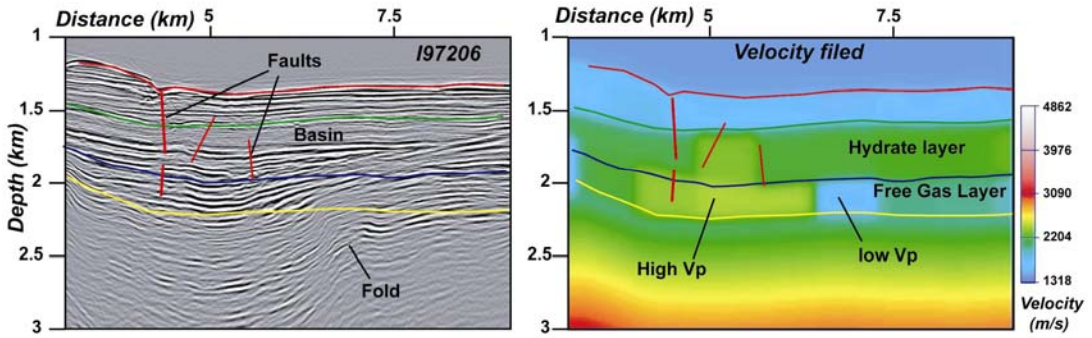

Figure 3. Part of seismic line I97206, located parallel to the margin (Fig. 1), depth migrated (left) with the final velocity field (right). The yellow line indicate the more probable BGR, with the blue line is indicate the BSR, the red line represent the sea-floor, and the green line a intermediate horizon recognized between the BSR and the sea-floor.

Slope instability

North to channel – fault controlled and folds, the investigated margin showed in the seismic section I97214 (Fig. 4, left) is characterized by sediments locally deformed, folded and lateral interrupted. This deformation involve the sea-floor conferring to the sediments the typical slump shape. In the deeper part, about 450 m bsf measured in correspondence of the distance of 1800 m, other discontinuities and lateral interruptions of reflectors are recognized. At this depth the BSR is present but discontinuous. By the preliminary analysis of seismic image (the analysis is still in progress) is possible to hypothesis the presence of a shallow slump and a probable deeper events. Between the distances 2050 and 2400 m, sediments are very chaotic and a clear BSR miss. Close to the body of the slump a conic sea-floor morphology and chaotic sediments are associated to a mud volcano. Below the volcano the BSR miss and sediments results more incoherent. The preliminary velocity field shows strong lateral velocity variations that could be explained by morphology and structures affecting this part of

the margin. The first layer below the sea-floor shows local low velocity in correspondence of the mud volcano and the body of the slump. The low velocity, determined by an excess of gas and fluids filling pore space of sediments, suggests that the ridge detected is a mud volcano, along which intense fluid outflow can realized. Moreover, the low velocity characterising sediments affected by slump and lateral interruptions suggests that the fluid escapes can happen along these discontinuities, as confirmed by the local missing of the BSR. These elements suggest that a direct relation exist between hydrate instability and slope instability, as already analysed along the Storegga Slide [31 - 34].

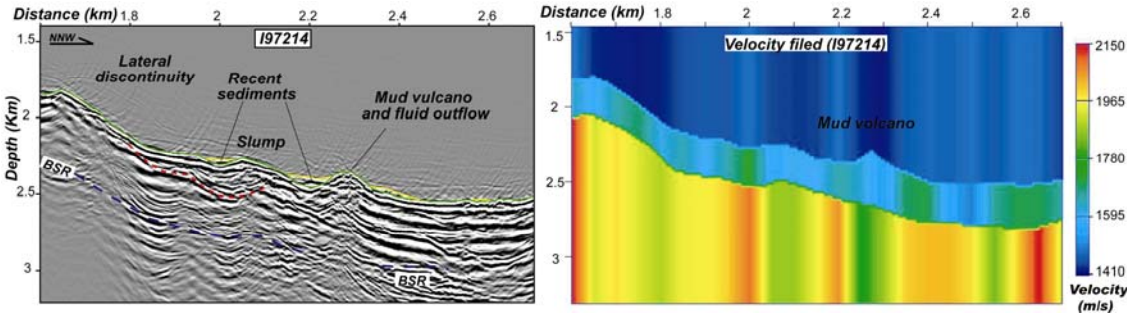

Figure 4. To left, part of the seismic line I97214, located orthogonal to the continental margin (red line in Fig. 1). To right, the velocity field used to implement the depth seismic section, the velocity field construction is in progress and here only the sea-floor and the horizon 1 are determined.

Actually, the sliding is not active as indicated by recent sub-horizontal sediments deposit within little depression (indicated with yellow lines), whereas the fluid escape continue to be active (Fig. 5b). Fluid escape from the sea floor along the slump detachment wall and close to the mud volcano is confirmed by high resolution seismic data (Chirp line 7; Fig. 5), acquired near the line I97214 (Fig. 1). The chirp profile shows a sedimentary deposit interpreted as a very shallow body of slump. Moreover in correspondence of CDP 390 (Fig. 5a) a weak reflection by a conic shape located on the top of a little collapse of the sea floor is detected, confirming our hypothesis based on the model proposed by Dillon and Max [35]. Close to the volcano several plumes located on the top of the sea-floor are detected (Fig. 5b), the releasing of gas is happening around it and not trough it suggesting that the fluids could be in overpressure condition.

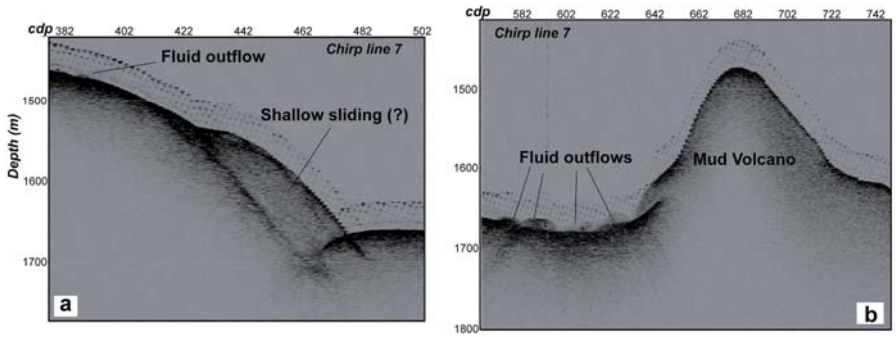

Figure 5. Shallow expression of a sliding (a) detected along the Chirp line 7; ridge interpreted as a mud volcano and close fluid outflows detected along Chirp line 7 (b) close to the seismic line I97214. See location map in Fig. 1, blue line.

Gas released by seepages and mud volcanoes at different water depth are completely [36] or in most part oxidised [11] before to reach the sea-level. But huge gas quantities abruptly released during sliding and hydrate destabilization could more likelihood to reach the atmosphere even if in a little percentage, contributing to climate change.

Gas estimation

Using a procedure developed at the OGS [29], velocity sections are translated in gas-phase concentration sections. This methodology takes into account a different gas distribution in the pore space of sediments that can be uniform or patchy. Here we analyse the section I97206 of gas-phase concentration, produced for uniform and patchy cases (Figs. 6 and 7).

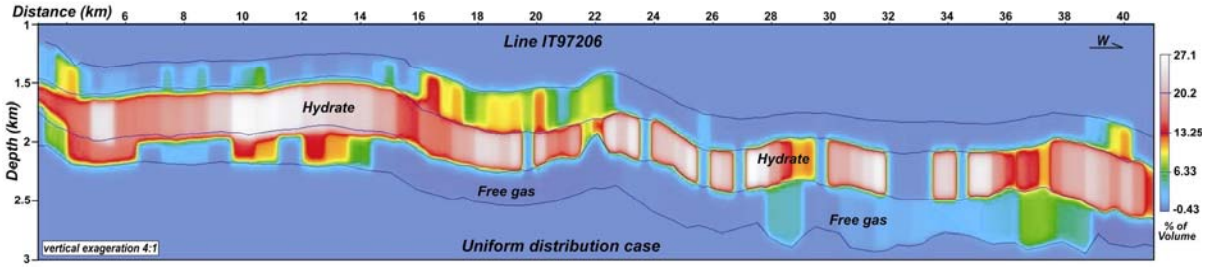

Figure 6. Hydrate and free gas concentration section derived by velocity filed, line I97206, considering a uniform phase-gas distribution. The hydrate gas percentage of total volume is expressed with positive value in the colour scale, whereas the free gas percentage is expressed with negative value in the scale.

Considering a uniform gas distribution, the concentration section shows a maximum gas hydrate percentage of about 27% of total volume, whereas the maximum free gas concentration results of about 0.4% of the total volume. The gas section, reflecting the velocity section, shows some areas characterized by low gas concentration controlled by tectonic activities In correspondence of the distance 22 km the hydrate layer is thinner and with low concentration, whereas the free gas layer result more thick. This variation of thickness is controlled by a fault that favours the upward fluids migration. These fluids probably destabilizes the base of hydrate stability zone, melting hydrate and consequently upwarding the BSR. Below it the free gas is trapped likely because the fault does not reach the sea-floor preventing fluid escape. The free gas concentration results low but more continuous in the central part of the line.

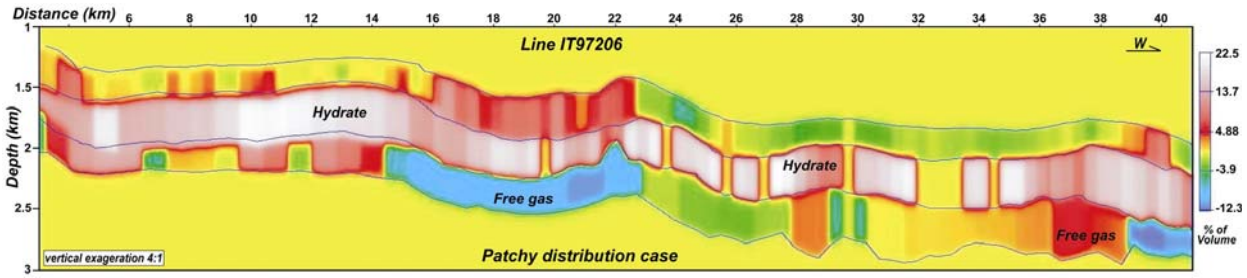

Figure 7. Hydrate and free gas concentration section of line I97206, considering a patchy gas distribution. The free gas percentage is expressed with negative value in the colour scale, whereas hydrate gas concentration is reported with positive value.

Considering a patchy distribution, the maximum gas hydrate concentration is about 22.5% of the total volume, differing in few percent from the uniform case. Whereas the free gas concentration increase dramatically until a maximum value of about 12% of the total volume, showing high concentration values in two main part of the line and indicated with light blue colour (Fig. 7). Based on [37], we can assume that in this area the gas hydrate layer is 345 m thick with a minimum concentration of 4.8% ± 1.0% and the free gas layer is 100 m thick with a minimum concentration of 0.3% ± 0.02% of volume. Because the area characterized by continuous BSR is about 1170 km^2, we can extrapolate that about 19.4 km^3 ± 4.0 km^3 of gas hydrate volume and 0.35 km^3 ± 0.02 km^3 of free gas volume are trapped in the marine sediments below the BSR. Note that these amount of gas are under-estimate the gas volume in the study area.

The work is in progress and the final focus is to produce a 3D velocity field to analyse the fluid circulation, physical properties of sediments, gas concentration of the entire reservoir and possible relations between gas destabilization and slope instabilities.

CONCLUSIONS

Gas hydrate and free gas strongly influence the propagation of seismic wave velocity; consequently the velocity field is a powerful tool to estimate the presence of gas phase in the pore space of sediments. The goodness of velocity field is controlled iteratively by the flatness of depth migrated horizons, in the CIGs, and by the quality of the pre-stack depth seismic sections.

Using the integrated analysis of velocity anomalies and morpho-structures, interpreted on depth seismic sections, the presence of possible relation between slope instabilities and gas hydrate destabilization are pointed out. Intense fluid or gas escape is realized along these instability zones. The estimation of gas amount, trapped in the hydrate and free gas layers, compared with a theoretical gas concentration can give an idea of the gas released in the ocean system, which could reach the atmosphere if the fluid escape produced by a catastrophic event, like slumps.

Acknowledgement
We are very grateful to Neslihan Ocakoglu for the support give to us. This study would not have been possible without the support of the crew and technicians of the R/V OGS-Explora during the acquisition. This work was partially supported by Italian *Programma Nazionale di Ricerche in Antartide (PNRA).*

REFERENCES

[1] Hyndman R.D. and Spence G.D., 1992. A seismic study of methane hydrate marine bottom simulating reflectors. *JGR*, **97**(B5), 6683-6698.

[2] Holbrook S.W:, Hoskin H., Wood W.T:, Stephen R.A:, Lizarralde D., 1996. Methane gas-hydrate and free gas on the Blake Ridge from vertical seismic profiling. *Science*, **273**, 1840-1843.
[3] Katzman R., Holbrook W.S., Paull C.K., 1994. Combined vertical incidence and wide-angle seismic study of a gas hydrate zone, Blake Ridge. *JGR*, **99**(B6), 17975-17995.
[4] Kvenvolden K.A., 1993. Gas hydrates-geological perspective and global change. *Reviewer of Geophysics*, **31**, 173-187.
[5] Paull C.K., Borowski W.S., Rodriguez N.M., Party O.L.S.S., 1998; Marine gas hydrate inventory: preliminary results of ODP Leg 164 and implications for gas venting and slumping associated with the Blake Ridge gas hydrate field, in: Henriet J.-P., Mienert J. (Eds.), *Gas Hydrate: Relevance to World Margin Stability and Climate Change, Geological Society of London, Special Publication,* 153-160.
[6] Vanneste M., De Batist M., Goldmshtok A., Kremlev A., Versteeg W., 2001. Multi-frequency seismic study of gas hydrate-bearing sediments in Lake Baikal, Siberia. *Marine Geology*, **172**, 1-21.
[7] McIver R.D., 1982. Role of naturally occurring gas hydrates in sediment transport. *Am. Ass. of Petroleum Geol. Bull.*, **66**(6), 789-792.
[8] Milkov A.,V., Sassen R., Novikova I. and Mikhailov E., 2000. Gas hydrates at minimum stability water depths in the Gulf of Mexico: significance to geohazard assessment. *Gulf Coast Ass. of Geol. Soc. Transactions*, L., 217-224.
[9] Nisbet E.G., 2002. Have sudden large releases of methane from geological reservoirs occurred since the Last Glacial Maximum, and could such releases occur again?. *Philisophical Transaction of the Royal Society of London,* **360**, 581-607.
[10] Kennet J.P., Cannariato K.G., Hendy I.L., Behl R.J., 2003. Mehtane Hydrate in Quaternary Climate change: the Clathrate Gun Hypothesis. *American Geoph. Union*, Washington, 216.
[11] Mienert J., Posewnag J. and Baumann M., 1998. Gas hydrates along the northeastern Atlantic Margin; possible hydrate-bound margin instabilities and possible release of methane. *Geol. Soc. Spec. Publ*., London, **137**, 275-291.
[12] Greinert J., Artemov Y., Egorov V., De Batist M., McGinnis D., 2006. 1300-m-high rising bubbles from mud volcanoes at 2080 m in the Black Sea: Hydroacoustic characteristics and temporal variability. *EPLS*, **244**, 1-15.
[13] Brooks J.M., Reid D.F. and Bernard B.B., 1981. Methane in the upper water column of the northwestern Gulf of Mexico. *JGR*, **86**, 11029-11040.
[14] Hovland M., Judd A.G. and Burke R.A., 1993. The global flux of methane form shallow submarine deposits. *Chemosphere*, **26**, 559-578.
[15] Judd A., Davies G., Wilson J., Holmes R., Barron G. and Bryden I., 1997. Contribution to atmospheric methane by natural seepages on the UK continental shelf. *Marine Geology*, **140**, 427-455.
[16] Leifer I. and Judd A.G., 2002. Oceanic methane layers: the hydrocarbon seep bubble deposition hypothesis. *Terra Nova*, **14**, 417-424.
[17] Maldonado A., Larter R.D. and Aldaya F., 1994. Forearc tectonic evolution of the South Shetland Margin, Antarctic Peninsula. *Tectonics*, **13**, 1345-1370.
[18] Kim Y., Kim H.-S., Larter R.D., Camerlenghi A., Gambôa L.A.P. & Rudowski S., 1995. Tectonic deformation in the upper crust and sediments at the South Shetland Trench. In: A.K. Cooper, P.T. Barker & G. Brancolini (Eds). *Geology and Seismic Stratigraphy of the Atlantic Margin, Antarct. Res. Ser.*, **68**, AGU, Washington, DC, 157-166.

[19] Larter R.D. & Barker P.F., 1991. Effects of ridge crest-trench inter-action on Antarctic-Phoenix spreading: forces on a young subducting plate. *JGR.*, **96**, 19583-19607.
[20] Bevis M., Smalley R.Jr., Taylor R. & Dalziel I.W.D., 1999. GPS studies of geodynamics in the Scotia Arc and West Antarctica. Paper presented at 8th International Symposium on Antarctic Earth Sciences, *S*ci. Comm. on *Antarct. Res*., Wellington, New Zealand.
[21] Loreto M.F., Della Vedova B., Accaino F., Tinivella U. and Accettella D., 2006. Shallow geological structures of the South Shetland trench, Antarctic Peninsula. *Ofioliti*, (under revision).
[22] Lawver L.A., Keller R.A., Fisk M.R., and Strelin J.A., 1995. Bransfield Strait, Antarctic Peninsula: Active extension behind a dead arc. In: B.Taylor (eds). *Back arc basin: Tectonics and magmatism volume: Amsterdam Plenum Press*., 315-342.
[23] Lodolo E., Camerlenghi A., Madrussani G., Tinivella U. and Rossi G., 2002. Assessment of gas hydrate and free gas distribution on the South Shetland margin (Antarctica) based on multichannel seismic reflection data. *Geophys. J. Int*., **148**, 103-119.
[24] Lodolo E., Camerlenghi A and Brancolini G., 1993. A bottom simulating reflector on the South Shetland margin, Antarctic Peninsula. *Antarctic Sci*., **5**(2), 201-210.
[25] Tinivella U., Lodolo E., Camerlenghi A. and Bohem, 1998. Seismic tomography study of a bottom simulating reflector off the South Shetland Islands (Antarctica). In: Henriet J.-P. and Mienert J. (Eds.), Gas Hydrates: Relevance to World Margin Stability and Climate Change. *Geol. Soc., London, Soc. Publ*., **137**, 141-151.
[26] Tinivella U., Accaino F. and Della Vedova B., 2006. New geophysical data to map the active fluid outflow in gas hydrate reservoir offshore Antarctic Peninsula. *Geo-Marine Let.* (under revision).
[27] Cohen J.K and Stockwell Jr.J.W., 2003. CWP/SU: Seismic Unix Release 37: a free package for seismic research and processing, Center for Wave Phenomena, Colorado School of Mines.
[29] TinivellaU., 2002. The seismic response to overpressure versus gas hydrate and free gas concentration. *J. of Seismic Exploration*, **11**, 283-305.
[30] Liu Z., 1995. Migration velocity analysis. PhD thesis, *Colorado School of Mines*, CWP 168.
[31] Paull C.K., Ussler W. and Dillon W.P., 1991. Is the extend of glaciation limited by gas hydrate? *Geoph. Res. Lett.*, **18**, 432-434.
[32] Mienert J., Vanneste M., Bünz S., Andreassen K., Haflidason H., Sejrup H.P., 2005. Ocean warming and gas hydrate stability on the mid-Norwegian margin at the Storegga Slide. *Marine and Petroleum Geology*, **22**, 233-244.
[33] Bouriak S., Vanneste M., Saoutkine A., 2000. Inferred gas hydrates and clay diairs near the Sroregga Slide on the southern edge of the Vøring Plateau, offshore Norway. *Marine Geology*, **163**, 125-148.
[34] Berndt C., Mienert J., Vanneste M., Bunz S., 2005. Gas hydrate dissociation and sea floor collapse in the wake of the Storegga Slide, Norway. In: Wanas, B.T.G., Eide E., Gradstein F., Nysteun J.P. (Eds.), *Onshore-offshore relationships on the North Atlantic Margin Norwegian Petroleum Society (NPF), Special Publ*., **12**, Elsevier, Amsterdam.
[35] Dillon W.P. and Max M.D., 2000. Oceanic gas hydrate. In M.D. Max (Eds.), *Natural gas hydrate in oceanic and permafrost environments*, 61-76. Dordrecht: Kluwer Academic Publishers.
[36] De Batist M., 2006. High-intensity methane venting at the sea floor – how much reaches the atmosphere? Results of the EC CRIMEA Project. *Final Eurodom Meeting*, Trieste – Italy.

[37] Tinivella U., Loreto M.F. and Accaino F., 2006. Regional versus detailed velocity analysis to quantify hydrate and free gas in marine sediments: the South Shetland Margin case study. Soc. Geol. of London, under revision.

AIR POLLUTION CONTROL PROGRAM IN THE METROPOLITANT CITY OF TEHRAN

H. Ganjidoust[1] and B. Ayati[2]

[1] IRIMO Atmospheric Chemistry, Ozon Depletion and Air Pollution Committee

Tehran, I.R. Iran, H-Ganji@modares.ac.ir

[2] Environmental Eng. Div., Dept. of Civil Eng.,Tarbiat Modarres Univ.,

P.O.Box 14155-4838, Tehran, I.R. Iran, Ayati_bi@modares.ac.ir

ABSTRACT

The metropolitan city of Tehran (The Capital City of the Islamic Republic of Iran) with populations of over twelve millions people had faced to serious air pollution problem. Population growth and industrial development are the main reasons for the air pollution problem. Due to the geographical condition in the area, inversion happens especially in fall and winter seasons.

Industries, traffic and houses and buildings' heating systems are the main sources of pollution. In recent years, original activities with short and long aims are done in different cities, separately. For example, researching and cooperating with different institutes, centers and countries like Japan and Sweden, implementing of more than 300 studying and researching plans in meteorology and dependent courses, establishing of the first meteorological research center and atmosphere sciences, three applicator meteorological research centers and more than 40 new stations in the country, Installation of newest computer systems in metrological information, using of wall map and continuous radio-traffic to announce traffic news, completing of subway construction in Tehran, forbidding of industrial activities in a definite distance away from Tehran and transferring them to suitable places, building of highways and freeways, improving of public transportation and gasifying them, developing of fuels quality and removing lead from them, gasifying of the heating systems in houses and buildings, are the main activities that are done in recent years.

Due to quick increase in the population because of peoples' migration from countryside to cities, and rate of growth in the early years after the revolution, air pollution was an important issue in Iran. Therefore, the main purpose of this study was to investigate the control mechanisms for Tehran air pollution problems, and the necessary action plans that were taken in recent years in the city.

INTRODUCTION

Recently, some researches related to air pollution problems in large cities of the Islamic Republic of Iran have been done. Famous institutes and research centers in countries like Japan, Sweden and Germany have been in cooperation with Iranian institutes in implementing the results.

Due to quick increase in the population because of peoples' migration from countryside to cities, and rate of growth in the early years after the revolution, air pollution was an important problem in I.R.Iran. Therefore, air pollution control is one of the main issues in major cities of I.R. Iran.

Islamic Republic of Iran (I.R. Iran) is located in the center of the Middle East. Because of its location, it is one of the important countries in the region. The population of I.R. Iran is over 60 millions in a surface land area of 1'648'195 kilometer squares. Seven cities of Tehran (The Capital City), Tabriz, Isfahan, Meshed, Kerman, Ahvaz and Shiraz with populations from two to twelve millions are the major industrialized ones. In recent years, these cities have faced to air pollution problems. Population growth, rapid urbanization, growing energy needs and fossil fuel consumption, industrial development, and traffic increase are the main reasons for the air pollution problem.

Tehran as one of the metropolitan cities of I.R.Iran with populations of over twelve millions people has faced to serious air pollution problem. In addition to the mentioned factors, the geographical condition in which mountains from north to east and wind direction from west to east surround it, the pollutants are concentrated in the city and cannot naturally removed. Presence of high buildings has limited circulation of air too. So, the inversion happens especially in fall and winter seasons. It is the objective of this paper to investigate the control mechanisms for Tehran air pollution problems, and the necessary action plans that were taken in recent years in the city.

SOURCES OF POLLUTION

Tehran has three main pollution sources of transportation, industry and heating system of buildings and houses. Table 1 shows the effect of each polluting source in the environment. In the following paragraphs each source will be briefly reviewed.

Table 1. ***Effect of Pollution Sourced In Tehran (%)***

Source of Pollutants	Mobile	Stationary		
	Transportation	Industry	Refinery and Power Plant	Buildings & Public Services
PM-10	87.3	8.8	1.4	2.5
CO	94	4.9	0.2	0.4
NO_X	29.3	41.9	17.7	11.1
SO_X	3.2	64	18.1	14.7
HC	70.2	18.2	14.1	13.2
Total	71.3	2.5	5.9	4.4

Transportation in I.R.Iran is divided into public, private, and government and cooperative ones. Annually, more than 15 milliard liters (1 cubic meter = 1000 liters) petrol and 6 milliard gasoline is consummated by different kinds of transport means in the country. In other hand, about 100,000 automobiles are produced each year. The number of different transport means, the amount of different produced pollutants and the suspended particulate matters in the air pollution of Tehran are illustrated in Tables 2 to 4 respectively.

Table 2. ***Number of Different Means of Transport in TEHRAN (1996)***

Kind	Number	Percent
Active automobiles	700000	59.56
Motorcycles	350000	29.78
Active and inactive buses	44260	3.77
Minibuses	4643	0.395
Taxies	23354	1.99
Other*	53000	4.5
Electric buses	66	0.006
Total	1175323	100

*Private cars that are used as taxies

Table 3. Produced Pollutions In Tehran (1997)

Pollutant	Tons
CO	280000
SO_2	17500
PM	21000
NO_X	105000
All kinds of HC	115000
Pb	More than 2000

Industries are stationary polluting sources that have less environmental effect than cars. It does not mean that they can be disregarded. Table 4 compares amount of NO_X and SO_X production in different industries.

Table 4. NO_X & SO_X Production from Industries

Kind of Industry	NO_X	SO_X
Nonmetal	11.4	31.8
Wood and Paper	1.3	1.8
Food	6.1	8.1
Textile	2.3	3.1
Iron	9.9	7.3
Chemical	4.5	4.7
Others	6.4	7.2
Total	41.9	64

In general, 30 percent of I.R.Iran industries are located in Tehran that is about 6500 units. Most of them are in west although wind direction is from west to east. So, in new management plan, establishment of industries is forbidden within the area of 120 kilometers around the city of Tehran unless in defined industry sites. Some polluting units should be move to another suitable site, too. Sometimes, numbers of polluting industries are prevented from activities but it doesn't seam to be an effective way. It is preferred to change and improve the industrial emission to reach the acceptable air quality standards.

Heating systems of buildings & houses are other stationary polluting sources. One of the actions in recent years is installation of natural gas piping in houses especially in main and great cities that has an important role in pollutant reduction.

AIR POLLUTION CONTROL PROGRAM

Present and future air quality control action plans are given in the following paragraphs:

Present Action Plans

The activities which have been studied and some were completed by now are considered as present action plan.General activities can be summarized as:

- Researching and cooperating with different institutes, centers and countries like Japan, Germany and Sweden.
- Implementing of more than 300 studying and researching plans in meteorology and dependent courses.
- Establishing of the first meteorological research center and atmosphere sciences, four applicator meteorological research centers and 36 new stations in the country.
- Installation of newest computer systems in metrological information canters.
- Using of wall map and radio-traffic to announce traffic news, continuously.
- Using of alternative fuels especially in improved engines.
- Analysis of air pollutants in different points in the main cities.
- Increasing of air pollution analysis stations for daily, weekly, seasonally and annually reports.
- Completion of subways construction in Tehran.
- Building of highways, bridges and sidewalks.
- Substituting new buses to the old ones and starting to change their fuel system to use natural gas instead of gasoline.
- Implementing limited traffic places and times in the center of Tehran that cars can't be entered from 6:30 am to 17 pm every day except on Fridays which are national weekend holidays.
- Implementing limited traffic places and times for odd and even cars' licens numbers in odd and even days respectively.
- Implementing even more limitation for vehicles to enter the downtown areas in pick air pollution days in Tehran.
- Implementation of different times for starting and ending of work hours in most of governmental and private administration, organizations, offices … in different times.

Future Action Plans

The future action plans are the ones that are studied in recent years and are expected to be completed by the year 2015. It is important to mention that these action plans are also considered to be implemented in other industrial cities.

- New transport means for major cities
- Advancing old cars with new ones
- Increasing and advancing public transportation
- Changing the fuel to the least pollution emission one
- More Technical car inspection

- Implementation of better Traffic management
- Organizing of training courses and workshops at different levels in the city

Solving of air pollution problem will be more important in future. Due to population increased in industrial cities in I.R.Iran, proper management, harmony among different organization and ministries should be applied. In addition, more public participation is necessary. Finally, more educational and training programs by any means will help to overcome the air pollution problems in the major cities.

REFERENCES

1) Air Quality Control Company (AQCC), 1998, Tehran Transport Emissions Reduction Project, Project Summary Report 1994-1997.
2) Air Quality Control Company (AQCC) & Japan International Cooperation Agency (JICA), 1997, Technical Workshops, 12-15 Oct. 1997, Tehran, I.R.Iran.
3) Ebtekar, T., 1995, Environmental Impact of Alternative Fuel on Tehran Air Pollution, Proceeding of the Intersociety Energy Conversion Engineering Conference, Tehran, Iran, pp 32-36.
4) Industry Ministry, Proceeding of Automobile and Environment, 1995, Tehran.
5) Iranian Statistics Center, 1999, Iran Statistical Yearbook, Tehran, I.R.Iran
6) Khan M.A., 2003, Kitakyushu Initiative Seminar on Urban Air Quality and Social Commission for Asia and the Pacific (UNESCAP) Institute for Global Environmental Strategies (IGES), 20-21 February 2003, Bangkok, Thailand
7) Theodore, L., Buonicore, A.J., 1992, Air Pollution Control Equipment (A. Torkian, Trans.), Volume 1 & 2, (Original Work Published 1988).

CO_2 EMISSION OF TURKEY'S PROVINCIES AND DISTRICTS WITH RESPECT TO INDUSTRIAL CLASSIFICATION

Ali Can[1], **Aysel T. Atımtay**[2]

[1]Turkish Statistical Institute, Ankara, ali.can@tuik.gov.tr
[2]Middle East Technical Uniersity, Ankara, aatimtay@metu.edu.tr

ABSTRACT

Earth's climate is changing and the human beings have played an important role on this change. The very rapid development of technology and multiplication of population has brought environmental crises to different regions of the earth. The release of greenhouse gases is one of the important sources of these changes. The most important greenhouse gas is the carbon dioxide (CO_2), because it is responsible for about 60% of the "Greenhouse Effect".

The results of the study showed that there are fluctuations in the CO_2 concentration throughout the years. The CO_2 emissions from industries are approximately 30% of the total emissions between the years 1995 and 2001. The results of the CO_2 emission inventory conducted in this study for these years showed that the CO_2 emission in 1997 is the highest with a value of 64.5 million tones. The highest regional CO_2 emissions from industries were observed in Marmara, Mediterranean, Black Sea and Aegean regions with annual average values of 12.87, 13.02, 13.01 and 11.96 million tones.

Keywords: CO_2 emissions, industrial classifications, IPCC method, GIS techniques

INTRODUCTION

CO_2 is emitted into the atmosphere with increasing quantities by years due to the combustion of coal, oil and natural gas [1]. Combustion of fossil fuels is responsible for 75-90% of all anthropogenic emissions of CO_2 [4]. The atmospheric concentration of CO_2 has increased from preindustrial value of 280 ppm to more than 370 ppm today and is increasing at a rate of 0.5%/year [5, 3]. Therefore, this increase contributes to the enhancement of the greenhouse effect, which results in atmospheric global warming and climate change [7].

The basic anthropogenic sources of the CO_2 emission were considered as households, thermal power plants, road vehicles and manufacturing industries. In this study, the CO_2 emission from manufacturing industries were studied. The necessary data for the annual fuel consumption in industries between 1995 and 2001 was obtained from the Turkish Statistical Institute (TURKSTAT) and Ministry of Energy (MOE).

The major objective of this study was to prepare an industrial CO_2 emission inventory of Turkey based on district and provinces by using the fuel consumption data with respect to industrial classifications. IPCC [6] method was applied to the annual fuel consumption data in order to calculate the CO_2 emissions and the results were mapped by using the GIS techniques.

METHODOLOGY

An emission inventory was prepared in this work by taking into account all possible emission sources. The basic source of CO_2 is the combustion of fossil fuels in households, manufacturing industries, thermal power plants and road vehicles. The carbon content and emission factors of the fuels used were the starting point for the estimation of CO_2 emissions.

The data for the annual fuel consumption between 1995 and 2001 was basically obtained from the published books [9] on energy consumption in the manufacturing industries of Turkish Statistical Institute (TURKSTAT) and energy balances tables [11] of Ministry of Energy (MOE). The data are aggregated according to the sectorial classifications. However, the formulas and studies published by Can (2006) was used for the determination of CO_2 emissions of industries according to its classifications and size.

The industries were classified as nine main parts as given in ISIC classifications [8]. These are;

- (31) Manufacture of food, beverages and tabacco,
- (32) Textile, wearing apparel and leather industries,
- (33) Manufacture of wood and wood products including furniture,
- (34) Manufacture of paper and paper products, printing and publishing,
- (35) Manufacture of chemicals and of chemical, petroleum, coal, rubber and plastic products,
- (36) Manufacture of non-metallic mineral products of petroleum and coal,
- (37) Basic metal industries,
- (38) Manufacture of fabricated metal products, machinery and equipment, transport equipment, professional and scientific and measuring and controlling equipment,
- (39) Other manufacturing industries.

The inventory results at the provincial and districts level are, then, mapped by using GIS techniques [10].

RESULTS AND DISCUSSIONS

According to the CO_2 emission inventory (1990-2003) which has been prepared by Can (2006), the average CO_2 emissions from industries are approximately 35% of the total emissios. The total provincial CO_2 emission is seen in the following Figure 1.

In the provincial total CO_2 emissions, the maximum annual CO_2 emission was observed in Istanbul with an average value of 30 million tones throughout the years. The amount of increase in the CO_2 emission of Istanbul in 2000 as compared to 1990 value (base year) was around 51.97%. In this year, the second highest CO_2 emissions were observed in İzmir, Ankara, Bursa, Kütahya and Muğla provinces with 16.5, 13.7, 11.2, 10.3 and 10.1 million tones, respectively. The main reason for these high emissions is the high rate of fuel consumption in thermal power plants and industries.

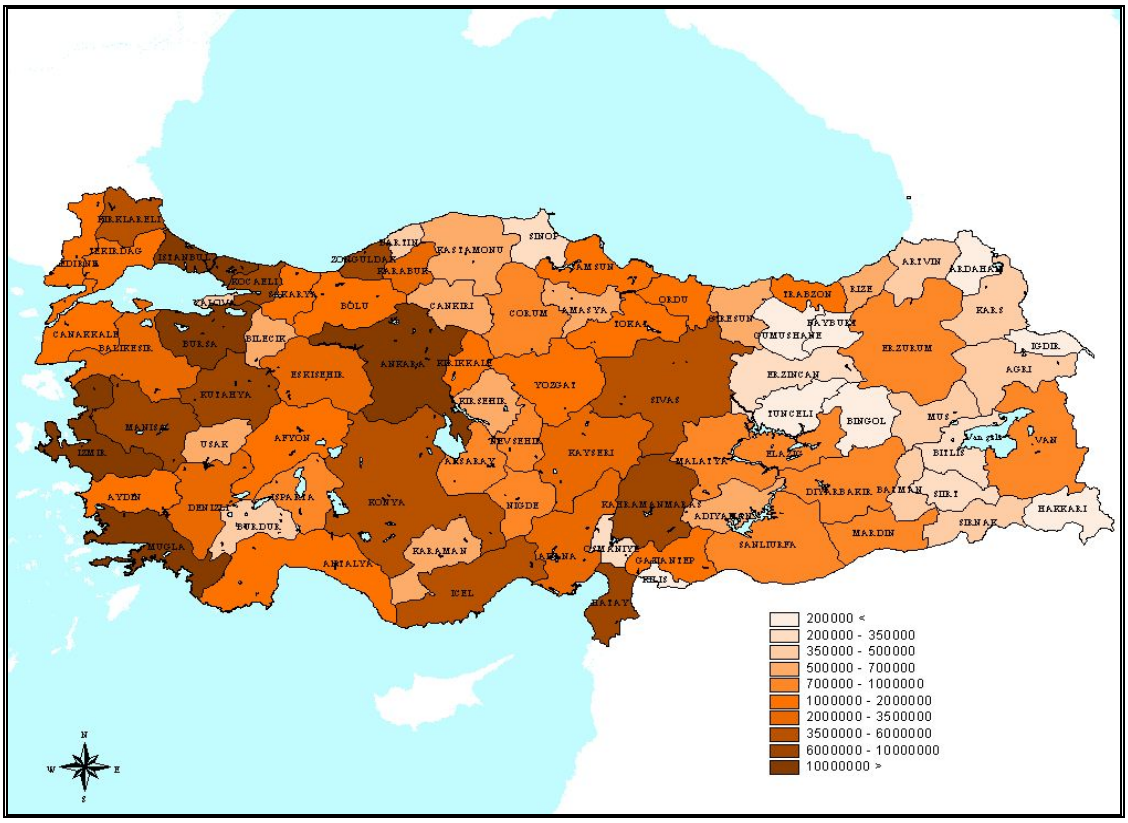

Figure 1. CO_2 emissions from provinces for 2000 in tones [2]

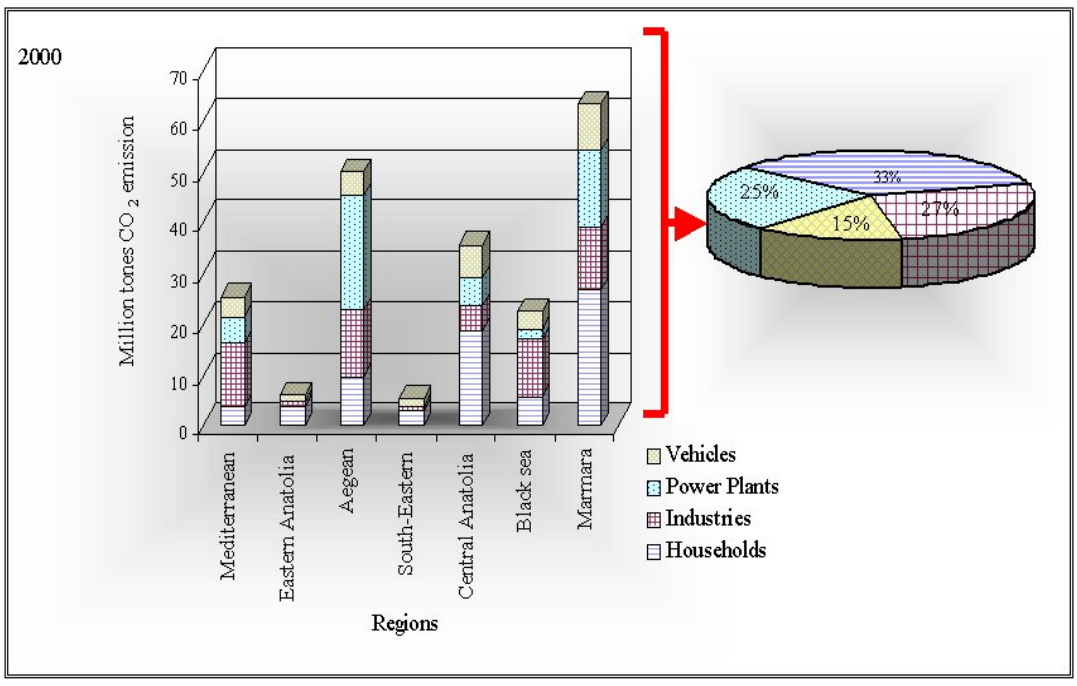

Figure 2. Regional and total CO_2 emissions from the sources for 2000 [2]

The Marmara Region showed the highest CO_2 emission with a 63.4 million tones in 2000 (Figure 2). The percentage emission increase as compared to the base year was found as

48.7%. The contribution of households, industries, power plants and road vehicles in this region to the annual total CO_2 emission of Turkey were 12.9%, 5.8%, 7.4% and 4.4%, respectively. The CO_2 emission from industries was approximately 27% of the total CO_2 emissions in 2000.

The total industrial CO_2 emissions according to its classifications for the years between 1995 and 2001 were given in Figure 3. As shown in this figure, the CO_2 emissions from the sector 37 (basic metal industries), sector 36 (manufacture of non-metallic mineral products of petroleum and coal), sector 35 (manufacture of chemicals and of chemical, petroleum, coal, rubber and plastic products) are the highest between 1995 and 2001. The average respective CO_2 emissions from these industries were 24.8, 12.2 and 8.3 million tones/year. In 2000, these industries contributed to the total industrial CO_2 emission with 43.84%, 21.57% and 16.8%, respectively. The result is shown in Figure 4.

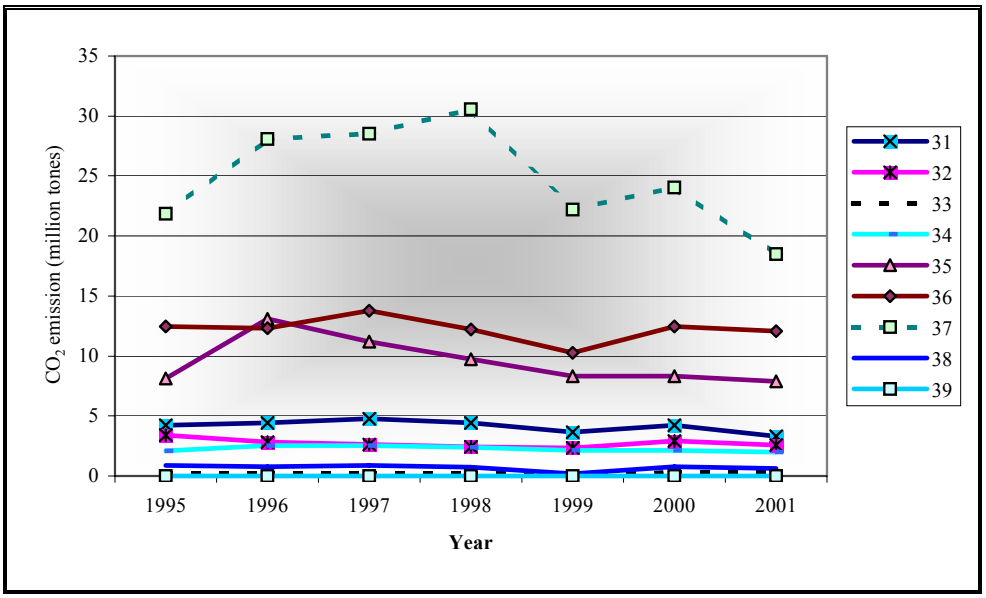

Figure 3. CO_2 emissions from the industries according to the its classifications for 1995-2001

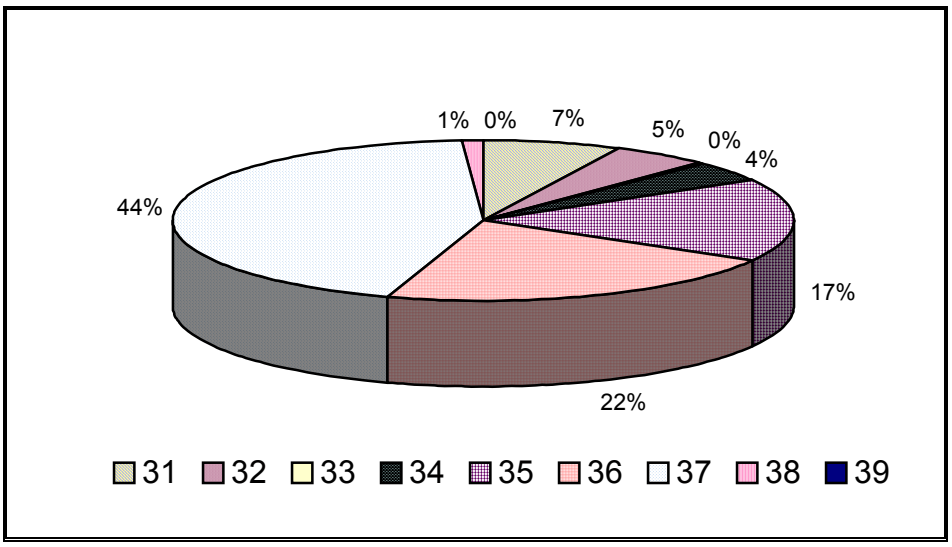

Figure 4. CO_2 emissions from the industries in 2000 according to the sector classification

As can be seen from Table 1, the highest CO_2 emissions were released from large size industries. About 55.7% of the total CO_2 emissions in 2000 were from the industries which have more than 1000 employees.

Table 1. CO_2 emissions from the industries according to the size and sector classification for 2000 in million tones

Size*	31	32	33	34	35	36	37	38	39	Total
10-24	0.0046	0.0015	0.0000	0.0000	0.0023	0.0365	0.0040	0.0021	0.0000	0.0510
25-49	0.0247	0.0138	0.0000	0.0057	0.0248	0.5573	0.0864	0.0029	0.0000	0.7156
50-99	0.1360	0.0634	0.0345	0.0690	0.0887	0.8822	0.1783	0.0017	0.0000	1.4539
100-199	0.5272	0.1478	0.0889	0.2170	0.1961	3.5297	0.2700	0.0526	0.0000	5.0294
200-499	0.8982	0.5347	0.1756	0.4486	0.7717	3.5433	1.5535	0.1927	0.0000	8.1182
500-999	1.8536	0.9614	0.0000	1.3378	1.3894	2.8598	0.4971	0.1959	0.0000	9.0948
1000+	0.8084	1.1771	0.0000	0.0772	5.8604	1.0376	21.4610	0.3078	0.0000	30.7295
Total	4.2527	2.8998	0.2990	2.1552	8.3335	12.4463	24.0502	0.7557	0.0000	55.1924

* The size of the industries are determined according to the number of employees

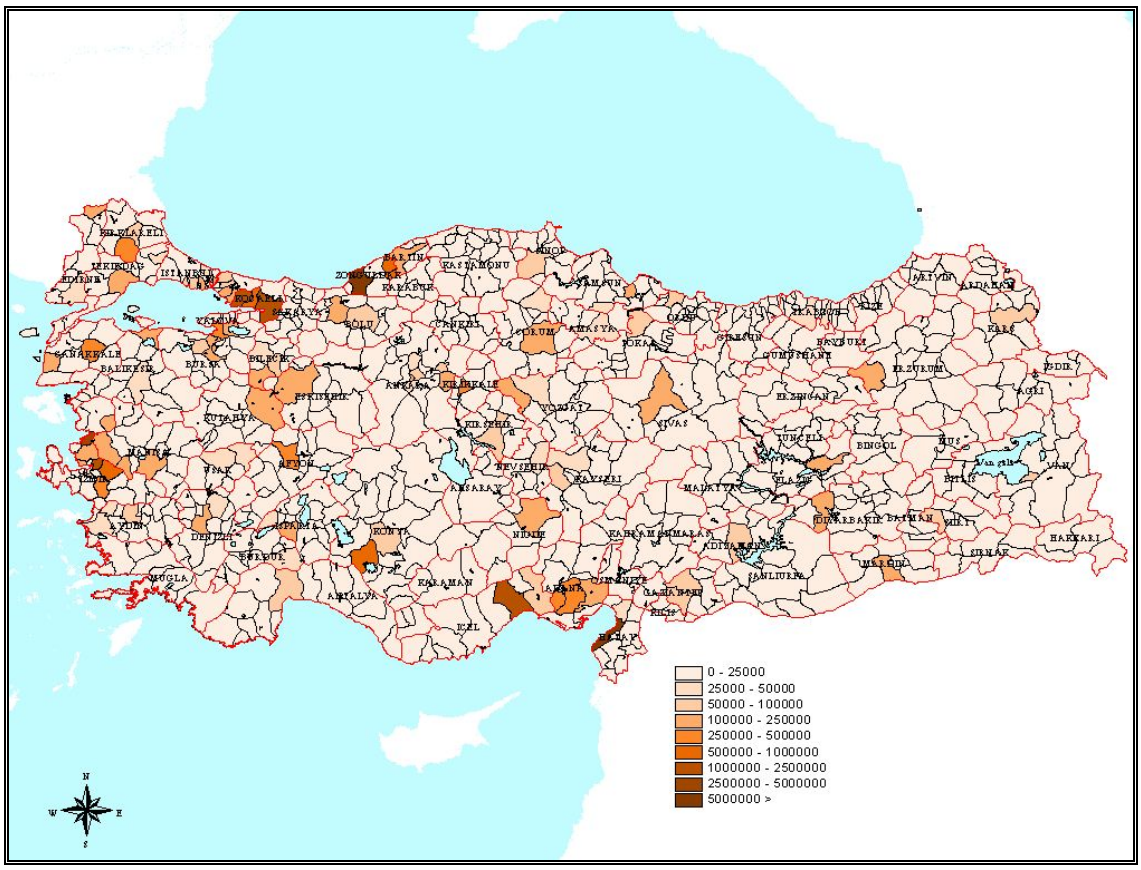

Figure 5. Total CO_2 emissions from the industrial sectors (35), (36), (37) in 1995

As can be seen from Figure 5 and Figure 6, the highest CO_2 emissions were seen in İzmir, Hatay and Zonguldak for the years between 1995 and 2001. Izmir province was the highest for the years 1995, 1999 and 2000 with an approximately 10 million tones CO_2 emission.

Hatay province was also highest for the years between 1996 and 1998 with an about 11 million tones CO_2 emission. For the year 2001, the highest industrial CO_2 emission was determined in Zonguldak with 5.76 million tones.
In 1995 for the sector (35), Aliağa (İzmir) district was estimated as a highest CO_2 emission province with 2.5 million tones/year. For the other sector (36) and (37), Bornova (İzmir) and Ereğli (Zonguldak) had the highest emission with respective values of 1.0 and 6.3 million tones.

Aliağa (İzmir) was also determined as a highest CO_2 emission district for sector (35) in 2000. The CO_2 emission was 2.2 million tones. İçel (Center) and İskenderun (Hatay) had the highest CO_2 emission with respective values 1.2 for sector (36) and 6.9 million tones for sector (37).

In 2001, the highest CO_2 emissions were seen in Kocaeli (Center) for sector (35), İçel (Center) for sector (36) and İskenderun (Hatay) for sector (37). The respective CO_2 emissions in these districts were 2.24, 1.41 and 5.33 million tones.

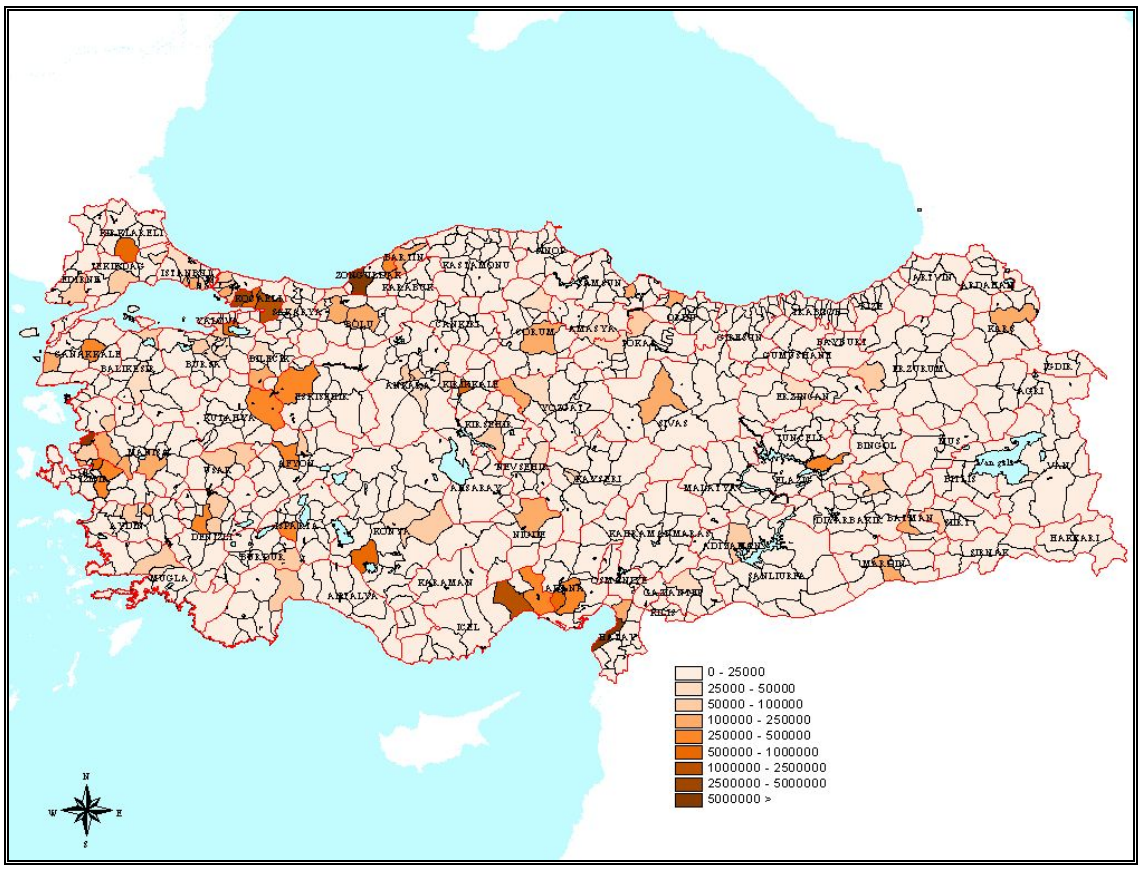

Figure 6. Total CO_2 emissions from the industrial sectors (35), (36), (37) in 2000

CONCLUSION

The results of this study have shown that CO_2 emission from manufacturing industries of Turkey has been fluctuating throughout the years and average emissions from industries are

approximately 30% of the total emissions between the years 1995 and 2001. The results of the CO_2 emission inventory conducted in this study for these years showed that the CO_2 emission in 1997 is the highest with a value of 64.5 million tones. Throughout the study period, Aliağa (İzmir) and İskenderun (Hatay) were almost determined as the highest CO_2 emissions districts from sector (35) and (37), respectively.

REFERENCES

[1] Alcoma J. , Krol M., Leemans R., Stabilizing Greenhouse Gases – Global and Regional Consequences – National Institute of Public Health and the Environment , the Netherlands. p. 1 – 10., 1995.

[2] Can, A., Investigation of Turkey's Carbon Dıoxide Problem by Numerical Modeling – PhD Thesis. p. 45-62., 2006.

[3] Carbon Dioxide (CO_2) - http://www.science.gmu.edu/~zli/ghe.html - visited on December 11, 2003.

[4] IGU - Climate Change – The case for gas, Internatıonal Gas union, Eurogas, Marcogaz: Printed by Van Marken Delft Drukkers. p. 6., 1997.

[5] IPCC - Intergovernmental Panel on Climate Change - Summaries for Policymakers and Other summaries. IPCC Special Report. p. 1 - 22, 43., 1994.

[6] IPCC - Greenhouse Gas Inventory Reference Manual - Revised 1996 IPCC Guidelines for National Greenhouse Gas Inventories. Vol I. p.1 - 19., Vol II. p. 1.1 - 1.31., Vol III p. 1.1 - 1.136., 1996.

[7] IPCC - Intergovernmental Panel on Climate Change - Climate Change 2001: The Scientific Basis. Cambridge University Press. p. 185 - 237., 2001.

[8] ISIC - International Standard ındustrial classification of all economic activities (Rev.2) – Manufacturing Industry classification. p.XXI-XXV., 1990.

[9] SIS - Energy Consumption in the Manufacturing Industry (1995-2001) - State Instıtute of Statıstıcs.

[10] Mahoney R.P., Land Information Systems-Geographical Information Systems-principles and applications-edited by J.Maguire, M.F. Goodchild, D.R.Rhind. p.101-114., 1991.

[11] MOE - The annual Energy and Petroleum Balance Sheets (1990-2010) – Ministry of Energy., 2003.

ANNUAL AND SEASONAL TREND PATTERNS OF CLIMATE CHANGE IN TURKEY

Ulas Im[1], Mete Tayanc[2]

[1]Bogaziçi University, Institute of Environmental Sciences, Bebek, İstanbul, Turkey, ulasim@boun.edu.tr,
[2]Marmara University, Dept. of Environmental Eng., Kuyubaşı, İstanbul, Turkey, mtayanc@eng.marmara.edu.tr

ABSTRACT

Climate change in Turkey is studied by analyzing the annual and seasonal temperature and precipitation trends of 53 climate stations during the period of 1950-2004. These stations are classified into two groups according to their populations; S1, including the large urban stations and S2, including rural and suburban stations. Normalized Mann-Kendall trend test statistics are calculated for maximum, minimum, mean temperatures and precipitation to determine the statistically significant climatic changes. Our results show that 29 stations produced significant warming trends in one or more of their maximum, minimum or mean temperature series. These stations are mainly located on western, southern and southeastern parts of Turkey. On the other hand, significant cooling trends are mostly experienced in the northern parts of the country with 5 stations yielding significant cooling in one or more of their temperature series. During regional analysis, the Mann-Kendall coefficients for the minimum temperatures, which are a signal of urbanization, resulted in an increasing trend in almost all of the regions except for the northeastern parts of the country. Maximum temperatures significantly increased in south, southeastern stations and in some western coastal stations. The average temperature profiles have shown almost the same behavior as maximum temperatures. 5 stations experienced significant increase in precipitation, 4 of them located in the northern regions and 1 in the southeast. 2 stations showed significant decrease in precipitation and are located in western and northwestern parts of Turkey. Significant warming has been detected on seasonal basis in especially minimum temperatures all around Turkey except for northeastern regions. Results also show that autumn precipitation has significantly increased for central and northern parts of the country.

INTRODUCTION

An increasing body of observations and analysis gives a collective picture of a warming world and other changes in the climate system. The global average surface temperature has increased over the 20th century by about 0.6°C. Climate change is threatening the food production, drinking water supplies and sustainable development throughout the world. Rising sea level, extreme weather events and desertification is just a few of the effects, especially threatening the millions of people living in less developed countries. Intergovernmental Panel on Climate Change report (IPCC, 2001) expresses that global warming mainly caused by human activities is a reality and there are growing fears of feedbacks that will accelerate this warming.

Within the last several decades, the increasing efforts to gain insight into the man-made climatic changes have resulted in much work on temperature records, mainly in the developed countries. Previously, much work had focused on North American and European countries owing to the ready availability of abundant data. With the expansion of the global climatic

datasets, a worldwide increase in the number of studies on climate variability has taken place, leading to a better understanding of climate system (Jones and Mann, 2004; Charlson and Wigley, 1994; Karaca et al., 1995, 2000; Karl et al., 1993; Kiehl et al., 2000; Nasrallah and Balling, 1993; Tayanç and Toros, 1997; Tayanç et al., 1997, 1998a, 1998b; Wigley, 2005; Ezber et al., 2006; WMO, 1992).

This study is aiming to conduct a research on climate variability in Turkey via historical observation data extending back to 1950s, determine the time and place of significant changes in temperature and precipitation, and comment on the possible effects of the climate variability. In this respect, this work proposes to compile up-to-date and historical meteorological data, carry out nonparametric statistical tests and determine any climatic changes in Turkey, find the threatened regions, and look to the future for any climate change dangers.

In the following section we first classify the 53 climate stations and explain the methods used in this study. In the Results section we look forward to find any climatic changes in the min, mean, max temperature and precipitation series, and comment on the findings and urbanization problems Turkey is now confronting.

STUDY AREA AND METHODS

The population of Turkey has grown almost 3.24 times between 1950 and 2000, from 20.947.188 to 67.803.927 [(State Institute of Statistics), 2000]. As can be seen in Figure 1, there is a sharp increase in early 1980's in urban share of this population. This increase of population in the favor of cities, has dramatic effects in the structure of land-use, convert the green areas to concrete buildings and this in turn may produce significant changes in the micro and meso scale climatic conditions.

To investigate the changes in climatic variability in Turkey, maximum, minimum and average daily temperature and daily precipitation data, provided by the National Meteorology Service, from 53 meteorological stations in Turkey are analyzed for a 55-years time period, between 1950 and 2004 in the study. The spatial distribution of stations used in the study is presented in Figure 2. The stations are classified into two groups according to the populations they represent; S_1 for stations with a population below 100000 and S_2 for stations with a population higher than 100000. Detailed information of these stations is provided in Table 1.

A computer code, which synchronizes the data by checking the missing dates or values, calculating the daily average for each day of a month throughout the whole available study period, and replacing the missing values with the calculated climatic averages is developed for this purpose. The months having more than 15 missing days and the years having no data available are excluded from the datasets in order to obtain more reliable bases for the trend analysis. The homogeneity of each station for each parameter is checked by producing difference series with their neighboring stations. The stations that have one jump in the whole study period are corrected by either adding or subtracting a value, which is obtained by taking the difference between the averages before and after the jump. The program then calculates the monthly, seasonal and yearly averages for each station and for each temperature and precipitation series.

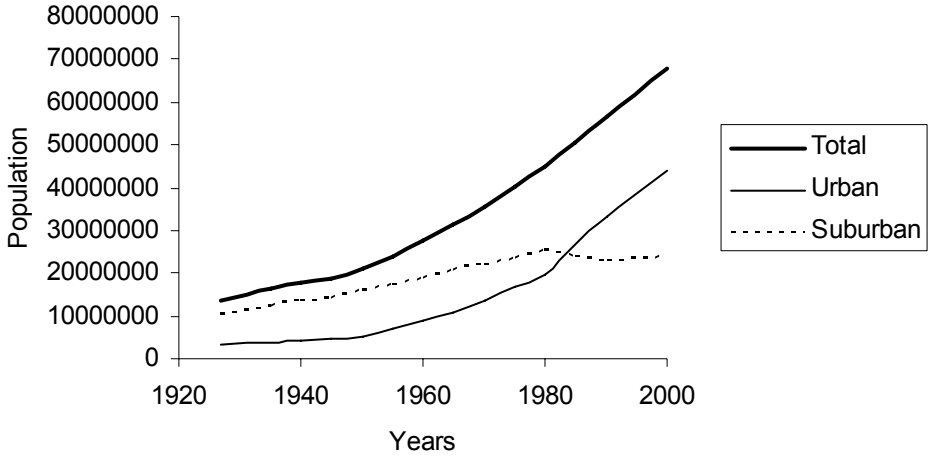

Figure 1. Population variability in Turkey between 1927 and 2000.

A non-parametric trend test, Mann-Kendall, is applied to temperature and precipitation series of all stations. If a Mann-Kendall statistic of a time series is higher than 1.96, there is a 95% significant increase in that particular time series. If the result is just the reverse, i.e. lower than -1.96, there is a 95% significantly decreasing trend in the series. The Mann-Kendall statistics are then plotted on a map in order to show the spatial distribution of both the significant and non-significant temperature and precipitation trends in Turkey. These plots are produced on monthly, seasonal and yearly basis to determine any significant climatic changes that might took place during the 55 years time period and to determine the critical months that were mostly affected by the climate change. To prevent unrealistic spatial prediction, the boundaries of the domain are set to 25 – 48° E and 34.5 – 44° N.

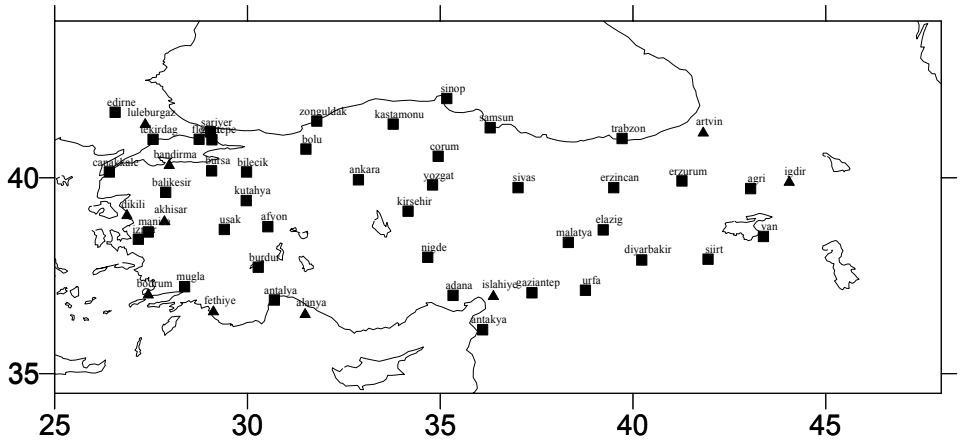

Figure 2. The spatial distribution of the meteorological stations (▲represents the stations characterized by populations up to 100 000, and ■ above 100 000).

Table 1. WMO numbers, Classifications, Coordinates and 2000 populations of 53 stations

WMO Number	Station Name	LAT	LONG	ALT	2000 URBAN POP	CLASS
17022	Zonguldak	41.45	31.8	137	250282	S2
17026	Sinop	42.02	35.17	32	101285	S2
17030	Samsun	41.28	36.3	4	635254	S2
17037	Trabzon	41	39.72	30	478954	S2
17045	Artvin	41.18	41.82	628	84198	S1
17050	Edirne	41.67	26.57	51	230908	S2
17056	Tekirdağ	40.98	27.55	4	395377	S2
17059	Kumköy (Kilyos - Istanbul)	41.25	29.03	30	1852	S1
17061	Sarıyer (kirecburnu)	41.17	29.04	58	219032	S2
17062	Göztepe (Kadıköy)	40.97	29.08	33	663299	S2
17070	Bolu	40.73	31.52	742	142685	S2
17074	Kastamonu	41.37	33.78	800	174020	S2
17084	Çorum	40.55	34.95	776	311897	S2
17090	Sivas	39.75	37.02	1285	421804	S2
17094	Erzincan	39.75	39.5	1218	172206	S2
17096	Erzurum	39.92	41.27	1869	560551	S2
17099	Agri	39.72	43.05	1631	252309	S2
17100	Iğdır	39.92	44.05	858	81582	S1
17112	Çanakkale	40.15	26.42	6	215571	S2
17114	Bandırma	40.35	27.97	58	97419	S1
17116	Bursa	40.18	29.07	100	1630940	S2
17120	Bilecik	40.15	29.98	539	124380	S2
17130	Ankara	39.95	32.88	891	3540522	S1
17140	Yozgat	39.82	34.8	1298	315156	S2
17152	Balıkesir	39.63	27.88	102	577595	S2
17155	Kütahya	39.42	29.97	969	318869	S2
17160	Kırşehir	39.15	34.17	1007	147412	S2
17172	Van	38.5	43.38	1671	446976	S2
17180	Dikili (Izmir)	39.07	26.88	3	12552	S1
17184	Akhisar (Izmir)	38.92	27.85	93	81510	S1
17186	Manisa (Izmir)	38.62	27.43	71	714760	S2
17188	Uşak	38.68	29.4	919	182040	S2
17190	Afyon	38.75	30.53	1034	371868	S2
17199	Malatya	38.35	38.32	898	499713	S2
17201	Elazığ	38.67	39.23	991	364274	S2
17210	Siirt	37.92	41.95	896	153522	S2
17220	İzmir	38.43	27.17	25	2732669	S2
17238	Burdur	37.72	30.28	967	139897	S2
17250	Niğde	37.97	34.68	1211	126812	S2
17261	Gaziantep	37.07	37.38	855	1009126	S2
17270	Urfa	37.13	38.77	547	842129	S2
17280	Diyarbakır	37.9	40.23	677	817692	S2
17290	Bodrum	37.05	27.43	27	32227	S1
17292	Muğla	37.22	28.37	646	268341	S2
17296	Fethiye	36.62	29.12	3	50689	S1
17300	Antalya	36.88	30.7	51	936240	S2
17310	Alanya	36.55	32.5	7	88346	S1
17351	Adana	37	35.33	20	1397853	S2
17600	Lüleburgaz	41.4	27.35	46	79002	S1
17636	Florya (Bakırköy)	40.98	28.75	36	208398	S2
17964	Islahiye (Urfa)	37.01	36.38	513	38770	S1
17984	Antakya (Hatay)	36.12	36.1	100	581341	S2

RESULTS

The yearly averages calculated for all temperature series show significant warming in southern and southeastern parts and significant cooling in northeastern parts of Turkey. Figure 3 illustrates the spatial distribution of Mann-Kendall statistics as circles. As can be seen from Figure 3a, there is a significant warming trend in the majority of the Mediterranean Region stations, some eastern Anatolia stations and in Lüleburgaz and in some İstanbul stations in the northwest. Looking at the big picture, one can conclude that almost all parts of Turkey are under a warming trend - mostly not significant - except for the northern parts. On the other hand, there is certainly a much more widespread significant warming trend in the minimum temperatures (Figure 3b). Almost all southern parts, western parts and continental regions of the country experienced a warming in minimum temperatures during the last half century. The increase in minimum temperatures can be easily attributed to urbanization and urban heat island effect. The increase in population, thus the increase in residential and industrial areas causes the heat to be absorbed by the buildings and air pollutants, and during the nighttime, when the minimum temperatures are observed, produces an artificial heating source that is called heat islands, increasing the minimum temperatures as well as leading to air pollution episodes.

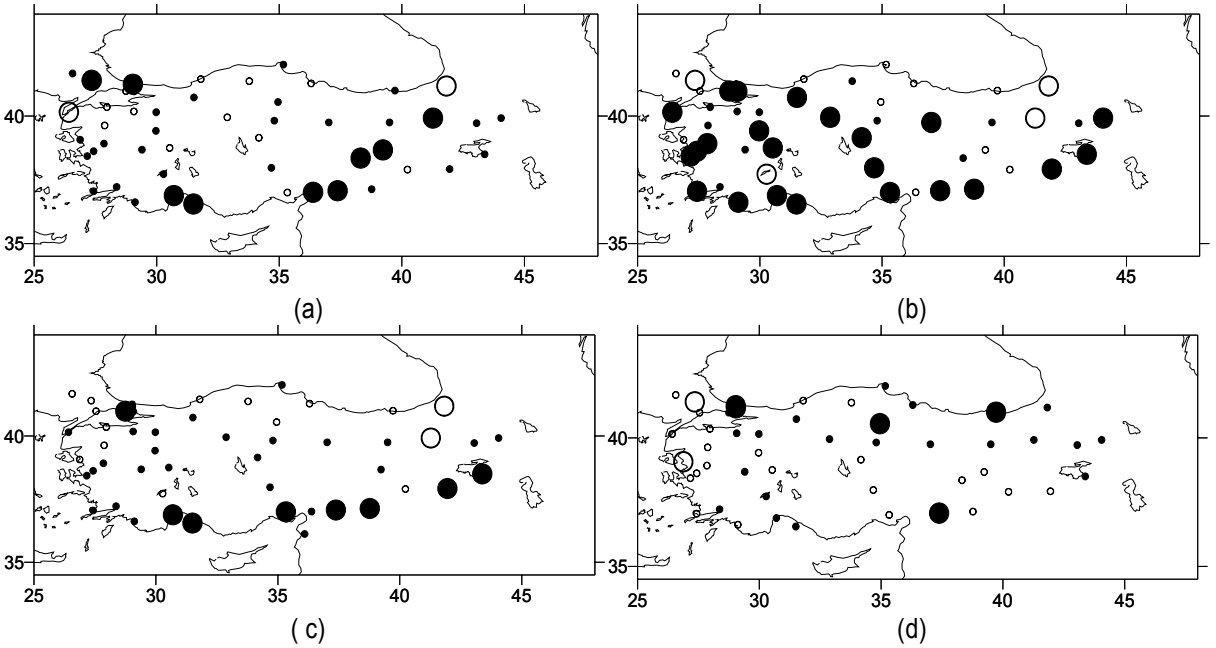

Figure 3. Spatial distribution of annual (a) maximum (b) minimum, (c) average temperatures and (d) precipitation series Mann-Kendall statistics in Turkey (● represents 95% significant warming, ● represents warming but not significant, ○ represent 95% significant cooling and ○ represents cooling that is not significant).

Figure 3c presents the trends in mean temperatures. Again the increase can be seen in most of the regions of Turkey, with the exception of northern regions. The southeastern regions experience significant warming. The significant increases the temperatures of the southern parts of the country is believed to be a result of desertification and the increasing frequency of the Africa and Middle East originated heat waves for the last half century. Another interesting result that can be seen in the figures is the stations in certain regions of the country that show

cooling trend in average temperatures but show a warming trend in maximum temperatures (e.g. Artvin, Tekirdağ, Edirne, Antalya). This is a result coming from the calculation of average daily temperatures. The formulation includes 0700, 1400 and 2100 LST observations but 2100 LST observation is included twice in the calculation. Thus, the daily average temperatures are more likely affected by a cooling trend observed in minimum temperatures.
Figure 3d represents the spatial distribution of precipitation throughout the study period. As can be seen from the figure, especially the trend in the southeastern, western and northern parts of the country agrees with the temperature changes discussed above. In the countrywide, there is not a significant change in precipitation series but on the northern parts, there is a significant increase in amount of precipitation received yearly. In the Aegean part of the country, though not significant, there is an opposite decreasing trend which is well correlated with the increasing temperatures in that region. Similarly, in the southeastern regions, generally there is a decreasing trend in the amounts of yearly rainfall agreeing well with the idea of desertification in that region.

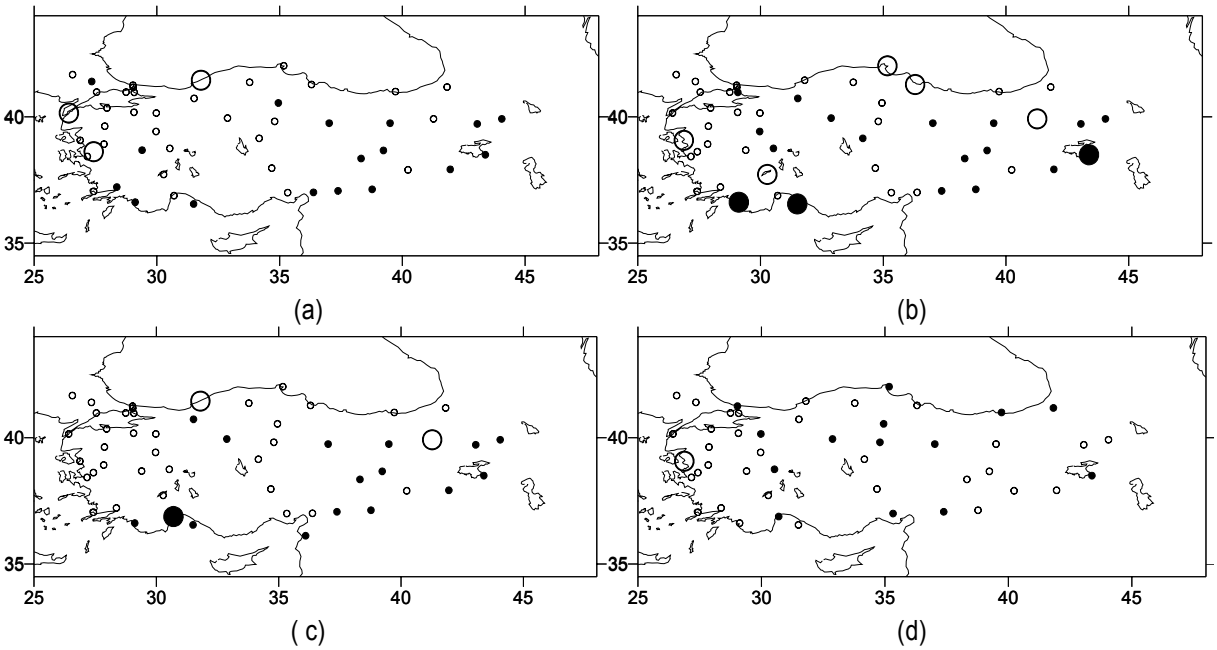

Figure 4. Same as Figure 3 for the winter season.

Regarding the seasonal variations in the temperature and precipitation trends, it is found that there is not much significant change in winter in either way, and that maximum temperatures did increase in the southwestern parts and decrease in the northern and continental (central) parts but these changes are not in 95 % significance level (Figure 4a). On the other hand, there is significant decrease in maximum winter temperatures in northwestern Turkey (Zonguldak) and in Aegean part (Çanakkale and Manisa). Minimum temperatures increased in central, southeastern and eastern part but decreased in western and northern parts (Figure 4b). These increases were significant in Alanya and Fethiye stations in southwestern Turkey and in Van station in eastern part of Turkey. Decrease in minimum temperatures were significant in Burdur station in southwestern part, in Dikili station in Aegean (western) region, Sinop and Samsun stations in northern regions (Black Sea Region) and Erzurum station in eastern part of Turkey. Average temperatures increased in eastern parts and

decreased in western parts (Figure 4c). Those changes were mostly not significant except for an increase in Antalya station and decrease in Zonguldak and Erzurum stations. There was decrease in amount of yearly precipitation in western and southeastern parts and increase in central and northeastern (East Black Sea Region) regions of Turkey (Figure 4d). The only significant change was detected in Manisa station as a decrease.

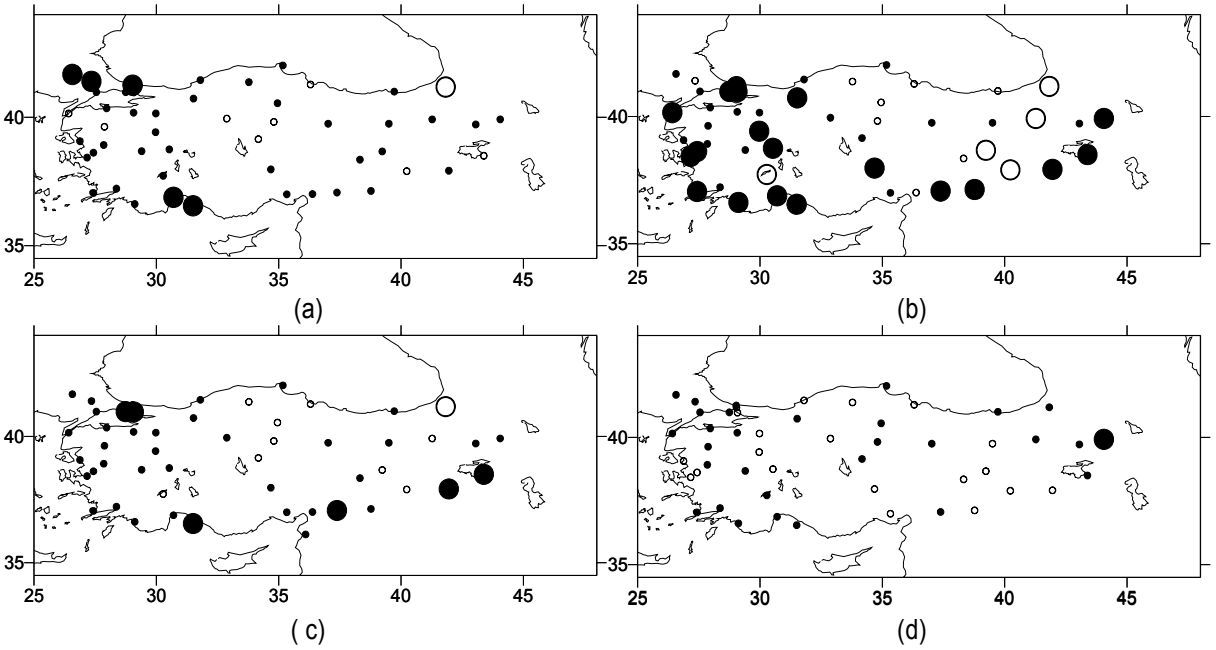

Figure 5. Same as Figure 3 for the spring season.

For the spring period, increase in all temperature series and precipitation series is found, especially in minimum temperatures (Figure 5). Significant increase in maximum temperatures in southern (Antalya and Alanya stations) and northwestern (İstanbul, Edirne and Trakya) regions were detected (Figure 5a). Minimum temperatures significantly increased in almost all western stations except for Burdur station (Figure 5b). Increase in southeastern regions was also in 95 % significance level. In Artvin and Erzurum stations in northeastern regions, together with Diyarbakır and Elazığ stations in southeastern parts experienced significant decrease in minimum temperatures. Increase in average temperatures in southeastern and northwestern and especially in western parts of the country are found, being mostly not significant (Figure 5c). Stations in Istanbul, Alanya station in southern Turkey, Gaziantep, Siirt and Van stations in southeastern Turkey showed significant increase in average temperatures. Precipitation amount generally increased in western, southwestern, central and northern parts, all being below 95 % significance level (Figure 5d). Decrease has mostly been experienced in southeastern regions and some stations in the western parts around İzmir, Bilecik, Kütahya and Afyon stations as well as some stations in north (Zonguldak, Samsun and Kastamonu).

For the summer period, it is clearly seen that significant warming exists in almost all regions, especially in minimum temperatures, including the northern regions (Figure 6). Max temperatures increased in almost all stations, mostly significant, and a couple of stations showed opposite trends in the northwestern parts (Figure 6a). The exceptions were Van in

eastern Turkey, Artvin station (significant) in northwestern Turkey, and Bandirma, Balikesir and Çanakkale stations in Marmara region (northwest). Minimum temperature series almost exhibited the same behavior as maximum temperatures (Figure 6b). The exceptions were mostly in eastern regions and not significant. On the other hand, Erzurum and Elazığ stations experienced significant decrease in their minimum temperatures. Average temperatures increased almost significantly throughout the country with the exceptions of Artvin, Erzurum and Elazığ stations in the east (Figure 6c). Decrease in precipitation in eastern, western and central parts; and increase in northern and southern parts are detected (Figure 6d). Summer precipitations significantly decreased in Erzurum station and increased in Sarıyer station in the Marmara Region. Decrease in western parts can be attributed to the positive NOA index values as explained before. The increasing temperature values and decreasing precipitation amounts in southeastern regions are a consequence of the desertification taking place in the Middle East Region. This result is almost clear in all seasonal and annual trends.

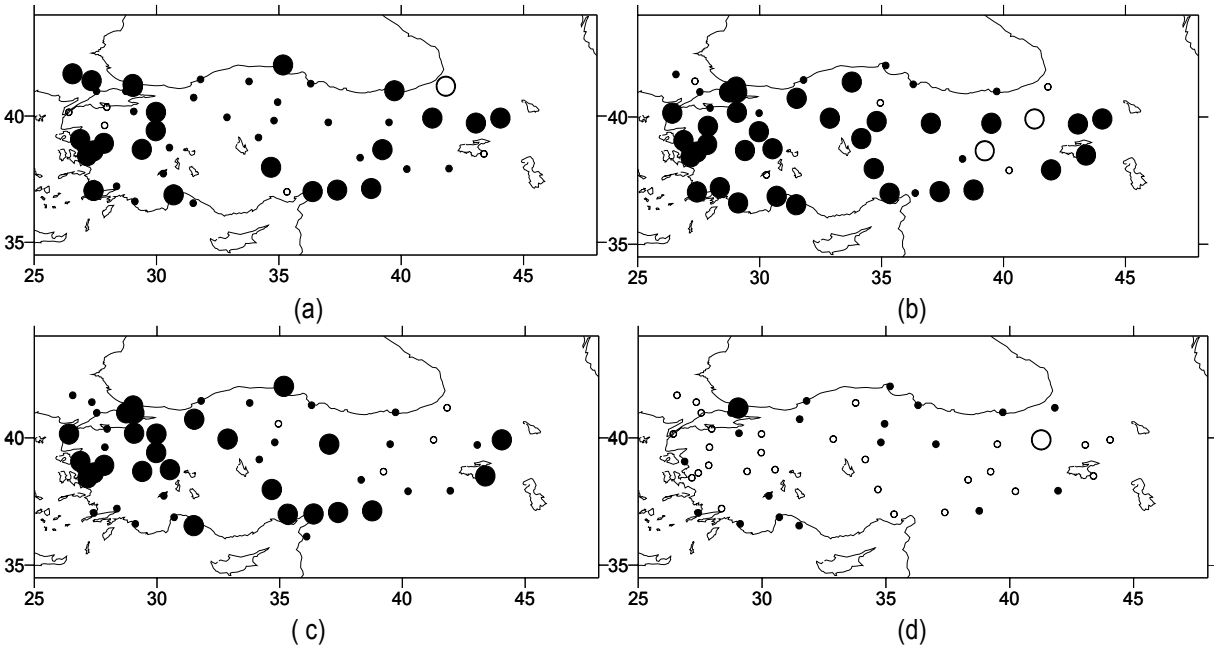

Figure 6. Same as Figure 3 for the summer season.

In autumn, increase in most of the country is experienced, being especially significant in minimum temperatures (Figure 7). Maximum temperatures increased in countrywide being below the significance level with exceptions of Antalya and Erzurum stations (Figure 7a). As can be seen in Figure 7b, minimum temperatures significantly increased except for the northern coastline, although the trend remains below the significance level. Decrease has also been detected in a few stations, being significant in Erzurum and Elazığ stations and not significant in Artvin, Çorum and Diyarbakır stations. Average temperatures increased in western, central and southern parts and decreased in southwestern parts (Figure 7c). Significant increase has been detected in Antalya, Alanya, and Adana stations in Mediterranean region, Kırşehir station in central region and Gaziantep in southeastern region. Increase in precipitation is clearly seen in all regions (Figure 7d). Significant increase has been detected in central parts and northwestern parts. Decrease has also taken place in northwestern parts but is not significant.

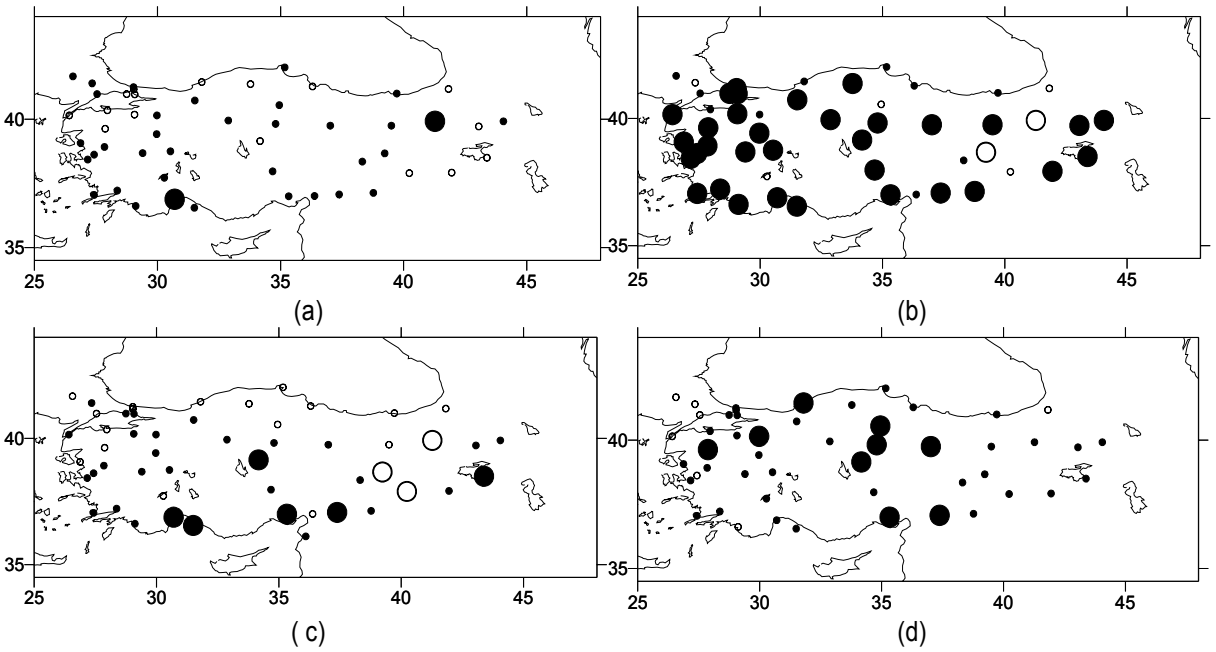

Figure 7. Same as Figure 3 for the autumn season.

CONCLUSIONS

In this study, annual and seasonal temperature and precipitation series from 53 stations are analyzed. Significant warming in southern and southeastern parts of the country is found. Cooling has also been detected in northern parts of the country that is not significant. Particularly, minimum temperature series show significant warming in almost all regions indicating the effect of urbanization. Significant warming in maximum and average temperature series as well as the significant decrease in precipitation, point to desertification in southeastern parts of Turkey. The decreasing precipitation rates in the Aegean part of Turkey can be related to the positive values of the North Atlantic Oscillation (NAO) in the recent years. Minimum temperatures in spring, summer and autumn shows significant warming trends. On the other hand, central and northwestern parts of Turkey experiences significant increase in precipitation in the autumn.

REFERENCES

Charlson, R. J., and T. M. L. Wigley, Sulfate aerosol and climatic change, Scientific American, 28-35, February 1994.

Ezber, Y., O. L. Sen, T. Kindap and M. Karaca, Climate effects of urbanization in İstanbul: a statistical and modeling analysis, Int. J. of Climatol., 26, 1225-1236, 2006.

IPCC, 2001, Intergovernmental Panel on Climate Change, Climate Change 2001--The Scientific Basis: Contribution of Working Group I to the Third Assessment Report of the Intergovernmental Panel on Climate Change, J. T. Houghton et al., eds., Cambridge U. Press, New York (2001).

Jones, P. D., and M. E. Mann (2004), Climate over past millennia, Rev. Geophys., 42.

Karaca M., M. Tayanç and H. Toros (1995) The Effects of Urbanization on Climate of İstanbul and Ankara, Atmos. Environ., Urban Atmospheres, 29, 3411-3421.

Karaca, M., A. Deniz, and M. Tayanç (2000) Cyclone Track Variability over Turkey in Association with Regional Climate, Int. J. of Climatol., 20, 1225-1236.
Karl, T. R., et al., Asymmetric trends of daily maximum and minimum temperature, Bull. of Amer. Meteor. Soc., 74, 1007-1023, 1993.
Kiehl, J.T., T.L. Schneider, P.J. Rasch, M.C. Barth, and J. Wong, 2000: Radiative forcing due to sulfate aerosols from simulations with the National Center for Atmospheric Research Community Climate Model, Version 3. J. Geophys. Res., 105, 1441-1457.
Nasrallah, H. A., and R. C. Balling, Spatial and temporal analysis of Middle Eastern temperature changes, Climatic Change, 25, 153-161, 1993.
State Institute of Statistics, Ankara, 2000
Tayanç, M. and H. Toros (1997) Urbanization Effects on Regional Climate Change in the Case of Four Large Cities of Turkey, Climatic Change, 35, 501-524.
Tayanç, M., M. Karaca, and O. Yenigün (1997) Annual and Seasonal Air Temperature Trend Patterns of Climate Change and Urbanization Effects in Relation with Air Pollutants in Turkey, J. Geophys. Res., 102 , No. D2 ,1909-1919.
Tayanç, M., H. N. Dalfes, M. Karaca, and O. Yenigün (1998a) A Comparative Assessment of Different Methodologies for Detecting Inhomogeneities in Turkish Temperature Dataset, Int. J. of Climatol., 18, 561-578.
Tayanç, M., M. Karaca, and H. N. Dalfes (1998b) March 1987 Cyclone (Blizzard) over the Eastern Mediterranean and Balkan Region Associated with Blocking, Mon. Wea. Rev., 126, 3036-3047.
Wigley, T.M.L, The Climate Change Commitment, Science, 18 March 2005, 1766-1769.
WMO, 1992, Monitoring, Assessment and Combat of Drought and Desertification, WMO/TD-No.505, Cenevre.

RELATIONSHIP BETWEEN SEA-SURFACE TEMPERATURE ANOMALIES AND PRECIPITATION ACROSS TURKEY

Bradford S. Barrett

University of Oklahoma, Norman, OK, USA and University of Graz, AUSTRIA, bradb@ou.edu

ABSTRACT

Due to their semi-arid climate and continued population growth, the major climate regions of Turkey are vulnerable to shifts in precipitation patterns and the associated cycles of groundwater availability. Previous analyses of rainfall data from stations throughout the country have revealed pronounced seasonality and inter-annual variability[1]. Cyclone track and frequency, proximity to the sea, local and regional orographic features, strength of anticyclonic flow, equatorward penetration of polar fronts, stage of the El Nino-Southern Oscillation and North Atlantic Oscillation, and strength and placement of 700 hPa height anomalies have all been shown to directly impact the quantity and distribution of precipitation[2],[3],[4],[5],[6]. Kadioğlu et al.[7] examined the regional variability of mean seasonal total precipitation and found that each region exhibited its own rainfall regime, especially in the high plateaus and rugged mountainous areas of Anatolia.

Taha et al.[8] and Martyn[9] found that most climate regions in Turkey were characterized by aridity and continentality, and thus they concluded that the influence of the surrounding Mediterranean and Black seas was restricted. However, because of the modulating influence of sea surface temperature (SST) anomalies on many of the factors identified by the above authors, it is important to re-examine its role. This study seeks to build on the Taha et al.[8] and Martyn[9] studies by identifying and examining the relationship between SST anomalies (from NCEP/NCAR reanalyses) in the Mediterranean and Black seas and rainfall in selected sites across Turkey (from the Turkish State Meteorological Agency). Pearson correlations coefficients will be computed and tested for significance. By isolating the relationship between SST anomalies and rainfall, community planning decisions can be made based on anticipated SST variation and subsequent rainfall expectations.

INTRODUCTION

Understanding climatic change and global warming is vitally important to human existence and continuance, and especially so in regions sensitive to shifts in water resources and precipitation[10]. Turkey is one such location. Because of the high year-to-year and seasonal variability in rainfall, much of the country lacks regular and sufficient water during the year[7]. Recent studies of precipitation distribution across Turkey[1],[6],[11] showed a noticeable decrease in both winter and annual rainfall in the Black Sea and Mediterranean precipitation regions. Also, periodic dry spells were noticed in the early 1930s, late 1950s, early 1970s, 1980, and the early 1990s. Several wet spells were observed to interrupt the dry conditions, especially in 1935-1945, around 1960, and in the late 1970s. Widespread dry conditions over much of Turkey were documented in the 1970s and 1980s[11].

The Turkish State Meteorological Service maintains a well-dispersed network of rain gauges across the several sub-climate regions of Turkey[10]. This precipitation data has been used by

several authors who examined the role of meso- and synoptic-scale atmospheric features in determining the precipitation amount and distribution over Turkey. Taha et al.[8] and Martyn[9] found that most climate regions in Turkey were characterized by aridity and continentality, and thus they concluded that the influence of the surrounding Mediterranean and Black seas was restricted. Other authors have identified several factors as directly impacting the quantity and distribution of precipitation across Turkey: proximity to the sea, strength of surface and mid-tropospheric anticyclones, equatorward extent and strength of cold fronts, mid-latitude cyclone track and frequency, local and regional orography, stages of the El Nino-Southern Oscillation and North Atlantic Oscillation, and location and intensity of 700 hPa height anomalies[2],[3],[4],[5].

Generally speaking, many of the worldwide climate research centers have recently focused their research endeavors in the area of global climate change. One popular research approach examines the sensitivity of global climate models (GCMs) to various initial condition and parameterization perturbations. However, a resonable physical interpretation of GCM output requires a priori knowledge of the current climatological system and its characteristics. One method helpful in understanding the earth-climate system is to systematically examine the near-historical record, looking for secular trends in the observations and drawing conclusions from the observations. This study is such a method, building on the earlier Taha et al.[8] and Martyn[9] research by investigating the relationship between sea surface temperature (SST) of the Mediterranean and Black seas and precipitation across twenty-seven selected sites across Turkey.

DATA

Sea surface temperatures from the period 1900 to 2006 were obtained from the U.S. National Climatic Data Center (NCDC), a division of the U.S. National Oceanographic and Atmospheric Agency (NOAA). The "extended reconstructed sea surface temperatures" (ERSST) dataset, version two, contains global monthly SSTs averaged on a two degree grid. Two points in the eastern Mediterranean basin were chosen as representative sea surface temperatures: 34°N, 30°E and 34°N, 22°E. One point in the western Black sea was chosen as a representative sea surface temperature: 42°N, 32°E.

Rainfall data were obtained from the NCDC's Global Historical Climatology Network (GHCN). Observing locations were selected across Turkey using several criteria: (1) length of the historical record available; (2) completeness of the historical record available; and (3) spatial distribution across Turkey's various climatic regimes. It is important to realize that, while this study aims to use only highest-quality data, inhomogeneities in both the precipitation (GHCN) and SST (ERSST) datasets are possible. However, no other observational data will be without similar problems, and the historical record (107 years for SST and an average of 75 years for precipitation) is sufficiently long that, in the author's opinion, some of the inaccuracies will be smoothed.

The twenty-seven selected precipitation sites, along with their abbreviations and the length of the historical record used in this study, are listed below in Table 1. Figure 1 (courtesy of M. Turkes) below plots the distribution of the selected sites. Notice the twenty-seven sites are spread roughly evenly through Turkey's identified climate regimes[10].

Table 1. The twenty-seven precipitation sites across Turkey used in this study.

WMO Code	City	Abbreviation	Period of Record
170220	ZONGULDAK	ZON	1938-2006
170400	RIZE	RIZ	1929-2004
170500	EDIRNE	EDI	1929-2006
170620	ISTANBUL / GOZTEPE	IST	1929-2006
170840	CORUM	COR	1931-2006
170900	SIVAS	SIV	1929-2006
170920	ERZINCAN	ERZ	1931-2006
170980	KARS	KAR	1931-2006
191120	KANAKKALE	KAN	1931-2006
171160	BURSA	BUR	1931-2006
171300	ANKARA / CENTRAL	ANK	1926-2006
171500	BALIKESIR	BAL	1937-2006
171700	VAN	VAN	1938-2006
171880	USAK	USK	1931-2006
171900	AFYON	AFY	1931-2006
171950	KAYSERI / ERKILET	KAY	1951-2004
172100	SIIRT	SIR	1938-2006
172200	IZMIR / GUZELYALI	IZM	1929-2004
172400	ISPARTA	ISP	1931-2006
172440	KONYA	KON	1931-2006
172500	NIGDE	NIG	1938-2006
172550	KAHRAMANMARAS	KAH	1961-2006
172700	SANLIURFA	SAN	1932-2006
172800	DIYARBAKIR	DIY	1929-2006
172920	MUGLA	MUG	1935-2006
173000	ANTALYA	ANT	1929-2006
173400	MERSIN	MER	1961-2006

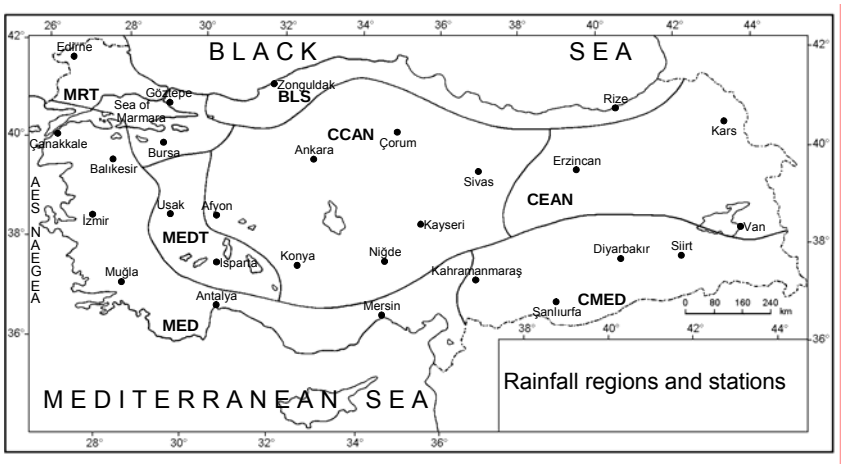

Figure 1. Location of the 27 stations over the rainfall regions of Turkey. Regions are identified as follows: **BLS**: Black Sea; **MRT**: Marmara Transition; **MED**: Mediterranean; **MEDT**: Mediterranean Transition; **CMED**: Continental Mediterranean; **CCAN**: Continental Central Anatolia; **CEAN**: Continental Eastern Anatolia. Figure provided courtesy of Dr. M. Türkeş[10].

METHODOLOGY AND RESULTS

To gauge the relationship between precipitation amount and SST, Pearson correlation coefficients were computed between the monthly precipitation data and the monthly SSTs. Because precipitation and sea surface temperatures exhibit strong seasonality[7], it is important to correlate monthly precipitation with the SST anomalies. Monthly SST data from 1900-2006 was averaged to calculate the mean. Then the mean was subtracted from each monthly value to compute the SST anomalies. Correlation coefficients were calculated between the SST anomaly and the precipitation value for each month where data was available. Annual correlation coefficients were also calculated between SST anomalies and rainfall data, but the values never deviated significantly from 0.00 (not shown). Monthly correlation coefficients between Mediterranean SSTs (at the grid point 34N, 22E) and precipitation data are summarized in Table 2 below. Correlation coefficients that exceed the "weak" threshold of relationship (above 0.30 or below -0.30) are highlighted in bold. No "strong" relationships (coefficients above 0.60 or below -0.60) were found, however several values do approach 0.50.

Table 2. Correlation coefficients between monthly precipitation and SST anomalies at 34°N, 22°E, in the Mediterranean Sea.

Station	Jan	Feb	Mar	Apr	May	Jun	Jul	Aug	Sep	Oct	Nov	Dec
ZON	(0.07)	(0.09)	(0.08)	**(0.37)**	(0.15)	0.20	(0.01)	(0.08)	(0.17)	0.04	(0.00)	(0.06)
RIZ	(0.13)	(0.11)	(0.15)	(0.29)	0.08	(0.10)	0.03	(0.08)	0.03	(0.17)	(0.08)	(0.10)
EDI	0.00	0.18	0.10	(0.10)	(0.17)	(0.15)	0.18	(0.10)	(0.16)	(0.02)	(0.04)	0.18
IST	(0.23)	(0.06)	(0.13)	**(0.30)**	**(0.31)**	(0.08)	(0.11)	(0.02)	(0.24)	(0.09)	(0.03)	(0.07)
COR	(0.12)	(0.08)	(0.07)	(0.13)	0.02	(0.12)	0.19	0.09	(0.04)	(0.23)	(0.00)	(0.15)
SIV	(0.20)	(0.11)	(0.10)	(0.05)	0.10	(0.04)	**0.36**	0.08	(0.10)	(0.09)	0.02	(0.07)
ERZ	(0.16)	0.10	0.20	(0.09)	0.00	0.12	0.25	0.14	0.07	(0.12)	(0.10)	0.06
KAR	(0.00)	(0.14)	0.19	0.20	0.22	0.09	**0.49**	0.13	0.04	(0.03)	0.14	0.05
KAN	(0.08)	0.21	(0.09)	(0.10)	(0.26)	(0.27)	0.01	(0.02)	(0.16)	(0.01)	(0.05)	0.17
BUR	(0.17)	0.11	0.01	(0.21)	**(0.31)**	(0.13)	(0.07)	0.06	(0.12)	(0.02)	0.05	(0.05)
ANK	(0.17)	0.08	0.05	(0.15)	0.00	0.13	(0.03)	(0.06)	(0.08)	(0.10)	(0.14)	(0.03)
BAL	(0.08)	0.22	(0.02)	(0.23)	(0.10)	(0.24)	(0.18)	**(0.32)**	(0.15)	(0.11)	0.09	0.05
VAN	0.05	(0.12)	0.11	(0.03)	(0.06)	**0.31**	0.14	0.25	0.26	0.11	0.13	0.09
USK	(0.08)	0.07	(0.03)	(0.15)	(0.05)	0.19	0.18	0.22	(0.04)	(0.16)	(0.04)	0.09
AFY	(0.18)	0.11	(0.13)	(0.12)	0.01	0.19	0.04	0.08	0.05	(0.12)	0.04	(0.08)
KAY	(0.27)	(0.06)	(0.05)	0.02	0.04	0.21	**0.34**	(0.07)	(0.23)	(0.12)	(0.15)	(0.09)
SIR	(0.10)	(0.27)	(0.09)	(0.12)	(0.02)	0.28	0.22	0.21	0.13	(0.09)	0.08	0.01
IZM	(0.13)	0.12	(0.15)	(0.27)	**(0.34)**	(0.22)	(0.24)	0.22	(0.01)	(0.04)	(0.03)	0.03
ISP	0.02	0.15	(0.19)	(0.05)	0.02	0.05	0.12	0.09	0.01	(0.12)	(0.04)	0.02
KON	(0.12)	(0.06)	(0.27)	0.03	0.15	0.15	0.14	0.08	0.02	(0.11)	(0.08)	(0.02)
NIG	0.16	0.09	(0.14)	(0.08)	0.07	0.24	**0.35**	0.04	0.06	(0.05)	0.11	(0.06)
KAH	(0.25)	0.15	(0.20)	(0.18)	0.05	(0.15)	0.07	**(0.35)**	0.09	(0.25)	0.14	(0.13)
SAN	0.05	(0.29)	(0.26)	(0.08)	0.05	0.13	**0.44**	0.21	0.19	(0.03)	0.21	(0.13)
DIY	0.01	(0.20)	(0.21)	(0.05)	0.15	0.04	**0.36**	(0.19)	0.33	0.05	0.07	(0.07)
MUG	(0.06)	0.13	(0.14)	(0.18)	0.02	0.02	0.28	0.24	0.12	(0.10)	(0.01)	0.14
ANT	0.18	0.09	(0.21)	0.00	0.14	0.07	0.25	0.17	0.04	(0.10)	0.00	(0.08)
MER	(0.25)	0.14	(0.28)	0.10	(0.05)	**0.34**	0.12	0.12	**(0.32)**	(0.27)	(0.02)	(0.13)

Most of the stations have very little correlation between monthly rainfall and SST anomalies, as evidenced by correlation coefficients between -0.20 and 0.20. However, the coefficients do reveal a few interesting relationships. First, the only weakly positive relationships (correlation coefficients greater than 0.30) are found in June and July, at stations SIV, KAR, VAN, KAY, NIG, SAN, DIY, and MER. This suggests that, for these locations, above-normal Mediterranean SSTs are related to increased summer precipitation. Second, the only weak negative relationships (correlation coefficients less than -0.30) are found in April-May and August-September at stations ZON, IST, BUR, IZM, BAL, KAH, and MER. This suggests that higher than normal Mediterranean SSTs are related to lower precipitation values. Third, no stations exhibit significant (either weak, or strong) relationships in the winter months (November-February), suggesting that Mediterranean SST anomalies are not related to precipitation during this season.

Turkey is bordered by not only the Mediterranean sea to its south and southwest, but also by the Black sea to its north and northeast. Thus, in addition to looking for relationships between Mediterranean SST anomalies and precipitation in Turkey, correlation coefficients were computed for the Black Sea (represented at the point 42°N, 32°E). The coefficients are presented in Table 3 below.

Like the correlations between Mediterranean Sea SST and precipitation, the correlations between Black Sea SST also reveal mostly no relationship (coefficients hovering around 0.00). However, several patterns similar to the Mediterranean emerge. For the month of July, seven stations' precipitation is weakly positively correlated (coefficients greater than 0.30) warm SST anomaly. Also, the weakly negative (coefficients less than -0.30) correlations are found in March-April and September-October. This suggests similar relationships exist between Mediterranean and Black Sea SST anomalies and precipitation across Turkey.

Table 3. Correlation coefficients between monthly precipitation and SST anomalies at 42°N, 32°E, in the Black Sea.

Station	Jan	Feb	Mar	Apr	May	Jun	Jul	Aug	Sep	Oct	Nov	Dec
ZON	0.16	(0.02)	0.01	**(0.36)**	(0.22)	0.17	(0.09)	(0.12)	(0.20)	0.05	(0.08)	0.02
RIZ	(0.10)	(0.04)	(0.23)	**(0.33)**	0.08	(0.06)	0.00	0.03	(0.08)	**(0.33)**	(0.23)	(0.29)
EDI	0.19	0.05	0.18	(0.10)	(0.24)	(0.11)	0.18	(0.05)	(0.08)	0.02	0.06	0.24
IST	0.06	(0.08)	0.02	**(0.32)**	(0.29)	(0.03)	(0.11)	0.01	**(0.31)**	(0.13)	(0.12)	(0.06)
COR	(0.05)	(0.15)	0.06	(0.17)	(0.08)	(0.15)	0.18	0.11	(0.04)	(0.25)	(0.10)	(0.10)
SIV	(0.22)	(0.20)	(0.08)	(0.15)	0.09	(0.03)	**0.43**	0.15	(0.07)	(0.16)	(0.13)	0.04
ERZ	(0.02)	(0.05)	0.14	(0.01)	(0.03)	0.16	**0.34**	0.15	(0.03)	(0.26)	(0.21)	(0.02)
KAR	(0.05)	(0.24)	(0.05)	0.11	0.17	0.06	**0.43**	0.08	(0.02)	(0.19)	0.02	(0.09)
KAN	0.15	0.10	0.03	(0.11)	(0.26)	(0.14)	0.01	(0.09)	(0.14)	(0.03)	0.05	0.16
BUR	0.05	0.10	0.17	(0.28)	(0.26)	(0.08)	(0.10)	(0.02)	(0.14)	(0.14)	(0.02)	(0.02)
ANK	0.02	(0.05)	0.14	(0.13)	0.01	0.17	0.08	0.01	(0.01)	(0.12)	(0.20)	0.05
BAL	0.08	0.17	0.07	(0.15)	(0.01)	(0.23)	(0.19)	(0.27)	(0.10)	(0.16)	0.10	0.20
VAN	(0.05)	(0.22)	(0.18)	(0.11)	0.06	0.19	0.17	0.23	0.25	(0.05)	0.08	(0.06)
USK	0.09	(0.05)	0.06	(0.23)	(0.04)	0.18	0.09	0.11	0.04	(0.12)	(0.04)	0.20
AFY	(0.10)	0.04	(0.02)	(0.23)	0.04	0.08	0.06	0.02	0.00	(0.17)	(0.08)	(0.05)
KAY	(0.17)	(0.25)	(0.08)	0.05	0.05	0.20	**0.30**	(0.15)	(0.29)	(0.27)	**(0.30)**	0.02
SIR	(0.10)	(0.28)	(0.37)	(0.14)	0.03	0.13	**0.30**	0.25	0.09	(0.16)	0.04	(0.11)
IZM	0.11	0.08	(0.02)	(0.25)	(0.27)	(0.08)	(0.23)	0.11	0.03	(0.02)	0.02	0.18
ISP	0.16	0.22	(0.10)	(0.14)	(0.01)	(0.00)	(0.00)	0.03	(0.06)	(0.11)	(0.08)	0.14
KON	0.07	(0.09)	(0.28)	(0.03)	0.23	0.12	0.15	0.09	(0.01)	(0.11)	(0.21)	0.07
NIG	0.25	(0.12)	(0.26)	(0.04)	0.09	0.25	**0.34**	0.07	0.07	(0.08)	0.04	(0.10)
KAH	(0.08)	(0.17)	**(0.40)**	(0.14)	0.07	0.01	(0.23)	**(0.40)**	0.08	**(0.39)**	0.02	(0.10)
SAN	0.01	(0.26)	**(0.35)**	(0.13)	0.10	0.07	**0.49**	0.22	0.13	(0.13)	0.10	(0.06)
DIY	0.04	(0.25)	(0.27)	(0.05)	0.15	(0.00)	**0.43**	(0.19)	**0.31**	(0.07)	0.05	(0.02)
MUG	0.12	0.08	(0.15)	(0.11)	0.08	0.09	**0.30**	0.09	0.11	(0.11)	0.08	0.25
ANT	0.26	0.07	(0.16)	(0.12)	0.02	0.10	0.20	0.04	(0.06)	(0.03)	0.03	(0.05)
MER	0.04	0.11	**(0.37)**	(0.05)	(0.18)	0.29	(0.01)	0.12	(0.26)	(0.26)	(0.03)	(0.23)

CONCLUSIONS

The data presented above reveal that precipitation across Turkey is largely unrelated to SST anomalies in both the Black and Mediterranean Seas. However, this study found indications that weak relationships may exist for some sites in some months. The correlation coefficients were not randomly dispersed throughout the year. Weakly positive coefficients were found in the summer months of June and July, implying that warmer than normal SSTs are connected with increased precipitation. Weakly negative coefficients were found in the transition months of March-April and August-September, implying that warmer than normal SSTs are connected with decreased precipitation.

Several possible reasons exist to explain these relationships. For the majority of sites across Turkey, precipitation has no relationship with SST anomaly. Precipitation is, in a basic sense, a function of local vertical motion and water vapor quantity. These two variables are influenced by a variety of global-, synoptic-, and meso-scale features, including planetary waves, mid-latitude cyclones, upper-tropospheric subsidence, mid-tropospheric humidity,

local topography, and local soil moisture. Therefore, it is not surprising to find little correlation between SST and precipitation.

However, it is interesting to examine the few sites and few months that do exhibit weak correlation. In the summer months of June and July, precipitation is mostly generated by random convective cells. As SSTs increase, boundary layer relative humidity will also increase. The stations that reported weakly positive correlations are mostly located in an arc across east-central Turkey, from NIG in the south-central to KAR in the northeast. This area is mountainous and its climate continental[10]. It is possible that in June and July, local orography acts to generate convective updrafts, and the greater boundary layer relative humidity (which must be transported to these locations, as they are not adjacent to either sea) enhances the convective precipitation. In this case, positive SST anomalies can be considered as one of the forcings for increased summer precipitation over the central and eastern interior of Turkey.

In the transition months of March-April and August-September, weakly negative correlation coefficients are found in an arc through northwest to northern to northeastern Turkey, from IZM to IST to RIZ. This area is in the Black Sea and Mediterranean Sea climate zones[6]. During these months, positive SST anomalies are possibly related to increased subsidence and thus increased solar radiation. The increased subsidence would act to suppress cloud cover and precipitation. Thus, in this case, positive SST anomalies are possibly responding to the same external forcing that causes decreased precipitation, and the two are therefore weakly negatively correlated.

Although mostly unrelated, future work is necessary to further define the relationship between SST anomalies and precipitation across Turkey. Examining wind direction and speed, and also surface temperature, would be beneficial in determining the causal relationship, i.e., if SST anomalies are able to force precipitation changes or if the two are related but forced by an external mechanism. Finally, it would be interesting to perturb SST in a GCM simulation and compare the results to the observations summarized in this study to see if similarities exist.

As the earth continues to warm, SSTs in the Mediterranean and Black seas will likely increase as well. If the relationships identified in this study hold during climate change, city planners, politicians, and citizens will be able to plan accordingly.

REFERENCES

[1]. Türkeş, M., 1996: Spatial and temporal analysis of annual rainfall variations in Turkey. *International Journal of Climatology*, 16, 1057–1076.
[2]. Chang, J.-H., 1972: *Atmospheric Circulation Systems and Climate.* Oriental Publishing, 326 pp.
[3]. Barry, R.G, and A. H. Perry, 1973: *Synoptic Climatology* : *Methods and Applications*. Methuen: London; 421.
[4]. Deniz A, and M. Karaca,1995: Analysis of cyclone tracks over Turkey (in Turkish). *Journal of ITU*, 53, 59–66.

[5]. Karaca, M, A. Deniz, and M. Tayanç, 2000: Cyclone track variability over Turkey in association with regional climate. *International Journal of Climatology*, 20, 122–136.
[6]. Türkeş, M., and E. Erlat, 2005: Climatological responses of winter precipitation in Turkey to variability of the North Atlantic Oscillation during the period 1930-2001. *Theor. and App. Climatol.*, 81, 45-69.
[7]. Kadioğlu, M., Y. Tulunay, and Y. Borhan, 1999: Variability of Turkish precipitation compared to El Ni˜no events. *Geophysical Research Letters*, 26, 1597–1600.
[8]. Taha, M. F., S. A. Harb, M. K. Nagib, and A. H. Tantawy, 1981: The Climate of the Near East, In Takahashi. K. and H. Arakawa (eds.), *Climate of Southern and Western Asia*, Elsevier, 183-241.
[9]. Martyn D. 1992. *Development in Atmospheric Science*: *Climates of the World*. 18, Elsevier, New York.
[10]. Türkeş M and Erlat E. 2003. Precipitation changes and variability in turkey linked to the North Atlantic oscillation during the period 1930-2000. *International Journal of Climatology*, 23, 1771-1796.
[11]. Türkeş, M., 1998: Influence of geopotential heights, cyclone frequency and southern oscillation on rainfall variations in Turkey. *International Journal of Climatology* 18, 649–680.